SIXTEENTH TRANSDUCER WORKSHOP

18 - 20 June 1991

SAN ANTONIO, TEXAS

TELEMETRY GROUP

RANGE COMMANDERS COUNCIL

WHITE SANDS MISSILE RANGE
KWAJALEIN MISSILE RANGE
YUMA PROVING GROUND
ELECTRONIC PROVING GROUND
DUGWAY PROVING GROUND

NAVAL AIR WARFARE CENTER-WEAPONS DIVISION
ATLANTIC FLEET WEAPONS TRAINING FACILITY
NAVAL AIR WARFARE CENTER-AIRCRAFT DIVISION
NAVAL UNDERSEA WARFARE CENTER, DIVISION NEWPORT

45TH SPACE WING
AIR FORCE DEVELOPMENT TEST CENTER
30TH SPACE WING
CONSOLIDATED SPACE TEST CENTER
AIR FORCE FLIGHT TEST CENTER
AIR FORCE TACTICAL FIGHTER WEAPONS CENTER

SIXTEENTH TRANSDUCER WORKSHOP

18-20 JUNE 1991

SAN ANTONIO, TEXAS

VEHICULAR INSTRUMENTATION/TRANSDUCER COMMITTEE
TELEMETRY GROUP
RANGE COMMANDERS COUNCIL

Published and Distributed by

Secretariat
Range Commanders Council
White Sands Missile Range,
New Mexico 88002-5110

DISCLAIMER

THIS DOCUMENT HAS BEEN PUBLISHED FOR INFORMATION PURPOSES ONLY. THE MATERIAL CONTAINED HEREIN DOES NOT NECESSARILY REPRESENT THE POSITION OR CONCLUSIONS OF THE RANGE COMMANDERS COUNCIL (RCC).

TABLE OF CONTENTS

TABLE OF CONTENTS

TELEMETRY GROUP COMMITTEES

Chairman, J. W. Rymer (NATC)
Vice Chairman,

Data Multiplex
RF Systems
Recorder/Reproducer
Vehicular Instrumentation/Transducer

MEMBERSHIP OF THE VEHICULAR INSTRUMENTATION/TRANSDUCER COMMITTEE

Raymond Faulstich (Chairman)
NAWC-WEPS - Code RD43
Patuxent River, MD 20670

LeRoy Bates
NSWSES - Code 4R13
Port Hueneme, CA 93043

William A. Xavier
EG&G Energy Measurements
P.O. Box 9051
Pleasanton, CA 94556

Lawrence Sires
NAWC-WEPS - Code 6213
China Lake, CA 93555

Archie Amos
6521 RANGES/TSRE
Edwards AFB, CA 93523

Normal E. Rector
Lawrence Livermore National Laboratories
P.O. Box 808. M/S 154
Livermore, CA 94550

Gary Bartlett
NAWC-WEPS - Code 3143
China Lake, CA 93555

Steve Kuehn
Sandia National Laboratories
P.O. Box 5800, Div 2543
Albuquerque, NM 87185

John Ach
AFWAL/FIBGA
Wright-Patterson AFB, OH 45433

Dennis Henry
Physical Science Laboratory
New Mexico State University
Las Cruces, NM 88003

Andrew Hooper
STEYP-MT-TE-T
Yuma Proving Ground
Yuma, AZ 85365

TRANSDUCER COMMITTEE OBJECTIVES

This committee apprises the Telemetry Group (TG) of significant progress in the field of transducers used in telemetry systems; maintains any necessary liaison between the TG and the National Bureau of Standards and their transducers' program or other related telemetry transducer efforts; coordinates TG activities with other professional technical groups; collects and passes on information on techniques of measurement, evaluation, reliability, calibration, reporting and manufacturing; recommends uniform practices for calibration, testing and evaluation of vehicular instrumentation components; and contributes to standards in the area of vehicular instrumentation.

WEDNESDAY, JUNE 19, 1991

0800 **Session 3: *Tutorials***
Moderator: **William A. Xavier,** EG&G
Presentations:
- "Lightning: Nature's Troublesome Transient," **Richard Hasbrouch,** Lawrence Livermore National Laboratory
- "Environmental Stress Screening," **Wayne Tustin,** Tustin Technical Institute, Inc.

1200 LUNCH

1330 Tour of Automotive Research Facilities, Lubricants Testing Area

1830 No-host social hour at hotel

1930 Banquet at hotel

THURSDAY, JUNE 20, 1991

0830 **Session 4: *Applications***
Chairman: **James Miller,** Redstone Arsenal
Cochairman: **W. B. Leisher,** Sandia National Laboratories
- "A New Solid-State Rotary Vibrometer," **P. W. Whaley,** Oklahoma Christian University
- "±70g Full Scale Accelerometer Designed to Survive 100,000g Overrange," **Robert D. Sill,** Endevco Corp.
- "Microprocessor Control of Transducer Signal Conditioning and Recording," **Peter Frazer,** Pacific Instruments, Inc.
- "Evaluation of Chamber Pressure Transducers for Large Caliber Weapons," **W. Scott Walton,** Aberdeen Proving Ground

1015 BREAK

1030
- "A High Frequency Piezoresistive Transducer for Measurement of Low Level Blast Overpressure," **W. Scott Walton,** Aberdeen Proving Ground
- "PVF2 Shock Stress Sensor Validation and Comparison Experiments," **David B. Watts,** Armament Lab., Eglin AFB
- "Recent Applications/Developments with the Two Wire Automatic Remote Sensing and Evaluation System," **E. A. Dahl** and **LeRoy Bates,** NSWSES

1130 Closing Remarks: General Chairman

1145 Workshop Concludes

General Information

The Sixteenth Transducer Workshop will be held June 18 - 20, 1991 at the Menger Hotel in San Antonio, Texas. The hosting agency is the Automotive Research Facilities.

Registration

The registration consists of a completed registration form, a written "Murphyism," and a fee of $80.00 (payable in advance or at the door) to:

LeRoy Bates, Treasurer
NSWSES
Code 4R13
Port Hueneme, CA 93043-5007

A "Murphyism" can describe any measurement attempt that went astray with the objective of learning from our errors and keeping our feet on the ground. It should be something generic rather than common human oversight; something from which we can learn. The tone should be anonymous to not embarrass any person, organization, or company. While a "Murphyism" is not a mandatory requirement, submissions are strongly encouraged and the best will be included in the program.

Advanced registration is desirable. Please use the enclosed registration form, include a check or money order for $80.00 payable to the Sixteenth Transducer Workshop, and mail to the Workshop Treasurer by May 16, 1991. (Note: Purchase orders are not acceptable)

The registration fee covers the cost of coffee, tea, soft drinks, doughnuts, and evening banquet, and a tour. A copy of the minutes of the workshop is supplied to all attendees. Late registration will be provided at the workshop registration desk in the hotel.

Hotel Accommodations

The official hotel for the workshop is the Menger Hotel, 204 Alamo Plaza, San Antonio, Texas 78205, (512) 223-4361. A fixed block of rooms has been reserved at the special rates

indicated on the enclosed hotel registration card. Early hotel reservations are strongly encouraged. Hotel registrations must be received by May 16, 1991 for workshop rates to apply.

No formal program will be provided for spouses or guests. However, they will be most welcome at the Social Hour on Monday and the banquet on Wednesday ($10.00 additional per guest for the dinner). Note: Final count for the banquet must be known by 11 am, June 17, 1991.

Tour – Wednesday Afternoon

A three hour tour of the Automotive Research Facilities is planned for Wednesday, June 19, 1991. Please indicate on the registration form if you will be accompanied by guests so that adequate transportation may be provided.

Format and Background

Workshops are just what the name implies: everyone should come prepared to contribute something from his knowledge and experience. In a workshop the attendees become the program in the sense that the extent and enthusiasm of their participation determines the success of the workshop.

Participants will have the opportunity to hear what their colleagues have been doing and how it went; to explore areas of common interest and common problems; to offer ideas and suggestions about what's needed in transducers, techniques, and applications. Several instrumentation experts have been invited to give presentations.

Additional Information

May be obtained from the General Chairman, or:

Proceedings Chairman and Treasurer
LeRoy Bates
NSWSES Code 4R13
Port Hueneme, CA 93043-5007
(805) 982-7568
(Autovon) 551-7568

Facilities Chairman
Dennis Henry
Physical Science Laboratory
Box 30002
Las Cruces, NM 88003
(505) 646 6340

Paper Chairman
Archie L. Amos
6510 TW/TSRE
Edwards AFB, CA 93523-5000
(805) 277-2785

LIST OF ATTENDEES

Ach, John T.
Wright-Patterson AFB
WL/FIBG
Wright-Patterson AFB, OH 45433-6553
513-255-5200

Alavarado, Joe
Alpha Tech
P.O. Box 423
Gales Ferry, CT 06335
203-464-8558

Amos, Archie L.
Edwards AFB
6521 RANS/TSRE
Edwards AFB, CA 93523-5000
805-277-2785

Appley, Kenneth E.
Vibra-Metrics Inc
1014 Sherman Inc
Hamden, CT 06415
203-288-6158

Banaszak, David L.
Wright-Patterson AFB
WL/FIBG
Wright-Patterson AFB, OH 45433
513-255-2543

Bartlett, Gary D.
Naval Air Warfare Center - WEPS DIV
Code 3143
China Lake, CA 93555
619-939-5942

Bates, LeRoy
NSWSES
Code 4R13
Port Hueneme, CA 93043-5007
805-982-7568

Benedict, Roger E.
Edwards AFB
Phillips Lab
OL-AC PL/RKCP
Edwards AFB, CA 93523-5000

Billia, Richard J.
Lawrence Livermore National lab
P.O. Box 808, L-113
Livermore, CA 94550
415-423-3400

Bohle, Robert J.
Kistler Instrumentation Corp
24952 Sebastian Lane
Mission Viejo, CA 92691
714-458-0919

Brady, Leo F.
Sandia National Laboratory
P.O. Box 238
Mercury, NV 89023
702-295-3928

Brown, Larry L.
Denver Research Institute
University of Denver
2050 E. Iliff
Denver, CO 80208
303-871-2616

Brown, Tom
Naval Air Warfare Center - AC DIV
Range Directorate: RD25
Patuxent River, MD 20670
301-863-1155

Busse, Donald W.
Sundstrand Aerospace
15001 NE 35th Street
Redmond, WA 98073
206-885-8817

Chamness, Stephen D.
Olin Rocket Research
P.O. Box 278
Marion, IL 62959
618-985-8211 352

Chu, Anthony S.
Endevco Inc
30700 Rancho Viejo
San Juan Capistrano, CA 92675
714-493-8181

Cooley, William H.
Endevco
1849 Old Bayshore Hwy
STE 304A
Burlingame, CA 94010
415-697-9887

Corrie, Scott
PCB Piezotronics Inc
3425 Walden Ave
Depew, NY 14043
716-684-0001

Crounse, Dave R.
Edwards AFB
Air Force Flight Test Center
6510 Test Wing/TSID
Edwards AFB, CA 93523-5000
805-277-2976

Dahl, Ernest A.
NSWSES
4L03
Port Hueneme, CA 93003
805-982-0908

Deyoe, Richard T.
Boeing Aerospace Operations
FA-81
Kennedy Space Center, FL 32899
407-867-2147

Donnelly, William J.
Electro-Motive Division of GMC
P.O. Box 10381
Dept 840
LaGrange, IL 60525-8031
708-387-6222

Esparza, Edward D.
Southwest Research Institute
6220 Culebra Road
P.O. Drawer 28510
San Antonio, TX 78228
512-684-5110

Estep, Harry
Travis Corporation
3636 Highway 49 S
Mariposa, CA 95338
209-966-2027

Faller, James G.
US Army Combat Systems Test Activities
STECS-EN-PM
Aberdeen Proving Ground, MD 21005-5059
301-278-4461

Fassola, Robert M.
Kinetic Systems Corporation
11 Mary Knoll Drive
Lockport, IL 60441
815-838-0005

Faulstich, Raymond J.
Naval Air Warfare Center - AC DIV
Range Directorate RD25
Patuxent River, MD 20670-5304
301-863-1155

Gardner, Lee S.
Edwards AFB
6521 RANS/RCP
Edwards AFB, CA 93523-5000
805-277-2628

Gilcrease, Billy J.
Boeing Commercial Airplanes
P.O. Box 3707
M/S 47-06
Seattle, WA 98124
206-655-8582

Gillis, Richard F.
Naval Air Warfare Center - AC DIV
Range Directorate: RD43
Patuxent River, MD 20670
301-863-1584

Gordon, Joseph
Eglin AFB
WL/MNGI
Eglin AFB, FL 32542
904-882-5375

Granath, Ben A.
PCB Piezotronics, Inc
3425 Walden Ave
Depew, NY 14043
716-684-0001

Hardin, James T.
Endevco
30700 Rancho Viejo Road
San Juan Capistrano, CA 92675
714-493-8181

Hartley, Frank
Jet Propulsion Laboratory
4800 Oak Grove Drive
Mail Stop 125/177
Pasadena, CA 91016
818-354-3139

Hasbrouck, Richard T.
Lawrence Livermore National Lab
P.O. Box 808, L-154
Livermore, CA 94550
415-422-1256

Hazelton, Elmer
Gulton, Servonic Division
1644 Whittier Ave
Costa Mesa, CA 92627
714-642-2400 313

Henry, Dennis G.
Physical Science Laboratory
New Mexico State University
P.O. Box 30002
Las Cruces, MN 88003
505-646-6340

Hinds, James J.
Ruska Instrumentation Corporation
3601 Dunvale
Houston, TX 77063
713-975-0547

Jaros, Dave
PCB Piezotronics Inc
3425 Walden Ave
Depew, NY 14043
716-684-0001

Johnson, Don
Ktech Corp
901 Pennsylvania NE
Albuquerque, NM 87110
505-268-3379

Kitchen, Walter R.
EG&G Energy Measurements, Inc
P.O. Box 1912 M/S B3-20
Las Vegas, NV 89125
702-295-2920

Klingaman, Kenneth W.
US Army ARDEC - Picatinny Arsenal
B-1501
Picatinny Arsenal, NJ 07806-5000
201-724-7250

Krizan, Richard W.
45th Space Wing
ESMC/DVEC
Patrick AFB, FL 32925
407-494-5107

Kubler, John M.
Kistler Instrument Corporation
75 John Glen Drive
Amherst, NY 14226
716-691-5100

Kuehn, Stephen F.
Sandia National Laboratories
Div 2542
P.O. Box 5800
Albuquerque, NM 87185-5800
505-844-8383

Lake, Robert E.
NASA/Marshall Space Flight Center
EP75
Marshall Space Center, AL 35872
205-544-1176

Lally, Rick W.
PCB Piezotronics Inc
3425 Walden Ave
Depew, NY 14043
716-684-0001

Leisher, William B.
Sandia National Laboratories
Division 7414
P.O. Box 5800
Albuquerque, NM 87185-5800
505-844-2755

Mandala, Stephen
Picatinny Arsenal
SMCAR-AEL Bldg 60
Picatinny Arsenal, NJ 07806
201-729-3330

Miller, James R.
US Army TMDE Support Group
AMXTM-S-EP
Redstone Arsenal
Redstone Arsenal, AL 35802
205-876-9494

Nicholson, Rickey L.
Vitro Technical Services Inc
P.O. Box 1898
Eglin AFB, FL 32542-1898
904-882-5188

Noyes, Roger P.
EG&G Energy Measurements, Inc
P.O. Box 1912, N-28
Las Vegas, NV 89125
702-295-2532

Painter, Darcy S.
Edwards AFB
6521 RANS/TSE
Edwards AFB, CA 93523-5000
805-275-8606

Palmer, Bruce M.
30th Space Wing
6595 Test & Evaluation Group/ENI
Vandenberg, CA 93437
805-866-2033

Payne, B. F.
NIST
Bldg 233, Room A149
Gaithersburg, MD 20899
301-975-6634

Perrin, Thomas
Frontline Management Inc
23151 Verdugo Drive, Suite 204
Laguna Hills, CA 92653
714-472-8631

Peterson, Edward L.
MB Dynamics Inc
25865 Richmond Road
Cleveland, OH 44146-1483
216-292-5850

Rahav, Amir
TEDEA
P.O. Box 2008
Herzliya, OH 46120

Rector, Normal L.
Lawrence Livermore National Lab
P.O. Box 808, M/S 154
Livermore, CA 94550
415-422-3994

Rendia, Gary M.
Endevco
30700 Rancho Viejo Road
San Juan Capistrano, CA 92675
714-493-8181

Rieger, James L.
Naval Air Warfare Center - WEPS DIV
Code 64203
China Lake, CA 93555-6001
619-939-2631

Rood, Richard
NASA Dryden
Box 273 XRF
Edwards AFB, CA 93523
805-258-2138

Schonthal, Ernst
Bruel & Kjaer Instruments, Inc
185 Forest Street
Marlboro, MA 01752
508-481-7000

Shay, William M.
Lawrence Livermore National Lab
P.O. Box 808, L-345
Livermore, CA 94550
415-422-7044

Sill, Robert D.
Endevco Corporation
30700 Rancho Viejo Road
San Juan Capistrano, CA 92765
714-493-8181

Sires, Lawrence M.
Naval Air Warfare Center - WEPS DIV
Code 6213
China Lake, CA 93555-6001
619-939-7404

Stein, Peter K.
Stein Engineering Services, Inc
5602 East Monterosa
Phoenix, AZ 85018
602-945-4603

Stonelake, Harry
Gulton Industries, Servonic Div
P.O. Box 1356
Ventura, CA 93002
805-658-1484

Supak, Wayne, A.
Caterpillar Inc
Technical Center Bldg A
P.O. Box 1875
Pedria, Il 61656
309-578-6851

Swiggers, Art
Precision Filters Inc
10221 North 32 Street Suite J
Phoenix, AZ 85028
602-953-0345

Walton, James S.

Talmadge, Richard
Wright-Patterson AFB
USAF WL/FIBG
Wright-Patterson AFB, OH 45433-6553
513-255-5200

Ronald B. Tussing
Naval Surface Weapons Center
White Oak Laboratory - R15
Silver Spring, MD 20910-5000
301-394-1187

Tustin, Wayne
Tustin Technical Institute
22 East Los Olivos Street
Santa Barbara, CA 93105
805-682-7171

Walton, James S.
4D Video
3136 Pauline Drive
Sebastopol, CA 95472
707-829-8883

Walton, W. Scott
US Army Aberdeen Proving Ground
STECS-DA-ID
Aberdeen Proving Gnd, MD 21005-5059
301-278-9485

Watts, David B.
Eglin AFB
Wright Laboratory Armament Dir
WL/MNGI
Eglin AFB, FL 32542-5434
904-882-5375

Whaley, Wayne
Oklahoma Christian University
P.O. Box 11000
Oklahoma City, OK 73136-1100
405-435-5424

Wiley, John T.
NASA Marshall Space Flight Center
EP75
MSFC, AL 34803
205-882-6556

Wilson, Jon S.
The Dynamic Consultant
32871 Via Del Amo
San Juan Capistrano, CA 92675
714-496-7135

Xavier, William A.
EG&G/DOE
1210 Marina Village Parkway
Suite 101
Alameda, CA 94541
415-748-8404

Yuen, Brian K.
LLNL
P.O. Box 808 L-154
Livermore, CA 94550
415-422-3328

TRANSDUCER WORKSHOP SUMMARY

Workshop Number	Date	Host	General Chairman	Number Attendees	RCC TG Transducer Chairman
1	March 1960	Albuquerque, NM			
2	25-26 July 1961	Holloman AFB Alamogordo, NM	W. H. Sanders Holloman AFB, NM	46	Paul Polishuk Wright-Patterson Dayton, OH
3	21-23 June 1962	NBS Washington, DC	Arnold Wexler NBS Washington, DC	106	Paul Polishuk Wright-Patterson Dayton, OH
4	18-19 June 1964	Wright-Patterson Dayton, OH	Jack Lynch NATC Patuxent River, MD	53	Jack Lynch NATC Patuxent River, MD
5	3-4 October 1967	NBS Gaithersburg, MD	Loyt L. Lathrop Sandia Labs Albuquerque, NM	106	Loyt L. Lathrop Sandia Labs Albuquerque, NM
6	22-24 October 1969	Langley Research Ctr NASA Hampton, VA	Paul Lederer NBS Washington, DC	49	Loyt L. Lathrop Sandia Labs Albuquerque, NM
7	4-6 April 1972	Sandia Labs Albuquerque, NM	W. G. James AEFDL Wright-Patterson Dayton, OH	111	Pat Walter Sandia Labs First Mfg's Panel Boo-Boos
8	22-24 April 1975	Wright-Patterson Dayton, OH	Pierre F. Fuselier Lawrence Livermore Labs Livermore, CA	74	Pat Walter Sandia Labs Albuquerque, NM
9	26-28 April 1977	Eglin AFB Fort Walton Beach, FL	Kenny Cox NWC China Lake, CA	100	William Anderson NATC Patuxent River, MD

Workshop Number	Date	Host	General Chairman	Number Attendees	RCC TG Transducer Chairman
10	12-14 June 1979	North American Air Defense Command Colorado Springs, CO	Richard Hasbrouck Lawrence Livermore Labs Livermore, CA	106	William Anderson NATC Patuxent River, MD
11	2-4 June 1981	Air Force Plant Rep Office, Det 9 Seattle, WA	Leroy Bates NSWSES Port Hueneme, CA	96	William Anderson NATC Patuxent River, MD
12	7-9 June 1983	Patrick AFB Melbourne, FL	Kenny Cox NWC China Lake, CA	116	William Anderson NATC Patuxent River, MD
13	4-6 June 1985	Naval Postgraduate School Monterey, CA	Richard Krizan Patrick AFB, FL	112	Leroy Bates NSWSES Port Hueneme, CA
14	16-18 June 1987	Air Force Academy Colorado Springs, CO	Stephen F. Kuehn Sandia National Labs Albuquerque, NM	118	Leroy Bates NSWSES Port Hueneme, CA
15	20-22 June 1989	ESMC, Patrick AFB Cocoa Beach, FL	John T. Ach WRDC/FIBGA Wright-Patterson AFB, OH	90	Leroy Bates NSWSES Port Hueneme, CA
16	18-20 June 1991	Automotive Research Facilities San Antonio, TX	Raymond Faulstich Naval Air Test Center Patuxent River, MD	81	Leroy Bates NSWSES Port Hueneme, CA

SIXTEENTH TRANSDUCER WORKSHOP

San Antonio, Texas
June 18 - 20, 1991

Sponsored by
Vehicular Instrumentation/
Transducer Committee of
Range Commanders Council
Telemetry Group

Participating Society

Test
Measurement
Division

Definition of The Transducer Workshop

History

The Workshop is sponsored by the Vehicular Instrumentation/ Transducer Committee, Telemetry Group of the Range Commanders Council. This committee develops and implements standards and procedures for transducer applications. The fifteen previous workshops, beginning in 1960, were held at two year intervals at, or near various U.S. Government installations around the country.

Attendees

Attendees are working-level people who must solve real-life hardware problems and are strongly oriented to the practical approach. Their field is making measurements of physical parameters using transducers. Test and project people who attend will benefit from exposure to the true complexity of transducer evaluation, selection, and application.

Subjects

Practical problems involving transducers, signal conditioners, and read-out devices will be considered as separate components and in systems. Engineering tests, laboratory calibrations, transducer developments and evaluations represent potential applications of the ideas presented. Measurands include force, pressure, flow, acceleration, velocity, displacement, temperature and others.

Emphasis

The Workshop

1. Is a practical approach to the solution of measurement problems,
2. Strongly focuses on transducers and related instrumentation used in measurements engineering,
3. Has a high ratio of discussion to presentation of papers, and
4. Shares knowledge and experience through open discussion and problem solving.

Goals

The workshop brings together those people who use transducers to identify problems and to suggest some solutions, identifies areas of common interest and provides a communication channel within the community of transducer users. Some examples are:

1. Improve the coordination of information regarding transducer standards, test techniques, evaluations, and application practices among the national test ranges, range users, range contractors, other transducer users, and transducer manufacturers;
2. Encourage the establishment of special sessions so that attendees with measurement problems in specific areas can form subgroups and remain to discuss these problems after the workshop concludes; and
3. Solicit suggestions and comments on past, present, and future Vehicular Instrumentation/Transducer Committee efforts.

General Chairman

Raymond Faulstich
Naval Air Test Center
Range Directorate: RD25
Patuxent River, MD 20670-5304
(301) 863-1155

Program

MONDAY, JUNE 17, 1991

2000 Social Hour, at the Menger Hotel, courtesy of the Vehicular Instrumentation/Transducer Committee
All attendees welcome!

TUESDAY, JUNE 18, 1991

0730 Registration

0800 **Ray Faulstich,** General Chairman
Sixteenth Transducer Workshop
Welcome: **Fred Parks,** EG&G Automotive Research, Inc
Introductions: **LeRoy Bates,** Chairman Vehicular Instrumentation/Transducer Committee, RCC/TG

0900 **Session 1: *Data Acquisition***
Chairman: **Richard Krizan,** Eastern Space and Missile Center
Cochairman: **R. P. Reed,** Sandia National Laboratories
- "Programmable Transducer Microchip Development," **Richard Talmadge,** Air Force Flight Dynamics Laboratory
- "A Couple Million Points of Light: Television, The Ultimate Transducer," **James L. Rieger,** Naval Weapons Center
- "Common Airborne Instrumentation Systems," **Raymond J. Faulstich,** Naval Air Test Center

1015 BREAK

1030
- "Compression Tradeoffs for Instrumentation Video," **James L. Rieger,** Naval Weapons Center
- "Image-Based Motion Measurement and Motion Reconstruction: Applications in Vehicular Dynamics," **James S. Walton,** 4D Video
- "Tourmaline Gauge in Use for Measurements of Underwater Explosion Phenomena," **Ronald Tussing,** Naval Surface Weapons Center

1200 LUNCH

1330 **Session 2: *Calibration Techniques***
Chairman: **Ronald Tussing,** Naval Surface Weapons Center
Cochairman: **Roger Noyes,** EG&G Energy Measurements
- "A Brief History of the Beginning of the Bonded Resistance Foil Strain Gage," **Peter K. Stein,** Stein Engineering Services, Inc.
- "Collecting, Managing, and Distributing Instrumentation System Calibration on Information in a High Volume, Data Production Environment," **Lee S. Gardner,** Edwards AFB
- "Automated Structural Gravimetric Calibration of Accelerometers with an Economical PC/Data Acquisition Board Combination," **Michael J. Lally,** University of Cincinnati
- "Multiple Accelerometer Frequency Response Evaluation," **David Banaszak,** Air Force Wright Aeronautical Lab.

1500 BREAK

1515
- "Absolute Calibration of Back-to-Back Accelerometers at High Frequencies," **B. F. Payne,** NIST
- "Vibratory Pressure Calibrations," **W. B. Leisher,** Sandia National Laboratories
- "Techniques to Optimize High Accuracy, Computer Controlled Pressure Calibration," **Martin Girard,** DH Instruments, Inc.

WEDNESDAY, JUNE 19, 1991

0800 **Session 3: *Tutorials***
Moderator: **William A. Xavier,** EG&G
Presentations:
- "Lightning: Nature's Troublesome Transient," **Richard Hasbrouch,** Lawrence Livermore National Laboratory
- "Environmental Stress Screening," **Wayne Tustin,** Tustin Technical Institute, Inc.

1200 LUNCH

1330 Tour of Automotive Research Facilities, Lubricants Testing Area

1830 No-host social hour at hotel

1930 Banquet at hotel

THURSDAY, JUNE 20, 1991

0830 **Session 4: *Applications***
Chairman: **James Miller,** Redstone Arsenal
Cochairman: **W. B. Leisher,** Sandia National Laboratories
- "A New Solid-State Rotary Vibrometer," **P. W. Whaley,** Oklahoma Christian University
- "±70g Full Scale Accelerometer Designed to Survive 100,000g Overrange," **Robert D. Sill,** Endevco Corp.
- "Microprocessor Control of Transducer Signal Conditioning and Recording," **Peter Frazer,** Pacific Instruments, Inc.
- "Evaluation of Chamber Pressure Transducers for Large Caliber Weapons," **W. Scott Walton,** Aberdeen Proving Ground

1015 BREAK

1030
- "A High Frequency Piezoresistive Transducer for Measurement of Low Level Blast Overpressure," **W. Scott Walton,** Aberdeen Proving Ground
- "PVF2 Shock Stress Sensor Validation and Comparison Experiments," **David B. Watts,** Armament Lab., Eglin AFB
- "Recent Applications/Developments with the Two Wire Automatic Remote Sensing and Evaluation System," **E. A. Dahl** and **LeRoy Bates,** NSWSES

1130 Closing Remarks: General Chairman

1145 Workshop Concludes

General Information

The Sixteenth Transducer Workshop will be held June 18 - 20, 1991 at the Menger Hotel in San Antonio, Texas. The hosting agency is the Automotive Research Facilities.

Registration

The registration consists of a completed registration form, a written "Murphyism," and a fee of $80.00 (payable in advance or at the door) to:

LeRoy Bates, Treasurer
NSWSES
Code 4R13
Port Hueneme, CA 93043-5007

A "Murphyism" can describe any measurement attempt that went astray with the objective of learning from our errors and keeping our feet on the ground. It should be something generic rather than common human oversight; something from which we can learn. The tone should be anonymous to not embarrass any person, organization, or company. While a "Murphyism" is not a mandatory requirement, submissions are strongly encouraged and the best will be included in the program.

Advanced registration is desirable. Please use the enclosed registration form, include a check or money order for $80.00 payable to the Sixteenth Transducer Workshop, and mail to the Workshop Treasurer by May 16, 1991. (Note: Purchase orders are not acceptable)

The registration fee covers the cost of coffee, tea, soft drinks, doughnuts, and evening banquet, and a tour. A copy of the minutes of the workshop is supplied to all attendees. Late registration will be provided at the workshop registration desk in the hotel

Hotel Accommodations

The official hotel for the workshop is the Menger Hotel, 204 Alamo Plaza, San Antonio, Texas 78205, (512) 223-4361. A fixed block of rooms has been reserved at the special rates

indicated on the enclosed hotel registration card. Early hotel reservations are strongly encouraged. Hotel registrations must be received by May 16, 1991 for workshop rates to apply.

No formal program will be provided for spouses or guests. However, they will be most welcome at the Social Hour on Monday and the banquet on Wednesday ($10.00 additional per guest for the dinner). Note: Final count for the banquet must be known by 11 am, June 17, 1991.

Tour – Wednesday Afternoon

A three hour tour of the Automotive Research Facilities is planned for Wednesday, June 19, 1991. Please indicate on the registration form if you will be accompanied by guests so that adequate transportation may be provided.

Format and Background

Workshops are just what the name implies: everyone should come prepared to contribute something from his knowledge and experience. In a workshop the attendees become the program in the sense that the extent and enthusiasm of their participation determines the success of the workshop.

Participants will have the opportunity to hear what their colleagues have been doing and how it went; to explore areas of common interest and common problems; to offer ideas and suggestions about what's needed in transducers, techniques, and applications. Several instrumentation experts have been invited to give presentations.

Additional Information

May be obtained from the General Chairman, or:

Proceedings Chairman and Treasurer
LeRoy Bates
NSWSES Code 4R13
Port Hueneme, CA 93043-5007
(805) 982-7568
(Autovon) 551-7568

Facilities Chairman
Dennis Henry
Physical Science Laboratory
Box 30002
Las Cruces, NM 88003
(505) 646-6340

Paper Chairman
Archie L. Amos
6510 TW/TSRE
Edwards AFB, CA 93523-5000
(805) 277-2785

LIST OF ATTENDEES

Ach, John T.
Wright-Patterson AFB
WL/FIBG
Wright-Patterson AFB, OH 45433-6553
513-255-5200

Alavarado, Joe
Alpha Tech
P.O. Box 423
Gales Ferry, CT 06335
203-464-8558

Amos, Archie L.
Edwards AFB
6521 RANS/TSRE
Edwards AFB, CA 93523-5000
805-277-2785

Appley, Kenneth E.
Vibra-Metrics Inc
1014 Sherman Inc
Hamden, CT 06415
203-288-6158

Banaszak, David L.
Wright-Patterson AFB
WL/FIBG
Wright-Patterson AFB, OH 45433
513-255-2543

Bartlett, Gary D.
Naval Air Warfare Center - WEPS DIV
Code 3143
China Lake, CA 93555
619-939-5942

Bates, LeRoy
NSWSES
Code 4R13
Port Hueneme, CA 93043-5007
805-982-7568

Benedict, Roger E.
Edwards AFB
Phillips Lab
OL-AC PL/RKCP
Edwards AFB, CA 93523-5000

Billia, Richard J.
Lawrence Livermore National lab
P.O. Box 808, L-113
Livermore, CA 94550
415-423-3400

Bohle, Robert J.
Kistler Instrumentation Corp
24952 Sebastian Lane
Mission Viejo, CA 92691
714-458-0919

Brady, Leo F.
Sandia National Laboratory
P.O. Box 238
Mercury, NV 89023
702-295-3928

Brown, Larry L.
Denver Research Institute
University of Denver
2050 E. Iliff
Denver, CO 80208
303-871-2616

Brown, Tom
Naval Air Warfare Center - AC DIV
Range Directorate: RD25
Patuxent River, MD 20670
301-863-1155

Busse, Donald W.
Sundstrand Aerospace
15001 NE 35th Street
Redmond, WA 98073
206-885-8817

Chamness, Stephen D.
Olin Rocket Research
P.O. Box 278
Marion, IL 62959
618-985-8211 352

Chu, Anthony S.
Endevco Inc
30700 Rancho Viejo
San Juan Capistrano, CA 92675
714-493-8181

Cooley, William H.
Endevco
1849 Old Bayshore Hwy
STE 304A
Burlingame, CA 94010
415-697-9887

Corrie, Scott
PCB Piezotronics Inc
3425 Walden Ave
Depew, NY 14043
716-684-0001

Crounse, Dave R.
Edwards AFB
Air Force Flight Test Center
6510 Test Wing/TSID
Edwards AFB, CA 93523-5000
805-277-2976

Dahl, Ernest A.
NSWSES
4L03
Port Hueneme, CA 93003
805-982-0908

Deyoe, Richard T.
Boeing Aerospace Operations
FA-81
Kennedy Space Center, FL 32899
407-867-2147

Donnelly, William J.
Electro-Motive Division of GMC
P.O. Box 10381
Dept 840
LaGrange, IL 60525-8031
708-387-6222

Esparza, Edward D.
Southwest Research Institute
6220 Culebra Road
P.O. Drawer 28510
San Antonio, TX 78228
512-684-5110

Estep, Harry
Travis Corporation
3636 Highway 49 S
Mariposa, CA 95338
209-966-2027

Faller, James G.
US Army Combat Systems Test Activities
STECS-EN-PM
Aberdeen Proving Ground, MD 21005-5059
301-278-4461

Fassola, Robert M.
Kinetic Systems Corporation
11 Mary Knoll Drive
Lockport, IL 60441
815-838-0005

Faulstich, Raymond J.
Naval Air Warfare Center - AC DIV
Range Directorate RD25
Patuxent River, MD 20670-5304
301-863-1155

Gardner, Lee S.
Edwards AFB
6521 RANS/RCP
Edwards AFB, CA 93523-5000
805-277-2628

Gilcrease, Billy J.
Boeing Commercial Airplanes
P.O. Box 3707
M/S 47-06
Seattle, WA 98124
206-655-8582

Gillis, Richard F.
Naval Air Warfare Center - AC DIV
Range Directorate: RD43
Patuxent River, MD 20670
301-863-1584

Gordon, Joseph
Eglin AFB
WL/MNGI
Eglin AFB, FL 32542
904-882-5375

Granath, Ben A.
PCB Piezotronics, Inc
3425 Walden Ave
Depew, NY 14043
716-684-0001

Hardin, James T.
Endevco
30700 Rancho Viejo Road
San Juan Capistrano, CA 92675
714-493-8181

Hartley, Frank
Jet Propulsion Laboratory
4800 Oak Grove Drive
Mail Stop 125/177
Pasadena, CA 91016
818-354-3139

Hasbrouck, Richard T.
Lawrence Livermore National Lab
P.O. Box 808, L-154
Livermore, CA 94550
415-422-1256

Hazelton, Elmer
Gulton, Servonic Division
1644 Whittier Ave
Costa Mesa, CA 92627
714-642-2400 313

Henry, Dennis G.
Physical Science Laboratory
New Mexico State University
P.O. Box 30002
Las Cruces, MN 88003
505-646-6340

Hinds, James J.
Ruska Instrumentation Corporation
3601 Dunvale
Houston, TX 77063
713-975-0547

Jaros, Dave
PCB Piezotronics Inc
3425 Walden Ave
Depew, NY 14043
716-684-0001

Johnson, Don
Ktech Corp
901 Pennsylvania NE
Albuquerque, NM 87110
505-268-3379

Kitchen, Walter R.
EG&G Energy Measurements, Inc
P.O. Box 1912 M/S B3-20
Las Vegas, NV 89125
702-295-2920

Klingaman, Kenneth W.
US Army ARDEC - Picatinny Arsenal
B-1501
Picatinny Arsenal, NJ 07806-5000
201-724-7250

Krizan, Richard W.
45th Space Wing
ESMC/DVEC
Patrick AFB, FL 32925
407-494-5107

Kubler, John M.
Kistler Instrument Corporation
75 John Glen Drive
Amherst, NY 14226
716-691-5100

Kuehn, Stephen F.
Sandia National Laboratories
Div 2542
P.O. Box 5800
Albuquerque, NM 87185-5800
505-844-8383

Lake, Robert E.
NASA/Marshall Space Flight Center
EP75
Marshall Space Center, AL 35872
205-544-1176

Lally, Rick W.
PCB Piezotronics Inc
3425 Walden Ave
Depew, NY 14043
716-684-0001

Leisher, William B.
Sandia National Laboratories
Division 7414
P.O. Box 5800
Albuquerque, NM 87185-5800
505-844-2755

Mandala, Stephen
Picatinny Arsenal
SMCAR-AEL Bldg 60
Picatinny Arsenal, NJ 07806
201-729-3330

Miller, James R.
US Army TMDE Support Group
AMXTM-S-EP
Redstone Arsenal
Redstone Arsenal, AL 35802
205-876-9494

Nicholson, Rickey L.
Vitro Technical Services Inc
P.O. Box 1898
Eglin AFB, FL 32542-1898
904-882-5188

Noyes, Roger P.
EG&G Energy Measurements, Inc
P.O. Box 1912, N-28
Las Vegas, NV 89125
702-295-2532

Painter, Darcy S.
Edwards AFB
6521 RANS/TSE
Edwards AFB, CA 93523-5000
805-275-8606

Palmer, Bruce M.
30th Space Wing
6595 Test & Evaluation Group/ENI
Vandenberg, CA 93437
805-866-2033

Payne, B. F.
NIST
Bldg 233, Room A149
Gaithersburg, MD 20899
301-975-6634

Perrin, Thomas
Frontline Management Inc
23151 Verdugo Drive, Suite 204
Laguna Hills, CA 92653
714-472-8631

Peterson, Edward L.
MB Dynamics Inc
25865 Richmond Road
Cleveland, OH 44146-1483
216-292-5850

Rahav, Amir
TEDEA
P.O. Box 2008
Herzliya, OH 46120

Rector, Normal L.
Lawrence Livermore National Lab
P.O. Box 808, M/S 154
Livermore, CA 94550
415-422-3994

Rendia, Gary M.
Endevco
30700 Rancho Viejo Road
San Juan Capistrano, CA 92675
714-493-8181

Rieger, James L.
Naval Air Warfare Center - WEPS DIV
Code 64203
China Lake, CA 93555-6001
619-939-2631

Rood, Richard
NASA Dryden
Box 273 XRF
Edwards AFB, CA 93523
805-258-2138

Schonthal, Ernst
Bruel & Kjaer Instruments, Inc
185 Forest Street
Marlboro, MA 01752
508-481-7000

Shay, William M.
Lawrence Livermore National Lab
P.O. Box 808, L-345
Livermore, CA 94550
415-422-7044

Sill, Robert D.
Endevco Corporation
30700 Rancho Viejo Road
San Juan Capistrano, CA 92765
714-493-8181

Sires, Lawrence M.
Naval Air Warfare Center - WEPS DIV
Code 6213
China Lake, CA 93555-6001
619-939-7404

Stein, Peter K.
Stein Engineering Services, Inc
5602 East Monterosa
Phoenix, AZ 85018
602-945-4603

Stonelake, Harry
Gulton Industries, Servonic Div
P.O. Box 1356
Ventura, CA 93002
805-658-1484

Supak, Wayne, A.
Caterpillar Inc
Technical Center Bldg A
P.O. Box 1875
Pedria, Il 61656
309-578-6851

Swiggers, Art
Precision Filters Inc
10221 North 32 Street Suite J
Phoenix, AZ 85028
602-953-0345

Talmadge, Richard
Wright-Patterson AFB
USAF WL/FIBG
Wright-Patterson AFB, OH 45433-6553
513-255-5200

Ronald B. Tussing
Naval Surface Weapons Center
White Oak Laboratory - R15
Silver Spring, MD 20910-5000
301-394-1187

Tustin, Wayne
Tustin Technical Institute
22 East Los Olivos Street
Santa Barbara, CA 93105
805-682-7171

Walton, James S.
4D Video
3136 Pauline Drive
Sebastopol, CA 95472
707-829-8883

Walton, W. Scott
US Army Aberdeen Proving Ground
STECS-DA-ID
Aberdeen Proving Gnd, MD 21005-5059
301-278-9485

Watts, David B.
Eglin AFB
Wright Laboratory Armament Dir
WL/MNGI
Eglin AFB, FL 32542-5434
904-882-5375

Whaley, Wayne
Oklahoma Christian University
P.O. Box 11000
Oklahoma City, OK 73136-1100
405-435-5424

Wiley, John T.
NASA Marshall Space Flight Center
EP75
MSFC, AL 34803
205-882-6556

Wilson, Jon S.
The Dynamic Consultant
32871 Via Del Amo
San Juan Capistrano, CA 92675
714-496-7135

Xavier, William A.
EG&G/DOE
1210 Marina Village Parkway
Suite 101
Alameda, CA 94541
415-748-8404

Yuen, Brian K.
LLNL
P.O. Box 808 L-154
Livermore, CA 94550
415-422-3328

SESSION 1

DATA ACQUISITIONS

MISSING PAGE

2

PROGRAMMABLE TRANSDUCER MICROCHIP PERFORMANCE

Kenneth E. Appley
Manager, Electrical Engineering
Vibra•Metrics, Inc.
Hamden, CT U.S.A.

ABSTRACT

This paper describes the performance and operation of the hybrid implementation of the Programmable Transducer Microchip[1] using a PC as the interface.

The functional goals of providing a common multiple transducer interface with on-line PC programmable signal conditioning have been demonstrated in a hybrid circuit. This circuit is housed in an in-line module and receives input from a charge accelerometer and a strain gage. Power, control, and data/signal connections are provided by a circuit board contained in the PC.

By responding to menu prompts an operator can: a) set conditioning and processing of the sensed input signal including impedance matching, filtering, gain selection, two stages of integration, and differentiation, b) establish a code that will be stored and returned to the interface on request to identify the particular sensor and its characteristics, and c) request a programmable frequency pulse train to be returned either through the sensing element or directly to the module output to evaluate signal integrity and calibrate the system.

Data is presented illustrating the operational characteristics of the system. Additional configurations of the module and interface are also given.

I. INTRODUCTION

An interim step in the development of the Programmable Transducer Microchip[1] was the fabrication and test of a hybrid of the circuit. The hybrid has the same performance and functional characteristics as the micro chip, but rather than being part of the transducer is encapsulated in a separate module (see Figure 1). The module provides filtering, integration, differentiation, and level control of sensed input signals from directly connected charge capacitive devices and dynamic resistive/bridge devices.

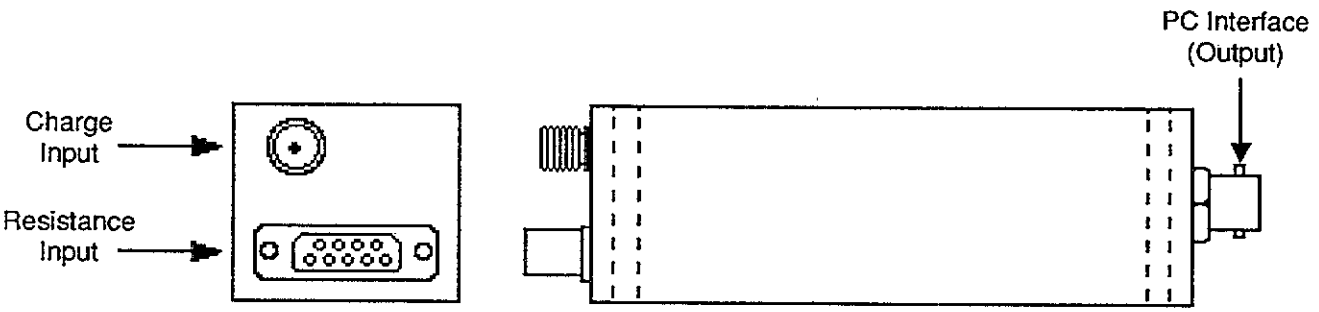

FIGURE 1. HYBRID MODULE

The module functions are field selectable, either pre-installation or on-line, using a PC containing a control/interface card.

When the module is connected to a PC on-line, test and ID functions can be initiated in addition to real time programming of the signal conditioning.

II. INTERFACE/OPERATION

The interface to the hybrid module is illustrated in Figure 2. The module accepts a charge input from a device that has a sensitivity between 1 and 100 pc/g and a capacitance range of 50 to 1000 pf, and a resistive input with a range of 100 to 5 KΩ operated from a 2ma constant current 12v source. Both devices may be connected simultaneously and selected by program control.

A PC Control Card supplies power, programs the memory, and accepts signal and pulse data by way of a coaxial cable to a distance of 500 ft. The signal and pulse data are available at the output of the Control Card as "signal" and "test" connectors. The module signal and pulse data is multiplexed onto the interface line and is available to be imbedded in the acquisition data ("signal" output) as an ID tag and a record of program settings. The test output is provided for an analyzer or oscilloscope connection to allow independent evaluation of the test pulse train.

The module is programmed at the PC by operator data entry in response to displayed menus. This procedure involves selecting a read or write operation, setting the desired mode (Program, ID, Test), and entering data. The programmed functions are changed and data output initiated by a read operation. Once initiated the test pulse train will be continuously generated until another mode is selected. The programmed selections and data are loaded into non-volatile memory in the module by the write operation. The last entered selections are automatically re-established each time power is applied.

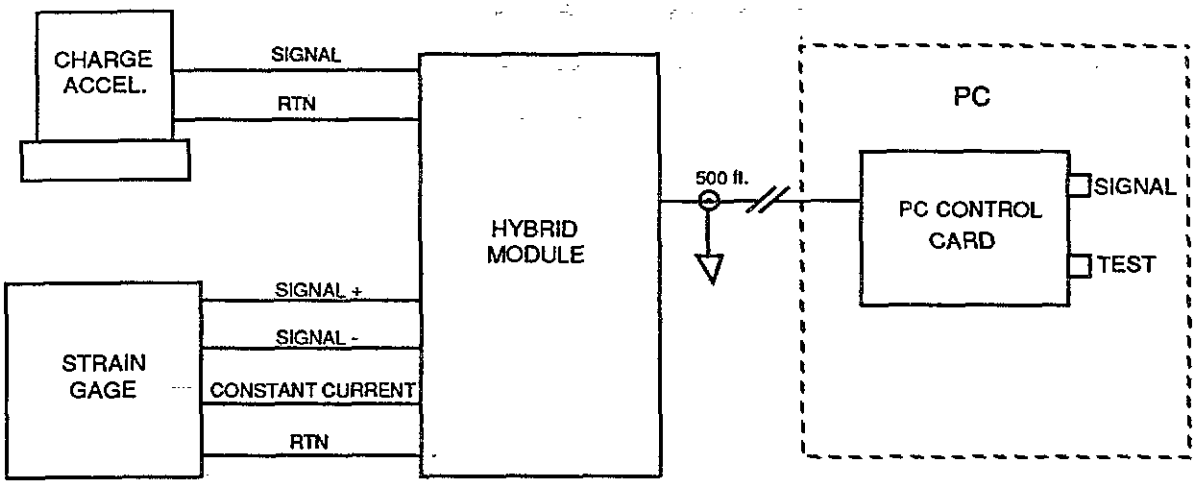

FIGURE 2. HYBRID MODULE INTERFACE

III. PERFORMANCE

In the basic system configuration the PC Control Card passes the module signal directly to the output connector (i.e., with no further signal conditioning). The system characteristics are therefore essentially those of the module given in Table I.

MODULE SIGNAL CHARACTERISTICS		
Linearity		±1% nominal
Noise	x1 Gain:	<20μv
	x100 Gain:	<2.5mv
Phase Shift (band edges) <5° unit to unit (without integration or differentiation)		
Output		
Impedance		50Ω
Bias		18 v (nominal)
Maximum Amplitude		±3v
Frequency (3db)		
Direct charge input		1.6 Hz to 30 KHz
Integrate		2 Hz to 5 KHz
Double integrate		2 Hz to 2 KHz
Differentiate		1 Hz to 2 KHz
Program pulse freq.		10 KHz (max.)
Direct resistive input		0.1 Hz to 10 KHz

TABLE I.

The programmable selections for signal processing, test, and ID are listed below.

A. SIGNAL PROCESSING

The signal processing selections consist of input, filter, and gain modifiers and the path of the input through the processing. The desired combination of these selections is coded into a single 16 bit data word. Sixteen of these data set-up words can be stored in the chip memory.

1. Input
   - Capacitive with charge sensitivity attenuation: x 1, x 0.5, or x 0.25
   - Resistive with resistance multiplier: x 2 or x 200
2. Filter corners (3db)
   - High Pass: 2, 5, 10 Hz (18 db/octave)
   - Low Pass: 0.5, 2.5, 10 KHz (24 db/oct)
3. Gain
   - x1, x10, or , x100

4. Processing path

The processing path from either input (gain applied to all) is:

- Direct from input
- High pass filter only
- Low pass filter only
- High and low Pass filters, and
- Single or double integration of filtered or direct input signal
- Differentiation of filtered or direct input signal

B. Test

The test output consists of a continuous square pulse train at one of 16 frequencies at either of two base frequencies. Pulses can be routed through the sensing element or direct to the output. The base frequency is factory set and the multipliers are programmed by a 16 bit data word. Eight test set-ups can be stored in the chip memory.

C. Identification

The unit ID output is a coded 16 bit data word which is returned directly from memory. The user may program up to eight of these words to indicate location, transducer characteristics, etc.

D. Program Timing

The specific control sequence (and therefore the program execute time) is application dependent. The time to complete a specific program operation can be determined from the following factors.

Read command:	3 msec
Write command:	30 msec
Switch between inputs:	1 sec
PC transfers:	1200 Baud

IV. DATA AND APPLICATION

Figure 3 shows the spectral response of the signal conditioning to a 15 mv 0-10 KHz random spectrum. In Frame A the 10 Hz high pass and 500 Hz low pass filters are selected. Frames B and C illustrate the effect of selecting single and double integration generating the velocity and displacement output. The velocity and displacement output shows the characteristic amplification of the low frequencies and attenuation of the high frequencies due to the integration.

Although the intent of the original development was just to be able to change the signal conditioning remotely and to generate ID and test functions in specific transducers, other possibilities become apparent when programming is available. Some of these are:

- Initialize to Last Set-up on Power Up: Eliminates need for re-programming after shutdown periods and allows transducers to be programmed off line.
- Multiple Set-ups Stored in Chip: Allows signal conditioning or test function to be changed by a single command instead of performing a reprogramming sequence.
- ID & Programmed Selection Returned to Interface: Permits 'tagging' data stream with setup and source code for archiving or for marking changed conditions during a test.

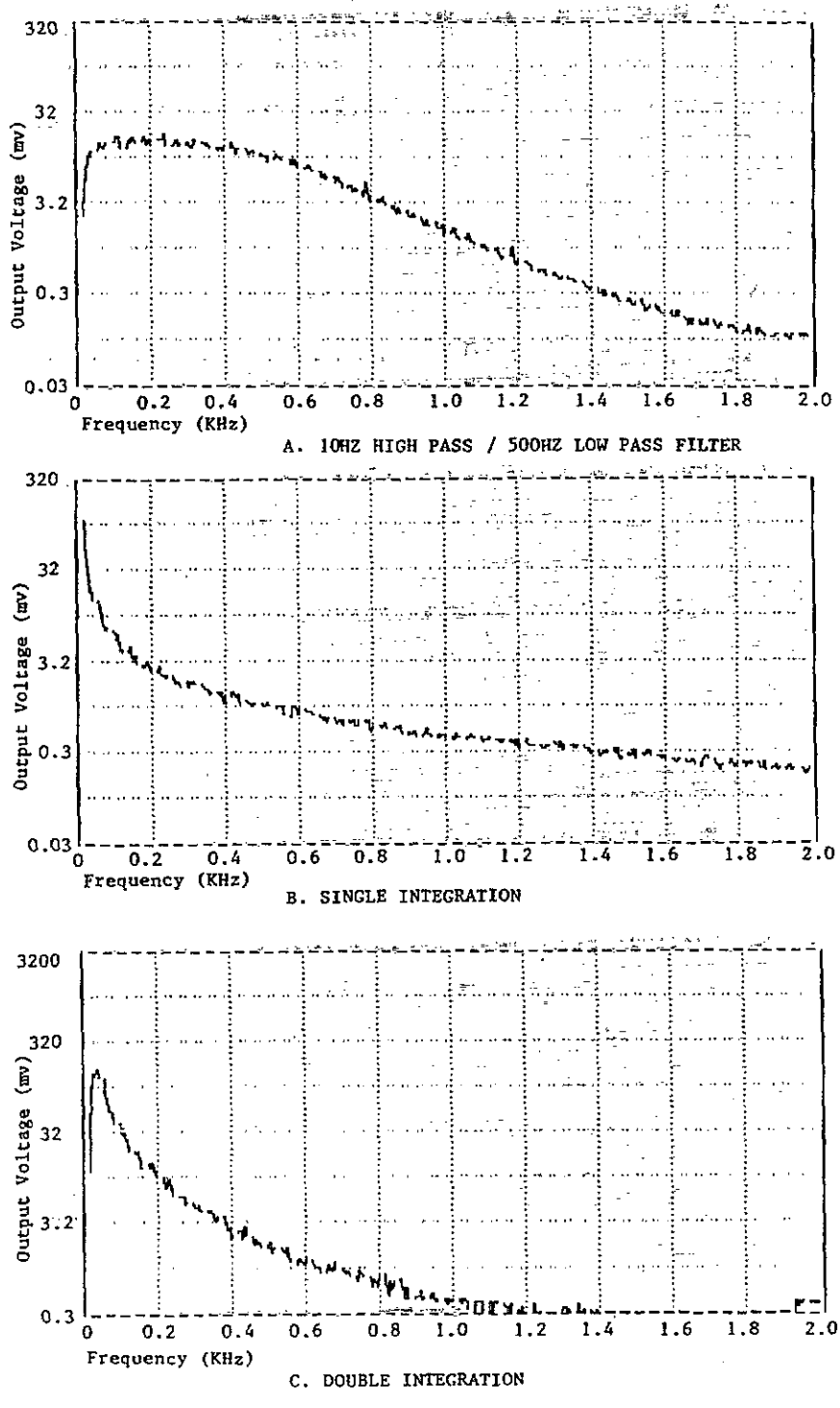

FIGURE 3. Processed response to 15mv random 0-10 KHz (Charge Input)

- Test Frequencies Related to x1000/x1 Oscillator: Allows verification of frequency response over wide range.

- On-Line Input Selection: Allows multiplexing various devices.

- Set-up under Software Control: PC software can program multiple transducers sequentially or as a block.

V. OPTIONAL CONFIGURATIONS

The separate module allows optional input configurations, i.e., (a) the programming capability can be applied in existing installations by connecting a low impedance accelerometer to the multi-pin connector and using the constant current drive, and (b), a temperature probe can be connected to the multi-pin connector to permit sampling temperature during data acquisition. The control and interface functions can also be separated from the PC by using a Control Module[2] communicating through an RS232 bus. The interface can also be adapted to multiplex more channels, to further condition the signal, to A/D convert, to communicate on other busses, and/or provide fault monitoring.

SUMMARY

All the programmable functions and signal conditioning specifications of the Programmable Transducer Microchip have been verified in the hybrid implementation. Although the hybrid module has application as a small signal conditioning unit in existing installations and the hybrid circuit itself could be placed in large transducers, the intended goal of the project will by met when the microchip is produced.

---

[1] Richard Talmadge and Kenneth Appley, "Programmable Transducer Microchip Development", Proceedings, Fifteenth Transducer Workshop, Range Commanders Council, June 1989

[2] Kenneth Appley, "Programmable Transducer Microchip Interface", Proceedings, Sensors Expo West, May 1990

PROGRAMMABLE TRANSDUCER MICROCHIP PERFORMANCE

SPEAKER: Ken Appley, Vibra Metrics, Inc

Q: Roger Noyes (EG&G). How do you calibrate this system?

A: Calibration is left up to the user. Actually, it is not much different except for the signal conditioning than is done for calibration now. We have the capability, and that is why we are going through this hybrid stage. We would like to get some of these hybrids out in the field to find out what really needs to be done before we commit ourselves. We know that the applications are going to be a lot more than we could foresee. That is one of the reasons we tried a little bit by sending the test signal back instead of through the crystal or through the sensing element. You see what test signal is going in there, what your interface, the communication link, is doing, and what noise is present. Then, when you send it through your sensing element you can see the differences. Now, calibration is one thing that we do not know how far we have to go with it and what we really want to do. If you have some inputs, I would be glad to talk to you afterwards.

Q: Bob Sill (ENDEVCO). What do you anticipate the environmental capability of your hybrid package will be, and what do you want it to do?

A: We don't anticipate any problems, because these are going to be plug-in modules into a bread board, and the temperature range is up to 200 when tested.

Q: Norm Rector (Lawrence Livermore). You went about half way to a digital system and all of a sudden you are using a PC to program this module. But yet, you still have an analog signal coming back. Did you ever plan to go to a completely digital system by digitizing in the transducer and sending back a serial strain?

A: That sounds neat but these A/D converters just chew up power. We are still running over two-wire interfaces. My analog designer did quite a bit of work in making things happen. Changing constant current to voltage is quite wasteful, and we don't get too much current out of it. Also, if you put many of these on the line, even 10 to 20 milliamps is a great deal of current when you multiply it by hundreds of units. There are some people who believe that digitizing the analog signal would do more harm than good. I know that it gets digitized before it gets into the computer at some point, but the earlier that you do that, the worse off you might be. I'm just not sure. Putting it into the chip is going to have to wait until we complete this one, and until some real advances are made in lower power electronics.

A Couple Million Points of Light: Television, the Ultimate Transducer

James L. Rieger and Sherri L. Gattis
Naval Weapons Center, China Lake, CA 93555-6001

March 26, 1991

Abstract

Television systems, designed as an experimenter's curiousity and used worldwide for entertainment, have considerable application in instrumentation and can provide large amounts of data suitable for interpretation by a human observer, a computer, or both. While there is no hard requirement for instrumentation television systems to conform, use of the entertainment or computer standards (as appropriate) for instrumentation video increases the variety of available and useful devices and decreases the costs, but the sometimes not-so-obvious differences between entertainment and scientific television requirements must be understood and dealt with. This paper examines some of the opportunities and limitations of using television in instrumentation systems.

1 Introduction

A *transducer* is a device which changes some physical quantity into another, to facilitate measurement of the original quantity in more convenient form. Imaging systems are concerned with the changing of light into electrical signals and/or vice versa, and a television system can be considered to be a multiplexing system sampling several hundred thousand points each 30 times per second or so. Television and still imaging can work in at least four ways, depending on whether the input and outputs are true images, or rather descriptions of something not in image form, as shown in Table ??.

Table 1: Imaging System Possibilities

	INPUT	
OUTPUT↓	Image	Description
Image	Image Processing	Graphics
Description	Image Analysis	Transformation

The *transformation* category includes systems which read printed material and prepare a report from it, by scanning the printed page, converting the characters read to text, and reversing the process after digesting the input's contents, to create, for example, a book report from a book without the bother of having some human read it.

2 Nature of Television

A television system in its most obvious form consists of a pickup on the sending end which converts a scene which it views into electronic signals which are reconverted on the far end to a visual display. As simple as

this appears, the system has all the elements of a telemetry system with two transducers, measuring light at one end and converting the signal back to light at the other.

The system described above has profound implications in instrumentation just as it is, because it allows observance of that which is not conveniently observed from wherever it's happening, but also leads to a number of additional generalizations that make television even more useful. First, the scene that is to be observed may not even exist, being rather a set of data to be arranged in some way to appear meaningful to a human observer on a screen. If the original scene is indeed an image, it may not be due to light, but instead a two-dimensional display of something observed with light of invisible wavelengths, like infrared or X-rays, or reconstructed radar or sonar images. At the receiving end, the "display" may not reconvert the scene created into light, and the "observer" may not be human. The scene may not be reproduced in near-instantaneous fashion, but rather delayed from a recording on film or tape. There may be more than one pickup, more than one channel, and more than one output device. All that's really necessary is that the output and input devices must agree on the format for the interchange of whatever is being sent, and that that format must be within the capability of the channel used between them.

2.1 Television Vs. Film

Television systems have been steadily replacing systems using film, in instrumentation systems as well as in entertainment. Because film is a medium that can be viewed directly, the stability of film images seems more permanent. Film also has greater resolution than does any form of TV, although the spatial frequency response of film does not behave as well as that of TV in either the vertical or horizontal directions. *Pin registration*, that is, the apparent motion of a motionless object on the screen, is not a problem with TV. Changing the width or height of a television image on a picture tube is not a problem; changing picture shape with film involves complex optics. Film can be shot and projected over a wide range of speeds; television signals are much more restricted except in special situations. But perhaps the advantage of TV that outweighs all else is that TV signals don't have to be taken to the drugstore to be developed—they can be viewed as they occur, and can be sent via wires, radio, or fiber optics for viewing somewhere else and can be recorded and played back immediately.

2.2 Serial Transmissions

Any rational television system is *scanned* both in its pickup and display systems,[1] reporting through the channel no more than the brightness of a single point, although some storage may exist at either end. Even if a video display consists of a single picture with no motion, the picture is constantly repeated ("refreshed") at the display end, at a rate of 25 to over 70 times a second, depending on the system.

2.3 Scanning Systems

The actual scanning system used between a pickup and a receiver is entirely arbitary, needing only to do whatever is needed to provide the resolution necessary to provide the desired picture quality. A system thus has resolution limits in six dimensions: vertical, horizontal, temporal, grayscale, and optionally two color dimensions, each of which may have resolution limits of their own. While the number of variations on these parameters is seriously infinite,[2] all television systems have certain aspects in common. For example, the scanning beam universally moves from left to right, and from top to bottom, almost universally with the left-to-right direction at a higher speed than the top-to-bottom speed, like a typewriter would type on a

[1] This is in contrast to a film system, where the input and output pictures are typically formed "all at once".

[2] Such expressions make mathematicians cringe, but are often necessary to indicate infinity raised to some power greater than one.

page. This scanning direction is used even in places like Israel and China, where the written languages are not read in the same directions. The shape of the screen on most systems is 4:3, conforming to the shape of a motion picture frame of the 1930's, which is $\frac{3}{4}''$ tall and $1''$ wide;[3] this shape is constant regardless of the number of "lines" in a picture nor its horizontal resolution. Beyond these similarities, systems worldwide differ in a number of respects.

2.4 Interlace

Entertainment television signals are typically *interlaced*, meaning that one set of lines is traced from the top to the bottom of the screen, ending halfway through the last one at the bottom, and starting again at the top halfway down the horizontal line and ending with a full line in the second vertical sweep. Because the horizontal lines are tilted slightly by the vertical sweep of the beam, the second group of lines fall between the first group, thus providing a picture that flickers far less than it would if the lines were all scanned at half the vertical sweep rate. As a consequence, objects in motion are viewed as they move but with only half the vertical resolution that would be afforded nonmoving objects, which the eye accepts (objects in motion are perceived less clearly), and an object so small that it appears only in one scan and not the other is seen to blink at half the vertical sweep rate. Interlace is the fundamental reason that television and motion picture film are basically incompatible, and any conversion of an interlaced television picture to film will involve significant loss of resolution.

2.5 Vertical Repetition Rate

The vertical sweep rate in the NTSC system used in the US and many other places is 60 Hz or nearly so.[4] European and some Asian systems use 50 Hz, and appear to flicker to anyone accustomed to the 60 Hz standard. Computers use not tightly-controlled frequencies from 50 to 72–73 Hz,[5] generally without interlace (although some high-resolution systems use interlace as well), and are optimized for viewing "up close". While the actual system selected is arbitrary, conversion from one system to another after the fact is seldom simple nor entirely satisfactory.[6] Hence there is a motivation to produce whatever television image is desired at the output by the input device in the first place, rather than trying to convert it later.

3 The NTSC System

Use of the NTSC system, or something close enough to it that many NTSC components will work with it is the best choice for any application that can work within its capabilities and limitations, principally because there's so much NTSC equipment around. The NTSC black-and-white standard dates back to 1941, with the compatible color standard added in 1953.[?] A television set purchased at the New York World's Fair in 1939 would connect to a modern camcorder, displaying the color picture captured on tape in black and white. Capabilities of the NTSC system are shown in Table ??.

While the quality limitations of NTSC seem apparent on a home receiver, the picture quality is actually quite good, allowing $8 \times 10''$ photos to be made from a television image. The major limit with displays is

[3] Wide-screen television formats have no single standard, but 16:9 is perhaps the most common. Some motion picture formats are as wide as 4:1.

[4] Standard color vertical frequency for broadcast is 59.97... Hz.[?]

[5] Motion picture film is projected in such a way that each frame is shown three times, thus creating a flicker rate of 72 per second, even though motion is at 24 frames per second. Computer pictures likewise typically change little from scan to scan.

[6] Motion picture film, for example, is shot at 24 frames per second. For playback in the NTSC system, one frame is scanned twice, the next three times, etc, to make 60 pictures per second. In 50 Hz systems, film is played back at 25 frames per second and scanned twice per frame. Both methods produce motion jitter and blur not present in a "live" picture. Converting from a 50 Hz to a 60 Hz system or vice-versa involves some compromises as well.

Table 2: NTSC Capabilities

Vertical	480 lines[1]
Horizontal	unlimited[2]
Temporal	30 FPS, interlaced
Grayscale	unlimited[3]
Color "I"	171 pixels H, 480 V
Color "Q"	57 pixels H, 480 V

1. System is defined for 525 lines including blanking. Broadcasting uses 483; some industrial systems use 512.

2. Limited to 4.2 MHz (approximately 450 pixels) for broadcasting; 6 MHz bandwidth (possible in closed-circuit systems) produces 640 square pixels.

3. Limited by channel and transducer signal-to-noise ratios [SNRs].

the line structure caused by the scanning and interlace processes, neither of which need be present. High-definition television [HDTV] systems hold out the promise of increasing the spatial resolution of television images by a factor of two or more, but limit the ways in which it can be recorded and transmitted.

Some "nearly NTSC" systems are found in the home and industry. If images are intended to be viewed one picture at a time rather than as the "live" image that created them, for example, looking at a single vertical scan rather than a complete frame reduces vertical resolution but prevents double images on objects which were in motion. Non-interlaced NTSC-type pictures can be produced by reducing the horizontal oscillator rate from 15,750 Hz to 15,720 Hz, thus reducing the number of lines in each vertical scan from $262\frac{1}{2}$, which produces interlacing, to 262.[7] Pictures viewed one at a time don't then bounce when jumping from one picture to the next. Videotape recordings from NTSC sources often have restricted bandwidths that require that the color information be recorded separately (your home VCR is of this type); such recorders reconstruct a NTSC color signal on playback. Newer VHS-S recorders have greater bandwidths and can provide the color information separate from the black-and-white part of the picture (called *luminance*) to provide a non-NTSC picture of greater picture fidelity than could possibly be broadcast on a modified receiver. Another NTSC derivative involves sending the red, green, and blue signals on separate cables, to provide color resolution equal to that of luminance. Many of these nearly-NTSC systems still work together, and when "true NTSC" isn't exactly suitable, some common extension of the standards is worth considering.

4 Pickups

Early television pickup devices were unfocused photocells, viewing the input scene through a rotating slotted disk or sensing light directed at the scene by scanning mirrors. Electronic scanning systems used three types of tubes, the *iconoscope*, the *image orthicon* and the *vidicon*, of which the most common today is the vidicon. However, tubes have largely given way to semiconductor devices, based on the fact that light hitting a semiconductor junction generates current. While a television picture could be created by switching an array of discrete photodiodes arranged in a rectangular grid, more practical methods exist for most uses.

[7] Of these 262 lines, from 240–256 are actually used for picture information, depending on the system.

4.1 Orthicon Tubes

The *image orthicon* or "immy"[8] was the first practical tube for studio use. Its salient characteristic is that it does not integrate the light hitting individual points on the tube, but rather scans what is happening at the instant the scanning beam crosses each individual point. As a consequence, a baseball thrown from pitcher to catcher may be seen only on a few scans, or not at all if it's a fast ball. A square coming toward the camera would be rendered on the display as a truncated pyramid. Objects in motion, however, are distorted by motion but not blurred, and thus object velocity can be measured using the information in a single picture.

4.2 CCDs

Charge-coupled devices are arrays of photodiodes arranged in a grid which permanently fixes their geometry, which is far more linear than that of tubes. Use of a two-dimensional array fixes forever the number of active lines in a picture, and each grid point in the array fills up some percentage of its cell with photosensitive area, making possible the loss of points of light that wind up between cells. Unlike the image orthicon tube (but like the vidicon tube) each cell integrates light between interrogations, and is unloaded with a parallel-in, serial out analog register which can overflow if any of the points in a line exceed a certain brightness, but since diode arrays are capable of a dynamic range exceeding ten bits (or 60 dB), it's possible to do some manipulation of the contrast curves and still present a noise-free picture. Since the photodiode arrays are sensitive to a broad spectrum of light, including infrared, they can be tailored for particular spectral responses by external filters. Color arrays can be created by using three arrays, or by putting color filters on individual dots and stepping the individual colors into registers for individual processing. A third technique uses *two* CCDs, one for the black-and-white image, the other to generate the two color separations.

4.2.1 Line Arrays

Line arrays are a single row of photodiodes, which create a television picture by mechanical motion in the tangent direction, much in the way a slit-camera shutter operates. Film scanners can operate in this way. The number of dots in the horizontal direction is fixed but is generally very large (corresponding to a very small scanning beam), and the number of vertical lines and sweep rate are controlled by external forces. Maps can be created by adjusting the scanning rate to operate proportionally with the rate of the aircraft or satellite containing the scanner, creating properly proportioned pictures at any speed.

4.2.2 Shutters

Since vidicon tubes and CCD arrays integrate the light incident upon them and dump the charge accumulated on each scan,[9] images in motion are blurred. When having an unblurred image is desired, use of a shutter that opens during the vertical blanking interval and shuts sometime before the next blanking interval decreases blur although it decreases the total light reaching the pickup as well. Since many arrays are quite sensitive, shutter opening times of millisecond or shorter duration can be used, possibly coupled to a strobe flash timed to the opening. This technique was first described and prototypes built at NWC,[?] and has found use in home video systems, where shutter dwell is used to regulate the amount of light hitting the pickup, rather than using a mechanical lens iris. Pictures shot with short shutter times when viewed in real time have a movie-like quality to them. Nothing prohibits opening the shutter once per *frame*

[8] After which the "Emmy" award for television is named.

[9] Actually, vidicon tubes don't completely erase images when scanned, but have been improved in this regard over the years.

rather than once per *field*, thus trading temporal resolution for vertical resolution.[10] The sixty-pictures-per second rate is often sufficient for measuring speeds, acceleration, and position if the individual pictures are sharp enough. When it isn't, shutters and changes in scanning rates allow placing more than one picture in the frame.

4.3 Electronic Sources

A picture can be generated entirely from a description of the objects in the scene. If the objects are described as to their shapes, positions, rotations, and colors rather than point-by-point, the resolution of the displayed image can be as good as the descriptors, no matter how many or how few points are available in the display. That means that high-resolution hard copy can be created. Some "real" scenes are amenable to storage as descriptors (or at least the important parts that need to be recovered and interpreted) and some are not. Conversion of a descriptor image to a display image should happen at the display end to keep the channel data requirements minimized.[?] As an example of this, the apparent high-resolution display of a video arcade game is often 128K or less, even though the display may have more than 307K of multicolored points. Sometimes there is a good reason to convert such a display file to an NTSC picture prior to transmission, but it's usually a desparation move.

5 Transmission Channels

While television can be used to look at something larger or smaller than life size with the camera and display in the same room, the major versatility comes from the ability to transmit or record the signal through some medium or channel. As a consequence, all synchronization and picture information are combined into a single signal in most cases. If a single channel is used, either DC coupling or DC restoration is used, and the transmission channel must be reasonably flat in response from the lowest frequency to the highest, typically several MHz.

5.1 Cable

A television image spans a greater range of octaves than does an audio signal. Neglecting the DC term, which can be reconstructed, an NTSC television image with square pixels requires a freqency range from 30 Hz (the frame rate) to 6 MHz, a span of 17.6 octaves; in contrast, an audio signal might require a frequency range of 20–20,000 Hz in the most optimistic estimate, a span of ten octaves. Moreover, phase delay as a nonlinear function of frequency is more apparent in video than in audio. As a consequence of these two factors, use of a constant-impedance system (typically 75Ω, unbalanced)[11] is required. For transmission distances greater than a few hundred feet, placing the video signal on an RF carrier decreases the effects of "tilt" in the cables, which attenuates higher frequencies at a greater rate than lower frequencies. Use of AM transmission, possibly using broadcast standard equipment, allows extending the signal for many miles; use of FM transmission allows television signals to be sent coast-to-coast and is the method used for terrestrial (and satellite) distribution of images in the most robust fashion. Cable TV systems using 36 or more channels of vestigal-sideband carrriers in systems resembling over-the-air commercial broadcasting can operate through tens of miles of cable and hundreds of amplifiers and can provide a signal-to-noise and signal-to-interference ratio of 46 dB or better on all channels. The limitation on intermodulation products

[10] If this is done on something other than a still camera, the display must use two fields from the same frame (shutter opening) to make a useful picture.

[11] Some instrumentation systems use 93Ω unbalanced or 124Ω balanced systems to overcome noise.

is due to slight nonlinearities in the amplifiers, which cover on the order of a decade of frequency range, from 54 to over 400 MHz.

5.2 Radio

The original transmission mode for television was (and remains) vestigal-sideband AM radio. The channel provided for television is 6 MHz wide, and involves rolling off the lower sideband of the signal below 1.5 MHz from the carrier, and an FM soundtrack subcarier is added 4.5 MHz above the picture, limiting the video signal to 4.3 MHz or so, of which a typical TV receiver displays but 3 MHz. Industrial transmissions, not necessarily intended for reception on a standard receiver, can produce NTSC pictures with information present at 10 MHz or higher, producing far higher horizontal resolution than available with commercial television. FM transmission by terrestrial relay or satellite transmission, also using FM techniques, can provide greater bandwidths as well. Properly-operating standard broadcast TV can provide a signal-to-noise ratio in a 4.5 MHz bandwidth of 55 dB or better, allowing a resolution of greater than 256 shades of gray.[12]

5.3 Fiber Optics

Fiber optics are waveguides for light, usually in the infrared range. Fiber optics are narrower in diameter than the copper wires they can replace, and can pass two very wideband signals in opposite directions. The signals sent can be binary PCM, analog, AM or FM carriers; phase coding isn't convenient because of the short wavelengths involved. Hundreds of megabits can be sent twenty or more miles between repeaters. A single fiber can send the output of several cameras and return control for the cameras electronics and aiming.

5.4 Recording

When a television image must be recorded, some compromises are typically necessary because of the wide bandwidth and dynamic range of the television signal itself. In the 1950s, television signals were recorded by pointing a film camera at a television screen, with frame rates of 24 or 30 per second depending upon the use, thus cutting the motion rate of the reproduced picture by at least half. Tape recording of television images involves use of a rotating head so that tape-to-head speed is high enough to allow recording of an FM carrrier containing a band-limited version of the input signal.[13] Typical professional videotape machines are limited to 4 MHz of response or so; typical cassette-type machines are limited to about 2 MHz, greatly decreasing the horizontal resolution of the recorded image. Signal-to-noise ratios from tape recording are typically lower than any other step in the chain. Digital recording techniques have become available to make recordings that are essentially "perfect". Videotape is lower in cost than film in price per minute, and unlike film, tape can be reused.[14] Video systems offer greater recording times than film packages of similar size. Most video recording formats have several audio tracks of greater fidelity and dynamic range than optical sound recording affords, which can be used for IRIG timing and voice annotation.

[12]The number would be higher but for the method used to combine picture and sync information for transmission. The number of gray shades a human eye can distinguish in the best of circumstances is on this order, but far fewer suffice in most real situations and scenes. Incidentally, the maximum contrast range a human can perceive is on the order of 100:1.

[13]In systems with limited bandwidth, the color signal is recorded separately from the black-and-white "luminance" component and reinserted in playback.

[14]Unlike instrumentation tape recorders, videotape recorders have erase heads, often with separate erase heads for audio and video tracks.

5.5 Computer files

Television pictures can be stored as a data file on a computer system. Files can be operated on by computer systems to enhance details, restore blurred images, remove interference, or recompose the scene entirely. Portions of a picture can be blown up for closer scrutiny, and pictures too large to be displayed can be examined piece by piece. While many of these operations can be done in the analog domain (or even with film images), the versatility and convenience of a computer for the task is clear.

6 Displays

The television image is generally intended, at least in part, for observation and interpretation by a human observer. The display may be such that it emits light (such as a typical kinescope display or a projection system), or such that light is reflected, such as an liquid-crystal display. Still photographs and transparencies made from a single picture or parts of a group of pictures can be produced.

6.1 Kinescopes

The most common type of video display is the *kinescope*, which uses an electron beam steered electrically and/or magnetically to light a phosphor[15] on the front of the tube. No more than one point on the tube is addressed at any given time, but the persistence of the phosphor and the viewer's eye create the impression that the entire scanned area of the tube surface is lit simultaneously. While this was sufficient in 1939, as it is today for entertainment television, high-quality "improved definition" television receivers can be made which use memory devices to redraw the lines of the receiver more often than they are actually updated through the channel, making the line structure and the flicker apparent from interlacing disappear entirely. Since these receivers aren't common, a photograph created by the same video source as that which produces the screen display appears to be of higher quality. Kinescopes with built-in lenses and a single-color phosphor can be used to make reasonable projected images, similar to the way in which film is displayed.[16]

6.2 Liquid-Crystal Displays

Since the kinescope is the last tube in a television system, it's no surprise that there are other ways under investigation (and available in stores) which eliminate tubes entirely. Like liquid-crystal displays in a wristwatch, little power is consumed, and the display simply passes or blocks light entering from the back or reflects incident light in front of a black backing. Unlike tubes, the number of pixels is fixed, typically at far fewer than the 480×640 necessary for an NTSC or VGA display, and contrast range is more limited than with tubes as well, although both are improving. Liquid crystal displays can be quite flat, both with regard to display shape and depth behind the display, and consume relatively little power. There are four differences from kinescopes that are worth noting:

- If the input contains more or fewer lines than expected, the display will react in a way that cannot be corrected through size and centering controls as would be the case with a kinescope.
- While the pixels are still addressed in the same scanning mode as with a kinescope, the display changes pixel by pixel or line-by-line, with all data remaining until rescanned. Since interlace is

[15] A "phosphor" may or may not actually contain phosphorus.

[16] Other, more costly projection systems are even more like film systems, using a light source projecting through or reflecting from a medium on which the picture is temporarily drawn. These systems, whether they draw pictures in an oil slick or create them with electronic "light valves", are capable of very large-screen displays of theatrical quality.

typically used, unless all lines are refreshed at each vertical scan, an object im notion will appear more blurry than with a kinescope display.

- Unlike a kinescope, it is generally easier to make a large LCD than a small one.
- As with a CCD pickup, linearity is inherent in the design.

6.3 Active Displays

A display made of a grid of light bulbs can supply an image in any size, bright enough to be viewed in direct sunlight. Displays of this type are used in sports arenas to show closeups, replays, and advertising. Active displays can be made with the resolution of a TV screen, but since 307,000+ light bulbs (921,000 or more for color) would be required, most have substantially lower resolution.

6.4 Hard Copy

The output of a television system can be directed to a hard-copy printer to produce a photograh, transparency, or motion-picture film, either by exposing photosensitive materials to light or by direct electron bombardment of the film. While images made this way may be of lower resolution than film alone, the results, especially when the original image was created in a computer, can be quite effective, as in the movies **Mary Poppins**, **Robocop**, and **The Last Starfighter**, for example.[17] An $8 \times 10''$ photo from an NTSC original has 60 lines per inch in the vertical direction, a structure which is not obvious at normal viewing distances.

6.5 Electronic Interpretation

Since the television signal is electronic in nature, it is often possible to eliminate or at least reduce human involvement from the process of interpreting certain types of images. Determining motion in the scene, for example, is easily done electronically, even if clouds are passing by and changing the illumination level. Displaying a signal on a screen and letting an operator place cursors on two items can allow machine measurement of the distance between them. Counting the number of red cells on a slide containing both red and white cells can be done easily. The electronics in all these cases treats the television signal as a PAM data signal or a still picture as a file.

7 Computer Graphics

Computers often produce an output on a kinescope or other type of video display, to serve as an interface between humans and the workings of the computer. The output produced may be lettering, or graphs and pictures. There is nothing sacred regarding computer displays, and in fact older computers communicated with their users through teletype machines and the like. Like a teletype machine which prints characters on paper and hence has no idea of what it has typed, a truly dumb video terminal cannot read nor retrieve what it is displaying. The practicality of a computer display as we know it today stems from the low cost of memory devices, which allow a signal to be written into a video memory and then scanned repeatedly to make a video display. While early display terminals could display 25 lines of 40, 64, or 80 characters (1000 characters in the last case) in two colors (typically black and green), present VGA (for "video graphics

[17] As an aside, when a purported computer display is part of a movie scene, the display is typically projected from film, because the scanning rate of the computer display will appear to flicker when shot on motion picture film due to a disparity in frame rates.

adapter") terminals can display a field of 640×480 points, each of which can take on as many as 256 shades of gray or assorted colors selected from a pallette of 262,144 or so. While this is indeed a lot of data, and a VGA picture exhibits higher horizontal and temporal resolution than an NTSC picture, a VGA image can only do a fair job of displaying an NTSC image and vice versa. The NTSC signal has far more color grades that can be displayed simultaneously. The VGA picture appears "sharper", although it contains less information ("entropy"). It is also easier for a computer to display a picture loaded into its memory than to change any or all of it; hence pictures made to make motion pictures are drawn at a slower rate than they will be projected.[18]

Capabilities of the VGA system are shown in Table ??.

Table 3: VGA Capabilities

Vertical	480 lines
Horizontal	640 pixels
Temporal	60–72 FPS, not interlaced
Grayscale	16 or 256
Color	shared with grayscale

Extended VGA modes are available with resolutions of 1024×768 pixels, typically with a limit of 16 simultaneous colors, are available for desktop computers. Pictures shot by satellite may have resolutions of 4096×4096 pixels, with 1024 shades each of 24 or more "colors", and must be reproduced as hard copy after manipulation by computer.

8 The Uses and Abuses of Color

Color television, introduced in the US in 1953 is the usual way we see pictures on TV, and color is used extensively in magazines, advertising, newspapers, and presentation artwork. As a consequence, users often imagine that color TV is the natural order of things, and should be used as well in instrumentation systems. NTSC color, which transmits the black and white image, sometimes consisting of a mixture of the three color "separations" that make the image, is sent at full resolution. The color difference signal that separates red from blue is broadcast at a resolution no greater than one-third that allowed for the monochrome image, and the green/purple difference is often more like one-eighth the resolution of the monochrome image in the vertical direction,[19] meaning that color differences are not well resolved. The color resolutions correspond to the color resolution capability of the eye, which was determined by experimentation in the early 1950s. Many tape recording systems exacerbate this problem still further, dealing with the color difference signals as a band-limited, relatively high noise signal.

Reduced color resolution is generally not a problem with entertainment TV, but may cause an incorrect impression when viewed frame by frame or for measurement purposes. Worse, the color information is interleaved with the black-and-white information in the transmitted signal, making certain black-and-white elements of the picture cause little blue and red flickering effects on the displayed picture. A newscaster's tweed jacket can set off a display like this, for example. This can be reduced by reducing the resolution of the image, but this is seldom the correct response in instrumentation video systems. Running the three

[18] The rate at which the screen display is refreshed limits the number of pictures per second that could be displayed in any event, but this is seldom the limiting factor.

[19] Systems such as the French SECAM system also have lower color resolution in the vertical direction, but NTSC provides full color resolution in the vertical.

colors to the monitors on separate coaxial cables provides full bandwidth for color signals, but creates a problem in videotaping or radio transmission.

8.1 Uses of Color

The use of color for instrumentation purposes is often a bad choice, but it is also true that color can provide data that could not be provided or perceived conveniently any other way. The three colors used need not be the same in the pickup as in the display, and there may not be three of them but rather only two. An example is a system which points an infrared camera and a black-and-white camera at the same scene. Properly encoded, the "hot spots" can be seen in red properly located within the black-and-white picture of how the scene looks to a human observer. Images obtained by radar mapping can be compared to visible images in the same way. Satellite photos may use as many as 24 bands, each representing a "color" which can be displayed three at a time to an observer with a color screen.[20] Camouflage can be detected by using different colors for pickup than those used for display, since the color spectra of decoys seldom matches that of the real thing, even though it may look the same to the unaided eye.

9 Picture Compression

For a picture to contain information of a form that can be interpreted by the eye, large amounts of redeundancy must be present. Examining a piece of motion picture film shows that most frames greatly resemble their neighbors.[21] The brightness (and color, if present) of any point in a picture is similar to those around it. Experiments showing that the analog television spectrum consists mainly of harmonics of the horizontal scanning frequency were conducted as early as 1934;[?] experimenters found that by adding teletype signals in the spectral spaces between the picture spectrum, better use of the channel could be made.[22] Moreover, the viewer was not even aware that such carriers had been added in most situations, because the eye integrated the carriers from the picture in time and space domains. Since the picture changes little from one frame to the next, the differences only could be transmitted. The picture could be fragmented into descriptors and only the primitive elements and their locations sent.[23] Clearly, to the extent that redundancy can be exploited, a picture can be compressed and restored with no loss whatsoever. Picture compression algorithms, however, are rarely so clever as the eye, and some degradation (especially of the unimportant "stuff" in the situation) can be tolerated if the main goal is to fit the picture into a channel of restricted characteristics. While compression may do major or minor harm to the picture, the digitization process may also assure that the signal is sufficiently robust that little further harm is done to it in subsequent transmission and recording. In most instrumentation applications, picture "beauty" is of less concern than some aspect of the picture that must be preserved. It is because of the differences in what is considered to be the important aspects of a picture that a system which may work fine for teleconferencing may be completely inappropriate for scientific or entertainment uses. Also, on any compression system that expects certain characteristics on its input picture and receives a picture of a different type will malfunction in a way from gracefully to fatally.

[20] A human cannot distinguish more than three or so colors; any color seen is a combination of those.

[21] The concept of a "cut" does not go back as far as motion picture photography itself. There is no real equivalent to a "cut" in a real scene as viewed by an observer.

[22] This discovery forms the basis of all composite color transmission systems.

[23] This technique works best for scenes created in a computer; most scenes produced by a camera are far too complex to separate into descriptors. The mathematical class of *fractals* hold some promise for descriptors of some types of complex scenes.

10 Conclusions

Television has many uses in instrumentation in addition to supplementing of film for the same purposes. Because the signal can be viewed instantly and because the signal can be manipulated for better human operator interpretation and can be directly interpreted electronically, television serves in ways not possible or practicable with film, if the limitations of television are observed. Finally, television is a cost effective way of doing experiments that could be done in other more complicated ways.

References

[1] LeBow, Leonard L.; Silberberg, George G.; Rieger, James L., and Koiner, Karl W.: **Integrated Range Television System**, NWC Technical Publication TP 5975, November 1977.

[2] Mertz, Pierre, and Gray, Frank: "A Theory of Scanning and its Relation to the Characteristics of the Transmitted Signal in Telephotography and Television", **Bell System Technical Journal**, July 1934, pp 464–515.

[3] National Television System Committee [NTSC]: **Color Television Standards**, McGraw-Hill, New York, 1955.

[4] Venetsanopoulos, Anastasios N.: "Digital Processing and Analysis", from **Signal Processing**, Elsevier Science Publishers B. V., 1987, pp 575–668.

COMMON AIRBORNE INSTRUMENTATION SYSTEM (CAIS)

Raymond J. Faulstich
CAIS Lead Engineer
Range Directorate; RD25
Naval Air Test Center
Patuxent River, Maryland 20670-5304

ABSTRACT

In March, 1991 the Naval Air Test Center awarded a design, development and limited production contract to SCI Technology, Inc. for a Department of Defense (DoD) Common Airborne Instrumentation System (CAIS). This system is being developed to meet the flight test needs of the Air Force, Army and Navy into the 21st century.

The CAIS will be a time-division multiplexed data acquisition system comprised of a standard modular complement of hardware and software. These systems will be used on both existing and future aircraft. CAIS will not be airframe or weapon system dependent nor will its use be restricted to any Test and Evaluation activity. This paper describes the CAIS system as specified and proposed for implementation.

BACKGROUND

Perceiving a universal need, the Office of the Deputy Director, Defense Research and Engineering (Test and Evaluation) initiated the concept of a tri-service Common Airborne Instrumentation System. Early in 1989, the Naval Air Test Center at Patuxent River, Maryland was designated as the DoD lead activity. The direction provided by the Office of the Secretary of Defense (OSD) was to develop an adaptable, reprogrammable, airborne flight test capability which will facilitate commonality of instrumentation among aircraft types and interoperability among test ranges. To that end, requirements and specifications for the CAIS were developed by the services. The procurement process was initiated and ultimately SCI Technology, Inc. of Huntsville, Alabama was selected as the developer of CAIS. The remainder of this paper will describe the CAIS concept, specifications and proposed solution to the OSD directive.

SYSTEM OVERVIEW

The CAIS is a time-division multiplexed digital data acquisition system. It consists of both airborne components/subsystems and a suite of ground based instrumentation support equipment. The airborne system includes all equipment traditionally found between the signal source and the telemetry transmitter or recorder.

The system is a family of modularized building blocks which are interconnected via a distributed serial communications bus (CAIS bus). The architecture is modular and open to allow the system to be user configured and expanded through the addition of data acquisition units (DAU) which

can be either centrally or remotely located throughout the test aircraft. System design is flexible to allow for easy and efficient expansion to accommodate new requirements without the need for redesign of the existing components or architecture. Figure 1 depicts a system level block diagram.

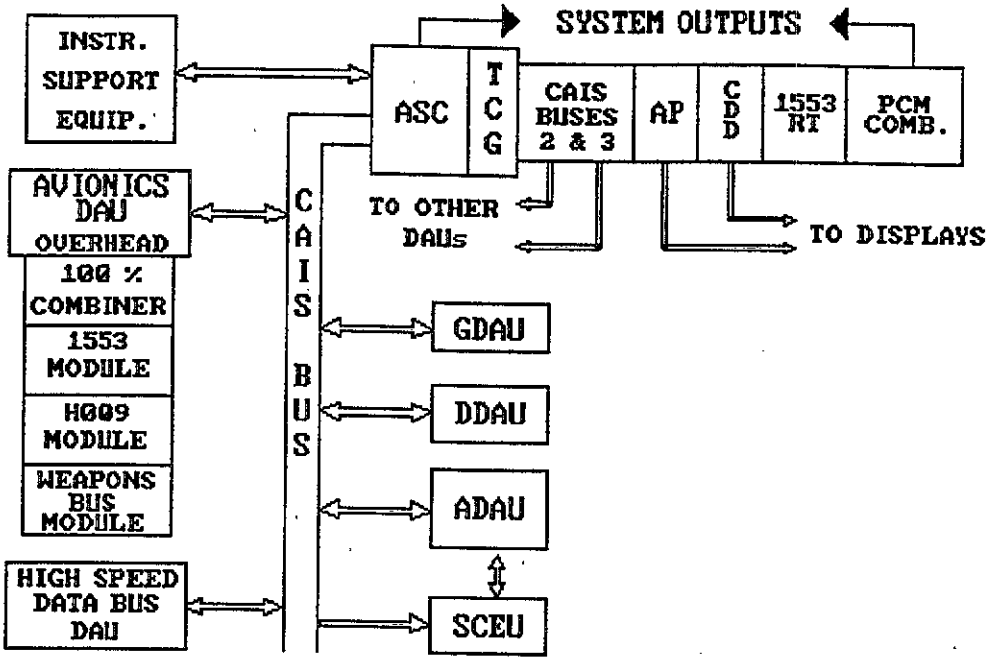

Figure 1. System Block Diagram

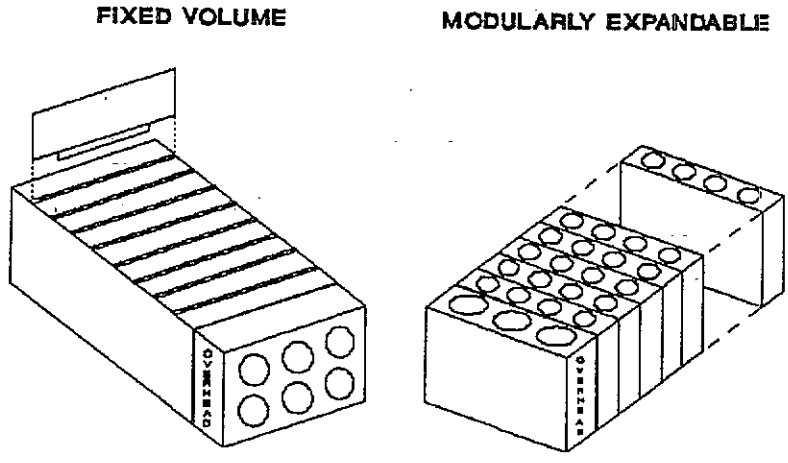

Figure 2. Packaging Concept

The modularized building block concept uses two levels, the line replaceable unit (LRU) which is changeable at the aircraft and the shop replaceable unit (SRU) which are submodules generally changeable in the shop or laboratory. LRU/SRU packaging is accomplished using both the fixed volume and modularly expandable approaches detailed in the specification and shown in figure 2. The open architecture readily permits system expansibility through the definition of common interface points, that is, the CAIS bus interface protocol and the interface definition for the signal conditioners.

System programmability is accomplished through the airborne system controller (ASC) over the CAIS bus to the various LRUs. The user has programmatic control over such parameters as format, channel gain, offset and cutoff frequency all under software control. The adjustment of potentiometers or jumpers on printed circuit cards are not required to configure or maintain the system.

CAIS BUS SYSTEM

The CAIS bus as specified is a serial daisy chain with the capability to operate in a star fashion when using bus splitter devices. The CAIS bus system proposed is identical to that developed for the Air Force Flight Test Instrumentation System and implemented in the Advanced Airborne Test Instrumentation System. The command/response bus carries commands from the ASC to the various data acquisition units and returns the collected data to the controller for formatting and output.

The bus is a 10 Megabit per second full duplex serial bus. Command and response functions are separate from one another. The command bus is designed to transmit continuously, through the use of filler bits, a technique which permits all the remote units to "lock onto" and synchronize with the system controller.

AIRBORNE SYSTEM CONTROLLER

The airborne system controller is the device which ties all the LRU components of the system together and orchestrates their operation. The system output rates are 2 KBPS to 50 MBPS with various user programmable values. The specification takes into consideration that many users may not require output rates exceeding 5 MBPS; therefore, a functionally modular approach was used to allow the user to expand bandwidth incrementally. The proposed system controller, using the modularly expandable packing approach, employs from one to three CAIS bus systems each with a 5 MBPS data capability. The three bus systems and a four input pulse code modulation combiner module extend the output capability to greater than 50 MBPS. Each CAIS bus subsystem is capable of servicing up to 63 data acquisition units. In addition to the CAIS bus modules and the PCM combiner module, an airborne processor, a display subsystem and a MIL-STD-1553B remote terminal are modularly available for user configuration into the ASC. This level of "personalization" makes this approach a technically attractive and affordable (buy only the capability required) solution for large and small users alike.

The MIL-STD-1553B remote terminal module provides the user with the capability to output CAIS acquired or processed data onto an aircraft data bus. The host MIL-STD-1553B system operational software must access the CAIS remote terminal. This feature may be used for such applications as test data display on production devices such as HUDs.

The ASC supports system word lengths from 12 to 16 bits and has a primary serial IRIG PCM output operating at the selected bit rate. Also available are reduced rate dedicated and programmable secondary output serial PCM streams. In addition to the serial data, a parallel output compatible with MIL-STD-2179A and ANSI ID-1 rotary head tape recorders is available.

Integral to the ASC is a high performance IRIG time code generator. This generator may be configured to operate on elapsed time or be externally synchronized through the application of an IRIG B signal.

The PCM combiner module and a 12 input Combiner Expander Module may be attached to a power supply module and used a separate LRU.

DATA ACQUISITION UNITS

Included in the CAIS data acquisition unit family are units to acquire conventional analog and discrete measurement data and units which are used to extract data from aircraft avionics buses. In the first category are the Analog-Discrete DAU or ADAU and the Discrete DAU or DDAU. The avionics systems DAUs include the Global Positioning System DAU or GDAU, the MIL-STD-1553 DAU or 1553DAU, the F15 avionics system DAU or H009DAU, the F16 weapons system DAU or WDAU and a High Speed Data Bus DAU for those newer fiber optic buses found on future aircraft such as the LHX and ATF.

ANALOG-DISCRETE DATA ACQUISITION UNIT

The fixed volume approach to packaging was selected for the ADAU. Included are an overhead section and a user configurable signal conditioning section containing eight card slots. The overhead of the ADAU contains format memory and control circuitry, a 12 bit analog to digital converter, a 32 channel differential input multiplexer for signals which do not require other signal conditioning and the necessary interface and control circuitry to accommodate up to four Signal Conditioning Expansion Units (SCEU). The sampling rate specified was 200K samples per second with a design goal to achieve 500K samples per second. The proposed system details methods which will be studied to achieve sampling rates approaching the goal of 500K. The data paths throughout the ADAU are 16 bits wide to facilitate growth to 16 bit analog to digital converters as they become readily available.

SIGNAL CONDITIONING EXPANSION UNIT

Signal Conditioning Expansion Units are specified to provide more signal conditioning capacity in a smaller volume than a ADAU. This goal is achieved by providing a fixed volume unit which accepts any of the ADAU analog output type signal conditioning cards without the burden of all the ADAU overhead. The analog outputs of the signal conditioners are multiplexed and the resulting PAM signal is routed to the ADAU for conversion and output to the ASC. The SCEU interfaces to the CAIS bus for the purpose of obtaining format and setup information. The unit is sized based on the requirement to house 32 channels of analog data filtering (eight card slots).

DISCRETE DATA ACQUISITION UNIT

Again using the fixed volume approach a DAU to accept only discrete (digital) data is being developed. This unit will have 128 input lines which will be configurable in a variety of ways. The output of the DDAU will be in eight groups of up to 16 bits each as requested by the ASC.

GLOBAL POSITIONING SYSTEM DAU

A data acquisition unit is being developed to interface with the Instrumentation Port (IP) provided by ICD-GPS-215 Global Positioning System tactical receivers. The GDAU will become one of the intelligent terminals connected to the IP for the purpose of commanding the receiver to supply specific data. Data such as time, space position and velocity are available from the GPS. The GDAU outputs are then formatted and sent to the ASC when requested.

AVIONICS DAU

The concept of a configurable avionics DAU permits the user to "build" an avionics bus monitor through the selection of particular bus receiver/interface modules. These modules are connected to an overhead section in a modularly expandable packaging arrangement. An architecture such as this allows mixing of bus types (MIL-STD-1553, H009, F16 Weapons) as necessary within the same unit.

Basically all three avionics bus monitors are designed to acquire both selected data and 100 percent of the bus traffic. Functionally the monitors include bus receivers, message decom memory, data memory, time tagging provisions, 100 percent acquisition and discrete digital interfaces. The message decom memory is used to identify the selected data to be acquired. Data memory is used to temporarily store the selected data prior to retrieval by the ASC. The data memory is configurable as one write/read block or in a double buffered mode where one half is dedicated to storing the incoming data while data is being read from the other half. These buffers then swap functions on command. This technique is used to preclude inadvertent data loss which could occur by writing over a memory location before it is read. The discrete digital input interface provides the user with 16 DDAU type inputs for each DAU slice. The 100 percent output is formatted in accordance with IRIG 106, Chapter 8. The H009DAU and WDAU outputs are formatted in a similar manner to the MIL-STD-1553 as detailed in chapter 8.

SIGNAL CONDITIONING

CAIS signal conditioning is designed on printed circuit cards 4.45 X 2.95 inches. These cards are utilized in the ADAU and the SCEU. A family of 19 different signal conditioners were specified to adequately cover the requirements of aircraft flight testing. To satisfy the requirement 18 different cards were proposed. Each card generally contains multiple identical circuits, with densities from one to eight channels. The conditioners are software programmable through the ADAU. The CAIS signal conditioners and a brief description of each are listed in Table 1.

Signal Conditioner	Feature/Characteristic
Analog Attenuator	Inputs to $\pm$ 175 volts
Analog Data Filter	F_c - 2 Hz to 10 KHz
ARINC 429 Monitor	1 K word storage capability
Auto-Range Conditioner	Gain 1 to 1024, 60 K samples/second
Control Signal Generator	Relay driver and TTL outputs
Digitized Audio Conditioner	CVSD modulation; 16 KBPS to 35 KBPS
Direct Input Expansion Mux	Provide additional ADAU direct inputs
Event Time Recorder	Time correlation to .01 millisecond
Frequency Converter/Pulse Totalizer	Converts 5 Hz to 256 KHz
Instrumentation MIL-STD-1553 Transducer Interface	Bus controller/monitor; 8 messages
Parallel Digital Conditioner	Versatile input configuration
Phase Sensitive Demodulator	20 Hz to 20 KHz excitation frequency
Serial Digital Conditioner	Inputs up to 128 bits
Simultaneous Sample Conditioner	On card 12 bit A/D
Synchro/Resolver Conditioner	15 bit resolution; 360 Hz to 1000 Hz
Thermocouple Signal Conditioner	Types J,K,E,T supported; external ref.
Transducer Excitation Supply	Programmable voltage supply
Variable Resistance Sensor Conditioner	Programmable current source

Table 1. Signal Conditioner Characteristics

STAND ALONE MODE

The CAIS data acquisition units, in addition to operating as remote units controlled by the ASC are capable of operating in a stand alone mode. In this mode, the DAU is able to collect data, convert and format it and generate IRIG PCM outputs. The ADAU is capable of operating stand alone and performing the task of controller for up to 62 other DAUs of any combination. One signal conditioning card slot is used in the ADAU to provide this capability. There are, however, limitations in format size, structure and bit rate. The output rates supported by the various DAU in the stand alone mode are listed here.

ADAU -- 1 MBPS
DDAU -- 1 MBPS
GDAU -- 1 MBPS
Avionics DAU -- 5 MBPS (selected data)
16 MBPS (100% data)
High Speed Data Bus DAU -- 20 MBPS

INSTRUMENTATION SUPPORT EQUIPMENT

The CAIS user will be supported with a complementary suite of ground-based Instrumentation Support Equipment (ISE). These systems range from a multi-user, multi-tasking Laboratory Support System to a dual channel Hand Held Decom. The support equipment systems are shown in Table 2.

Instrumentation Support Equipment	Function
Laboratory Support System (LSS)	Check-out/development system
Instrumentation Support Unit (ISU)	Portable version of LSS
Portable Pre-Flight Unit (PFU)	Hand carry; set-up, decommutate & display
CAIS Bus Decommutator (CBD)	CAIS bus analysis/check-out
Signal Simulators (SS)	Provide test stimuli for DAU
Time Code Head (TCH)	Time Code Generator setup/display
Hand Held Decom (HHD)	Dual channel raw PCM display

Table 2. Instrumentation Support Equipment Systems

LABORATORY SUPPORT SYSTEM

The key features of the LSS include; format generation and loading, airborne processor software development, airborne system configuration verification, quick look decommutation, semiautomatic check-out of the airborne system, exercising initiated BIT and acceptance and fault isolation testing. The LSS employs three computer systems (SUN SPARC station 1+ and two PC compatibles), a telemetry front end and other commercial test equipment to perform these functions. The operating systems used are SUN OS (UNIX) and MS DOS. The operational software is written in Ada with the exception of existing code.

INSTRUMENTATION SUPPORT UNIT

The ISU is intended to support an aircraft installed CAIS system in a flight line environment. It functionally is identical to the LSS except for some fault isolation and the acceptance test capability. The ISU is being developed in a rack-mounted configuration for user installation in vehicles or on towable carts.

PORTABLE PRE-FLIGHT UNIT

An alternative pre-flight tool is required for those times when an ISU is unavailable or impractical. This capability, although reduced from that of the ISU, resides in a one person transportable system based on a Greco Systems ruggedized PC compatible. The PFU operates from aircraft power and performs format generation and loading, decommutation, limit checking, configuration verification and initiated BIT.

SYSTEM DESIGN FEATURES

CAIS is designed in accordance with numerous military standards and specifications, with the objective of building in reliability, maintainability and producibility. Each CAIS item will exhibit a Mean Time Between Failure greater than 1000 hours. The system is designed with Built-in-Test (BIT) provisions. Periodic BIT operates continuously and does not interfere with normal system operation while Initiated BIT interrupts system function but runs more extensive tests. The results of BIT are reported via the PCM stream during flight and directly analyzed by the ISE when initiated during a ground check-out.

CAIS is specified to withstand a wide variety of adverse environmental conditions. Included among the specifications are operating temperature limits of $-55^{o}C$ to $+85^{o}C$, shock, vibration and electromagnetic interference.

SOFTWARE SUPPORT

All new CAIS software is being developed to the guidelines and procedures detailed in DOD-STD-2167A. The high order language used throughout CAIS is Ada. Some exceptions to the Ada requirement occur when qualified Ada compilers do not exist for particular devices or when previously developed code is being reused.

SUMMARY

In response to the OSD directive, CAIS is being developed. The system as specified and proposed will satisfy the majority of the flight test instrumentation needs of the Air Force, Army and Navy well into the next decade. The architecture developed insures CAIS longevity through its openness and flexibility to accommodate future requirements.

REFERENCES

Lamy, Michael F. "Air Force Flight Test Instrumentation System", 1984 International Telemetering Conference (ITC) Proceedings, Volume XX.

Compression Tradeoffs for Instrumentation Video

James L. Rieger, PE/PTBW*

March 27, 1991

Abstract

Compression of a raw data file is often desired to allow it to be stored or transmitted in more compact form. Compression can be lossless, or can cause subtle or sometimes serious distortion in the reconstructed data file. Compression of still and moving images is possible because of redundancies in the three to six types of redundancy that exist in any rational image. For a compression system to be of use in an instrumentation system, any distortions introduced by the process must not interfere with the original intent of the picture, must never cause a rational but wrong display in the reconstructed output, and must be able to withstand or recover from overloads caused by the compression algorithm's local failure. This paper examines some of these tradeoffs, especially with regard to the HORACE data compression protocol described in RCC document RCC/TCG-210 and the future extension of the standard to color.

1 Introduction

The HORACE data transmission protocol[3] was envisioned as a system by which digitized, compressed video for a variety of instrumentation uses could be transmitted through data channels of whatever bandwidth is available. Available channel capacities investigated ranged from 44.732 Mb/s DS-3 microwave links down to a 16 kb/s link using a KY-58 encryptor connected to a UHF aircraft comm link.[2] In any system, the usual starting point is to determine the maximum bit rate available for the link. Options for a given bit rate for any use include user-selected horizontal resolution, grayscale resolution, field or frame rate, and the order in which fallback modes are engaged to prevent overflow. The receiving decoder reads the settings used by the sender and adjusts itself accordingly. If color or 3-D images are transmitted, several other resolution options are available to the user as well. These tradeoffs are not a limitation of the HORACE system alone, but in most video compression systems are not selectable by the user. Also, many commercial teleconferencing systems assume two-way conversations, and are sold only as *transceivers*; most instrumentation uses of television are one-way only.

2 Compression Ratios

The term *compression ratio* is used to indicate how well a compression system decreases the total amount of data sent in comparison to what it would be if no compression were used. For compression ratio to be a real measure of anything, though, it should refer to the compression ratio achieved when completely reversible algorithms are used—in other words, a compressor that achieves a 2:1 compression ratio and restores the original picture, no matter

*Mr. Rieger is a Fellow of the Naval Weapons Center, at China Lake, California, and works for the Telemetry Division, Code 64203.

what the picture contained—in its original form is as useful as a system that compresses the picture by a factor of 100:1 but looks awful or goes crazy if the camera zooms in on the subject. One form of "compression" involves taking fewer than all horizontal lines in the original picture and chopping the ends off lines to reduce the amount of data sent or stored. Depending on whether one wants to specify a large or a small number for the HORACE system, a ratio on the order of 4:1 to 1000:1 can be justified, depending "on whether you're buyin' or sellin'". Because the expression is imprecise, we advise not using it. That a suitable signal can be transmitted in a channel of a given bit rate is the important criterion, not a number whose meaning is suspect.

3 Selecting a Bit Rate

The first decision a user must make is what bit rate to use. The bit rate that is highest is best, if the major concern is to be able to reproduce the original picture in its entertainment-grade beauty. Failing that, the limitations of the channel(s) through which the signal must pass are the governing factor. The HORACE protocol has no inherent operating bit rate, although encoders can be provided with one or more internal clock frequencies. The telephone switching heirarchy, including the integrated switched data network [ISDN] can provide a number of bit rates which while sufficient for voice or high-speed data are quite restrictive for pictures, notably 16 and 64 kB/s. The digital telephone heirarchy, which is also used for microwave and cable distribution at many test ranges, has certain "magic numbers" that can be a basis for selection of rates. In telemetry transmissions, which usually use binary frequency-shift keying (*i.e.*, FM), the bit rate is limited to slightly less than the channel bandwidth allowed, which means about 800 kB/s for a standard channel and no more than about 5 Mb/s in any case. "Magic numbers" are harder to identify, but may be limited by receiver IFs and tape recorder speeds. Use of digital modems with analog channels might limit the user to powers of two times 300 b/s (19.2K, 38.4K, etc.).

4 Picture Elements

A standard NTSC *frame* contains 525 lines, of which about 483 actually display picture information. The rest of the lines are taken up during the retrace period or involve transmission of test signals and perhaps teletype data—all of which look irritating if actually displayed. The HORACE system transmits and displays exactly 480 lines; no compression is used in the vertical direction.[1]

4.1 Interlace

In a standard NTSC TV signal, the scanning beam starts at the top left-hand corner of the screen and paints a line from left to right, tilted down slightly by the vertical sweep, and ending at the middle of the bottom of the screen. The beam starts the next sweep at the middle of the top of the screen, and traces lines in between all the lines generated in the first vertical sweep. Thus the display on the screen consists of about 240 lines in each sweep, a pair of sweeps constituting a *frame*. These individual sweeps are called *fields* or in some instrumentation literature simply (and somewhat confusingly) as *pictures*. The interlace is caused by the odd number of lines in a frame; if the horizontal rate is decreased slightly, interlace can be turned off, making a 60 pictures per second of half the vertical resolution of a frame, which has a repetition rate of 30. When objects in motion are viewed on a picture-by-picture basis, it's frames, not fields, that are examined.[2]

[1] Systems which compress the signal in the vertical direction scan the picture vertically and can reduce the resulting bandwidth by lowpass filtering.

[2] The exception to the above is a system which uses a shutter triggered at the frame rate. Individual frames would then not blur objects which were in motion in the original scene,

Hence the vertical resolution of a *field* is 240 lines, and the vertical resolution of a *frame* is 480 lines.[3]

4.2 Horizontal Resolution

The horizontal resolution of a television picture is more difficult to quantify. With tube-type scanners and displays, the horizontal line is represented by a signal of variable brightness, hence the bandwidth in the horizontal direction limits the resolution, but so too does the size and shape of the scanning beam on both ends. Pickups and displays using solid-state scanners are indeed quantified in the horizontal direction as well, but may be limited still further by system bandwidth. Assuming that the smallest element in the display is a round or square dot whose vertical and horizontal dimensions are identical (which would be optimum as far as the viewer's eye is concerned), and noting that the width to height ratio of the display is 4:3, the optimum number of picture elements (called "pixels") would be 640 for frame images and 320 for field images. Standard interlaced broadcast NTSC television uses a bandwidth restricted to about 4.2 MHz, so the number of horizontal pixels is around 450, a compromise between resolution and bandwidth that takes into account losses in vertical resolution due to moving objects and interlace. Most television receivers are incapable of even the 450 pixel resolution, and images recorded on a home videotape recorder have resolutions on the order of 220–240 pixels per horizontal line. The HORACE protocol allows the user to specify the horizontal resolution as 225, 256, 320, 450, 512, 640, 900, 1024, or 1280 pixels per line, depending upon the characteristics of the picture to be observed. When the HORACE transmit buffer is in danger of overflowing on an especially complex picture, a fallback to half the resolution is allowed on randomly-selected lines. The HORACE decoder senses the number of pixels in a line and adjusts the display automatically.

4.3 Correlation

Doubling the horizontal resolution in a system such as HORACE does not double the bit rate necessary for transmission, because pixels taken closer together have a higher corellation with each other than those taken further apart. The exact ratio varies with picture content, but using test slides with 512 7-bit pixels in a horizontal line changed from pixel to pixel by an average of 1.8 bits using the HORACE scheme while 256-pixel versions of the same images required 2.5–2.7 bits.

4.4 Pixel Stagger

If the major purpose of some instrumentation television system is to measure the distance between to objects or with respect to the horizontal edges of a frame, use of the highest number of pixels in the horizontal line that produces noticeable changes is appropriate. Failing that, the HORACE protocol permits staggering of the pixels in such a way that if the odd-numbered lines of a picture contains 256 pixels, the even-numbered ones contain 255, aligned like a brick wall. The edge or any object more than two lines tall can then be measured with 511-pixel precision, almost double that obtained without stagger. The decoder notes that pixel stagger is engaged and adjusts automatically. Pixel stagger will produce unpleasant results if the horizontal pixel resolution is close to the horizontal resolution of a mosaic pickup.

but the motion rate is cut in half.

[3]On displays made of rows of lights (such as those found in a baseball area) or liquid-crystal displays, the horizontal lines are not tilted downward on their trace across the screen. The reproduced picture on displays such as these is rotated counterclockwise slightly, and would leave a half-line at the top and bottom of the display. Consequently, these lines are not reproduced, so a display panel can have a maximum of 482 lines in the vertical trace, usually limited instead to 480 to make square elements possible.

5 HORACE Overhead

The HORACE encoding removes the synchronization intervals from the analog version of the picture, to allow sending of the actual picture portion of the signal at a lower rate. To allow the decoder to attain and lock synchronization to the source, some overhead is necessary. The overhead is in the nature of the header transmitted at the beginning of each picture line, which consists of a 12-bit code (000000000001), followed by a 10-bit code which identifies the resolution for the line to follow and the line's position in the vertical scan, followed in the most compact case by a single zero. Hence the overhead for each line is 23 bits, no matter what horizontal resolution is selected. If a 320-pixel line is used, and assuming two bits per pixel is necessary to transmit the resulting grayscale, overhead is $\frac{23}{320 \cdot 2 + 23} = 3.47\%$, far lower than the 20% figure for analog television. At higher resolutions, the overhead is lower. A "vertical data channel" can provide about 100 bits of data per picture, enough to specify the camera mount position, for example, with no change in overhead.[4]

6 Grayscale Resolution

The resolution of a black-and-white television image is such that eight-bit quantization of the image is indistinguishable from an analog original; some say that seven bits is enough, but since eight-bit words are common, the eight bits are used anyway. The analog television signal occupies an arbitrary 141-point scale which has the synchronization information between –40 and zero and video information between +10 and 100. As a consequence, the video signal occupies $\frac{90}{140} \times 256 = 165$ possible levels, which is slightly more than 7 bits of actual brightness resolution. The bit rate necessary for a black-and-white picture of 4.2 MHz bandwidth which is indistinguishable from the analog original is thus about 67.2 Mbits/second.[5] Compression in the HORACE system comes from bracketing the changes in gray level, transmitting a signal to tell the output to stay the same, or to brighten or darken a little or a lot, based on previous history from the last two pixels. Since "stay the same" is more likely than "change a bunch", the codes for the likelier condition are shorter. Hence a 7-bit brightness image is coded into a figure on the order of 1.5–3 bits per pixel in almost all cases.[6] The coding levels used for HORACE are discussed in references [1] and [3].

7 Temporal Resolution

While 30 frames or 60 fields per second are needed for measurement of objects in motion if the motion itself is to be measured, many subjects and uses lend themselves to transmission at a lower rate. Even if the picture replacement rate is reduced to a picture every few seconds, the display continually paints the screen to eliminate flicker—that's why movies, shot at 24 frames per second are projected through a shutter operating at 72 (or higher) pulses per second. A television system operating on every other field will have a motion rate of 30—still higher than film—but take about half the bandwidth of the "full motion" version, and in many cases will be indistinguishable from the full motion case. The HORACE protocol allows transmitting as few as one picture in 16, creating a field rate of slightly greater than 4 pictures per second, sufficient for many uses. A second mode allows transmitting of a picture at random intervals, whenever the channel can hold one, replacing the old displayed picture with the next when it has been re-

[4]Several thousand bits per picture can be added between video lines if required, although this raises the overhead.

[5]Because of the ephemeral nature of this type of calculation, numbers quoted can be higher or lower than this. Color NTSC images are often quoted as containing 112 Mb/s of raw data.

[6]The worst picture to encode is one in which there are no redundancies to exploit. Blank channel noise on a TV receiver is of this type.

ceived completely. The difference between the fixed and variable modes is that no resolution reduction is ever triggered by variable-skip mode, so all pictures sent are of full resolution. Variable-skip mode can be used down to bit rates as low as 300 b/s or so, but resemble a slide show. At 56 kb/s, a 256-pixel image can be sent every 3–4 seconds or so, suitable for teleconferencing or mapmaking.

8 Inappropriate Uses

The HORACE protocol is quite versatile, but because of the assumptions made by the system to effect compression, some uses are inappropriate and actually result in a data rate greater than that which can be attained by other means. While the HORACE system will always do something in these cases, the results may not be as heartwarming as expected.

8.1 Still Images

In systems with no motion, sending more than one picture is redundant. Continuous retransmission of a still picture, rather than display from a file at the receiving end is a waste of spectrum, equipment, and money. A still image can be treated as a *file*, with a definite beginning and end, unlike a continuous picture signal.

8.2 Slowly-moving Images

Slowly-changing pictures, especially when blurred motion is acceptable, can be coded to a much lower bit rate by transmitting picture-to-picture differences rather than redrawing the picture every time.

8.3 Alphanumerics

Even a simple computer screen can display 25 lines of 80 characters, for a total of 1000. Each character is made up of a series of dots, and a 640×200 or so grid describes the contents of the screen. While such a signal takes a 5–6 MHz analog frequency response to transmit, which would be similar to the 60 Mb/s used in an NTSC picture, the screen really contains nothing but 1000 7-bit characters, and even if the entire screen changed 60 times per second (which would make it tough to read), no more than $1000 \times 7 \times 60 = 42$ kb/s would be required to transmit the signal—a difference of more than 1000. In fact, any picture composed of blobs and shapes, as would be generated in a computer (or a video game) is much more compactly expressed by those descriptors than as a television signal.

8.4 Noisy Pictures

Noise and granularity of any input image is regarded as data, and causes sharp edges that shouldn't be present in the first place. The recovered picture is never better than the input picture, which may in fact exacerbate the limitations of the original. Coring and/or lowpass filtering of the picture prior to encoding may help in these situations.

8.5 Color Images

Input images fed by an NTSC color source contain a color subcarrier whose intensity varies with the saturation of individual objects in the picture and whose phase varies with the actual hue. The subcarrier is seen by a black-and-white encoder as fine detail, which can overload the system with undesired artifacts. If a color signal must be used, filtering of the color subcarrier with a 3.58 MHz trap is necessary.

9 Dealing with Color

NWC Code 642A has been tasked with the responsibility of adding a set of color compression standards to the basic HORACE standard now in print. Because the uses of color as an instrumentation tool differ, so too do (or at least should) the options for

adding color. The HORACE color standards are *compatible* in the same sense as the NTSC color system, so that a color signal received by a black-and-white decoder will be displayed in black-and-white, and a black-and-white signal will be displayed in black-and-white by a color decoder.

9.1 NTSC Color Encoding

A standard NTSC picture, with a black-and-white signal ("luminance") bandwidth of 4.2 MHz, uses two subcarriers to transmit the color difference signals. One of these is the red-blue separation component, with about a 1.5 MHz bandwidth, and the other is the green-purple separation, with a bandwidth of about 500 kHz.[7] The NTSC system takes advantage of the lower acuity of the eye to color differences than to brightness differences. The luminance and red-blue components are delayed slightly to make the color blobs wind up where they are supposed to be in the displayed picture. Most videotape systems (super VHS included) restrict the color signals to about 600 kHz bandwidth in any case, because the color signal is recorded in a different way than the luminance signal. These frequency restrictions reduce the horizontal color resolution to one-eighth or less of what the luminance resolution is. An encoding system such as color HORACE[8] presented with an NTSC composite can do no better than these resolutions. On the other hand, full resolution on each of the three primary colors would require three times the bandwidth of a black-and-white signal.

9.2 SECAM Color Encoding

The color system used in France and the USSR uses a restricted bandwidth on the color signals, which are defined slightly differently, but only transmit one color at a time per line, so that the color for a single line uses the color information from the previous line as part of the data, cutting the color resolution by a factor of two on a field basis and a factor of four or a frame basis. While this loss seems extreme, the resolution is no worse in SECAM in the vertical direction than in the horizontal.

9.3 HORACE Color Encoding

The HORACE color coding system allows user-selected color separation transmission modes which transmit one or both color signals on each line and allows the user to select a resolution of 1, 2, 4, or 8 luminance pixels per color pixel. Because the colors of scenes are mainly of low saturation or don't change much over the scene, color transmission requires only about 50% greater bit rates in most situations. Since the color separations represent a difference between the brightness of elements of the picture, the color separation signals can take positive and negative values, but their ranges decrease with luminance in the brightness signal.

9.4 Two-Color Systems

While a standard NTSC transmission system assumes three colors for transmission and reception, transmission of a single color difference, perhaps between blue-green and red-orange (the two colors that look most different to the human eye), or receiving a color signal and decoding the color subcarrier in one axis only can produce a two-color system which looks a great deal like the original scene if the original scene isn't there for comparison. The brain attached to the observer's eyes fills in most of the missing colors, as long as the observer knows what the colors "should" be. That two properly-selected colors could regenerate a good impression of a color scene was discovered by Dr. Land (of the Polaroid Corporation) in the late 1940s. A two-color decoding of the NTSC signal was used for low-priced receivers in Mexico in the 1950s—decoding one color signal only, even

[7] "Super NTSC" from Faroudja Laboratories uses 1.5 MHz bandwidths for both color signals.

[8] A HORACE of a different color?

when used with an unmodified three-color kinescope took several tubes fewer than a three-color decoder, and was less sensitive to certain type of interference reception. Two-color liquid-crystal displays are far simpler to produce than three-color ones, so interest in two-color color exists even today. While using a two-color original doesn't change the statistical properties of an NTSC composite much (and doesn't make much sense on SECAM), the HORACE color system can be locked in a two-color mode resulting in decreasing by half the amount of added color data, allowing the user either to use a lower bit rate, or a higher resolution in the luminance or color channel with the original bit rate.

9.5 Anaglyphics

A three-dimensional picture can be sent by using two colors, often blue-green and red. When viewed on a color display and with the viewer wearing colored glasses, a single three-dimensional view is produced. Such a view may be quite informative in miss-distance measurements and bomb scoring. To be sensible, a view produced in this way must be such that most of the scene appears the same in either view; this point may be the background or the fixed target. Most of the detail that makes the 3-D image is contained in the differences on horizontal edges between the two views,[9] and not in the low-resolution "blobs" that suffice for color, hence the coding for rapid contrast changes is optimally different from that of a color image. While commercial transmissions and videotape recordings using NTSC encoding have been used for this type of 3-D transmission, performance is marginal. Note also that the difference between two views can be a positive or negative number equal to the difference between whitest white and blackest black, hence the separation component has twice the dynamic range of the main picture itself.

[9]Some vertical information may be present in some situations.

10 Available Equipment

The HORACE protocol itself does not describe packaging for encoders and decoders, nor such user-specific requirements as the data format (TTL, AMI, etc.), operating temperature range, power supply voltages, etc., which are often different at the two ends of the link. While the protocol describes many features, the decoder need not have them all and the encoder need have even less. At NWC, we have two specifications for encoders[4] and decoders,[5] which allow many but by no means all of the HORACE features.[10] The encoder specification describes five packaging styles, the first three of which have been built by several manufacturers, including a 19″ rack-mounting version and a 12 cubic inch version suitable for missile applications. Both specifications allow the user to specify the maximum operating bit rate (there is no minimum), input power supply voltages, etc., by exercising options in the ordering data section (§6.2.1). Copies of these specifications can be obtained from the author. Nothing, of course, prohibits a user from creating his own specification or (in a pinch) ordering from a catalog data sheet. Miminum size limit for the encoder using hybrid construction seems to be about 2–3 cubic inches, including the camera.

11 Conclusions

The HORACE television compression protocol, like many over-the-counter medications, is safe and effective when used as directed, and more versatile than any other known system with regard to bit rates and resolutions. Because of its versatility, ground station equipment can be used with a variety of sending equipment, thus reducing the amount of hardware needed to handle various customers and projects. Because it is a published protocol, several manufac-

[10]It can be pointed out that, for example, we communicate with each other using a small subset of the English language.

turers can provide compatible equipment.

References

[1] Rieger, James L., and Gattis, Sherri L.: **HORACE Presentation-Level Protocol Standard for Digital Transmission of Television Images**, NWC Technical Publication TP 7115, China Lake, CA, October 1990.

[2] Gattis, Sherri L., and Hill, J. Ward: **Video Compression Using Digitized Images**, NWC Technical Publication TP 7028, China Lake, CA, April 1990.

[3] Range Commanders' Council, Telecommunications Group: **HORACE Presentation-Level Protocol Standard for Digital Transmission of Television Images**, document number RCC/TCG-210, White Sands Missile Range, NM, 1991.

[4] Naval Weapons Center: "Critical Item Product Function Specification for Encoder, Digital Video", specification number NWC 2421, China Lake, CA, current revision.

[5] Naval Weapons Center: "Critical Item Product Function Specification for Encoder, Digital Video", specification number NWC 2422, China Lake, CA, current revision.

IMAGE-BASED MOTION MEASUREMENT AND MOTION RECONSTRUCTION: APPLICATIONS IN VEHICULAR DYNAMICS

James S. Walton, PhD, President, 4D Video

In the course of normal events, this investigator has undertaken various projects which involve the use of imaging techniques for quantifying vehicular motions. Briefly, photogrammetric principles are being applied to cinematographic and videographic sequences to recover the trajectories of moving objects. Using state-of-the-art instrumentation, displacement data are automatically recovered from standard film and video images and are subsequently manipulated by custom computer software to produce detailed, two and three dimensional, kinematic descriptions of complex events. This is generally achieved with high accuracy and high precision under conditions which would normally prohibit the use of traditional electronic transducers.

A variety of tests have been conducted for all three of the major US automobile manufacturers, and for government test laboratories. Among those tests considered to be particularly challenging are those which have been conducted "on-board" the vehicle at highway speeds. Typical of such tests are those performed to investigate road wheel dynamics, wheel-well envelopes, engine mount vibrations, control arm bushing compressions, and dynamic camber, caster and toe. It can be shown, for example, that it is possible to measure camber, caster and toe to within 0.1 degree at highway speeds.

This paper describes the methods used to acquire such data and perform interactive graphic reconstructions using solid modeling techniques.

IMAGED-BASED MOTION MEASUREMENT AND MOTION RECONSTRUCTION: APPLICATIONS IN VEHICULAR DYNAMICS

SPEAKER: James Walton, 4D Video

Q: John Wilson (Independent Consultant). All of your targets seem to be bright. Can you use a dark target on a white background?

A: It works equally well. It is just a matter of separating one from the other. If you look at the plot of one line, that is, the intensity of one line, it either goes up and then drops down or it drops down and then comes back up again. All we are doing is establishing a reference somewhere within that range. Where the intensity traverses that reference, we take those pixel locations as our raw coordinate data.

Q: How do you compensate for camera motion like the frame on the automobile? I am sure when you're going over bumps the camera must be moving.

A: That is correct. First, tie the cameras down as hard as you can. You put the cameras on a common ground, so they are on a fairly stiff plate. Second, you can put reference targets out on the ground. Then, you get relative motion of everything tied to the ground targets and subtract out motions caused by the cameras. In that way, you can get around camera motion. Quite frankly, although we always provide those reference targets, in 90 percent of the cases they are not needed. In the case of the wheels, we found that we had more fore-aft shimmying than vertical motion, which was our real concern. Being suspended from the vehicle, we were getting more of fore and aft motion, and we were having problems initially bracing it that way.

Q: Roger Noyes (EG&G). You talked about changing camera speed a couple of times. Did you have any trouble with aliasing and if so, how did you handle it?

A: If you have frequencies that are too high, then you do have problems with aliasing. We obviously can't compete with the frequency response of an ENDEVCO transducer, for instance. But, if we are looking at these wheels, and we look at the frequency, we do find our FFTs on our data. Generally, the people we are working with are fairly knowledgeable about the frequency content of their signals. We work with them and try to understand what their limitations are, that is, what they are trying to find out about their data. In the case of the vehicle, everything they were interested in was below 20 Hz. We were well within the bounds of our 60 Hz sampling rate, so we had no problems aliasing there; however, it is obviously a problem. The accelerometer is very good at the very small displacements, high frequency. We

are great for space structures with low frequency, large displacement. So somewhere in the middle, there is an overlap where one method takes over from the other.

Q: Wayne Supak (Catepillar). In the vehicle test engines, do you ever have problems with dust and oil messing up the contrast? Do you have some kind of filter on the lens, and if so is it a problem?

A: No, the only thing that caused significant problems was salt on the road at General Motors Proving Ground. The salt would take large chunks out of the front of the lens. These lenses cost $100 each, so you almost have to look at them as a disposable element. Occasionally, one is lost. We've not had problems with the thresholding end of it, because if you have problems like that, you get more lighting. My lights give me all the intensity I need. We have special lights, arranged in a ring light, that take eight ELH bulbs. We have looked at road wheels of tanks for FMC in bright California sunlight at 120 feet away with no problems at all in bright sunlight. Of course, it is optimum if we can do the work in the evening as we did when examining the wheels. In the evening, we can minimize all of the reflections such as the sunlight and the spurious signals.

Q: On one graph you were showing a resolution better than 0.1 millimeters. Is that the case?

A: Yes. You are getting down to subpixel resolution. I didn't have time to put all of this information up on the accuracy, precision, and resolution of this system. If you talk with biologists--give or take a foot is fine, but, if you talk to engineers, they want bounds on the data. Typically, we are getting 1 part in 2000, one standard deviation rms across the field. What you need to do is just tighten the field. Then, if that is not enough, take multiple cameras and the average results. It sounds crazy, but as long as you can produce a video image when you are finished, everything is fine. You can use infrared cameras as we did on a Navy project looking at the horizon. In situations where standard videos will not come through, you can run through a conversion process that produces an RS-170 signal and then digitize that signal.

Q: What is the cost on a per-camera basis?

A: It is really not a per-camera basis. Many cameras performing 2-D analysis are cheap. Once you start working underwater or in 3-D, then it depends on the complexity of the test. Generally, I have a figure to work with, but it really does vary tremendously from one set of tests to another, depending on the constraints.

THE TOURMALINE GAUGE IN USE FOR MEASUREMENTS OF UNDERWATER EXPLOSION PHENOMENA

R. B. Tussing, R15
Naval Surface Warfare Center
White Oak Lab.
Silver Spring, MD 20903-5000
301-394-1187,1170

ABSTRACT

The measurements of underwater explosion shock wave phenomena present some formidable tasks for an underwater pressure gauge and the peripheral calibration and interfacing instrumentation. The tourmaline gauge has traditionally been the gauge of choice because it is linear and bulk sensitive. The oil booted gauge as fabricated by NAVSWC (Naval Surface Warfare Center) has long been used to gather data and develop the similitude equations that are archived for all the Navy explosives. The tourmaline gauges are piezoelectric and require high input impedances to achieve the input time constants required for measurement of long duration shock waves. This requires that the impedance matching preamplifiers be stable and have low frequency responses, frequently to less than 0.01 Hz. gauge connecting cables experience varying and various temperatures as they are deployed over hot decks down into the ocean through the thermocline. The Q-step method of calibration is used so as to negate the variations in cable capacitance and also allows for termination of the gauge cable such that the high frequency reflections traversing the "transmission line" are minimized with a pseudo-termination, resulting in the desired result of both a high and low frequency response for the measurement system. Some of the gauge and instrumentation problems encountered are discussed covering a variety of typical requirements from the largest to the smallest of charges, free field and against ships and models.

INTRODUCTION

The pressure transducer and instrumentation used for measuring underwater explosion shock wave and bubble phenomena must meet a myriad of stringent and sometimes mutually conflicting requirements. This often leads to a number of compromises that have to be optimized for the particular experiment. The

shock wave and bubble phenomena are shown graphically in Fig. 1. The use of a piezoelectric gauge does dictate certain unique specifications for the input cabling and impedance matching circuitry; and each of these warrants a detailed treatment. Generally, the measurements of underwater explosion pressure phenomena require an order of magnitude better accuracy than do response measurements such as strain, displacement, velocity and acceleration. The comparison of explosive types, characterization of each, and the yield requires about the best precision available. The peak pressure is a function of the cube root of the charge weight, so that when measurements are made for as crude a purpose as determining complete detonation, the measurements must have at least the accuracy required for response measurements (10-20%). To put this in perspective, a 10 percent decrease in peak pressure (to 90%) would indicate that 73 percent of the charge detonated [$(.9)^3 = .729$], while a 20 percent decrease would indicate that only 50 percent detonated. Another way to view this, is that if one were trying to determine if another explosive were 10 percent better, the difference in the pressures would only be about 2 percent, requiring a system capable of resolving this accurately.

THE TOURMALINE GAUGE

The tourmaline gauge has been the gauge of choice for over 40 years because it is piezoelectric, linear, and bulk sensitive. The bulk or hydrostatic sensitivity simplifies the fabrication of the gauge, since no axis need be shielded. Thus, no metal housings or diaphragms with their complexities are required. A waterproof coating on the gauge is required however, and can greatly affect the gauge response and the resulting accuracy. Gauge coating studies done at NAVSWC over 20 years ago revealed that a Tygon boot filled with silicon oil reduced the standard deviation of peak pressure measurements by a marked amount[1]. Another study[2] showed that the transfer function of the oil-booted gauge closely matched the calculated geometric rise response (Fig. 2), increasing the time of the rise by only half again (1.5X)the transit time of the bare gauge. As shown in Fig. 2, the calculated rise is shown as a solid line, while the points measured for the response of an oil-booted gauge facing edge-on to an exponential shockwave are superposed. The "real" gauge includes the effects of the gauge coating. For example, a 1/4" oil-booted gauge has the sensitivity(or gauge constant) of the 1/4" bare crystals or discs, but the transit time of the 3/8" bare discs. No other coatings were found that did not adversely change the shape of the rise or the gauge constant in non-repeatable ways. The response time or transit time of the gauge is affected by the diameter of the gauge, or its high frequency response is directly affected by the element size. The criterion for gauge size is based upon the acceptable error in the peak pressure and the ratio of shockwave time constant θ to the transit time of the gauge t_D or θ/t_D[2]. Most NAVSWC gauges are fabricated with 4 elements or discs paralleled for greater output sensitivity, and ruggedness. Some gauges are fabricated with a single element, as well as some with 8 elements. A line drawing of a NAVSWC oil-booted tourmaline gauge is shown with the elements mounted to a feed-through in Fig. 3. The NAVSWC oil-booted gauge has served as a standard internationally for data comparisons for over 15 years, and has been made available at cost for this purpose.

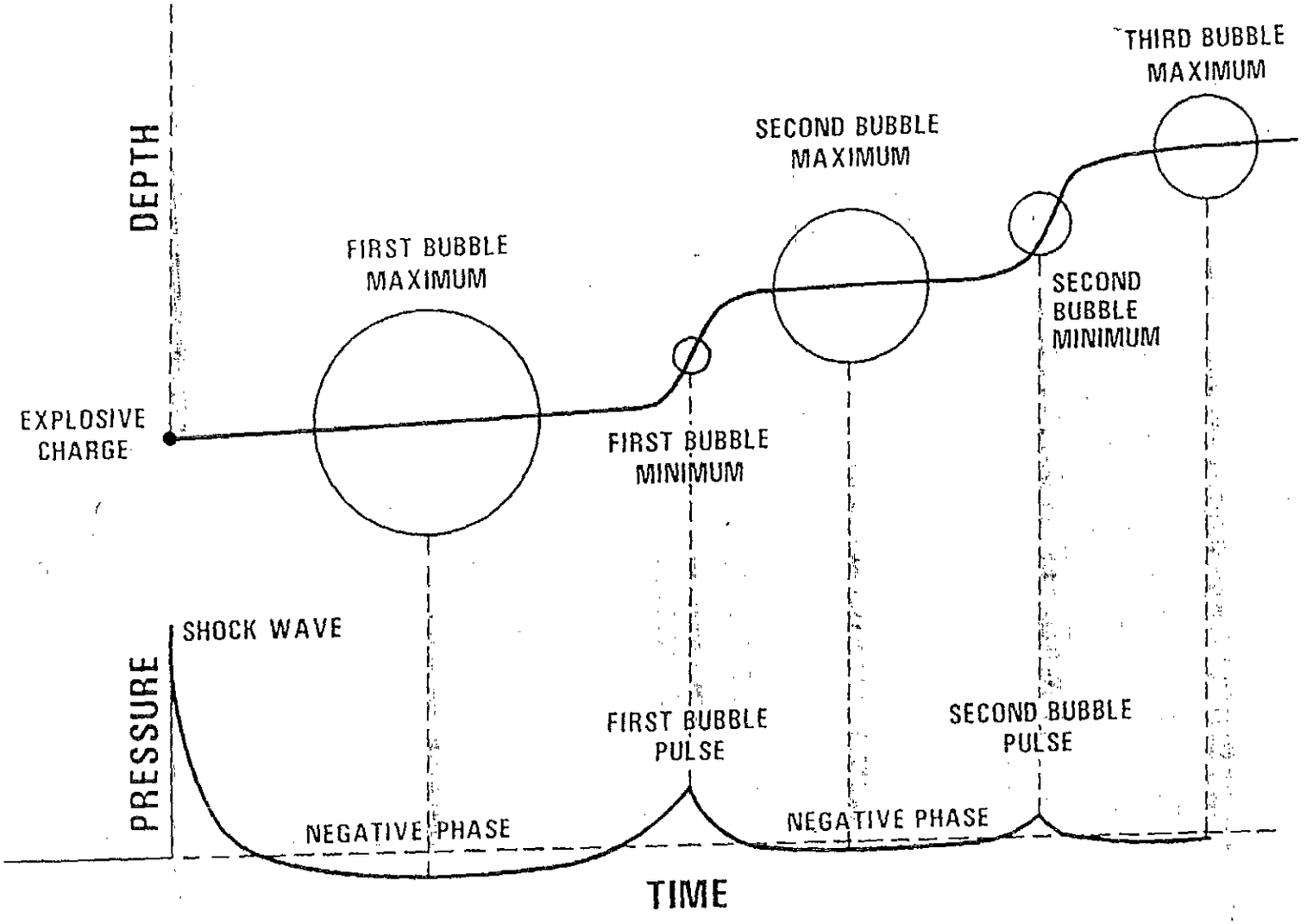

Fig. 1 Explosion Bubble and Pressure-Time History

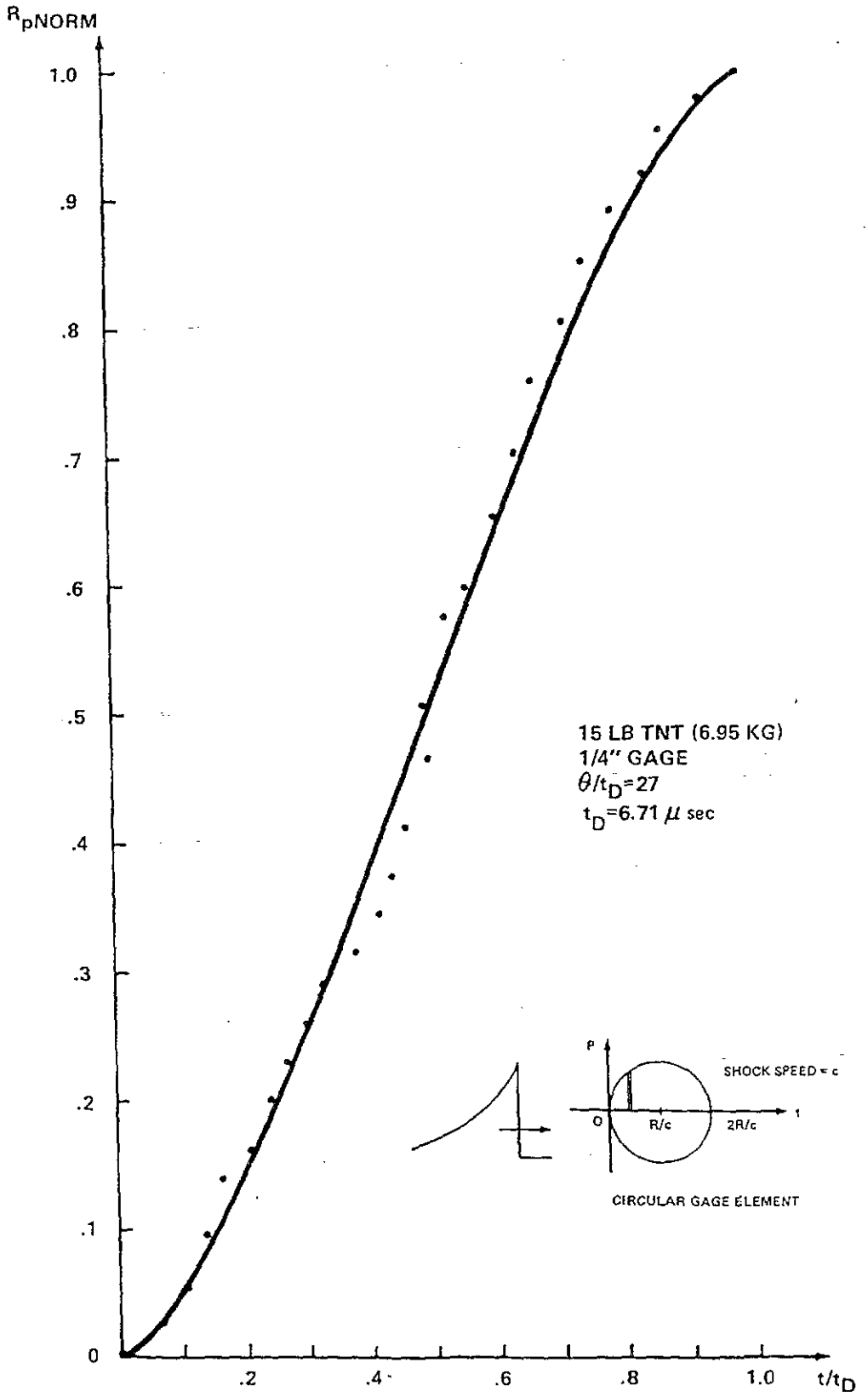

Fig. 2 Actual Vs. Geometric Rise 1/4-Inch Gauge

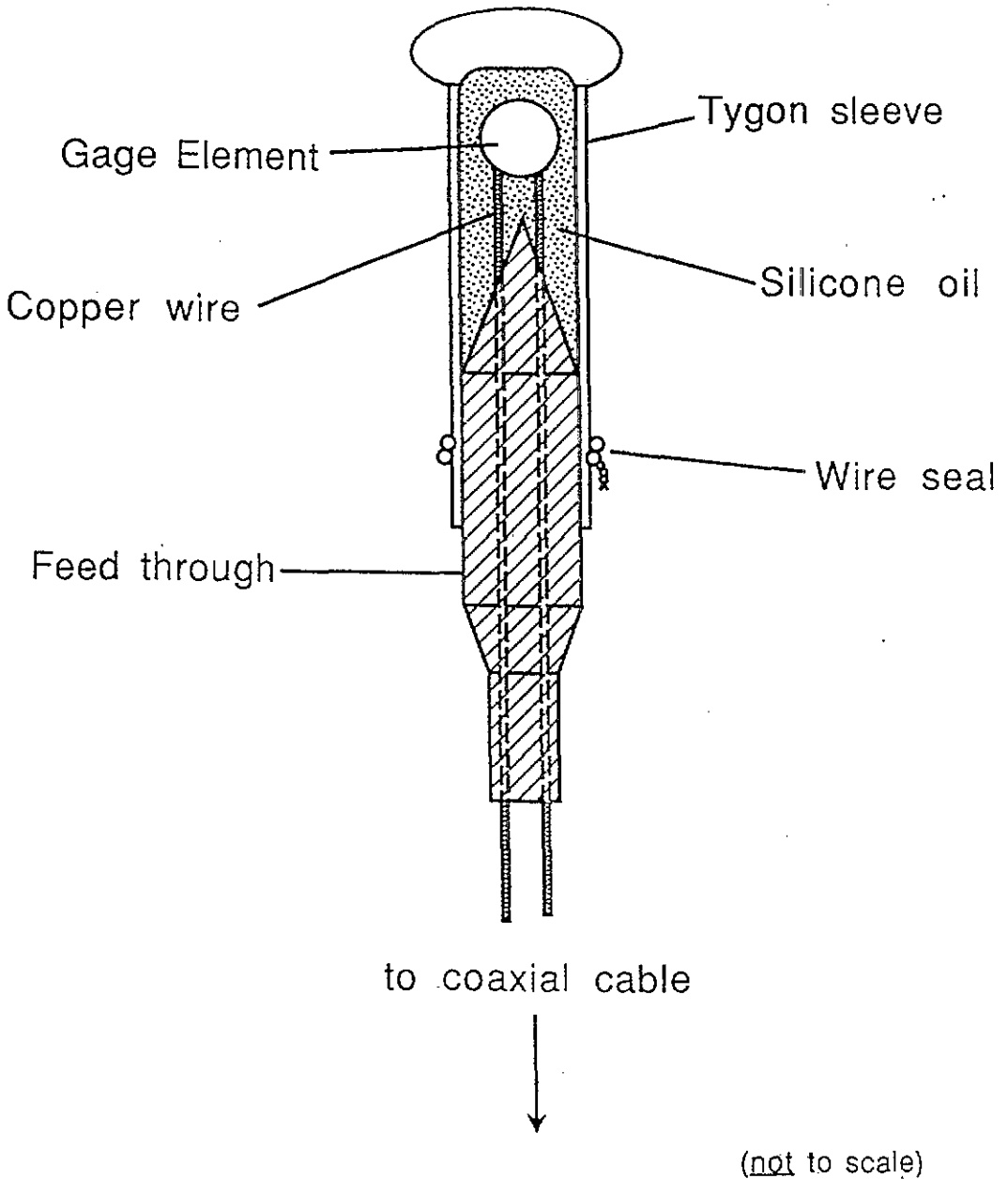

Fig. 3 NAVSWC Tourmaline Gauge Diagram

A tourmaline crystal or disc, cut perpendicular to the optic or z axis, generates a charge on the opposite faces when squeezed or immersed in a pressure field. The charge Q is directly proportional to its material sensitivity constant K and the area of the disc A, thus, the gauge constant is referred to as the "KA". The circuit equivalent for a piezoelectric gauge is shown in Fig. 4, and is simply an ideal voltage source V_g of value Q/C_o in series with its capacitance C_o. The charge Q is proportional to the product of KA and the pressure P, or $Q = KAP$. Thus, the voltage source V_g has the value KAP/C_o.

While the high frequency response of the gauge is dependent upon its size or the transit time of the shock front crossing, the low frequency response of a piezoelectric gauge can be shown to be dependent upon the input time constant of the total system.

INTERFACING THE GAUGE

The piezoelectric or tourmaline gauge must be interfaced or connected to the recording and calibration system through a cable and a preamplifier, each of which must have certain unique characteristics.

The Cable

Most gauges are fabricated to be single ended and must be shielded from electro-magnetic noise by the use of shielded cable. All cables are subject to the triboelectric effect or the electrostatic charges generated by friction when the cable is flexed, struck or hit by a shock wave. "Low noise" (for triboelectric effect) cable is fabricated with a conductive coating between the conductors and their insulation to reduce this effect; graphite was used in the past, conductive rubber or plastic coatings are used currently. Even these cables generate some noise when struck, thus it is important to orient the cables lengthwise to the shock phenomena when at all possible, and to use the largest or highest sensitivity gauge permissible (for an acceptable error in the peak pressure).

Equivalent circuits for coaxial cables range from a simple element to distributed multiple L-filter sections using R,L,C elements. The acceptable equivalent circuit or simulation depends upon the frequencies of interest, the driving source (gauge or preamplifier) and the application. For most underwater explosion studies related to characterizing explosives, damage to models or weapon output, the cables can be treated as a single lumped capacitance (C_c) when used with the tourmaline gauge driving the cable directly. The output of the gauge is effectively capacitance divided down by the cable and input (termination and preamplifier) capacitance. Thus, (from any first circuit's book) the Thevenin equivalent circuit (Fig. 5) for the gauge and cable is simply a voltage source with a value equal to the gage output voltage divided down by the total capacitance, in series with a capacitor equal to the total capacitance. A preamplifier input circuit can be represented by a shunt parallel combination of the input resistance and capacitance. The Thevenin equivalent of this addition places the shunt input capacitance with the total circuit capacitance, dividing down the value of the voltage source as seen in Fig. 6. Thus, the equivalent circuit is simply a

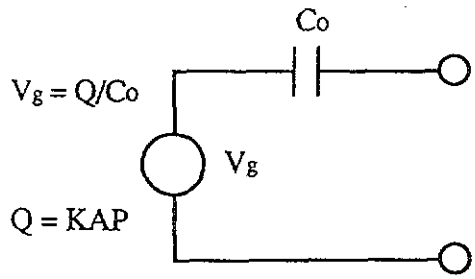

Fig. 4 Equivalent Circuit for Tourmaline Gauge

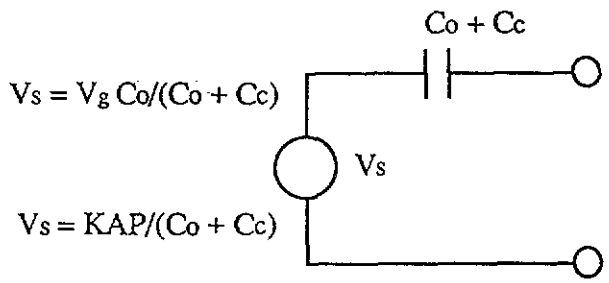

Fig. 5 Thevenin Equivalent For Gauge and Cable

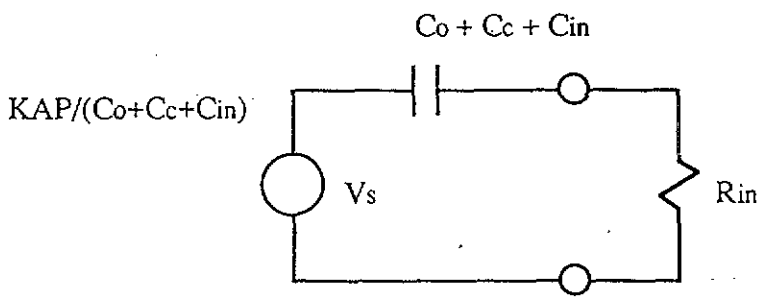

Fig. 6 Thevenin Equivalent for Gauge, Cable and Input Preamplifier

voltage source driving a high pass RC filter with the low frequency cut-off f_L, where $f_L = 1/(2\pi RC)$ for a high pass filter . Another way to view this is to consider that the response to a unit step will decay with the time constant $\tau = 1/(RC)$ or the output is equal to $e^{-t/RC}$ or $e^{-t/\tau}$.

The shock wave is often approximated as an exponential function out to one time constant θ, at which time the shock wave falls off at a slower rate. The equation for the shockwave pressure P(t) is:

$$p(t) = P_m \cdot e^{-t/\theta} \quad (1)$$

where, P_m is the shock wave peak pressure.

The system response to a unit exponential shock wave input ($P_m = 1$) can be shown to be an exponential that decays somewhat faster than the input, and in proportion to the input time constant of the equivalent circuit:

$$V_o(t) = [1/(1 - (\theta/\tau))]\ [e^{-t/\theta} - (\theta/\tau)\ e^{-t/\tau}] \quad (2)$$

The output response is the difference of two exponential terms: the input exponential shock wave minus the unit step response of the input circuit, which is reduced by the ratio of the shock wave time constant θ to the input circuit time constant τ. When this ratio is small, as it should be when $\tau >> \theta$, the output lags the input exponential, or decays slightly faster than the input. The bracketed multiplier in front of the bracketed exponential terms is usually close to, but greater than 1.0. This multiplier serves to adjust the initial output amplitude exactly to the input at time equal to zero.

The bottom line is that the higher the input resistance R_{in}, the more closely the output follows the input. The impulse I of a shock wave is the integral of the pressure-time [p(t)] curve or the area under the curve and the energy flux density E is the integral of the pressure-squared-time [$p^2(t)$] curve multiplied by the reciprocal of the acoustic impedance of water(density ρ times sound velocity c):

$$I = \int p(t)\, dt \quad (3)$$

$$E = (1/\rho c) \int p^2(t)\, dt \quad (4)$$

Generally, accuracies in impulse and energy are adequate when the input time constant is 100 times or more greater than the shock wave decay θ or, $\tau >> \theta$. Curves are shown in Fig. 7 for values of the input time constant τ of 10 to 500 times the shock wave time constant θ. For large charges, the time constant θ is in the milliseconds (msec) range, which means the input time constant should be in seconds (sec). The low frequency cutoff f_L required would then be less than 0.1 Hz, and typically less than 0.01 Hz.

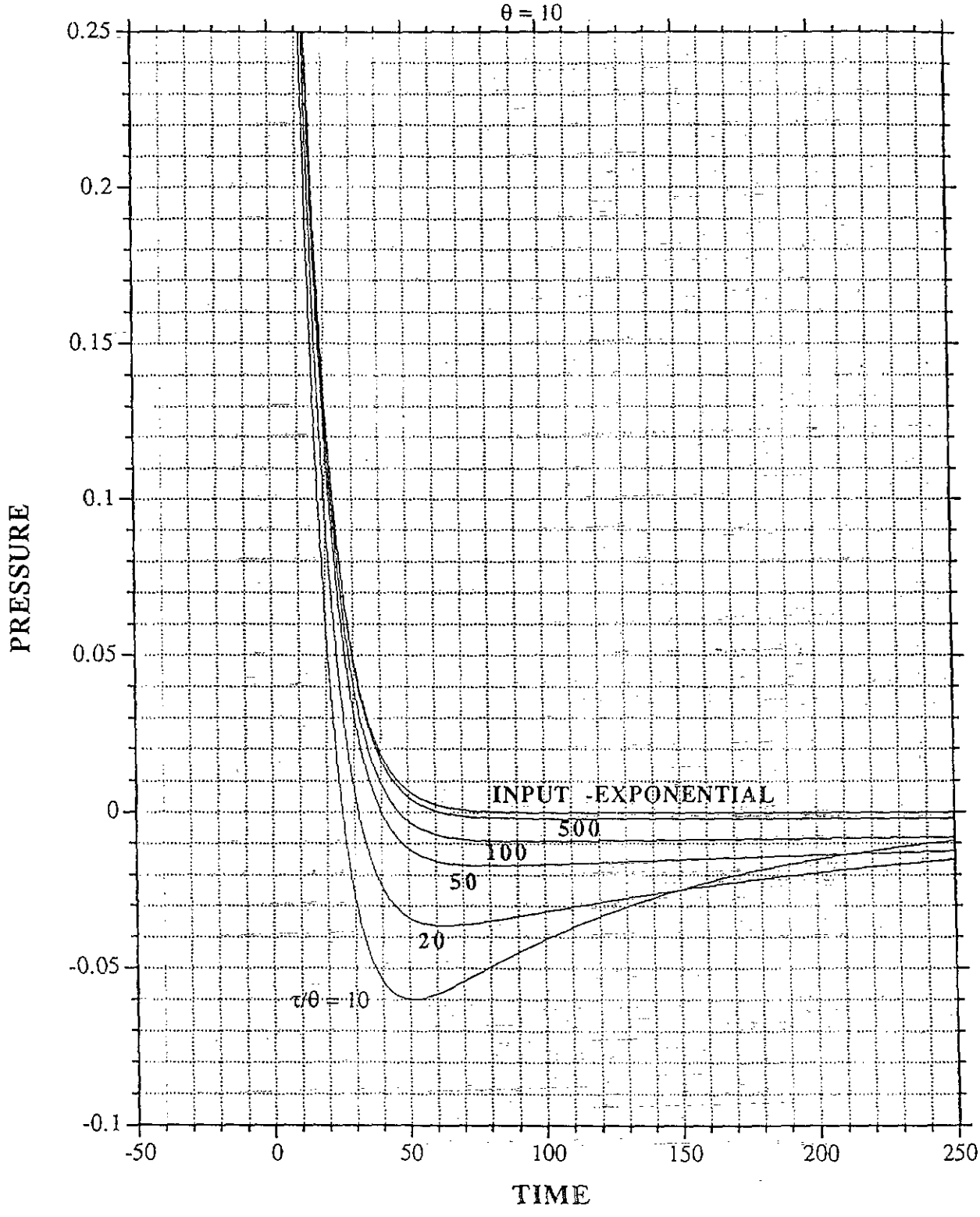

Fig. 7 Output Response To Exponential Shock Wave ($\tau = 10\ \theta$ to $500\ \theta$)

The Dilemma

Transmission line theory tells us that good practice is to terminate both ends of the cable in its characteristic impedance to eliminate the multiple reflections from the ends of the cable; characteristic impedances are usually between 50 and 75 ohms. For studies of the shock wave at or near the peak (the high frequency part of the waveform), where the time scale is expanded, or for short duration shock waves, this is still the best practice. But this would violate the gauge's need to see a high input impedance in the hundreds of megohms to preserve the low frequency response, i.e. the large input time constant. This dilemma could be solved by placing a preamplifier with a high input resistance near the gauge, one that could stand the high shock wave pressures without noise or failing. Frequently, long cables are required by the geometry of the experiment, requiring that the preamplifier be able to drive the long cables with adequate current levels to quickly charge the cable capacitance. Often, preamplifiers that can withstand high shock levels do not have the power to drive the cables and preserve the high frequency response. Though their output resistance is specified to be low, in actuality the preamplifier output usually goes into current limiting, with the characteristic slow linear ramp rise, rather than the expected faster exponential rise. For these cases, another solution to the dilemma is required.

Many years ago, prior to integrated circuits, no preamplifiers could withstand the high shock levels and it was always necessary to drive long cables with the gauge directly. This led to a clever compromise solution attributed to Lampson[3]. The Lampson network was a simple RC circuit at the recording or preamplifier end of the cable (Fig. 8). Lampson also had a less popular double ended network that was not often used, though it did terminate both ends of the cable; the network at the gauge end was usually destroyed by the explosion, or added to the complexity of the waterproofing. The single ended network had to be a non wire-wound variable resistor with very low inductance, called the Surge Resistor (R_S). The shunt capacitance was a high quality temperature stable capacitor that must exhibit very low dielectric absorption, referred to as the Standard Capacitor (C_S). With a square wave driving the gauge end of the cable through a capacitance equivalent to the that of the gauge, the surge resistance was adjusted for the "best" termination ($R_S \approx 1.46\, Z_0$), given the value of the standard capacitance (best found empirically to be twice C_c). The result was that the cable appeared to be terminated in its characteristic impedance for the high frequencies, minimizing the reflections on the cable, while preserving the high input time constant for the lower frequencies. The standard capacitor is a low impedance for high frequencies, making the cable to appear to be terminated in the surge resistance, or the series combination of R_S and C_S. The standard capacitor is a high impedance for low frequencies, making the cable to appear to be coupled into the high input resistance of the preamplifier, preserving the large input time constant that the gauge circuit requires for closely following the shock wave exponential decay. The dilemma is solved as both ends of the frequency spectrum are satisfied by this solution. This is a simplified explanation that is not intended to be rigorous, but it does offer a quick understanding of this proven technique that works well for most shock wave recording applications. This technique is still in general use because it compliments the Q-step calibration technique to be described separately and has several other advantages over the preamplifier near the gauge, which is the only other solution.

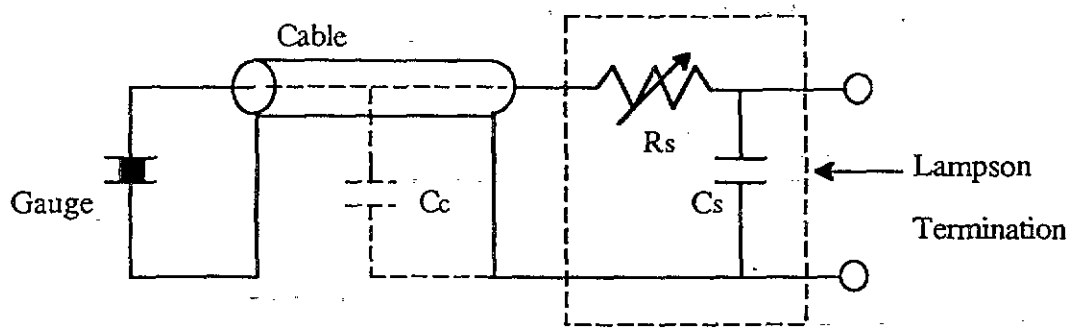

Fig. 8 Gauge And Cable Terminated In Lampson Network

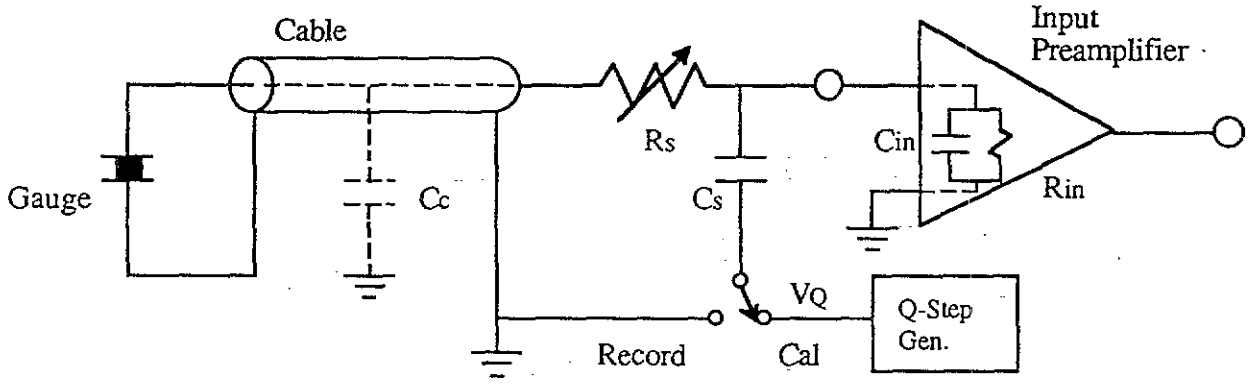

Fig. 9 Input Circuit For Shock Wave Recording and Q-Step Calibration

AMPLITUDE CALIBRATION

There are two generally accepted methods for calibrating the amplitude of a system. One is the Voltage Calibration Method (V-Cal) and the other is the Q-Step Method[4]. A step voltage for both methods was convenient in the past for viewing the system time constant, for oscilloscope displays of both the shock wave and calibration, and for hand analysis of records, but currently, a square wave is more easily handled for automatic computer analyses. With the V-Cal Method the input cables are removed physically or by way of relay switching, and a precision voltage source is attached to the input of the system, calibrating from this point through the recording device (tape or transient recorder). Usually this is done near the recorder and calibrates the preamplifier and the recorder, but does not account for the gauge and cable capacitance. The cable capacitance must be measured under the conditions and at the time of use, to account for temperature variations in capacitance as the cables lay on hot decks, as well as the temperature variations as the cables traverse the temperatures down to the colder gauge measuring depths. The separate measurement of the cable and gauge capacitance can be cumbersome and inconvenient right near the time of the charge detonation and recording. When a preamplifier is used near the gauge, rarely is a calibration done at the front end, because the switching circuitry would also have to withstand the shock phenomena, thus, any variations in capacitance and gain caused by temperature variations must be known to be small, since ignoring these would directly affects the system's accuracy. The second method, the Q-step Calibration, has some definite benefits in both accuracy and expediency of operation.

The Q-Step Method

With gauge cables still attached for recording, a precision voltage source is connected through a capacitor to each of the recording channels. For the case where the gauge directly drives a cable back to the impedance matching preamplifier near the recorder, the bottom end of the Standard Capacitor (C_S) is lifted and the calibration voltage V_Q is injected through this capacitance (Fig. 9). Thus, a charge equivalent to $V_Q C_S$ is injected to calibrate each channel of recording: cable and gauge capacitance, preamplifier and recorder. When this is done right at recording time, the variations in capacitance and gain are automatically taken care of in the calibration. The Thevenin equivalent circuits for the shock recording position and the calibration position are shown in Fig. 10, a and b. The surge resistance is small and can be ignored; the initial rise of the Q-Step is set by the ratio of the surge resistance and the generator's internal resistance plus surge resistance, while the final peak value used for calibration is determined by the ratio of the Standard Capacitance to the total of the gauge C_O, cable C_S, Standard C_S, and preamplifier C_{in}[5]. The calibration charge is adjusted close to that expected by the gauge circuit upon the arrival of the shock wave. Another way to view this is that the voltage caused by the Q-Step at the point of injection is set to match closely the voltage generated by the gauge/cable circuit by the shock wave at the same point. The equation for the voltage V_S at the input to the impedance matching preamplifier caused by the shock wave is:

$$V_S = KAP/(C_O + C_C + C_S + C_{in}) = KAP/C_T \quad (5)_{\text{where,}}$$

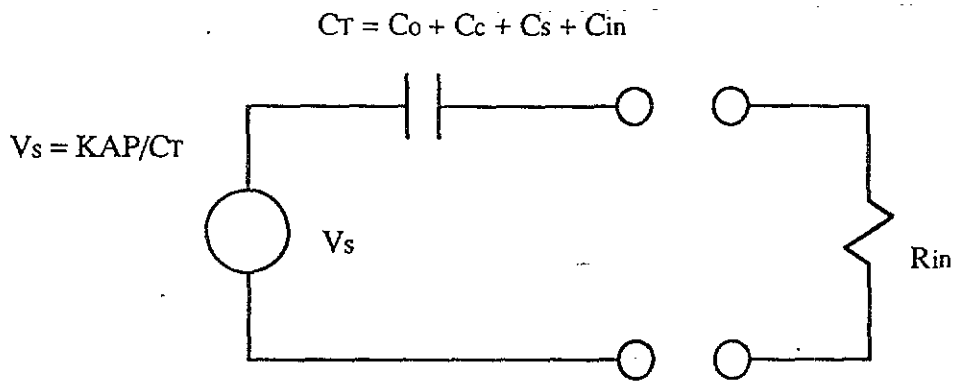

Fig. 10(a) Thevenin Equivalent for Shock Wave Recording

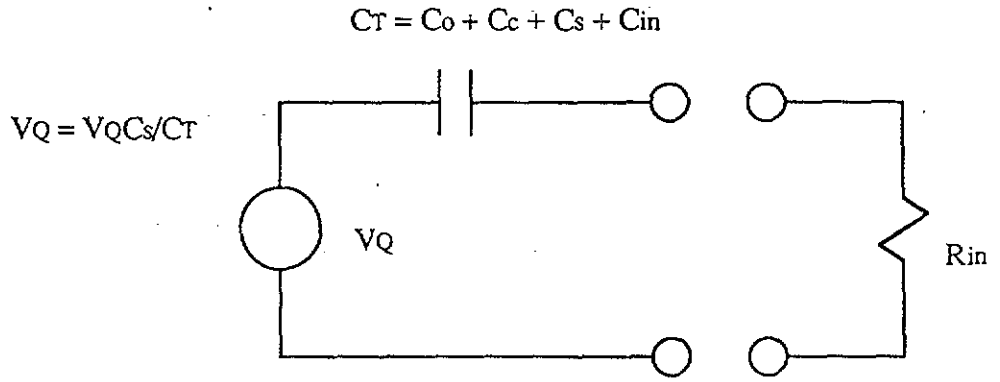

Fig. 10(b) Thevenin Equivalent for Q-Step Calibration

$$C_T = C_o + C_c + C_s + C_{in} \quad (6)$$

and the charge injected is,

$$Q = KAP \quad (7)$$

The equation for the voltage V_c at the input to the impedance matching preamplifier caused by the Q-Step is:

$$V_c = V_Q C_s/(C_o + C_c + C_s) = V_Q C_s/C_T \quad (8)$$

Dividing the shock voltage by the calibration voltage:

$$V_s/V_c = (KAP/C_T)/(V_Q C_s/C_T) \quad (9)$$

Note that the total capacitances (C_T's) cancel out, thus, so do all the variations in the cable and gauge capacitances. This is the real advantage of the Q-Step method! The voltage ratio is really just a unit-less amplitude ratio comparing the "height" of the shock wave to the "height" of the calibration. Note that this ratio is also the ratio of the charge generated by the gauge (KAP) and the calibration charge injected to the circuit ($V_Q C_s$), therefore the name, charge or Q-Step Method.

Now, solving for the pressure P:

$$P = (V_Q C_s/KA)(V_s/V_c) \quad (10)$$

The term ($V_Q C_s/KA$) is the pressure equivalent for the calibration amplitude containing the items that must be measured accurately: the precision calibration voltage source V_Q, the Standard Capacitor C_s and the gauge calibration constant KA. The shock wave amplitude is then scaled by the calibration amplitude after recording, and multiplied by the pressure equivalent to get the pressure P. The Q-Step decays with the rate of the input time constant of the system and can be used as a diagnostic to indicate inadequate impedance matching caused by wet cables or gauges that go low resistance because of pin-holes or bad splices, or other causes such as faulty coupling capacitors or preamplifiers. This is an important trouble-shooting tool prior to recording in the field and an important check for analysts, after the fact.

THE INPUT AMPLIFIER

As mentioned previously, the input impedance matching amplifier or preamplifier, may be placed near the gauge or at the recording end of the cable, both with advantages and disadvantages. The amplifier may be a charge or a voltage amplifier. The charge amplifier appears to the gauge and cable as a large capacitance. The cable and gauge capacitance are swamped and therefore, insignificant. While this lends an apparent simplicity to the setup and calculations, it doesn't "terminate" the cable and the signal-to-noise ratio (S/N) suffers because the loss in signal amplitude is recovered by use of high gains in the preamplifier. In the past, charge amplifiers have also tended to have stability problems. The voltage amplifier with a gain near one has been the preferable amplifier in use. These amplifiers are simple, stable, wideband preamplifiers with good S/N ratios. Early on, cathode followers were used, then came source followers using field effect transistors, and now voltage followers using integrated circuit operational amplifiers. The input impedance has easily been increased with these, using bootstrapping techniques. An important consideration for any preamplifier whose input is connected to the gauge and cable is that the standing voltage on the amplifier's input must be adjusted to be zero d.c., requiring a positive and negative balanced power supply. Any cable with a voltage standing on it and subjected to the shock wave will generate a "noise" signal as the cable is "squeezed" and the cable capacitance changes, simply the effect of $Q = CV$. This signal cannot be decoupled from the gauge signal by analysis later; near the gauge, the signal can appear to increase the impulse and energy of the shock wave, making an explosive look better than it is, leading to erroneous conclusions. The deleterious affects of this noise, depends upon the duration, direction and arrival time of the phenomena of interest, which unfortunately cannot always be predicted beforehand.

The Recording End

The configuration of the preamplifier at the recording end of the gauge cable has been the most used for the Navy's large scale underwater explosions testing. Early on, tube type cathode followers were used and they could not take the shock very close-in. When used, there were even bigger cabling problems: the filaments required low voltage/high currents and the plates, high voltage/low currents. This was certainly formidable for underwater field testing; some amplifiers housed in heavy water-tight containers with heavy multi-conductor cables were still used on some deep ocean tests in the early 1960's. Later, power transistors were tried, but the internal wires would break when shocked. Even today, there are no power preamplifiers in common use close-in, to drive long cables. There are some lower power integrated circuit commercial preamplifiers available that will withstand the shock close-in; these will be discussed in the next section. The historical problems with preamplifiers close-in are not the over-riding reasons for using the preamplifier at the recording end, however. Large scale tests with explosive charges from one pound to several hundred pounds are necessary because the explosive characteristics of, and effects from smaller charges frequently do not scale up. As charges get larger, the safe stand-off distances for the recording stations also increase, increasing the cable lengths required. But fortunately, the gauge sizes and sensitivities can also increase without loss in the required frequency response.

There are several benefits of being able to use the gauge driving a long cable back to the preamplifier and recorder. Certainly, simplicity in waterproofing and field handling of the cables are important to the operations. On tests such as ship/submarine shock and model tests requiring large dynamic ranges, the tourmaline gauge being linear can drive several recording channels in parallel, each with higher gains to overlap as wide a dynamic range as could be required. A gauge driving a preamplifier up close, immediately loses this advantage. The Q-Step Calibration Method can be used with this configuration, with all the advantages of canceling out the temperature variations caused by thermoclines, the varying temperature-depth profiles of the water, and the changes in air temperature throughout the day. This is not only an accuracy advantage but, the method quickens the calibration procedures operationally. This configuration has the added advantage that everything except the gauge and cable are housed in one location in a temperature and humidity controlled environment, thereby stabilizing all the components in the measurements instrumentation. The fabrication of the preamplifiers, as well as the termination units, are simplified because the severe environmental, size and shock constraints are eliminated. The condition of the entire system from the gauge and cable through the recorder can also be monitored and verified at any time. The integrity of the gauges, splices and cables can be frequently monitored easily and directly at the recording station as to their impedance; typically gauges and cables must read greater than 10,000 megohms when "megged", otherwise, the water-tight integrity has been breeched, and can lead to erroneous measurements, particularly in impulse and energy.

The Gauge End

There are a few conditions under which there is a distinct advantage to having the preamplifier near the gauge. These tests usually involve recording low pressure signals of short duration, requiring high frequency response, or tiny single crystal gauges with short transit times, generating very small charges or signals. Under these conditions, even a short piece of cable may capacitively divide the signal down into the noise. These conditions are more often dictated by laboratory tests using small scale models and tiny charges; here the cables can usually be short and are not exposed to the phenomena. Much emphasis has recently been placed upon small scale tests because of the economics. Great caution should be exercised in scaling down, for at least two reasons. Sometimes scaling doesn't hold and poor quality or erroneous data is not better than "no data". The finite gauge size may actually interfere with the phenomena, as well as not be fast enough to render accurate results.

Some have used the preamplifier driving the cable configuration to avoid problems caused by water leaks in splices and pin holes in the cables. The high impedance must be maintained for the gauge-to-preamplifier input circuit to preserve the low frequency response, whether the preamplifier is near the gauge or at the recording end. A low impedance driving the cable would not be affected by an impedance drop into the megohm range caused by water leaks, whereas, the input circuit impedance must typically be maintained to greater than 10,000 megohms. Maintaining the impedances at these levels has been no particular problem even at sea with cable arrays as long as 2000 ft for over 40 years of testing at NAVSWC. Reasonable routine care of cables and splices have avoided losses in data caused by water

leaks. There might be tests where the low impedance drive could prove to be advantageous in avoiding the impedance loss caused by water leaks.

The low impedance drive configuration is not as vulnerable to rf pickup since the high impedance input circuit is shielded by the water. This may not prove to be of great advantage for many tests because under high fields, as with certain radars on ship shock testing, all cables including those for low impedance strain gauges must be shielded on deck anyway. Generally with explosive testing, there is little problem with rf pickup even with high impedance cables because radar and radio transmissions are prohibited while the charge is armed, until after the explosive charge is detonated. Pickup problems of any kind are certainly less of a problem with a low impedance drive, and this configuration may prove particularly advantageous for certain tests or conditions.

Other conditions of advantage might include long duration signals of very low amplitude, where the signal must not be divided down, but the whole input time constant must be high, now made up of the small input capacitance and almost solely of the high input resistance of the preamplifier. There is a limit here though, because very long time constants cannot be achieved by the input resistance of the preamplifier alone (10^{10} ohms), added capacitance is required to further boost the time constant, while at the same time this divides down the signal. An example of a case that would require additional capacitance is the recording of the negative portion of the shock and bubble pulse. Typical shallow water bubble periods run about 0.1 sec, which requires an input time constant greater than 10 sec to faithfully reproduce this long negative phase. The capacitance required would have to be greater than 10,000 pf or 0.01 μf. When capacitance of this magnitude must be added, it might well be better to just drive a long cable with the equivalent capacitance, using a larger gauge. There is seldom a correct solution, more like shades of better ones.

There are many varieties and geometries of tests where the gauge/preamplifier as a unit or gauge and preamplifier close-in can be used. There may be no particular advantage in doing so, other than having them on-hand, available for the tests. An example would be testing of large charges that may not require high frequency response; even though the preamplifiers may go into current limiting while driving long cables, the rise time or frequency response may still be adequate for the requirements. There likely would be some other disadvantages, even with this example, but they would have to be weighed against the purpose of the tests. There is one caution even when current limiting doesn't occur. A piezoelectric gauge appears as in Fig. 4, a voltage source in series with a capacitor driving the cable capacitance. As mentioned earlier, the compromise is a loss in sensitivity and not in the high frequency response or rise time. This is not the case with a piezoresistive gauge or a preamplifier; the equivalent is a voltage source in series with an internal resistance R_o driving the cable capacitance C_c, or a low pass filter. Here the compromise is a loss in high frequency response or rise time, and not the sensitivity. When the power to drive the cable capacitance is inadequate, current limiting occurs and the cable capacitance is charged linearly and thus, more slowly, than with the exponential rise. The caution is that at least the simple

calculation for the low pass equivalent must be made as a check on the limitation of the upper frequency cutoff $f_H = 1/2\pi R_O C_C$. The rise time t_r can then be calculated with the useful relationship $t_r f_H = 0.35$[6].

The use of the close-in preamplifier does lead to a number of marked disadvantages, most of which are just the opposite of the advantages of the preamplifier used at the recording end. Temperature stability of components directly affect the accuracy, such as variations in gain and capacitances; these variations would have to be known for the operating variations, such as in thermoclines. The status of the gauge and cable condition cannot be monitored at the recording end, since this is blocked by the preamplifier. A calibration through the whole system is not possible. The dynamic range of a gauge and preamplifier combination cannot be expanded by paralleling, though the tourmaline is linear over many orders of magnitude of dynamic range, thus, a gauge/preamplifier combination becomes a fixed or limited range transducer because of the S/N range of the preamplifier. The fabrication of the preamplifiers is more complex because of the severe shock and water environment. The waterproofing and splicing of tiny cables connected to small preamplifiers renders them fragile; when coaxial connectors such as microdot or BNC are used, there are center pin contact noise problems after just a short use. Frequently, rugged small preamplifiers do not have the power to maintain their low output resistance to drive the cable capacitance of long cables; the output goes into current limiting with the typical slow ramp rise and thus, they fail to maintain a high frequency response and mask any need for a cable termination. Even though the long cable back to the recording station is driven by a "low impedance", triboelectric effect remains a problem, requiring the same special "low noise" cable when exposed to the shock environment. The preamplifiers that acquire their power by sharing the signal leads back to the recording station render the cable vulnerable to the noise generated by the shock wave hitting the cable and changing its capacitance. And, signal cables sharing the power drive are rarely terminated, even in a "pseudo-termination".

There is one other "popular" and important reason for using a gauge/preamplifier combination; there is one available commercially. Because large pieces of crack-free tourmaline are rare, gauges must be made from tiny pieces and hence, have a low sensitivity requiring a preamplifier at the gauge. The output capacitance of a crystal may well be less than 10 pf, whereas the capacitance of most coaxial cables is at least 30 pf/ft; therefore, it doesn't take much cable to divide the signal down into the noise level. NAVSWC has a great supply of large tourmaline crystals with few cracks; these allow the fabrication of large discs and gauges that can drive long cables without the need for preamplifiers near the gauge. The Navy or NAVSWC oil booted gauge has been the standard for data comparisons, even internationally. Thus, it has been made available at cost. The lack of available large high quality tourmaline crystals for commercial fabrication is currently the most frequent reason for the use of a preamplifier at the gauge.

THE RECORDER

The remainder of a recording system would be comprised of additional amplifiers for gain and a recorder, transient or tape. All a.c. coupling after the input circuit must have time constants that exceed the input

time constant. An earlier example required a 10 sec time constant. If an amplifier's output were a.c. coupled out to an FM tape recorder with 20,000 ohms input, a coupling capacitor greater than 500 μf would be required. If a transient recorder with a one megohm input were used instead, the coupling capacitor would only have to exceed 10 μf. Should two or more channels be paralleled, the coupling capacitor would have to be increased appropriately, double for two, triple for three. The "total system" time constant must be kept in mind. The "direct record" mode of most instrumentation recorders cuts off at about 600 Hz on the low end, thus, the FM record mode must be used with its DC or zero HZ lower end response.

SUMMARY

The tourmaline gauge remains the transducer of choice for the measurements of underwater explosion phenomena. The NAVSWC oil-booted gauge serves as a standard of comparison, even internationally: thus, is made available at cost. For large scale testing, interfacing the gauge with the cable and a high input impedance voltage amplifier can usually best be done with the preamplifier at the recording end of the cable using a termination network named for Lampson. The cable appears to be terminated in its characteristic impedance for the high frequency reflections, while providing the high input time constant required for the low frequency decay of the shock wave. The Lampson termination lends itself well to the Q-Step Calibration Method, which compensates for gauge and cable capacitance variations caused by variations in temperature encountered as the cable traverses hot decks and then, the thermocline of the water environment. The advantages of this configuration are many, though there are a few times when the preamplifier close-in to the gauge has an advantage. The advantages and disadvantages of each configuration were enumerated. The response time or frequency response (both high and low) of the total system must be considered, which includes the gauge, cable, termination, impedance matching preamplifier, amplifiers for gain, and the transient or tape recorder.

REFERENCES

1. Dempsey, J. B. and Price, R. S., "Reduction of Scatter in Underwater Shock Wave Measurements Made with Piezoelectric Gage", NOLTR 72-12, Feb 1972.

2. Tussing, R. B., "Accuracy and Response of Tourmaline Gages for Measurement of Underwater Explosion Phenomena", NOLTR 82-294, JUL 1982.

3. Lampson, C. W., "Cable Compensation For Piezoelectric Gages", NDRC Memorandum A-63M, JAN 1943.

4. Cole, R. H., Underwater Explosions (Princeton University Press, 1948).

5. Tussing, R. B., "Accuracy and Calibration Requirements of Oscilloscope Recording Systems", NOLTR 65-77, Oct 1965.

6. Millman and Taub, Pulse and Digital Circuits (McGraw-Hill Book Co., 1956)

THE TOURMALINE GAUGE IN USE FOR MEASUREMENTS OF UNDERWATER EXPLOSION PHENOMENA

SPEAKER: Ron Tussing, NSWS

Q: Jim Rieger (NAWC-WEPS DIV). What kind of voltages are you actually talking about, millivolts, volts, microvolts?

A: If you mean for recording shock waves, usually millivolts up to volts. A gauge can put out 50-100 volts. Of course, its capacity is divided down then. You try to get in the 0.50 volt range. You can use amplifiers, but try to stay in the millivolt range or higher. You can also use large charges and get away with things even if it goes into current limiting. So, there are many things that you can do with it, but you can't do probably quite as well as putting the preamp in the control environment. If you want your technicians to select gauge sizes, we go with gauge sizes. Then, you have to look at the frequency content and see if your gauge is actually going to be adequate. If you fabricate one size gauge and make it very small, you put a preamp there. Next, you can shunt it with capacitors and change its gain. So that is an advantage, too.

MISSING PAGE

62

SESSION 2

CALIBRATION TECHNIQUES

MISSING PAGE

64

1936 - A BANNER YEAR FOR STRAIN GAGES AND EXPERIMENTAL STRESS ANALYSIS

A HISTORICAL PERSPECTIVE FOR THE UNITED STATES OF AMERICA (*)

by Peter K. Stein, M.Sc., P.E.

Stein Engineering Services, Inc., Phoenix, Arizona, U.S.A.

DEDICATIONS

THIS PAPER IS DEDICATED IN HONOR OF

DR. JULIUS RUDOLF BEER
Institute for Mechanics
Technical University of Vienna

On the Occasion of the Celebration
Of His 65th Birthday

My Long-Time Colleague on Technical Committee TC-15
Measurements in Experimental Mechanics
International Measurement Confederation (IMEKO)

THIS PAPER IS DEDICATED TO THE MEMORY OF

WILLIAM M. MURRAY, Sc.D.

April 24, 1910 - August 14, 1990

It was in Bill's course on Experimental Stress Analysis that I first was introduced to strain gages, brittle coatings and photoelasticity. I was his Graduate Assistant and, later, Instructor from 1950-55. He was my teacher, mentor, supporter and friend. We first met at M.I.T. in Spring 1949.

He was also the founder of the Society for Experimental Stress Analysis, now Society for Experimental Mechanics and was invited by BLH Electronics to attend the early meetings of Western Regional Strain Gage Committee as its Honorary Chairman, to lend distinction and credibility to this unusual group.

Bill came to Massachusetts Institute of Technology in 1932 with his BS degree in Mechanical Engineering from McGill University. He received his MS and ScD degrees from MIT in 1933 and 1936, and remained there until his retirement in 1973 when he was appointed Professor Emeritus of Mechanical Engineering at MIT and then Visiting Professor of Civil Engineering at University of Houston, in Texas.

He was the great educator in Experimental Stress Analysis, offering the first course on photoelasticity, strain gages and brittle coatings in a college/university curriculum, and the first Summer Sessions one-and-two-week courses for practicing engineers, scientists and managers from industry starting in 1953 and continuing for two decades; first at MIT and later at UCLA and in many other locations in the US and in Mexico. S.E.S.A. was run out of his office for over a decade. His professional contributions and honors are legion. S.E.M.'s annual Murray Lecture is awarded in his honor.

To this pioneer and educator in experimental stress analysis I humbly dedicate this paper of a history to which he contributed so much!

Laboratory for Measurement Systems Engineering - Lf/MSE
Stein Engineering Services, Inc., 5602 E. Monte Rosa, Phoenix, AZ 85018, USA February 1991

(*) But also see Appendix 5

1936 - A BANNER YEAR FOR STRAIN GAGES AND EXPERIMENTAL STRESS ANALYSIS

SPRING: E. H. HULL OF GENERAL ELECTRIC CO USES HIS "AQUADAG" A GRAPHITE EMULSION IN WATER, PAINTED ON SURFACES FOR STRAIN MEASUREMENT

APRIL 7: ROY CARLSON'S PATENT "A TELEMETRIC DEVICE" USING UNBONDED WIRE STRAIN GAGES, ISSUES. HE HAS MANUFACTURED THEM FOR SOME YEARS

MAY 20: THE FRANKLIN INSTITUTE AWARDS THE LONGSTRETH MEDAL TO A. V. DE FOREST AND WILLIAM E. HOKE FOR THE INVENTION OF MAGNAFLUX

JUNE: J. HANS MEIER ARRIVES AT M.I.T. WITH HIS DIPL-ING DEGREE FROM SWITZERLAND. HE WILL DEVELOP THE BONDED STRAIN GAGE UNDER PROF ARTHUR C. RUGE WHO IS ALREADY AT M.I.T. AS IS A. V. DE FOREST

JULY: BALDWIN-SOUTHWARK ISSUES BULLETIN 132: "THE McCOLLUM-PETERS TELEMETER INVENTED IN 1923, BASED ON THE UNBONDED CARBON GAGE

EARLY AUG: CHARLES M. KEARNS INVENTS THE BONDED CARBON STRAIN GAGE AT HAMILTON STANDARD PROPELLER. ITS USE SPREADS LIKE WILD FIRE

AUGUST 10: EARLE KENT & LeROY PASLAY FILE FOR A PATENT WHICH CONTAINS THEIR UNWITTING INVENTION OF PRINTED CIRCUITS. THE U.S. PATENT WILL INVALIDATE ALL FUTURE ONES IN THE U.S., ESPECIALLY EISLER'S

SEPT 10: EDWARD E. SIMMONS, JR AT CAL TECH, SUGGESTS BONDING A WIRE TO A BAR TO MAKE A LOAD CELL. THE BONDED RESISTANCE WIRE GAGE IS BORN. IT IS UNRECOGNIZED AS SUCH. LIES DORMANT FOR 2-1/2 YRS

SEPT 16: DR.-ING. PAUL EISLER RECEIVES U.K. PROVISIONAL PATENT FOR THE PRINTED CIRCUIT. HE IS STRUCK BY THE IMMENSITY OF ITS POTENTIAL APPLICATION AND BECOMES THE "FATHER OF THE PRINTED CIRCUIT"

FALL: GREER ELLIS ARRIVES AT M.I.T. HIS MASTER'S THESIS IN A.V. DE FOREST'S LAB IN 1938 RESULTS IN "STRESSCOAT" BRITTLE COATING

FRANK HINES TRANSFERS TO M.I.T. HE WORKS FOR PROF RUGE IN SPRING 1938 AND SPENDS HIS LIFE ON BONDED WIRE TRANSDUCERS. THE TEAM WHICH WILL INVENT & DEVELOP THE BONDED WIRE GAGE IS IN PLACE

DECEMBER WILLIAM M. MURRAY EARNS HIS DOCTORATE AT M.I.T. HE WILL BE THE PRIME EDUCATOR IN EXPERIMENTAL STRESS ANALYSIS & FOUND S.E.M.

1936 - A BANNER YEAR FOR STRAIN GAGES AND EXPERIMENTAL STRESS ANALYSIS

- CARBON STRAIN GAGES
  - UNBONDED
    - McCOLLUM-PETERS TELEMETER
      - BURTON McCOLLUM (1880-1984)
      - ORVILLE S. PETERS (1883-1942)
      - FRANCIS G. "FRANK" TATNALL (1896-1981)
  - BONDED
    - LIQUID
      - AQUADAG
        - EDWIN H. HULL (1902-1964)
    - SOLID
      - CHARLES M. KEARNS, JR. (1915- LIVING IN TUCSON, AZ)

- METALLIC STRAIN GAGES
  - UNBONDED WIRE GAGES
    - ROY W. CARLSON (1900- LIVING IN BERKELEY, CA)
  - BONDED WIRE GAGES
    - CALIFORNIA INSTITUTE OF TECHNOLOGY, PASADENA, CALIFORNIA
      - EDWARD E. SIMMONS, JR. (1911- LIVING IN PASADENA, CA)
      - GOTTFRIED DATWYLER (1906-1976)
      - DONALD S. CLARK (1906-1976)
    - MASSACHUSETTS INSTITUTE OF TECHNOLOGY, CAMBRIDGE, MASSACHUSETTS
      - ARTHUR C. RUGE (1905- LIVING IN LEXINGTON, MA)
      - J. HANS MEIER (1913- LIVING IN VESTAL, NY)
      - FRANK F. HINES (1913- LIVING IN HUDSON, NH)
      - WILLIAM M. MURRAY (1910-1990)
      - ALFRED V. "A.V." DE FOREST & WILFRID L. "BILL" WALSH
        - MAGNAFLUX (1888-1945) & (1893-1967)
        - SCRATCH GAGE
        - ELECTRICAL STRAIN SENSITIVE (ESS) - STRIP
        - BONDED WIRE GAGE (CATALYST)
        - "STRESSCOAT" BRITTLE COATING (CATALYST)
  - PRINTED CIRCUITS - FOIL STRAIN GAGE PRECURSOR
    - EARLE KENT (1910- LIVING IN ELKHART, IN)
    - LeROY PASLAY (1907- LIVING IN MANALPAN, FL)
    - PAUL EISLER (1907- LIVING IN LONDON, ENGLAND)

- BRITTLE COATINGS
  - "STRESSCOAT" (1910- LIVING IN GREER ELLIS (MATTAPOISETT, MA)

- MECHANICAL STRAIN GAGES
  - DE FOREST SCRATCH GAGE
  - HUGGENBERGER EXTENSOMETER

1936 - A BANNER YEAR FOR STRAIN GAGES AND EXPERIMENTAL STRESS ANALYSIS: SUMMARY AND OUTLINE

Spring: E. H. Hull of General Electric Co applies "Aquadag", a graphite emulsion in water, to be painted on surfaces for strain measurement. It has many problems but is used.

April 7: Roy Carlson's patent on a "Telemetric Device" based on unbonded strain-sensitive wires is issued. He has manufactured his transducers for some years. He will receive his ScD from M.I.T. in 1939 together with Prof A. C. Ruge and J. Hans Meier. His office and lab at M.I.T. are next door to Ruge's.

May 20: The Franklin Institute awards the Longstreth Medal to Alfred V. "A.V." de Forest and William E. Hoke for the invention of Magnaflux (RTM). De Forest has already commercialized his Scratch Gage through Baldwin-Southwark and founded Magnaflux. He is destined to be the catalyst for commercializing the bonded resistance wire gage through Baldwin, and "Stresscoat" through his Magnaflux Corporation.

June: J. Hans Meier arrives at M.I.T. with his Dipl.-ing. degree from Switzerland. He obtains his MSc under William M. Murray and becomes Prof. Ruge's Assistant. He develops the bonded resistance strain gage invented by Prof Arthur C. Ruge, April 3, 1938 and writes the first and definitive, still pertinent doctoral dissertation on the new bonded strain gage.

July: Baldwin-Southwark issues Bulletin 132: "McCollum-Peters Electrical Telemeters", 32 pages of operating principle, static and dynamic applications and commercial forms. It was invented at NBS, seen by Francis G. "Frank" Tatnall, commercialized by him and sold through Baldwin-Southwark for whom he travelled extensively. He did the same for many other mechanical strain gages. After initial opposition to the bonded wire gage, he becomes its most enthusiastic supporter and propagandist.

Early August: Charles M. Kearns, Jr., a recently-hired Penn State EE grad invents the bonded carbon strain gage during Hamilton Standard Propeller Co's vacation period. Within 4 years, in-flight propeller failures will go from dozens/year to none. The carbon gage is sold, copied, spreads like wildfire world-wide.

August 10: Earle L. Kent and LeRoy Paslay file for a patent on an "Apparatus for Generation of Musical Tones". In it they describe the manufacture and use of printed circuits. They did not realize what they had invented, but this patent, 20 years later, will invalidate all then-existing printed circuit patents in the U.S., especially Eisler's.

September 10: Edward E. Simmons, Jr., at Cal Tech suggests to Dr. Gottfried Dätwyler that he bond a wire to a bar to make a load cell for measuring forces in an impact machine. The bonded wire resistance strain gage is born but not recognized as such. It lies dormant for 2½ years until Prof Ruge's reinvention at MIT.

September 16: Dr.-ing. Paul Eisler, a Viennese PhD in electrical engineering with extensive experience in lithography and printing, obtains a U.K. Provisional Patent for The Printed Circuit. He is struck by "the immensity of its potential application." He becomes the "Father of the Printed Circuit."

Fall: Greer Ellis arrives at M.I.T. He has his BS in Physics and lands up doing his Master's Thesis in A. V. de Forest's lab where he perfects a nondestructive brittle coating which he calls "Stresscoat" (RTM). His thesis is completed in 1938. Stresscoat is commercialized through "AV"'s Magnaflux Corp and by 1940 is a success. He founds Ellis Assoc, an instrument company, now part of Measurements Group, Inc.

Frank F. Hines transfers to M.I.T. from West Virginia U. The courses he needs in Spring 1938 are not offered; he takes a "temporary" job in Prof. Ruge's lab, helps develop the strain gage Ruge invents and spends his life with bonded resistance transducers. He is now Chairman of the Board of RdF Corp, Hudson, NH.

December: William M. Murray earns his doctorate from M.I.T. He remains there until his retirement in 1973 and becomes the prime educator in experimental stress analysis, especially bonded resistance strain gages, brittle coatings and photoelasticity. He founds the Society for Experimental Stress Analysis in 1943, now Society for Experimental Mechanics.

In 1936, Arthur C. Ruge is Research Associate in Engineering Seismology at M.I.T. He will invent the bonded resistance strain gage as a deliberate solution to a strain measurement problem, April 3, 1938. Hans Meier and Frank Hines will help him perfect the invention, and with "A.V." to commercialize it by mid-1939. By Fall 1936 this team is assembled at M.I.T.

Comments: Note that both the first printed circuit (out of which grew the bonded foil gage) and the first bonded wire gages were "unwittingly invented". Kent and Paslay did not appreciate the significance of their invention. Simmons thought his was too simple to even document; and no one on the Cal Tech Impact Project realized the significance of the invention.

Not until later commercialization by Eisler and Ruge was the significance appreciated !

1936 - A BANNER YEAR FOR STRAIN GAGES AND EXPERIMENTAL STRESS ANALYSIS

by Peter K. Stein, Stein Engineering Services, Inc., Phoenix, Arizona, USA

INTRODUCTION

As the Outline and Summary shows, 1936 was a turning point in the history of experimental stress analysis and strain gages. The events were listed approximately chronologically in the Outline. The body of the paper, however, will divide the events by subject:

CARBON STRAIN GAGES

- Unbonded
  - The McCollum-Peters Telemeter
- Bonded
  - Liquid - Aquadag
  - Solid - The Kearns Gage

METALLIC STRAIN GAGES

- Unbonded Wire Gages
  - The Carlson Gage
- Bonded Wire Gages
  - Simmons at Cal Tech
  - Ruge at MIT
- Printed Circuits - Foil Gage Precursor
  - Kent and Pasley in the U.S.
  - Eisler in the U.K.

STRESSCOAT BRITTLE COATING

- Greer Ellis

All of these methods either originated in 1936 or achieved a "critical mass" which assured success or reinforced it.

CARBON STRAIN GAGES

The Unbonded Carbon Gage:

In July 1936, the Southwark Division of Baldwin-Southwark Corp in Philadelphia, published Bulletin No. 132, "McCollum-Peters Electrical Telemeters". The 32-page booklet contained a description of the device and a large number of practical field applications along with a catalog of the available hardware and prices. The bibliography included some 25 references to the Telemeter's use on aircraft in flight, concrete structures, oil well tests, railroad tests, rolling mill pressures, transmission towers, automotive applications, elevator cable and general-usage-and-description. The Partial List of Telemeter Users included 110 organizations in the U.S. and over a dozen in 8 other countries. Even though the basic strain gage version was fairly large (3/4" x 1-7/8" x 8½") and heavy (1 lb), it is obvious that the device invented by Burton McCollum and Orville S. Peters, electrical engineers at the National Bureau of Standards, had "arrived".

Burton McCollum had been hired by NBS in the early 1910s to help solve a problem of electrolytic corrosion of water and gas mains due to current straying from trolley tracks. He then became engaged in investigations of sound-ranging and sound-detecting equipment for locating distant or concealed enemy guns during World War I. He also worked on geophones and seismographs to detect enemy mining operations in the trenches, and special microphones for underwater sounds until well after the armistice. The work was done in the Electrolysis Section.

McCollum left the Bureau in 1926 to work in the oil-prospecting industry.

Orville S. Peters was born in Nov 1883 and joined NBS in 1910 working his way up from Assistant Physicist to Electrical Engineer by 1929. In 1930 he became Consulting Engineer. At the Bureau he worked on electrolysis in concrete, together with McCollum. In 1923 he co-authored a paper which seems to be the first publication on the carbon-based "Telemeter", with R. S. Johnston: NEW DEVELOPMENTS IN ELECTRIC TELEMETERS, (Proc. ASTM, Vol. 23, Part II, 1923, pp. 592-601). That paper already showed operational hardware and practical applications such as field tests on bridges, dynamometers, pressure gages, and stresses in airplane stay-cables during flight.

The traditionally-cited paper by McCollum & Peters: A NEW ELECTRICAL TELEMETER, appeared in Technologic Papers of the Bureau of Standards No. 247, January 4, 1924; part of Vol. 17.

It describes a carbon-pile displacement transducer with two differentially coupled elements shown in the illustration as D_1 and D_2. Each element consists of from 20 to 55 carbon rings, carefully lapped, under an initial pressure of some 180 psi, produced by preloading the frame, A. When the tongue, B, held by a frictionless fulcrum, C, was moved up or down, it would increase the compression in one element and decrease it in the other. Since the elements were in adjacent arms of a Wheatstone Bridge (i.e., differentially coupled), the non-linearity of response in each element was cancelled by that in the other.

The movement of the tongue could be produced by force, pressure, torque, acceleration, etc., and the basic frame could be adapted to serve in a wide variety of transducers.

In about 1930, Peters set up his own instrument company. It is believed that Frank Tatnall was instrumental in this transition. (*)

Francis G. "Frank" Tatnall was then working

(*) See Appendix 7

inductor telemeter

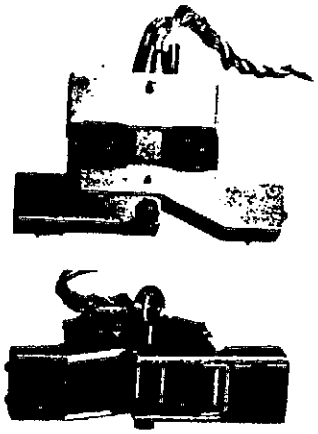

FIGURE 34

FORCES, loads, and pressures are transformed into electrical values by changes in the reluctance of two magnetic circuits as an armature is moved in an air gap under action of the mechanical forces to be measured. High frequency alternating current is used in a Wheatstone bridge circuit.

To date the Inductor Telemeter has been mainly used in pressure plug equipment for measuring rolling mill screw down loads and in drop testers where units have been employed for measuring hydraulic pressure, impact loads, stresses and strains in various parts of airplane landing gears. For similar applications where displacement does not exceed 0.010 in. in a 2-in. gage length, particularly where temperature changes are wide, it will be found more practicable than the carbon pile telemeter.

The complete unit consists of the telemeters, a control box weighing approximately 50 lb, a high-frequency generator set and a special Westinghouse oscillograph for making permanent records.

Complete information on the Inductor Telemeter will be given upon request.

McCollum-Peters electric telemeters

LOADS, forces, pressures and accelerations vary the resistance in a Wheatstone bridge circuit, unbalancing the bridge. The gage is composed of carbon piles. Their electrical resistance is varied by strain which causes pressure changes on the contacts. The instrument is supplied in several forms: (1) strain gage for static and dynamic stress and strain measurements, (2) pressure gage for fluctuating pressures in fluids and gases, (3) accelerometer, (4) pressure plug for measuring and recording direct loads.

Some actual applications include the measurement of strain in concrete dams, loads on rolling mills, vibration in steam turbines, explosions in internal combustion engines and the impact of waves against bulkheads. For rapidly changing values or for permanent records oscillograph equipment is supplied. In addition to this and the telemeter unit proper, a calibrator control board and other special equipment are required.

Bulletin 132 describes the McCollum-Peters Telemeter in detail.

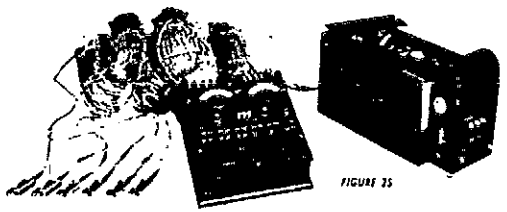

FIGURE 35

THE PRINCIPLE OF THE BURTON McCOLLUM - ORVILLE S. PETERS
CARBON PILE "ELECTRIC TELEMETER"
FROM BADLWIN-SOUTHWARK CORPORATION BULLETIN NO. 132, JULY 1936

FROM 20 TO 55 RINGS UNDER ABOUT 180 PSI PRESSURE
DEPENDING ON THE APPLICATION

"EXCLUSIVE RIGHTS GRANTED UNDER CONTRACT WITH EMERY-TATNALL COMPANY"

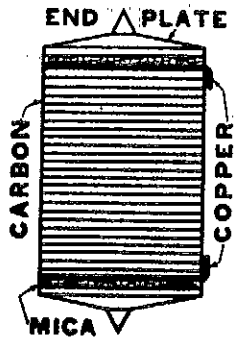

Fig. Z-107.

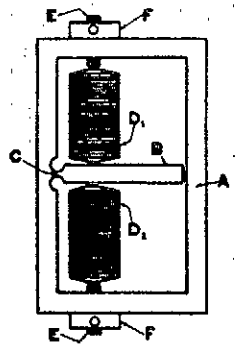

Fig. Z-100.

THE PRINCIPLE (ABOVE) AND HARDWARE (LEFT) OF THE McCOLLUM-PETERS TELEMETER

The units were made by the O. S. Peter Company, later absorbed into Baldwin-Southwark. The Inductor Telemeter was also made by O. S. Peters Co. Frank Tatnall saw an early unit at the National Bureau of Standards where McCollum and Peters developed it. In 1936 the unit was at the height of its popularity, soon to be displaced by Carlson's Unbonded Wire-Based Transducers. From Bulletin 153, 1940, Baldwin Southwark Co.

for the Baldwin-Southwark Corporation, selling testing machines and associated equipment. He travelled widely and knew everyone there was to know in the testing business, and what they were doing. In his charming and sometimes imaginative autobiography: TATNALL ON TESTING (American Society for Metals, 1966) he relates his discovery of numerous strain gages in use by imaginative inventors in various laboratories he visited. It is believed that Frank often helped these inventors set up their own businesses, had an interest in those, and then arranged to sell the devices through Baldwin-Southwark.

Baldwin's Bulletin 132 does carry the footnote: "Exclusive rights granted under contract with Emery-Tatnall Company", and Frank also relates his meeting with H. L. Whittemore, Chief of the Mechanics Section an NBS, whose invention was also treated in that manner and sold by Baldwin as the Whittemore Strain Gage for many years.

Roy Carlson remembers using one of these McCollum-Peters Carbon Gage transducers embedded in the Stevenson Creek Dam for measurement of forces, displacements and pressures, and being frustrated by the instabilities and temperature sensitivity of the carbon elements. They were, indeed, better suited for dynamic studies. It was this experience with carbon gages which drove Carlson to develop his own transducer based on unbonded wires, to be discussed in a subsequent section.

In 1936, however, the McCollum-Peters Telemeter was at the height of its popularity, although, also in 1936, Carlson's patent for his unbonded-wire transducer, was granted.

Frank Tatnall recalls that when he first heard of the Telemeter and went to NBS, McCollum had already left, which he did in 1926. By May 19, 1927, Frank had already written an: "UNOFFICIAL OBSERVER'S REPORT ON TELEMETER TESTS ON FREIGHT CAR TRUCK SIDE FRAMES BY AMERICAN STEEL FOUNDRIES, published in mimeographed form by Baldwin Southwark. This would appear to date the arrival of the "Telemeter" on the commercial scene, to 1927.

The Bonded-Painted Carbon Resistance Gage:

Among the early attempts to paint a liquid, carbon-based substance to surfaces for strain measurement was A. Bloch's publication in Nature Magazine, August 10, 1935. He was with the Physics Dept at Trinity College, Dublin.

It was E. H. Hull's application of AQUADAG at General Electric Company in 1936, however, that, at the time, came close to a small, weightless, bondable strain gage. It was no panacea, however. A. V. de Forest describes AQUADAG in his paper: MEASUREMENT OF PROPELLER STRESSES IN FLIGHT, Jnl of Aeronautical Sciences, Vol. 4, No. 6, April 1937, in which he is listed as affiliated with Hamilton Standard Propellers Div, United Aircraft Corp, a fact of interest in the next section.

"In its first form, this pick-up consists of an insulating layer of paper cemented to the metal surface, and carrying lead-in contacts of tin foil cemented to the upper surface of the insulating paper. The paint, applied between the two metal contact strips, was made of very finely divided graphite either in water or alcohol suspension. The steady resistance of the strip varies in an irregular manner at zero load due to temperature, moisture and perhaps other disturbances. To avoid this difficulty, the strip was connected so that only changes in resistance with strain were measured. If the stress variation is above 30 cycles per minute, the amplifier only records the cyclic fluctuations and is not sensitive to slow changes in resistance.

"Calibration of such strips at the General Electric Company, at Hamilton Standard Propeller and at M.I.T., showed that the measurement of strain was almost independent of frequency and closely proportional to strain amplitude. The resistance could be made quite high, 1000 to 50,000 ohms, and a considerable voltage applied to the system. In this way, slip ring difficulties were largely avoided. The weight of the pick-up was infinitesimal and the measurement could be carried out anywhere on the (propeller) blades regardless of the centrifugal loading.

"The major difficulties were the necessity for calibration of each paint strip under vibratory stresses, and the change in sensitivity due to temperature and moisture. The device is, in effect, an extreme refinement of the carbon pile telemeter as originally developed by Peters of the Bureau of Standards and marketed by Baldwin-Southwark Company for the last 10 years."

Frank Tatnall recalls that: "it was impossible to reproduce the thickness, gage length and resistance." Charles M. Kearns, Jr., inventor of the bonded (solid) carbon strain gage (see next section) recalls that powdered sulfur would be mixed with the solution, and the gage, once painted on, would be heated to melt the sulfur and solidify the installation. He also prepared such strain gages on paper strips befor mounting them to the test specimen. His memory of Aquadag is associated with the vile smell of heated sulfur.

The (Solid) Bonded Carbon Resistance Gage:

As related by Charles M. Kearns, Jr: "I had the good fortune, after graduating in June 1936 from Penn State, to join Hamilton Standard, then a division of United Aircraft Corp. I was

(See Appendices 7 & 8 for details)

assigned to the problem of doing something about propeller blade fatigue stress failures (in flight). After a couple of months of working with a terrible mixture of sulfur and graphite (Aquadag) which did indeed change its resistance with stress, but also with just about everything else, I was left alone during the vacation period of the company (the first 2 weeks of August). Having been a ham radio but -- in fact I still am - I got to thinking: a microphone provides a resistance change when carbon granules are compressed. What we need is a more rugged substance than a carbon granule button, and, having used carbon resistors, I simply ground one down, cemented it to a beam, and sure enough, it changed resistance with strain more or less linearly." The calibrations were on a bar against a Huggenberger Tensometer. "With this type of gage we made hundreds of thousands of propeller stress measurements and succeeded in reducing the incidence of propeller failures from a major problem to, in some years, zero problem; and I think we saved a lot of lives. I was mainly interested in solving the problem of safety in flight. The strain gage was an important means to that end but not the end itself...we viewed ourselves as having responsibility to the whole aviation community to spread the word of what we were doing. I published a paper in 1937 in the Jnl of Applied Mechanics: VIBRATION STRESS MEASUREMENTS IN STRONG CENTRIFUGAL FIELDS. (Dec, A 156-59, with Ralph Guerke)

"Between the years 1931 to 1938, propeller failures in flight ran anywhere from 8 to 41 times a year. By 1938 we had begun to study all the installations in the field and restricting them so that they did not operate under conditions of severe vibrations. In 1939 there were 6 failures and in 1940 there were none. I am proud of that because it has led to improved safety in flight."

The Kearns gage was widely copied, but also made for sale by Hamilton Standard who sold many thousands all over the world. It was replaced in 1938 by a more flexible carbon gage, which obsoleted not only his first invention but also the Electric Strain Sensitive Strip (ESS-Strip) developed by A. V. de Forest and Wilfrid L. "Bill" Walsh at MIT in 1937. In fact, the Kearns Carbon Gage and its copies were used at least through 1944 and probably later.

Kearns retired in 1975 as Staff Vice-President of United Technologies, the parent company of Hamilton Standard, Pratt & Whitney and others. He now lives in Tucson, AZ. He was awarded many honors including the Longstreth Medal of the Franklin Institute in 1942.

It is interesting to note that bonded carbon-film gages are still used today in shock pressure measurements at very high pressures, as developed by Dr. Jacques Charest, Dynasen Inc, 20 Dean Arnold Place, Goleta, CA 93017.

Unbonded Wire Strain Gages:

U.S. Patent No. 2,036,458 on a Telemetric Device was granted to Roy W. Carlson on April 7, 1936. He had applied for it August 4, 1934. The attorney preparing the patent was Roy's cousin, Chester F. Carlson, the inventor of the xerographic copying method and founder of Xerox.

Roy achieved international fame, acclaim and honors in the field of dams and large concrete structures, especially in their instrumentation. He got his BA in Mathematics from University of Redlands, worked for Southern California Edison for a year, attended California Institute of Technology for a year (1923-24) but left without a degree. After teaching a year at U of Redlands he returned to Southern California Edison and worked on the Experimental Arch Dam on Stevenson Creek in 1925 where he began his work on dams and concrete technology. "Every type of instrument known at the time for measuring structural action was used to test that dam," he wrote for a February 3, 1978 lecture in São Paulo, Brazil, "including strain meters of a carbon resistance type. These strain meters, (the McCollum-Peters Telemeter) were fairly good for quick changes in dimension, but were worthless for long-time measurements....The Stevenson Creek Experimental Dam was probably the most researched dam in the world ... built ... solely for the purpose of testing theories for arch dams." All told, Carlson helped determine the safety of 37 dams for Southern Cal Edison. He was then Testing Engineer on some 10 dams for County of Los Angeles, 1927-31, and Assistant Director of Research on Materials for Hoover Dam until 1934. During that time he earned his MSE an U of California at Berkeley in 1933 and taught there as Associate Prof in 1935, when he went to M.I.T. for his doctorate.

In the early 1930s, culminating in his 1936 patent, he designed his own instruments for dam investigations, based on unbonded wires, pretensioned in a frame which differentially coupled the responses of two loops of wires. Very much as in the McCollum-Peters pre-compressed carbon stack, the movement of Carlson's frame, increased the tension in one winding as it reduced the tension in the other, giving a linear, temperature-compensated output. He found that carbon steel, when drawn small enough (about 0.01" diameter) approaches 700,000 psi tensile strength with a gage factor of 3.6. 2000 of his strain meters were used in Glen Canyon Dam; 1600 in Flaming Gorge Dam. They are still manufactured by Carlson Instrument Co and (in copy form) by Kyowa Electronic Instruments.

In 1935 he went to M.I.T. where he earned his doctorate in 1939 on DEVELOPMENT AND ANALYSIS OF A DEVICE FOR MEASURING COMPRESSIVE STRESS IN CONCRETE. At the same time as he received His doctorate, so did Arthur C. Ruge and Hans

April 7, 1936. R. W CARLSON 2,036,458

TELEMETRIC DEVICE

Filed Aug. 4, 1934 2 Sheets-Sheet 1

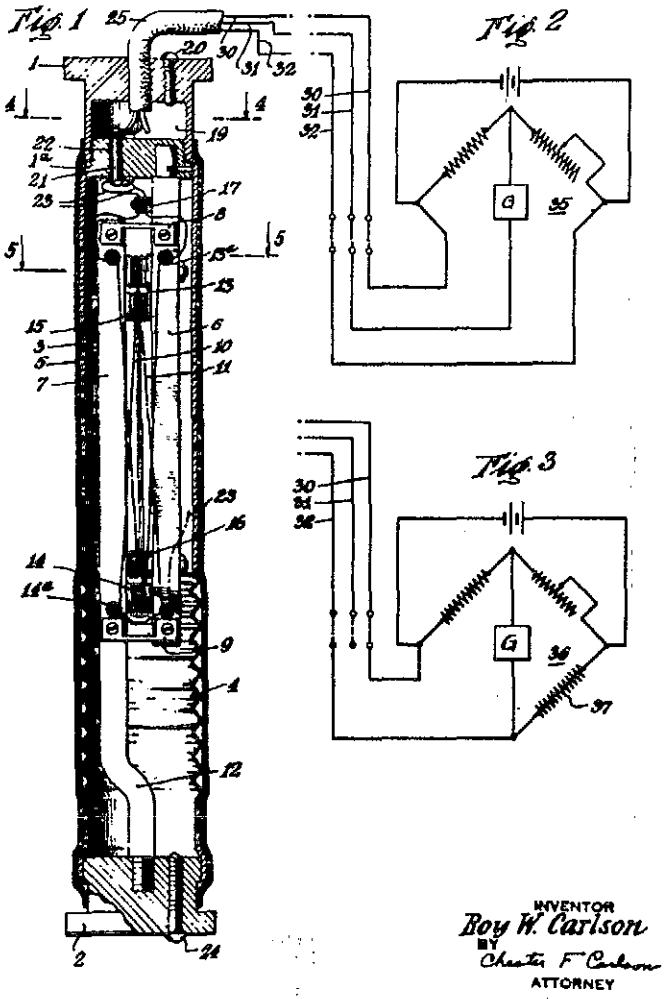

ROY CARLSON'S PATENT FOR HIS UNBONDED WIRE TRANSDUCER

Feb. 21, 1939. E L. KENT ET AL 2,147,948

APPARATUS FOR THE GENERATION OF MUSICAL TONES

Filed Aug. 10, 1936 4 Sheets-Sheet 4

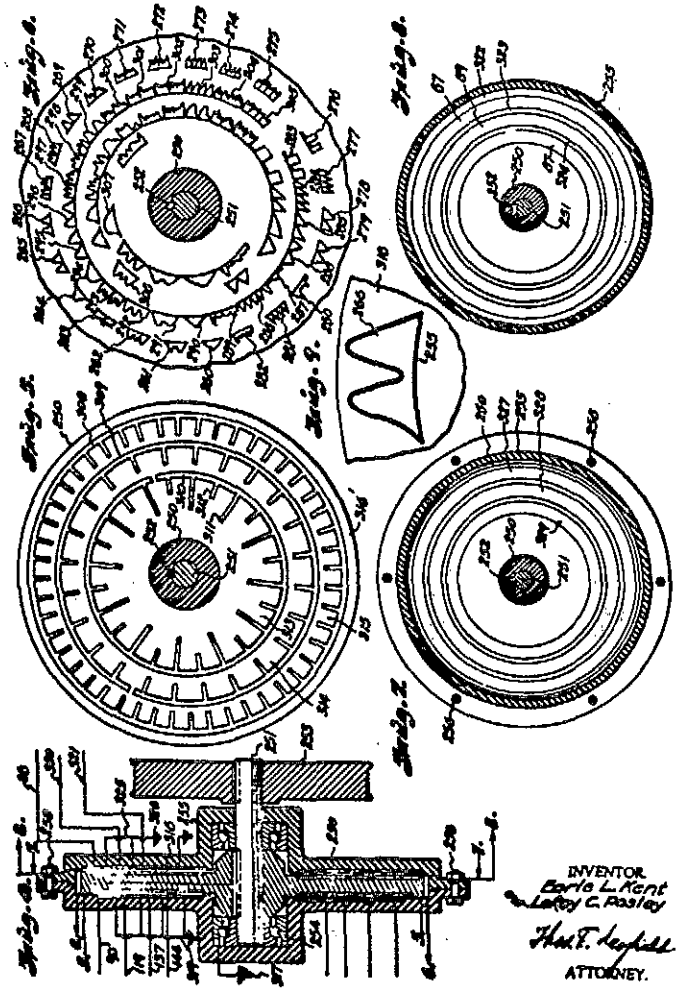

EARLE L. KENT'S AND LeROY C. PASLEY'S PATENT FOR AN ELECTRONIC ORGAN, IN WHICH THEY INVENTED THE PRINTED CIRCUIT, SEE TOP LEFT FIGURE 6.

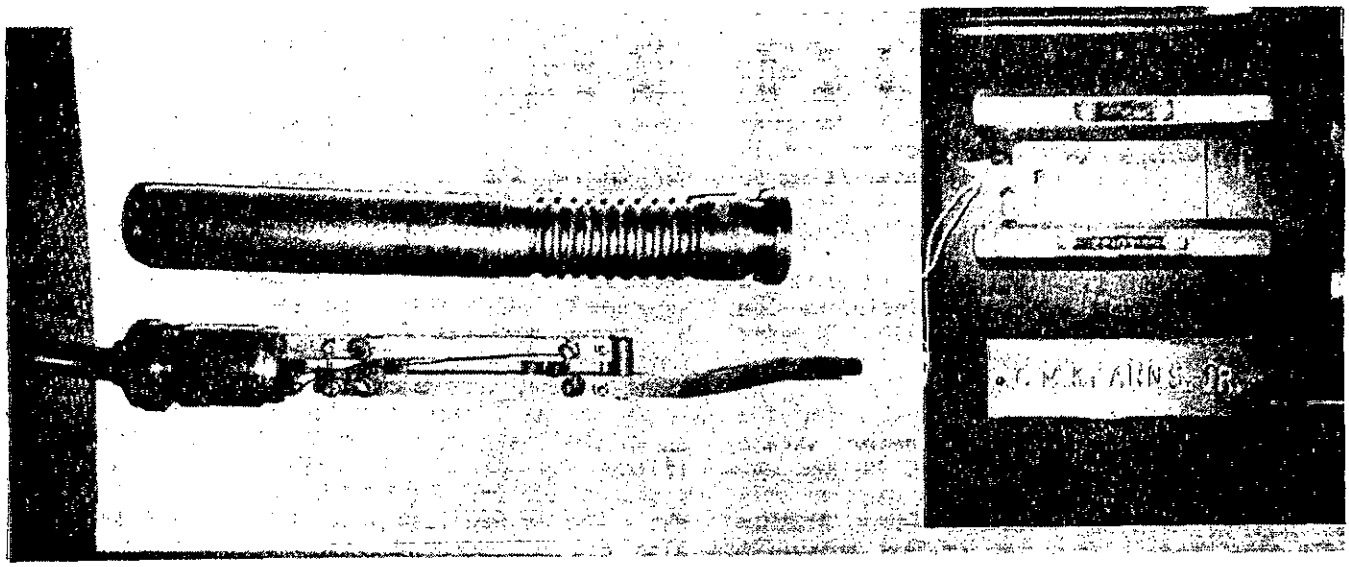

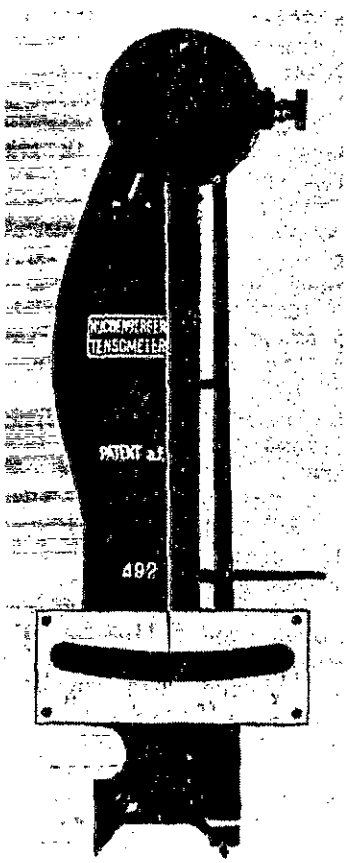

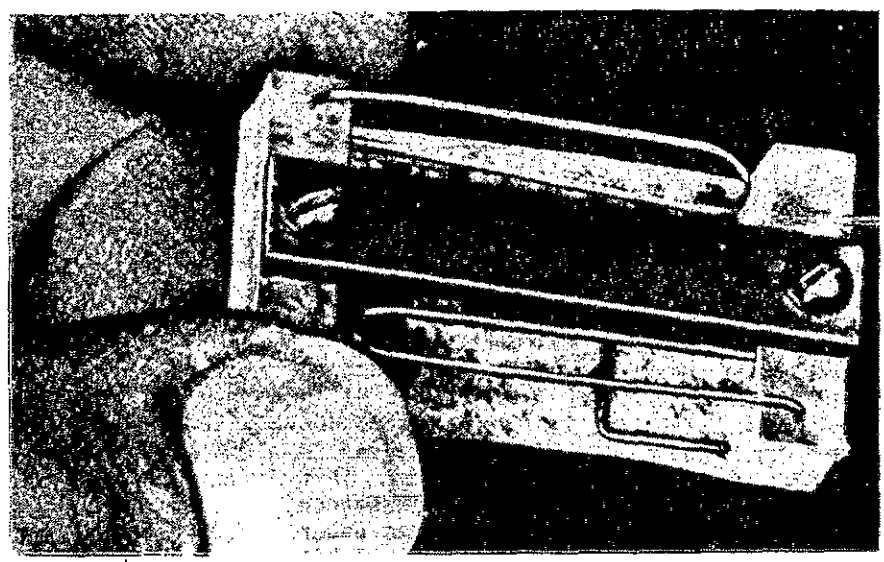

TOP LEFT: A Carlson Unbonded Wire Transducer. About 25 cm, 10 inches long. Force applied at left end increases the tension in one pair of pretensioned wires, and decreases the tension in the other pair. TOP RIGHT: Examples of the Kearns Bonded Carbon Gage. The plaque was presented to Kearns when he left the group. Bottom Gage: Serial No 22103, original design; Top: Serial #M1174, more flexible design. BOTTOM LEFT: Huggenberger Extensometer with 1200 magnification. Invented by A. U Huggenberger in Switzerland it was sold by Baldwin-Southwark in the US; one of the most popular strain gages of 1936. BOTTOM RIGHT: One of the first SR-4 "Metalectric" Bonded Wire Resistance Strain Gages of the SR-4 type invented by A. C. Ruge and sold through Baldwin-Southwark starting in 1939-40. The team which perfected and commercialized it was in place at M.I.T. in 1936.

Meier. Frank Hines received his bachelor's degree by mail that year - he was too busy making the SR-4 bonded wire strain gages which Prof. Ruge had invented April 3, 1938 and which Hans Meier had developed as his doctoral dissertation. These invididuals appear in this story a little later. But it is interesting to note that Carlson and Ruge had side-by-side offices and labs in the basement of Building I, Civil Engineering Dept, at M.I.T.

Roy Carlson, living in Berkeley, CA accumulated numerous honors and awards including the Southern Cross of Brazil, recognizing his years of involvement with construction and testing of concrete dams in that country. He is noted for 3 major inventions for understanding the behavior of concrete: the stress meter, strain meter and conduction calorimeter. He had envisioned the unbonded-wire strain gage as only for applications to concrete. Louis Statham built many other transducers on that principle: force, displacement, acceleration, pressure, fluid flow, etc. He infringed on Carlson's patent until he was finally forced to buy it, paying Carlson a 3% royalty on all Statham transducers while collecting 50¢/transducer which Carlson sold. In some forms, the unbonded wire strain gage is still available today.

Bonded Resistance Wire Strain Gages:

It was during the first two weeks of September 1936, that Edward E. Simmons, Jr., an inventive MS EE graduate from California Institute of Technology (also 1936) was consulted by Dr. Gottfried Dätwyler about a better way of measuring the dynamic forces produced by an impact testing machine at Cal Tech.

Dätwyler had received his Dipl.-ing. degree from the Federal Technical Institute (ETH) in Switzerland in 1929, and, to please his mother, continued for a doctorate which he received in Aerodynamics from ETH March 19, 1934. That same year he appears at Cal Tech as Research Associate in Aeronautical Engineering under Prof. Theodore van Karman, who had under his wing, in the Guggenheim Aeronautical Building all sorts of "orphan projects" which could not find a home in other departments. One of these was the Impact Research Project headed by Dr. Donald S. Clark. (°) See Appendix 9.

Exactly how Dätwyler came to work on that project with Clark we now (°) know. Simmons had been involved for some time as a "consultant" to many of the projects in the building because of his inventiveness especially of measuring apparatus and instrumentation. Dätwyler had tried Aquadag and other electrical strain gages of the day, but nothing worked under the high-speed transient conditions of impact.

Ed Simmons suggested that Dätwyler try bonding a fine wire to the surface of a prismatic bar and to use that as a load cell. He even went to the Physics Stock Room and got a spool of No. 40-gage insulated constantan wire for Dätwyler to try. Dätwyler bonded it to a piece of clock spring and tested it cantilever beam style - September 10, 1936. It was linear, repeatable and hysteresis-free. The bonded wire strain gage had been born, and its immediate derivative, the strain-gage-based loads cell.

It is interesting to note that no one realized that a significant invention had been made. Simmons the electrical engineer, Dätwyler the aerodynamicist and Clark the metallurgist were apparently unfamiliar with the intense search by stress analysts for just what Simmons had conceived. Simmons recalled his thought at the time: "Patent such a ridiculously simple thing?"

It was an invention which solved a problem, as we shall see again for the Printed Circuit. It was not an aim in itself. Although the sponsors of the Impact Project read like a Who's Who in American industry at the time, it also did not occur to the recipients of the periodic progress reports to note anything significant about the way in which the dynamic impact forces were measured. Even when Clark and Dätwyler presented their paper at the ASTM Meeting, June 1938, in Atlantic City, none of the discussants whose comments were published, noted anything significant about the measurement system - not even Dr. Louis B. Tuckerman, of the National Bureau of Standards and inventor of the Tuckerman Gage, and who was in the audience, commented about the load cell. (*)(#)

The sponsors were: Allis Chalmers Manufacturing Co., Caterpillar Tractor Co., General Petroleum Corp of America, Hughes Tool Co., Lane-Wells Co., National Supply Co., Arnold Pfau. A. O. Smith Corp., Union Oil of California and W. M. White - all of whom had also given permission to publish the results of those invetigations.

The volume of ASTM Proceedings containing the paper was not published until January 1939 and not until after Prof. Arthur C. Ruge, at M.I.T. had requested a patent release from M.I.T. on February 20, 1939 for his (re)invention of the bonded wire gage, did the M.I.T. team find out about Simmons' work ! (+)

Dätwyler returned to the ETH in Switzerland September 25, 1938 and developed a line of hot-wire anemometers and associated instrumentation which he made and sold through his company: Polymetron, for many years. He also designed, produced and sold large and medium-sized wind-tunnels throughout Europe, and cross-flow compressors/fans as Dätwyler-Hausamann-Diesler in the early 1950s. He grazed the field of strain gages only once, briefly, like a comet.

In 1936, Arthur C. Ruge, whom everyone called "Prof" as though it was his first name, was a Research Associate in Engineering Seismology at M.I.T. J. Hans Meier appears at M.I.T. with his Dipl.-ing. degree from Switzerland, gets his Master's Degree under William M. Murray in 1937 and becomes "Prof's" assistant. Also in 1936

(*) See Appendix 1 (+) See Appendix 2 (#) See Appendix 6

Aug. 11, 1942. E. E. SIMMONS, JR 2,292,549

MATERIAL TESTING APPARATUS

Filed Feb. 23, 1940 2 Sheets-Sheet 2

Fig. 3

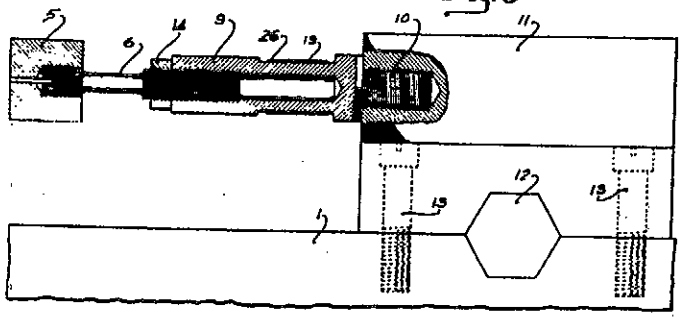

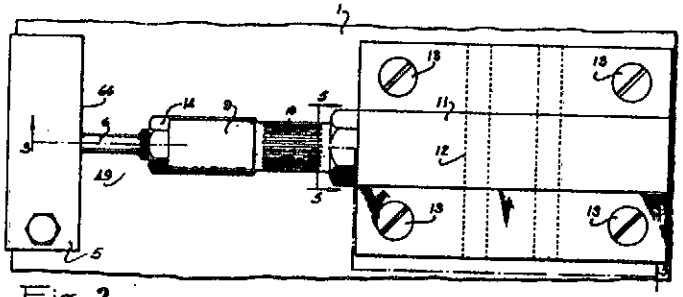

Fig. 2

Fig. 7

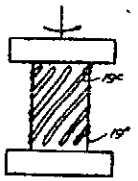

Fig. 8

INVENTOR
EDWARD E. SIMMONS, JR.
BY
ATTORNEY

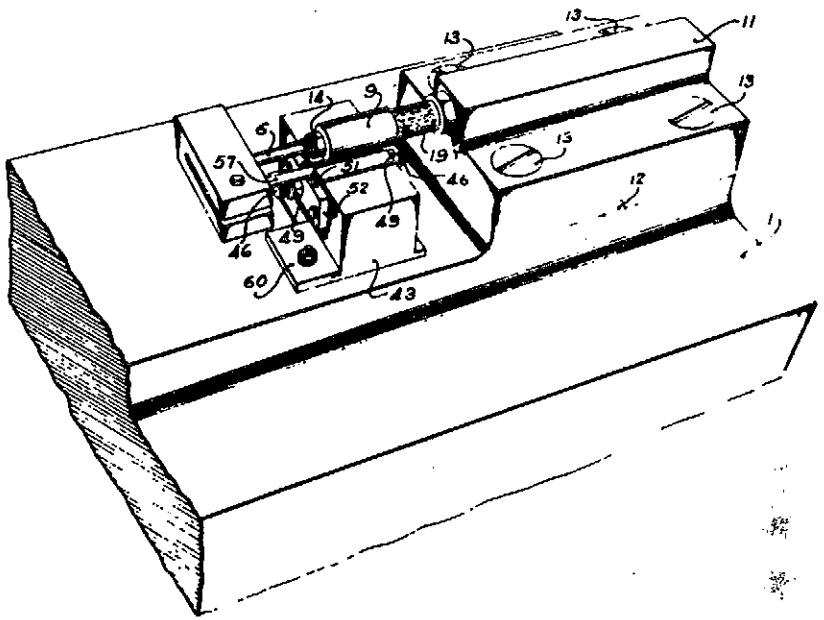

THE SIMMONS PATENT FOR THE BONDED WIRE RESISTANCE STRAIN GAGE

Invented in early September 1936 by Edward E. Simmons, Jr., 1936 Cal Tech MS EE and reduced to practice by Dr. Gottfried Dätwyler on the Impact Project under Dr. Donald S. Clark. 14 feet (4¼+ meters) of No. 40 AWG insulated Constantan wire were bonded on the 4 faces of a 7/8"x3/4"x4-5/8" long steel bar (24¼mmx19mmx117½mm). The patent shows a round bar (9) with strain sensitive wires (19).

Simmons, the Electrical Engineer didn't think such a simple thing was worth documenting or patenting; Aerodynamicist Dätwyler didn't realize what had been invented, and Metallurgist Clark was interested only in the impact properties of the material he tested. The gage languished for 2½ years before re-discovery and commercialization by Arthur C. Ruge.

Frank Hines transfers to M.I.T. from West Virginia University. He had won the 1931 Fisher Body (General Motors) competition for a hand-made exact model replica of Napoleon's Wedding Coach. The prize for that National Competition was a $5000 (1931 dollars!) scholarship, which enabled him to attend college.

As happens with many transfer students, the courses he needed in Spring 1938 were not offered and he took a semester off to work for the M.I.T. Hobby Shop. By luck and chance he got a job in Prof Ruge's lab to maintain the notoriously failure-prone earthquake-simulating machine. The team to which we owe the bonded wire strain gage as we know it today, has now been assembled!

In December 1936, William M. Murray earns his doctorate at M.I.T. where he will remain until his 1973 retirement. He will be the educator in experimental stress analysis, the first to incorporate strain gages, brittle coatings and photoelasticity into the undergraduate curriculum of an institution of higher learning. He is also the founder of the Society for Experimental Stress Analysis now the Society for Experimental Mechanics. He died at age 80 in August 1990. See dedication.

Prof. Ruge received a research contract from an insurance company to study the behavior of water towers under earthquake conditions, since the major damage in earthquakes is from fires rather than the quake itself. Hans Meier, his Assistant, is to predict and measure the stresses in the double-curved thin-shell vibrating structure. They try every strain measurement method known to them, but none will do the job. Finally, in desperation, Prof has a "Eureka-Experience" early Sunday morning, April 3, 1938. He unwinds the wire from a precision resistor, bonds it down on a test beam, and it works! Hans Meier develops the gage on his doctoral dissertation which changes from an emphasis on the water tower to an emphasis on the strain gage. Frank Hines with his unusual manual dexterity and devotion to detail, which won him the Fisher Body prize, is an invaluable member of the team and spends the rest of his life on bonded resistance transducers - first strain gages and now temperature sensors. He is Chairman of the Board, RdF Corporation, the last remaining vestige of Ruge-de Forest Consulting Engineers.

Ruge and Meier, not having a galvanometer to read the output of their Wheatstone bridge, conduct their first experiments in A. V. de Forest's Lab in Mechanical Engineering on the 3rd floor of Building I. When they see how well it works, they each recognize exactly what has been discovered and spend the rest of their lives developing (Ruge, de Forest and Hines), making and using (Meier) the gages, and transducers based on them.

(*) For today's Scratch Gages see Appendix 3.

Alfred V. "A.V." de Forest:

"A.V." deserves a separate section in any history of experimental mechanics. In 1936, he and William E. Hoke receive the prestigious Longstreth Medal from the Franklin Institute "For the Detection of Hidden Defects in Magnetic and Current-Carrying Materials," commercially exploited as Magnaflux Corporation which de Forest founded in 1934. In 1928 he noted that small iron particles tend to collect on cracks in magnetized steel parts. He found that by passing heavy currents through the material under investigation, the sensitivity of the test could be greatly increased, and his development of circular polarization completed this very powerful non-destructive testing tool. He found that his original patent application had been pre-empted by Major William Hoke, who in 1918 also noted small iron particles collecting around cracks but never used the process commercially. De Forest overcame his disappointment and realized that although Hoke may have the basic papent, he, de Forest, would have the improvement patents, so they joined forces and de Forest soon bought out Hoke's interest. By 1936 Magnaflux had "arrived".

De Forest had also invented the "de Forest Scratch Gage", a small, light-weight mechanical self-recording strain gage which he commercialized through Baldwin-Southwark Corp. The last Catalog Bulletin which the author has on the Scratch Gage is dated 1947 ! So late into the history of strain gages was that simple device still made and sold. (*)

The Scratch Gage consists of a polished target which is attached to the test specimen, adhesively, with screws, solder, etc., and a pointer with abrasive material at the tip, which sits on the target. The pointer is held in place by a frictional joint, but near its other end it is bent in the third dimension to form a torsional spring, the restoring force of which overcomes the frictional force in the joint under vibratory (but not static) conditions. The "other end" of the pointer is, in turn also attached to the specimen so that a 2" gage-length strain gage (usually) results - non-electrical, without lead wires, self-recording (the scratches on the target), self-contained and light-weight.

Wilfrid L. "Bill" Walsh worked with "A.V." as his technician/associate from the early 1920s to "A.V."'s untimely death in 1945. Together they moved from American Chain Company to M.I.T. in 1934. It is correct to assess their partnership as follows: every idea which "A.V." had and every invention he made was reduced to practice and built by Bill Walsh. He made the first Magnaflux equipment, all the Scratch Gages until after "A.V."'s death, and all the other devices which "A.V." needed.

The consumate entrepreneuer/inventor, "A.V."

BALDWIN

Slightly over two inches long, weighing less than two grams, and self-contained, the deForest Scratch Gage has many applications in measuring strain in fast moving machine parts.

THE deForest Scratch Gage is a self-contained recording strain gage, weighing less than two grams which records deformations below the elastic limit and ranging from 0.0001 to 0.050 of an inch over a two-inch gage length. It may also be used to measure high rates of vibration, such as harmonics up to frequencies in the sonic range. The presence of a torsional strain, and its frequency in terms of longitudinal vibration, are indicated but are not measured quantitatively.

It is the smallest, lightest and lowest cost recording strain gage ever devised.

The record is in the form of a scratch which indicates the exact value of the deformation. It can be measured or photographed at suitable magnification under a metallographic microscope. The record does not, however, give an indication of time, although this can sometimes be inferred from other data.

The gage may be fastened to a member in various ways; screws, solder, spot welding and clamps have all been used. Because of its small size and light weight it may be attached to such members as airplane propellers or rapidly moving parts of high speed machinery.

CONSTRUCTION AND OPERATION

The Scratch Gage consists of only two parts — the *scratch arm* and the *target*. The target and the fulcrum end of the scratch arm are rigidly attached to the member which is to be tested in such a way that the scratch arm is parallel to the direction of strain, and lies closely on the center line of the target.

The tip of the scratch arm carries a special abrasive and is in contact with the polished, chrome plated recording surface of the target. Deformation of the member causes the scratch arm and target to move longitudinally in relation to each other, and this movement is recorded as a scratch on the recording surface.

The unique feature of the gage is the method by which the scratch arm is caused to progress across the target at a right angle to the direction of strain, so as to produce a continuous record. The portion of the scratch arm near the fulcrum is so designed that it constitutes a spring. When the gage is made ready for the test, the tip of the scratch arm is pushed to the left or right. This sets up a restoring force in the fulcrum spring and, incidentally, marks a zero line on the recording surface.

One part of the target functions as a friction bar, pressing down on the scratch arm with enough force to hold it in place when the test surface is static. When strain occurs, however, this friction is insufficient, and the force exerted by the fulcrum spring causes the scratch arm to move slightly toward the center of the target at the same time that the deformation of the member causes movement in a longitudinal direction.

The force of the fulcrum spring may be reduced by reducing its thickness; friction may be varied by bending the friction bar. By varying these, the record may be obtained packed or spread out, as desired.

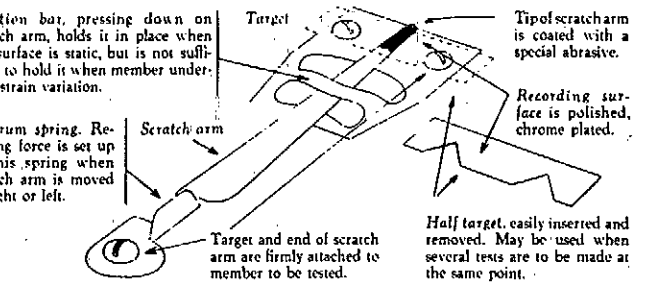

APPLICATIONS

It is not possible in a brief bulletin to even enumerate the many uses which have been found for the deForest Scratch Gage. Some have been mentioned, others may be suggested by the illustrations on this page. To a very great extent, however, the applications of this gage will depend on the imagination and ingenuity of the user.

deForest Scratch Gages mounted on airplane propeller blade for analysis of different modes of vibration.

High frequency vibration, 3,100 lb. per square inch, superimposed on repetitions of principal stress of 39,600 lb. per square inch.

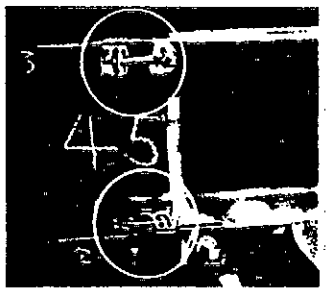

Scratch Gages attached to rail. Use of half-targets facilitates obtaining many records without removing gage.

Close packed record from airplane propeller. Density of record may be varied within wide limits. Magnification: 500x.

Open scale record of vibration in propeller. Magnification: 500x.

Combined torsional and longitudinal stress in angle iron vibrating as a cantilever beam. Magnification: 300x.

PRINCIPLE - HARDWARE - APPLICATIONS OF THE DE FOREST SCRATCH GAGE - POPULAR STRAIN GAGE IN 1936

Both sides of Bulletin 265 of April 1947 ! So late was it still in use. It was made by Wilfrid L. "Bill" Walsh, de Forest's associate until de Forest's death in 1945. Some time after that, Bill sent his tools and fixtures to the O. S. Peters Co, who continued making the gage for Baldwin-Southwark. In 1936 the Scratch Gage was very widely used as a self-recording strain gage.

commercialized the Scratch Gage through Baldwin-Southwark who sold them by the thousands. "A.V." was M.I.T. Class 1911 and the only Full Professor on the faculty with only a BS degree. He was very proud of that.

It is his ability to overcome disappointments, as with the Magnaflux patent, and to commercialize on his inventiveness, as with the Scratch Gage, which are responsible for the commercialization, in the form in which we know them today, of the bonded wire strain gage - the SR-4 "Metalectric" Gage and of Stresscoat brittle coating (through Magnaflux). He is also the author of the first publication on the bonded resistance strain gage: LETTER TO THE EDITOR, Jnl of Aeronautical Sciences, Vol. 7, No. 7, November 27, 1939. (*)

Bonded Wire Resistance Strain Gage: Continued

The Simmons gage, starting in the first two weeks of September 1936, was made of INSULATED wire, pre-mounted on a paper carrier, and mounted PAPER-SIDE UP, WIRE-SIDE DOWN on the test specimen. The Ruge gage, starting in April 1938 was made with bare wire, pre-mounted on a paper backing or carrier. IT was mounted PAPER-SIDE DOWN, WIRE-SIDE UP, so that the paper provided the insulation.

When the patent and contract negotiations started between Simmons and Clark at Cal Tech with Baldwin-Southwark, Simmons was happy for Cal Tech to get the royalties because he was told they would pay his salary on the Impact Project by which he was fascinated. When his employment and then the entire project were terminated in 1941, he found that the royalties had gone to the general fund. He sued Cal Tech for fraud and recovered $125,000 in back royalties when the California Supreme Court found in his favor in 1949 [Edward E. Simmons, Jr. v. Cal Tech (34 C2d 264; 209 P. 2d 581) L.A. No. 19484, In Bank, Sept. 16, 1949], and about $1 million total over the life of the patent. He lives today in Pasadena, California, wearing only Renaissance costume, still with an interest in engineering and science and with total and instant recall of the details of the early days. He received the Longstreth Medal of the Franklin Institute in 1944 for his invention of the bonded wire gage. It should be noted that he NEVER bonded a gage down in his life. "I've always had others to do that," he says even of the very first gage which Dätwyler bonded. But because he had the idea, his were the patent and the royalties.

Printed Circuits: Precursors of the Foil Gage

The bonded resistance strain gage of choice today, is the foil strain gage manufactured primarily by printed-circuit etching methods. The die-cut strain gage had a brief period of success but is not commercial today.

August 10, 1936, Earle L. Kent and LeRoy Paslay filed for a patent on an "Apparatus for the Generation of Musical Tones", issued as # 2,147,948 February 21, 1939. It was an electronic organ ! In its construction and in the patent, they describe in complete detail the still-pertinent manufacture of a printed circuit.

Since their aim was an electronic organ, they paid no attention to the printed circuit technique by which they made it, and, as in the case of Simmons and Cal Tech, did not recognize the significance of their invention.

September 16, 1936, Dr.-ing. Paul Eisler received his Provisional Patent Application # 24,543 in London, England, for "Production of Electrical Apparatus and Components for Weak Current Purposes." As a doctor of electrical engineering with practical experience in the printing and lithography industries in his birthplace, Vienna, Austria, he had his "Eureka Experience" while walking with friends in Regents Park, London, and "was struck by the immensity of its potential applications!" He knew what he had invented and went on to become the Father of Printed Circuits all over the world, except, ironically, not in the U.S. where the Kent & Paslay patent invalidated the Eisler patents in a bitterly fought series of law suits of which Technograph Printed Circuits Ltd v. Admiral Corp, Civil Action 62C671 in U.S. District Court for the Northern District of Illinois Eastern Division, 1964, and Technograph Printed Circuits v. Bendix Aviation Corp Civ. A. No. 11421, U.S. District Court D. Maryland, May 27, 1963; appealed U.S. Court of Appeals, 4th Circuit # 9085, decided Jan 17, 1964 for the Defendant, are prime examples.

Earle Kent was born in 1910 in Adrian, Texas. He was a professional musician playing clarinet and saxophone in concert bands from 1927-35. He also developed an early interest in electronics and helped build and operate one of the first regularly scheduled experimental TV broadcasting stations in the nation: W9XAK at Kansas State Univ where he met LeRoy Paslay who directed the project.

While at Kansas State he invented an electronic organ (mentioned above) which incorporated the modern printed circuit in its manufacture, working with Paslay from 1933-36. In 1935 he received his BS EE and in 1936 his MS EE. from 1936-40 he was Instructor in EE at Armour (now Illinois) Institute of Technology in Chicago. He earned his PhD from Univ of Michigan in 1952.

In 1940 he had joined C. G. Conn, manufacturer of musical instruments and set up their electronic organ engineering department. During World War II he directed research on defense products for government agencies. He has over 2 dozen patents to his credit. In his 29-year-long career with C. G. Conn, Ltd, he disting-

(*) See also Appendix 2

uished himself in the design of both electronic and acoustical instruments. "We used strain gages in wind instruments and piano research!" he wrote in October 1990. He won several awards and honors. He retired in 1971 after 29 years as Director of Research, Development and Design. He has his own consulting firm and even at 80 is doing computer programming for the County Court System in Elkhart, Indiana where he and Nina live. His civic activities, awards publications and presentations fill pages.

LeRoy C. Paslay was born in Manhattan, Kansas in 1907. He acquired his BS EE at Kansas State in 1930, joined General Electric Co for 2 years and returned for his MS EE which he received in 1934. He remained as Assistant Prof until 1935; also as Director of Research.

It is of that period that he wrote on November 2, 1990: "I was mostly engaged in television research when Earle Kent approached me for help in development of an electronic organ he had been working on. The idea seemed great and I agreed to go into it with him....we decided that a means of scanning exact wave forms of organ sounds was indicated (as obtained on oscillograms and translated to polar coordinates). The system..required a lot of carefully laid out conducting forms on an insulated disc. My father was a commercial photographer with some photoengraving experience and with a fully equipped shop in the same town, so with that knowledge and expertise available, it seemed logical to produce these forms and the connecting circuits with printed circuits, and it worked like a charm.

"We made several models, got a patent, and tried to find a way to raise money and get into the organ businesns but without success."

"I joined the National Geophysical Co of Dallas, Texas, as Director of Research and Development of electronic instruments for use in seismic exploration for oil and gas structures. That put the organ pretty much on hold.

"During World War II I became head of the Underwater Sound Division of Naval Ordnance Laboratory in Washington, DC where my division developed crystal pressure transducers for various mine applications. With this, then new, practical application using various crystal materials, I was able to develop, after the war, and patent, an entirely new method of oil exploration in water-covered areas that has since been the means of finding almost all the underwater structures containing oil, in the world." His device is known today as the Paslay Streamer. He has received many awards and honors and held numerous high positions with various organizations. He still maintains his office in Dallas, Texas and remains professionally active, living in Manalpan, Florida.

Dr.-ing. Paul Eisler earned his doctorate in Electrical Engineering at the Univ of Vienna in 1933, and, as a Jew, could not find employment in already-Nazi-contaminated Austria. He did acquire a marvelous background in printing technology and lithography, and in making the music played on electrified trains free of noise and static, a major problem in those days.

May 15, 1936 he left Vienna for London. "As an alien, however, I was not permitted to work," he wrote in his biography MY LIFE WITH PRINTED CIRCUITS, LeHigh Univ Press / Associated University Presses, 1989. "It was in the warm sunny days of early autumn 1936," he wrote on December 18, 1990, "I had met a friend ... we were taking a walk in Regents Park. Suddenly out of the blue sky, without any conscious association I got the idea of Printed Circuits and was struck by the immensity of its potential applications. I got in touch with my patent agent... ...my application for a Provisional Patent got the number 24543." (*)

When he offered his printed circuit invention to industry, it was rejected. Eventually, after much hardship, he succeeded in interesting H. V. Strong, proprietor of an old, established firm of music printers; but he was required to sign an agreement that conferred title of all related future patents to Strong.

Eisler then constructed the first radio set incorporating printed circuits. He demonstrated the set to the Allied Missions and received a highly favorable response. The Americans used printed circuits in proximity fuses, and these were supplied to the anti-aircraft batteries for the defense of London and of the Antwerp bridgehead.

Technograph Printed Circuits, Ltd was formed and he developed a unique facility for making printed circuits. These eventually "conquered the world" and he got patents in many countries including the U.S. It wasn't until after Eisler left Technograph in 1956 that Technograph tried to enforce their patents in the U.S. and launched some 100 law suits, that the Kent & Paslay patent was found by Bendix lawyers. It invalidated all the Technograph patents.

Paul Eisler has numerous other inventions to his credit and still maintains a Consultancy in London, where he lives.

Foil Strain Gages as such, came much later, in the early 1950s and do not form part of this story. In 1936, however, the groundwork was all laid and the technology and people were in place.

(*) "Production of Electrical Apparatus and Components for Weak Current Purposes."

BRITTLE COATINGS

Strain gages have always pre-supposed knowledge of where to mount them, in stress analysis applications. The locations and directions of the highest strains on a structure are usually unknown, but unless the strain gage is placed there, even the best strain gage and instrumentation system are powerless to predict failure, in general. (Continued on page 18)

THE STRAIN GAGE / BRITTLE COATING PIONEERS OF 1936 FEATURED IN THIS PAPER

TOP ROW - LEFT TO RIGHT

Burton McCOLLUM (photo courtesy of Univ of Kansas Alumni Assoc)(June 1, 1880 - July 20, 1984). Burton was a Univ of Kansas BS EE 1903 and went into power plant operations, 1903-07. He returned to Univ of Kansas as Assistant Prof in EE, 1907-09 when he joined the National Bureau of Standards until 1926. His work with the unbonded carbon gage, culminating in the "McCollum-Peters Telemeter" was done at NBS.

He entered the geophysical field, first in private research and in 1924 as President, McCollum Exploration Co and McCollum Geological Exploration, Inc. It appears that some of these ventures overlapped his stay at NBS.

He was a pioneer in oil field exploration by means of seismographs and located the first oil well by seismographic methods, ever so found, in 1924. Subsequently he developed many new devices and inventions. He lived in Houston, Texas after leaving NBS. He apparently touched the strain gage field only once, at the National Bureau of Standards as co-worker with Orville S. Peters, who stayed in the field.

Orville S. PETERS (photo from the 1907-08 Montanan, Alumni Assoc, Montana State Univ) (November 30, 1883 - August 24, 1942.) Orville graduated from Montana State with a BS EE in 1909 and was Instructor in EE there for a year. In 1910 he joined the National Bureau of Standards as Associate Physicist and rose to Electrical Engineer.

Presumably under the influence of Frank Tatnall (see body of paper) he set up the O. S. Peters Co in 1930, manufacturing the McCollum-Peters Unbonded Carbon "Telemeter" and added many other mechanical and electrical strain-related instruments to his line over the years. He was under contract to Baldwin Southwark who marketed his devices and eventually acquired the company by exchange of stock. Frank Tatnall tells "The O. S. Peters Story" well in his book: Tatnall on Testing (ASM, Metals Park, Ohio, 1966).

Francis G. "Frank" TATNALL (photo by Ferdi Stern)(March 9, 1896 - December 5, 1981). As related in the body of this paper, Frank was the catalyst who brought together inventors of strain-measuring instruments, mostly mechanical, manufacturing facilities and the marketing function through Baldwin-Southwark. Many of the devices he "found" were made by the O. S. Peters Co.

Edwin H. HULL (photo courtesy of Yale University Alumni Assoc)(November 17, 1902 - November 7, 1964). Hull was Yale, Class of 1924 when he went to work for General Electric Co Research Lab in Schenectady, New York. He held patents on elastic mountings, high speed motor design, etc. He had an interest in lubricants. Originally issued as Trademark 31,075, April 28, 1908, Aquadag is still manufactured as a general lubricant by Acheson Colloids Co, in Port Huron, MI. It is "a colloidal graphited water for various use in the industrial arts." Its use by Hull as a liquid-carbon resistance strain gage is described in this paper. Trademark #290,211, Dec 22, 1931 is also for Aquadag.

SECOND ROW - LEFT TO RIGHT

Alfred V. "A.V." de FOREST (April 7, 1888 - April 5, 1945). His story is told in the paper.

Wilfrid L. "Bill" WALSH (July 23, 1893 - September 19, 1967). His story is told in the paper.

Roy W. CARLSON (photo from M.I.T. 1939 Yearbook and at the Reception for the Carlson Chair, which he endowed at U C Berkeley, November 1984 courtesy of MATRIX, Karen Holterman, Editor.) (September 20, 1900 - living in Berkeley, Calif)

BOTTOM ROW - LEFT TO RIGHT

Dr. Arnold U. HUGGENBERGER (1895 - 1981) of Switzerland. See Appendix 4. He is the inventor of the Huggenberger Extensometer, one of the most durable mechanical strain gages, used from 1924 through the 1960s and even today. Photo '65.

Dr. Earle L. KENT (May 22, 1910 - living in Elkhart, Indiana). One of the two "unwitting" inventors of the printed circuit in 1936; see body of paper. Photo from 1960.

Dr. LeRoy C. PASLAY (December 26, 1907 - living in Manalpan, FL). The second of the two "unwitting" inventors of the printed circuit, fore-runner of the foil strain gage, in 1936. Photo from 1985. See body of the paper.

Dr.-ing. Paul EISLER (May 5, 1907 - living in London, England,) the deliberate inventor of today's printed circuit. Photo circa 1989. He is holding the first radio set using a printed circuit chassis and aerial coil. Photo courtesy of Maurice Hubert, Multitech, UK, with permission of Lehigh University Press, from his book: My Life with the Printed Circuit, 1989.

CONTINUED FROM PAGE 18.

Greer ELLIS (June 7, 1910 - living in Mattapoisett, Massachusetts, inventor of Stresscoat, at the 50th Jubilee Celebration of his invention.

Dr. William M. MURRAY with his wife, Joan, at his retirement from M.I.T. in 1973.











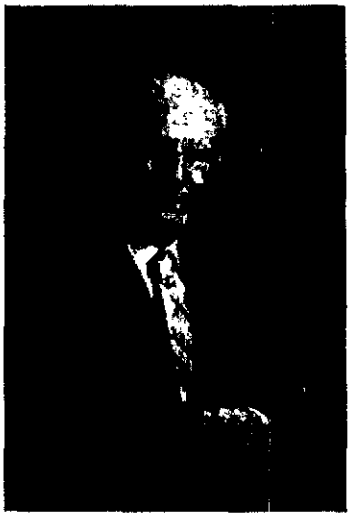


(Continued from page 16)

It is fortuitous that in the same year and at the same institution, and even in the same laboratory in which the bonded resistance strain gage, as we know it today, was developed, the first commercially successful brittle coating was developed as the result of a Master's Thesis.

In 1936, Greer Ellis had arrived at M.I.T. with his BS in Physics and practical experience at the National Bureau of Standards. He received his Master's Degree in Aeronautics in June 1938 and for his Thesis had worked in A. V. de Forest's lab developing a brittle coating which could be sprayed on to parts, and which would crack before the parts themselves were over-strained. He called the coating Stresscoat (RTM). It was commercialized by "A.V." through his Magnaflux Corporation and by 1940 had become a successful adjunct to strain gage work and often sufficient in itself to solve important stress analysis problems. After some years propagating his invention, and doing consulting work, Greer started his own company, Ellis Associates, designing and manufacturing electronic instruments, primarily signal conditioning and readout instruments for strain gage and transducer work. His designs still survive, and the BAM-1 Bridge, Amplifier and Meter is still made substantially as he designed it in the early 1950s, a true tribute to a great designer.

Vishay Intertechnology bought his company in the 1970s and it is today part of Measurements Group, Inc. Ellis lives in Mattapoisett, Massachussetts where he celebrated his 80th birthday in 1990.

COMMENT

Of necessity, the descriptions and biographies presented here, are abbreviated. A much fuller version of the contributions of each of the pioneers presented here, will be found in THE GOLDEN BOOK OF STRAIN GAGES, LOAD CELLS AND BRITTLE COATINGS - The History, Not Only of the Technologies but of the People Who Made Them Possible. The book includes the Proceedings of 4 Golden Jubilee Celebrations held between June 1988 and January 1990 to celebrate 50 years since the commercialization of these valuable experimental stress analysis methods.

NOVA SCIENCE PUBLISHERS, INC., 283 Commack Road, Suite 300, Commack, NY 11725-3401; $195 available in 1991, over 1000 pages, 8½"x11", featuring over 120 authors from 22 countries. Edited by Peter K. Stein, Jubilee Organizer & Arranger; Prof. Tamas Kemeny, Secretary-General, International Measurement Confederation (IMEKO) and Karolina Havrilla, IMEKO Secretariat.

THE STRAIN GAGE / BRITTLE COATING PIONEERS OF 1936, FEATURED IN THIS PAPER - CONTINUED

TOP ROW - LEFT TO RIGHT

Charles M. KEARNS, Jr. (March 20, 1915 - living in Tucson, Arizona.) Inventor of the bonded carbon gage, see body of paper.

Dr. Gottfried DÄTWYLER (January 13, 1906 - July 30, 1976). He made the first bonded resistance strain gage in 1936 at the suggestion of Edward E. Simmons, Jr, at Cal Tech.

Dr. Donald S. CLARK (December 26, 1906 - November 17, 1976). He was in charge of the Impact Project at Cal Tech for which the bonded resistance strain gage was invented.

Edward E. SIMMONS, Jr. (March 30, 1911 - living in Pasadena, California) in white, showing the Longstreth Medal awarded him by the Franklin Institute, to Frank Tatnall (on the right) and to Baldwin-Southwark management (left). The ceremony was held Spring 1944.

SECOND ROW - LEFT TO RIGHT

Edward E. SIMMONS, Jr. with Peter Stein at the February 1989 meeting of the Southern California Section of Society for Experimental Stress Analysis.

"Prof" Arthur C. RUGE (July 28, 1905 - living in Lexington, Massachusetts). 1938 photo by Hans Meier of "Prof" with his model water tank, strain gaged with his (re)-invention: the bonded wire strain gage.

J. Hans MEIER (October 9, 1913 - living in Vestal, New York). 1938 photo of Hans with the Wheatstone Bridge he used for his doctoral dissertation on bonded resistance strain gages.

THIRD ROW - LEFT TO RIGHT

Dr. J. Hans MEIER and "Prof" Dr. Arthur C. RUGE who has just been awarded the Inventor of the Year Award by the Boston Museum of Science in 1986. Photo by Maarten Spoor.

Frank F. HINES in 1939 on his Bachelor's Thesis concerning strains on a pulley, as measured with the new bonded resistance strain gage. (December 5, 1913 - living in Hudson, NH)

Dr. William M. MURRAY (April 24, 1910 - August 14, 1990) in January 1960, Phoenix, Arizona.

BOTTOM ROW - LEFT TO RIGHT

Frank F. HINES from the 1939 M.I.T. Yearbook and at the 1989 Jubilee Celebrations, 50 Years of Strain Gages, Load Cells & Stresscoat.

Continued on page 16 .








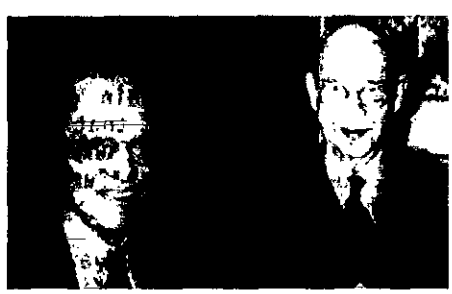





APPENDIX

(1) "Stress-Strain Relationships under Tension Impact Loading", by Dr. Donald S. Clark and Dr. Gottfried Dätwyler, Assistant Professor of Mechanical Engineering and Research Fellow in Aeronautics, respectively, California Institute of Technology, Pasadena, California. Symposium on Impact Testing, ASTM June 1938. Proceedings printed in January 1939, Copyright 1939. Proceedings of the 1938 Annual Meeting.

(2) When the team of "Prof" Ruge, Hans Meier and Frank Hines at M.I.T., heard about the Clark & Dätwyler paper (cited above) some time after February 20, 1939, great disillusionment and despondency descended on them. They were readying their version of the bonded wire resistance strain gage for commercialization. Hans Meier remembers: "I just had time to include the reference in my doctoral dissertation!"

It was "A.V." de Forest who had gone through the same situation in 1929 with the Magnaflux patents, who saved the day. He told Ruge that Simmons might get the basic patent but that he, Ruge, would have any improvement patents; that the promise of commercialization and financial return was great, and that he should go ahead. It was also "A.V.", with his existing ties with Baldwin-Southwark through his Scratch Gage, that brought Ruge together with Baldwin, who, in turn, approached Simmons to join the enterprise.

Without "A.V."'s experience and business acumen, the history of experimental stress analysis would have developed along quite different lines.

(3) Scratch gages are still used today. Two surviving varieties used in applications ranging from off-shore platforms to all first-line aircraft in the U.S. Air Force utilize their distinct advantages: it is diver-installable and retrievable, operates unattended, is self-recording, requires no electrical connections or lead wires, is radiation resistant, and can be self-temperature compensated. Two manufacturers are:

Prewitt Associates, Scratch Gage Div, P. O. Box 365, Lexington, KY 40501. Their gage is suitable for low-frequency work such as the off-shore platform application.

Leigh Instruments Ltd., Avionics Div., Box 820, Carleton Place, Ontario, Canada, K0A 1J0. A removable cartridge contains a roll of steel tape on which the record is inscribed. In aircraft applications, the cartridge will record 150 flight-hours of vibration experience and can then simply be exchanged for a new one.

(4) - OTHER STRAIN GAGES IN USE IN 1936

Although the author is not aware that 1936 was a crucial year for the many mechanical and inductive strain gages used for stress analysis and in some transducer applications, the one mechanical strain gage which should be mentioned is the Huggenberger Tensometer. It was perhaps the most widely used gage for many decades.

In 1924, Dr. Arnold U. Huggenberger in Switzerland, invented a compound-lever mechanical strain gage. The two popular models had magnifications of 700 and 1200. It was sold in the U.S. by Baldwin-Southwark already before 1930 and the author used them through 1955.

It had to be clamped to the test specimen by one of a variety of ways - mechanical, magnetic, electro-magnetic, and was suitable only for static measurements. A line of sight was required to read the position of the pointer against a scale.

Dr. Huggengerger (1895-1981) was a world-renowned expert in instrumentation of dams and large concrete structures. His company also manufactured bonded resistance wire strain gages based on the method of Dr. Gotthard Gustafsson (November 14, 1902 - March 5, 1975) which circumvented the Simmons patent. He also copied Roy Carlson's unbonded wire strain gage transducers and sold them along with a line of electrical/electronic strain indicators and signal-conditioning/read-out instrumentation.

Dr. Gustafsson was with the Aeronautical Research Institute of Sweden, and the gage was known as the G-H Tepic, for Gustafsson-Huggenberger Tensio Pickup.

(5) Twenty-one countries besides the United States, report on the state of strain gage technology in the 1930s and 1940s and the arrival of the bonded resistance strain gage in each country. The circumstances of that arrival and the pioneers involved in the early work, are described in the GOLDEN BOOK, referenced in the "Comments" section above.

(6) It is interesting that the very first successful application of bonded resistance wire strain gages was on a problem still considered challenging: high-speed transient force measurement during impact. Electrical engineer (with a Master's degree) Ed Simmons developed circuitry, triggering and single-current-pulse techniques which are still modern, on that first application in 1936 !

==========

Note: The author is still "excavating strain gage history". Any help will be most welcome if you have additional information or corrections.

(7) A. Bloch, "New Methods for Measuring Mechanical Stresses at Higher Frequencies," Nature, Vol. 156, No. 3432, August 10, 1935, pp. 223-224. Discusses carbon pile and piezo-electric transducers as well as a painted carbon film.

(8) E. H. Hull,"Alternating Stress Measurement by the Resistance Strip Method", General Electric Review, August 1937, pp. 379-380 presents Edwin Hull's Aquadag (RTM)-based painted carbon strip. In 1935 he had experimented with the method by painting a small strip of paper with India ink. This gage he had used successfully in measuring strain concentrations in fillets on steam turbine shafts, as reported in: Claude M. Hathaway, "Electrical Instruments for Strain Analysis", Proc., Society for Experimental Stress Analysis, Vol. I, No. 1, 1943, pp. 83-93. Claude Hathaway, (December 20, 1902 - ?), got his BS EE at University of Colorado in 1927 and his MS EE in 1928. From 1929-1939 he worked at General Electric Company, Schenectady, New York, mostly in the General Engineering Consulting Laboratory. He started Hathaway Instrument Company in Colorado in about 1938/39 and sold it to Hamilton Watch Company in January 1955.

While at GE, Hathaway made and worked with electromagnetic strain gages and the signal conditioning and galvanometers for recording their output, starting in 1934. He did preliminary experiments on strain sensitivity of wires and conceived of bonding a wire to the surface of a test speciment for strain measurement in 1937.

"In those days it was very difficult to sell anyone outside of the communications field, electronics; they were all afraid of vacuum tubes," he said in his June 23, 1958 deposition (72 pages) in the landmark law suit: Baldwin-Lima-Hamilton Corporation and Edward E. Simmons, Jr., vs. Tatnall Measuring Systems Co., and the Budd Company, U.S. District Court, E.D. Pennsylvania, Dec. 1, 1958, Civil A. No. 23505.

"Throughout all industries except the communications industry, heavy machinery industry, the Central Station industry were all afraid of vacuum tubes." "Because the wire gage was about 1/100 as sensitive as carbon resistance gages, the practical application of this type of gage had to wait a few years until industrial electronics caught up with it." "It was impossible - at least I was unable to, sell the resistance strain gage to industry at the time. Although I, personally felt that it had potential and that we could develop a satisfactory electronic equipment to use it. I was unable to sell it." By the time he had his own company, the SR-4 "Metalectric" bonded wire strain gage of Prof. Ruge was already commercially available. He was not allowed to follow his research in that field, at G.E. !

(9) From Dr. Gottfried Dätwyler's Deposition of February 9, 1958 in the same law suit referenced in Appendix (7), some interesting facts emerge which fill holes in the story as previously available.

After receiving his doctorate in Switzerland in 1934, he spent about 6 months in the family plant in Altdorf, Switzerland. The plant produced electric wires and technical rubber goods amongst other products. They were having some problems with the wire drawing process.

In September 1934 he landed in the U.S. and drove across the country to Cal Tech. Prof. von Karman had assured him a Research Fellow position in Aerodynamics, his major field. At Cal Tech, however, he found that the wind tunnel "was busy with confidential work, and as an alien I couldn't get into the tunnel. After I got tired of just pencil pushing, I got in contact with Prof. Clark, Professor in Metallurgy and Testing Materials. We got to talk about various problems of metals, mostly in connection with the copper wire drawing problem which they had in Altdorf, and then I got more into the field of testing materials."

Dätwyler described the start of the Impact Project at Cal Tech, and the meeting at which some $10,000 were raised by a group of sponsors.

Work started June 20, 1936. By July 29, he was working with Aquadag, all the way through September 8. He was aware of Carlson's unbonded wire strain gage and of Kearns' work at Hamilton Standard Propeller of just a few weeks before, through private correspondence with the Hamilton group, but apparently did not use the Kearns gage.

September 10, 1936 was the date when Ed Simmons suggested using a bonded wire, and when No. 36 gage, cotton-wrapped Advance (constantan) wire was bonded to a spring steel strip with Glyptal cement. Later he used No. 40 gage varnish-insulated wire.

"I had just a straight piece of wire, varnished on to a spring steel strip. By bending the steel strip into a U-shape, resistance increased by 0.25 ohms. The initial resistance was 17 ohms ... No shifting of zero after several tests; wire finally broke." The 1.4% resistance change would be 7000 microstrain!

The Aquadag-based strain gage had shown incurable zero-shifts, drifts and hysteresis effects which made in useless for his purposes.

Impact Research Report # 1 - Confidential, was signed by Dätwyler, Prof. Don Clarke and Professor von Karman. It was released to no one outside the Impact Project except its sponsors.

==========

Author: Peter K. Stein, M.Sc., P.E., President
STEIN ENGINEERING SERVICES, INC.
5602 East Monte Rosa, Phoenix, AZ 85018, USA
Telefon & FAX: 602-945-4603

Arranger and organizer of the Golden Jubilee Celebrations for Strain Gages, Load Cells and Brittle Coatings, 1938-1940 / 1988-1990.

COLLECTING, MANAGING, AND DISTRIBUTING INSTRUMENTATION SYSTEM CALIBRATION INFORMATION IN A HIGH VOLUME, DATA PRODUCTION ENVIRONMENT

Lee S. Gardner
6521 Range Squadron
Air Force Flight Test Center
Edwards AFB, CA

ABSTRACT

The Air Force Flight Test Center (AFFTC) at Edwards AFB handles a large number of highly diverse flight test programs on a continuing basis. Projects requiring real-time telemetry (TM) and/or post-flight data analysis use one or more of the data production systems in Ridley Mission Control Center (RMCC). In order for these various systems to perform engineering units conversion on TM and other flight test data, the airborne instrumentation system and the ground-based analysis system must be compatible. Telemetry formats, measurement calibrations, frequencies, etc. must correspond.

In the past, this process used individual calibration sheets for each aircraft instrumentation system change. The data from these calibration sheets were then entered into ground-based analysis system setup files manually. This manual process was prone to transposition and other data entry errors. In addition, some of the analysis system files reflected information valid for only one flight. This closed, manual system had limited capability to maintain an historical record of project instrumentation changes.

With the increasing sophistication of instrumentation systems, the time required to set up the airborne systems for a test decreased. However, the larger number of measurands has resulted in unmanageable growth in labor hours to complete the manual update process. The time required to prepare ground-based analysis systems has increased, causing widening disparities between the setup times required for airborne and ground systems.

This paper discusses the calibration handling problem and describes the Aircraft Information Management System (AIMS) currently being operationally deployed in the 6521 Range Squadron to solve the problem.

INTRODUCTION

Airborne weapons system testing requires measurements of critical physical system characteristics while the system undergoes a specific test scenario. System actions and reactions to the test conditions are recorded and/or transmitted in real-time to provide the foundation for detailed analysis of test results. This analysis is performed by ground-based real-time and post-flight systems. The system under test transmits and records information during the test and ground systems analyze that information during and after the test.

Instrumentation systems provide the physical means for collecting, transmitting, and recording the required measurements. They use electrical devices called transducers that react to the quantity being measured by changing the way the transducer behaves in an electronic circuit. The voltages or amperages of these transducer circuits are organized into a formatted signal that is transmitted during real-time system monitoring and recorded on special magnetic tape for post-experiment analysis.

Other data sources onboard are also recorded. These may include a Global Positioning System (GPS) or an Inertial Navigation System (INS), computer bus mes-

sages, system state variables, time code generators, etc. All these measurands can be included with transducer measurands in the transmitted and recorded signals. For each measurand type some method of regaining the content of the original measurement is needed.

Two critical pieces of information are necessary to decode these formatted signals and recover the original engineering units for analysis: decommutation data and calibration information. The decommutation information explains how to divide the formatted signal into pieces representing each measurement. The calibration information describes how to convert these pieces, which represent amps or volts, into the original physical quantities measured on the test vehicle.

Future instrumentation systems and ground-based analysis systems may share even more information. Descriptions of data displays, video links, as well as real-time air-to-air and air-to-ground data link signal definitions may soon become part of the information required to support a flight test project. Any comprehensive information management system design must include the flexibility to adapt to new ways of capturing, storing, and distributing measurement and other information during a test.

The AIMS provides a way to collect these types of information, manage them, and selectively distribute them to the systems that perform the actual decommutation and conversion algorithms.

CHALLENGES AND REQUIREMENTS

Instrumentation systems on test aircraft may be provided by a contractor, they may be provided by the test organization, or they may be a mixture. The collection of decommutation and calibration information from contractors and from the in-house instrumentation group presents a significant challenge to any system proposing to manage that information. Although there are standards governing instrumentation system configurations, there is still great variability between manufacturers. Any system designed to manage decommutation and calibration information must have a flexible input processor to accommodate all the different ways instrumentation groups maintain that information.

The sophistication of all these different instrumentation systems is increasing. It used to be that decommutation information was very stable. Once a transmission/recording format was defined, few changes were made throughout the life of the project. Calibration information might change only when one transducer was swapped for another due to failure.

Modern instrumentation systems are completely programmable. The stability of the past is giving way to total flexibility. Testers can literally program the instrumentation system for one test in the morning and a completely different test in the afternoon. This implies a vast increase in the number and volume of possible changes made during a test program. Since flight test project engineers require the capability to replay or recalibrate any previous flight from original recordings, the calibration handling system must retain a complete historical record of all changes during the life of that project.

The flexibility of the airborne instrumentation system requires similar capability in the ground analysis systems. To achieve this flexibility, the setup time required for ground-based systems must more closely correspond with the airborne system setup times. This means less reliance on manual processes in the exchange of decommutation and calibration information. Also, the data exchange must be accomplished with an increase in the certainty that the information and the mission setup are correct for all analysis systems used on a program. The system that receives decommutation and calibration information from the instrumentation group must quickly, efficiently, and accurately pass that information on to ground-based test support systems.

Ground-based analysis systems have considerable variability in the syntax of the instruction sets they use for setup. Although they all require the same information, the details of how that information is presented to each system differ greatly. The system that creates these setup files must have a flexible output processor to accommodate the input needs of different analysis systems.

Any system that truly manages decommutation and calibration information must: (1) have a flexible input processor to accommodate information from many different instrumentation groups, (2) maintain an efficient historical record of all changes in the instrumentation

system throughout a project, (3) have a flexible output processor to provide various set-up files required by ground analysis systems, (4) be capable of rapid transfer of information via high speed networks and/or magnetic tape, and (5) process the information quickly and accurately to keep pace with the set-up speed of airborne systems.

CURRENT SYSTEM

At the AFFTC, decommutation and calibration information is currently maintained in several different file types depending on which real-time or post-flight system (or systems) a particular flight test project is using for analysis. One or more of three main systems are used on most projects: The Integrated Flight Data Processing System (IFDAPS), the Standard Analog to Digital System (SANDS), and the SCI System (named after its primary contractor).

Each ground-based analysis system uses a different instruction set which is created and maintained via a mostly manual process. Calibration sheets are produced by the engineers in the responsible instrumentation organization and passed on to the 6521st Range Squadron for distribution to all the processing systems that the project uses. The systems are then manually updated for each flight test for every project.

The IFDAPS is used for real-time mission support and post-flight data playback. Decommutation and calibration information is stored in separate sections of an IFDAPS Source Language (ISL) file, which is manually updated from handwritten calibration change sheets for every flight. The ISL files from previous flights are maintained for some projects, but IFDAPS does not generally maintain an historical record of previous calibration changes and setups for earlier flight replays.

The SANDS system is really two systems: The Post Flight Processing System (PFP) and SANDS itself. The PFP does the decommutation producing a digital tape which contains tagged data. The SANDS reads the PFP output tape and performs the engineering units conversion on the tagged data. The Decom deck is the instruction set to the PFP System. The Project History is the

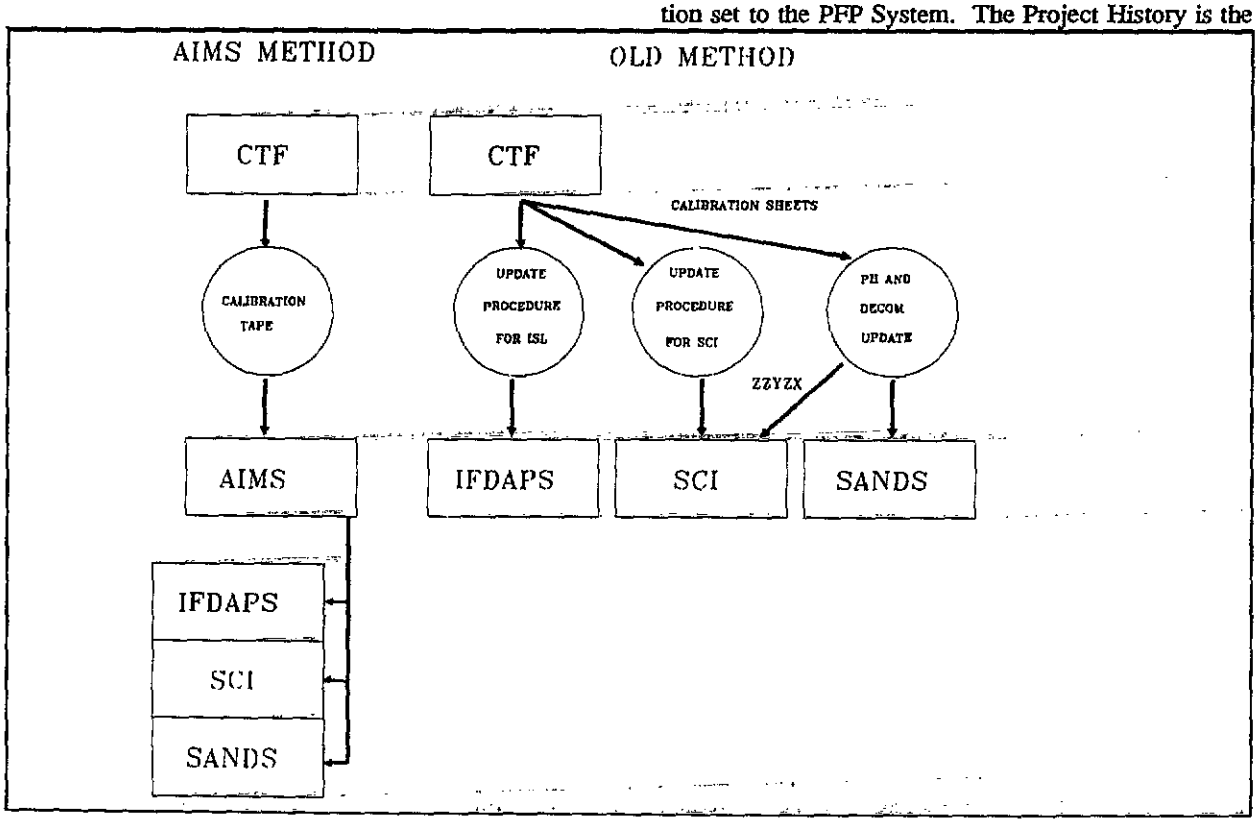

Figure 1 - Existing System Diagram

instruction set for SANDS. Both Decom Decks and Project Histories maintain an historical record of calibration changes which makes redigitization and calibrations of data from earlier flights routine. The maintenance and updating of both these files is largely manual, with some automated quality checking.

The SCI system uses a file called an SCI Deck which contains both decommutation and calibration information. Like ISL, the construction and maintenance of SCI Decks is mostly a manual process. The SCI Decks can be produced from a Project History File, however, which provides some automation. Also like IFDAPS, the SCI Decks from previous flights can be saved, but there is no inherent historical function that can be used to get valid information for earlier flight replays.

The existing calibration and decommutation information handling system has difficulty as the number of changes since last flight increases. With thousands of transducers whose measurements can be organized into several new formats per test flight, update times of minutes per change must be compressed to seconds. Manual processes simply cannot keep pace with the increasing volume of information that must be stored and distributed rapidly and accurately.

The large number of parameters per aircraft and the rapidly changing nature of the data about those parameters are overwhelming the existing Project History File construct and the manual process that supports it. Project Histories store parameter attribute information in 80 column IBM card images. Many existing projects already have several Project History Files per aircraft, emphasizing the need for a more efficient information storage structure.

AIMS DATA FLOW

The Aircraft Information Management System, AIMS, is designed to be the bridge between an instrumentation group's database and the real-time or post-flight analysis systems. The decommutation and calibration information for a project flows from the instrumentation database through AIMS to the ground-based analysis systems. Here are the steps in the process.

1. All the changes to the instrumentation system since last flight are extracted from the instrumentation group's data system. These changes are extracted in an agreed format as documented in an Interface Control Document (ICD) and transmitted via the agreed media, a network file transfer or magnetic tape to the 6521st Range Squadron's Main Scientific Computer.

2. An AIMS translator transforms the external data files into its standard file structure, the keystream.

3. The keystream from the translator is then used to update the AIMS file, the repository of historical instrumentation system information. Only changes are stored.

4. A keystream is selected from AIMS which includes either all of the information for a flight or just the changes since last flight, depending on the ground-based system's requirements.

5. That keystream is post-processed to conform to the data exchange structure between AIMS and the ground-based analysis system as described in another ICD.

6. The analysis system uses the post-processed file to setup for the mission.

AIMS KEYSTREAM

The AIMS uses a standard input/output file called a keystream. It is a parameter oriented ASCII file with free formatted records. Each record is of the form

keyword = value(s)

A parameter section begins with the keyword PARAMETER whose value is the parameter name. Subsequent records contain keywords and values that describe the decommutation and calibration information for that parameter. The section ends with an ENDPAR keyword (with no value associated). The following is an example parameter section from an AIMS keystream (References 1 and 2).

```
PARAMETER = ALT
    TITLE = 'MSL ALTITUDE'
     WORD = 4
     FRAME = 0
     UNITS = FT
     NCOEFS = 2
     COEFS = 0.0, 1.0
ENDPAR
```

AIMS TRANSLATORS

The AIMS has associated software programs, called translators, that transform an instrumentation maintenance group's computerized decommutation and calibration data into a keystream. These translators are written as required based on an Interface Control Document (ICD).

The ICDs describe in detail the media, files, records, and bits (if necessary) of the information exchanged between two groups. An ICD is negotiated between the groups and represents a formal agreement to stabilize the information exchange.

The ISDs can also describe standard keywords that carry the same meaning for all projects. The use of standard keywords in AIMS allows cross-project continuity and eases the training load for people who work on data for several projects.

AIMS DATA STORAGE AND RETRIEVAL

The AIMS command "Update" processes the keystream from the translator. Update checks existing records in the AIMS file and stores only changed information. Update writes a changes file in keystream format that represents all the changes accepted.

When all the updates have been processed for a particular flight, the team responsible for data processing requests the calibration and decommutation data for that flight.

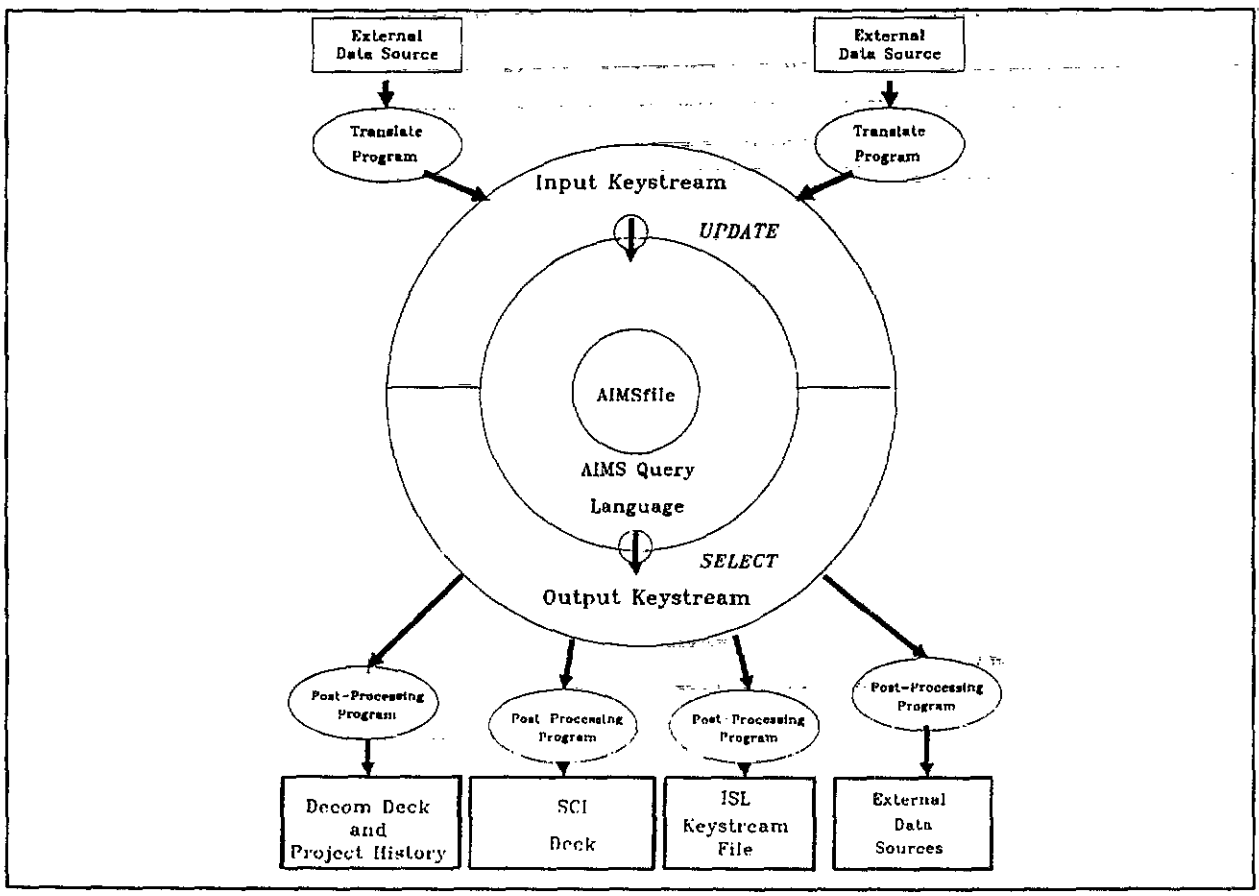

Figure 2 - AIMS Data Flow

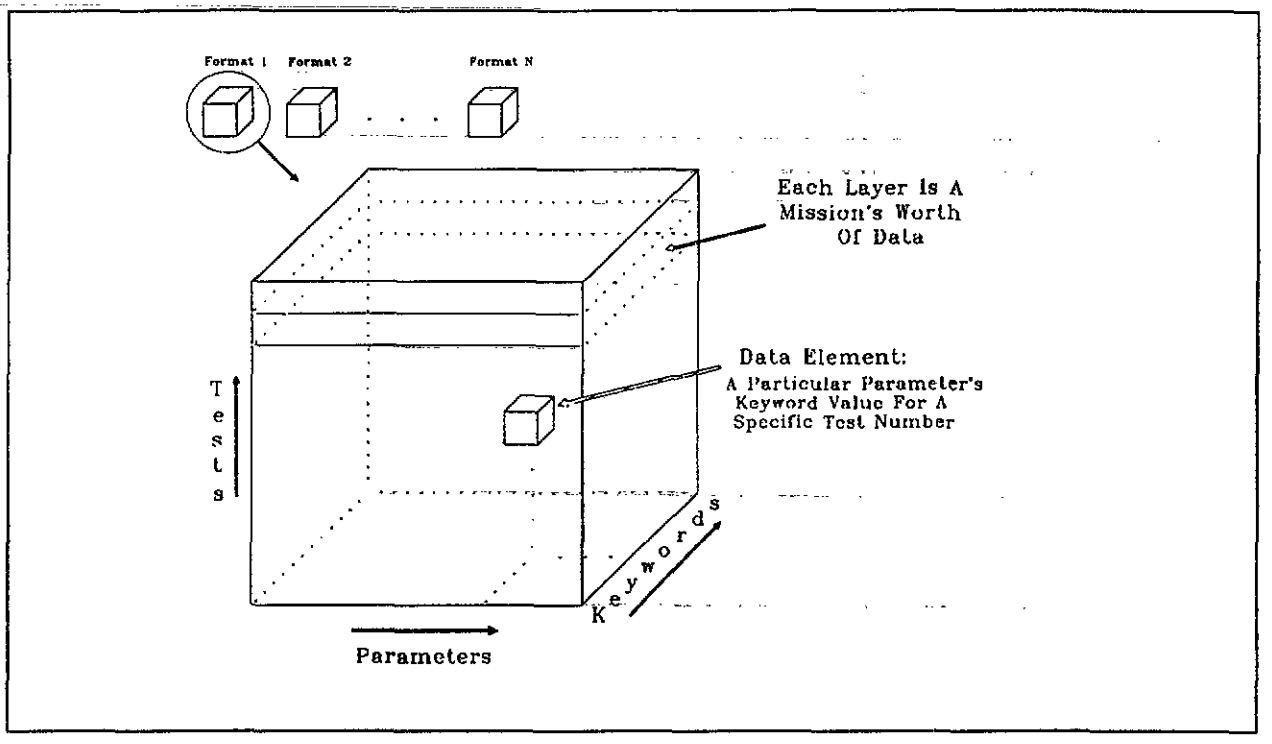

Figure 3 - AIMS File Structure

The AIMS "Select" command provides this capability with a variety of options. Select produces an output keystream that contains the desired data.

AIMS POST-PROCESSING

This output keystream is then post-processed into the format required by the real-time or post-flight systems being used by the project. These post-processing programs are also written based on previously negotiated ICDs. If the projects choose to use standard keywords in their AIMS files they can often share post-processors.

DETAILS OF THE AIMS DESIGN

The design of the AIMS file facilitates its functionality. The AIMS file is organized hierarchically, like the data it contains. At the highest level of the file is the parameter list. This is a linked list of individual parameter records which is always maintained in lexicographic order. Visualize this list as comprising one edge of a data cube.

Subordinate to each parameter is another linked list of keywords, which describe that parameter's attributes. The keywords are also in lexicographic sequence in this second list. To handle projects with multiple transmission/recording formats, keywords can have a format specific suffix. Thus multiple formats implies multiple entries with different suffixes for each affected keyword. The keyword list comprises the second dimension of a data cube.

The lowest level is the data for each keyword. This is maintained in a third linked list subordinate to each keyword. The data elements in this lowest level list represent the change history for that keyword, with the most recent change at the head of the list. Visualize this as the vertical dimension of the AIMS data cube. This design stores data in minimal space. Only data that has changed is maintained and data access is quick and direct.

In addition, the AIMS has some other unique features. It has a flexible parser based on formal language theory which parses both the keyword stream and the command

line input. This parser is easily ported to become the input portion of an AIMS post- processor. AIMS has a small set of user commands (two main commands and three auxiliary commands including "HELP") which use a consistent set of options. This feature makes AIMS easy to learn and use. The AIMS design has also been implemented to work in both batch processing and interactive processing modes, which allows users further flexibility in how they use AIMS and how they manage their AIMS workload (References 1 and 2).

PRACTICAL RESULTS

Preliminary tests show a mean processing time of 2.4 seconds per parameter (actual clock time under busy system conditions) based on an Update of 939 parameters with all new information into an empty AIMS file and then a Select of all the data in the file (28 minutes for Update, 10 minutes for Select). This test is on the first implementation of AIMS without planned optimization reviews. Additional tests show translation times of 0.05 second of processing time per parameter and 0.33 second to post-process into a SANDS Project History and Decom Deck. The total processing time of a parameter through AIMS is less than 3 seconds clock time, beating the 10 second worst case requirement with better times depending on system traffic.

The initial implementation of AIMS was on a CDC 994 CYBER computer running the Network Operating System (NOS). The modification of four statements, the file open, close, read, and write allowed the software to be transferred in total to the NOS/VE (Virtual Environment). The software requires an ANSI FORTRAN 77 Compiler, and FORTRAN callable routines to access a word (or byte) addressable file structure.

The calibration information previously stored in Project History card images in eight NOS words (ten characters per word) are stored in 1 word per calibration coefficient in AIMS. This amounts to an average of 2.7 to 1 storage savings for real-valued data.

CONCLUSIONS

The AIMS system has met performance requirements even before fine tuning. The preliminary performance studies show ten to sixty times the productivity to update decommutation and calibration information over the existing manual processing system. The AIMS is also immune from transposition and data entry errors, since people do not interact with the actual data.

The resulting system is highly portable. It requires changing four file access statements to port the code to another system. The system must have a FORTRAN compiler and a word or byte addressable file structure to support the AIMS.

The system meets storage minimization requirements in that it stores a minimum of data required in the smallest space. Overhead for AIMS list constructs has not been taken into account in the data compression estimates. Data for only a few tests have been stored in any project AIMS file so far, so the total storage capability per project question remains unanswered.

The keystream provides a standard I/O interface that can be read and checked for quality. This idea of a standard file structure for both human and machine consumption is so important that members of the AIMS design team are promoting the keystream structure for acceptance by the instrumentation and real-time and post-flight processing communities.

Translators and post-processors provide the flexibility required to import/export external calibration and decommutation file types. A project negotiates a decommutation and calibration information exchange media and structure in an Interface Control Document (ICD) which forms the basis for development of translators or post-processors. Organizations that can produce and ground systems that can accept the standard keystream file require no translator or post-processor.

The set of parameter attributes required to support a particular ground analysis system depends on that system's capabilities, but certainly there is a critical kernel of information required by all systems. The AIMS has a standard set of parameter keywords that represent that kernel and allows flexibility in adding attributes for particular systems. For example, SANDS and IFDAPS use the keywords "word," "frame," and "depth" to indicate word location in subframe, subframe number, and the number of repetitions across subframes (subcommutation depth). These parameter decommutation attributes are in the kernel. But IFDAPS drives graphical devices and requires standard and critical limit attributes to con-

trol color changes on real-time displays. The SANDS produces an engineering units tape and has no such need. The AIMS can contain the extra limits for IFDAPS without affecting how keystreams are post-processed for SANDS (or any other system).

The AIMS should be considered to replace manual calibration handling procedures wherever timeliness and accuracy of instrumentation decommutation and calibration information are critical.

BIBLIOGRAPHY

Jones, Charles H. (author), Hoaglund, Catharine M., Flanders, Joey B. (eds), *AIMS Aircraft Information Management System User Guide*, Software Library, Computer Sciences Branch, 6521 Range Squadron, Edwards AFB, CA.

Jones, Charles H., Hoaglund, Catharine M., Flanders, Joey B., *AIMS Aircraft Information Management System Programmer's Guide*, Software Library, Computer Sciences Branch, 6521 Range Squadron, Edwards AFB, CA, Preliminary as of May 91.

COLLECTING, MANAGING, AND DISTRIBUTING INSTRUMENTATION SYSTEM CALIBRATION ON INFORMATION IN A HIGH VOLUME, DATA PRODUCTION ENVIRONMENT

SPEAKER: Lee S. Gardner, Edwards AFB, California

Q: Peter Stein (Stein Engineering): Are the data from the contractors with whom you work compatible with your file? Is their data base compatible with what you need?

A: So far, my experience has been no, but that has been limited somewhat. We have been able to accommodate their data structures in most cases or meet somewhere in middle ground. We typically develop an interface control document with that company or group. There is great variability among those systems.

Q: Are you proposing some sort of a standard format in which contractors may want to keep their data base, so compatibility can be achieved all the way around? That would be a great step forward.

A: Yes it would. No, we haven't proposed such a thing, but I think there is some committee in the group that is working on something like that. I heard at a DR&CG meeting last February that a committee is working on standardization.

Q: Frank Hartley (JPL). Isn't the 1553 bus the standard used in the aircraft industry for a lot of this instrumentation?

A: Yes, the 1553 bus is a standard. Although it is a standard, there is still a lot of variability.

Q: In terms of automized test support and collecting the information, can you still use the information protocol of that system to work in your telemetry system?

A: Yes, you could still use the protocol, but there is great variability among 1553 bus information in my experience.

Q: Did you look at that rather than PCM data, telecommunication?

A: Traditionally, we use quite a lot of PCM systems. They're still around, so that is what we're accommodating.

Q: But you're moving away from the A column card, too. It would seem like that would be a good place to look.

A: The project we're supporting right now, which is a pilot project, is just getting into resolving the 1553 bus issues they have on the system. We're learning more and more about the 1553 bus as we go through that project.

AUTOMATED STRUCTURAL GRAVIMETRIC CALIBRATION OF ACCELEROMETERS WITH AN ECONOMICAL PC/DATA ACQUISITION BOARD COMBINATION

Michael J. Lally, University of Cincinnati

Usually time consuming and troublesome, calibration is often neglected prior to performing an structural measurement. Providing a degree of automation, an economical PC/Data acquisition board combination with the Structural Gravimetric Calibration method expedites the calibration process. Results can be obtained by a drop test (accelerometers and force sensors) and by random excitation (accelerometers) with automated curve fitting and archival. Calibration data can also be obtained from single frequency "1 g" exciters. All pertinent data is stored into a data base for trending and quality assurance purposes.

AUTOMATED STRUCTURAL GRAVIMETRIC CALIBRATION OF ACCELEROMETERS WITH AN ECONOMICAL PC/DATA ACQUISITION BOARD COMBINATION

SPEAKER: Rick J. Lally, PCB.

Q: Bob Sill (ENDEVCO). How do you account for the mass of the cables going in the accelerometers? During this drop they are not going.

A: They are attached as well. As a matter of fact, what you generally do in the first place when you are doing high frequency calibration, is find the lightest, flimsiest cable you can get your hands on, so its effect doesn't create a lot of transverse motion in your test fixture or in your drop calibration test. The masses of cables become essentially negligible in either test set-up, whether its a drop test or the frequency response test.

Q: How much do they contribute? You have mass in the cables. What do you use as your effective mass?

A: The cables must be attached during the drop test. The drop test accommodates the amount of mass on the test fixture in the first place. If, in fact, the cables represent a significant mass through the system, the lightweight cables effects are negligible or less than 1 percent. Essentially in the drop test, the cables are attached, and you can let the same amount of cables lay free as in the frequency response test and use the mass as some weighting value. Effectively, you are chasing around a very insignificant detail. You are going to run into far more difficulties with the basic fixturing of the transducer on the shaker in trying to create one degree of freedom-of-motion and not sensing other parameters.

Q: Scott Walton (U.S. Army Aberdeen Proving Ground - Combat Systems Test Activity). I don't understand how you're getting 100 kHz frequency response. This question is in three parts. Are you shaking this thing up to 100 kHz or are you giving it a step function with a sharp rise time? Do you really trust the load cell up to 100 kHz? Even if I did trust that load cell, if I had anything I could excite it with that had content up to 100 kHz, but there's no such thing as a rigid body above 2-5 kHz.

A: These are pretty common questions, and they're not simple ones either. Yes, yes, and the last one wasn't a yes or no question. I'll take the questions in order. First question: How do you know it works to 100 kHz? What I told you was that for it to do that, the force sensor would have to be an idealized spring. There would have to be no modes of vibration on the spring. Now, the things that do the sensing of the force sensors are crystals, whose natural frequencies are 1 MHz. If, in fact, that crystal is behaving as an ideal spring, then you can measure force to 100 kHz without any problem. Force on one end will equal force on the other.

Q: I'll buy the crystal as being the ideal spring, but it is the rest of that stainless steel around it.

A: Exactly. That's a really good observation. In fact, to make this work to 100 kHz takes a fairly special force sensor. You can't just use general purpose force sensors to go to very high frequencies because of contamination from housings and connectors. But consider for a minute, if you took a 1/4-inch piece of stainless steel, what is the natural resonant frequency?

Q: Seems like it takes about 200 kHz just to transverse and then come down.

A: Basically we use 1-inch steel. At the speed of sound, you have approximately 100 kHz resonance. So, if you drop it back to about 1/4 of a hertz, you end with about 400 kHz resonance for the speed of sound. This mode of vibration basically messes up your measurement.

Q: That's exactly what I'm worried about, if I'm within a third of that 400 kHz, then I'm in trouble, particularly if I'm going to talk about 1 dB.

A: I would like to calibrate to 100 kHz.

RICK LALLY: I finally found a customer. That theory is exactly what you have to apply, what you have to think about if you really want to scale the value. In addition to those other things I talked about in variance and actually putting the transducer down and really getting something repeatable, you mount it up to 100 kHz. I highlighted that because that's far more significant. The surface finish mounting torque will change your results by tens of decibels. Remember when I showed you how the resonant frequency was at 150 kHz, and we did come up with 1 dB at 50 kHz. We can and have done that a number of times. Experimental information indicates that we are getting correct scaling values at those higher frequency regions. Not knowing how else to measure them is the basic problem I have. All I know is over the normal bands we calibrate, I validated the method. Every time I could put that in and show we're within 1 percent, we've got the same result. My contention is then, this thing really is behaving as the system we're predicting and calculating. Because if it's not 1 dB here, it is going to effect things back at 20 kHz. If there is a significant rise of 50, there's going to be some rise at 20 kHz as well, and we're not measuring it there. We haven't seen it at 50 kHz based on our experimental results. In reality, if we approach it intelligently, we seem to be getting the right information. The bottom line is that we don't have any other way to get the information. How else are you going to get a scaling number? There's no other technique. At least, we're offering a technique that has some theoretical support and a lot of experimental validation over standard ranges. The second question was: How do you excite it? Anyway you want to as long as its got some

energy in it at the frequency you want analyzed. You can impact excite it. We shaker it, we electrodynamic shaker excite it. You don't need very many g's. You don't need very much displacement at all at 50 kHz to get a few g's to give you a reasonable signal-to-noise ratio. Actually, that's never been the limitation. The limitation has been "Can we create one degree of freedom?"

Q: But, your shaker does go up to 100 kHz?

A: The fact of the matter is that everybody's does.

Q: Mine does, but after 12 kHz, I don't believe it.

A: The bottom line is that it's moving, isn't it. All we care about is that we put some motion in there, because we're going to measure it with the reference sensor. We use a spectrum analyzer to sort the frequency content in the FFT process. We don't rely on sinusoidal excitation. As a matter of fact, what we do is a swept sign with an FFT process, which gives you great signal to noise. Basically, digital signal processing is how you get an accurate signal up to very high frequencies. I would have to demonstrate it for you to really appreciate the amount of capability. Thank you very much.

MULTIPLE ACCELEROMETER FREQUENCY RESPONSE EVALUATION

David Banasak, Air Force Wright Aeronautical Laboratory

This mini-paper describes a technique to obtain simultaneous frequency response calibrations of accelerometers. The technique involves mounting accelerometers to a rigid circular plate attached to a shaker. Random noise excites the shaker. A digital pulse code modulation (PCM) data system acquires and stores the responses on instrumentation tape. The data on tape is reformatted for computer analysis. The computer calculates each transducer's frequency response. The computer derives transfer functions between 15 unknown transducers and a DC responding reference accelerometer. This multiple accelerometer calibration technique compares well with four methods of single channel laboratory calibrations. The Structural Dynamics Branch tested the multiple accelerometer technique in the laboratory and in the field. The technique was used on a ground vibration test of a F-16 wing. The branch evaluated the frequency response of 37 accelerometers over a range of 0 to 100 hertz.

Exciting multiple accelerometers ensures calibration of each transducer at the same temperature, humidity and force input levels. The technique provides a quick, automated, end-to-end frequency response calibration. Sensitivities versus frequency correlate well with single accelerometer calibration.

MISSING PAGE

100

ABSOLUTE CALIBRATION OF BACK-TO-BACK ACCELEROMETERS AT HIGH FREQUENCIES

B. F. Payne
National Institute of Standards and Technology
Gaithersburg, MD 20899

ABSTRACT

Back to back accelerometers are becoming widely used as standards in vibration laboratories. Many problems arise in calibrating these standards at high frequencies. Until recently, these standards were calibrated by comparison to a single-ended accelerometer mounted on the top surface of the back to back pickup. In this paper, a method is presented for absolute calibration of back to back accelerometers in the frequency range of 5 - 20 kHz. A laser interferometer is used in this calibration method and the measurements are made at 121.1 nm displacement. This paper describes the measurement procedure and gives data for a back-to-back accelerometer for several calibration masses attached to the top surface.

INTRODUCTION

The back-to-back (BTB) accelerometer is used by many laboratories as a laboratory standard. This type of transducer has certain advantages as a laboratory standard. The primary advantage is that it can be attached to a shaker table and used to calibrate vibration pickups by mounting them directly on the top surface of the BTB accelerometer. The advantage of this arrangement is that the shaker does not need to have provision for mounting a reference accelerometer inside the shaker table. Also it is much easier and quicker to mount the reference pickup on the outside of the shaker table. The disadvantage of the BTB pickups is that the sensitivity of the pickup changes with the mass attached to the top surface. In order to achieve maximum accuracy, the BTB accelerometer must be calibrated as a function of the mass attached. This paper presents an absolute method for calibrating the BTB accelerometer for a range of masses.

BACKGROUND AND EXPERIMENTAL METHODS

This subject was treated in two previous papers (1,2). In these papers, it was shown that a BTB accelerometer can be calibrated by an absolute method by the use of a laser interferometer. In this previous work calibrations were made using zero mass and a single mass of 19 g. Also for the previous work, the BTB pickup's surface was polished so that the laser light could be reflected from it's surface.

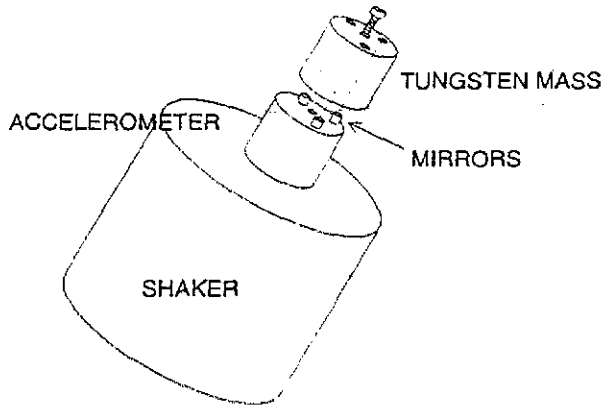

Figure 1. Mounting Arrangement for the BTB Accelerometer and Loading Mass

The present work uses a modification of this technique. Instead of polishing the accelerometer surface, three small mirrors were attached to the top surface of the BTB accelerometer with fast drying glue as shown in figure 1.

Three tungsten masses were used, each with three concentric holes, so that the mass can be mounted on the shaker table with a bolt through the center (also shown in figure 1). The experiments referenced in (1,2) also used a laser interferometer. In that case, however, the interferometer utilized the J_1 null method as described in NBS tech. note 1232 (3). That interferometer was used to make measurements at 193 nm and was not computer controlled. In the experiments described in this paper, the J_0 automated fringe-disappearance interferometer was used. This interferometer makes measurements at 121 nm (3,4). The automated fringe-disappearance interferometer operates over the frequency range of 3 - 20 kHz and is also described in (3).

Figure 2 shows the high frequency fringe-disappearance interferometric accelerometer calibration system schematic. This system uses a Michelson interferometer with one of the mirrors attached to the vibrating surface to be measured. The accelerometer is mounted by a screw to the center of the shaker table. The reference mirror of the interferometer is attached to small piezoelectric driver so that the path length difference Δ, of the two arms of the interferometer can be modulated by an oscillator tuned to a low frequency of 0.5 Hz. The details of the experimental process is given in (4). For a HeNe laser with a wavelength λ of 632.2 nm, the vibration displacement for fringe-disappearance is 121.1 nm.

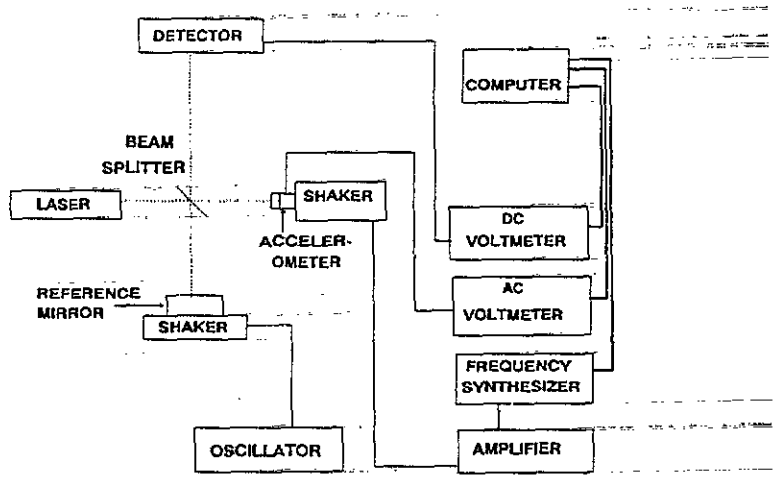

Figure 2. Fringe-Disappearance Interferometer for 121 nm displacement

EXPERIMENTAL RESULTS

A BTB accelerometer was calibrated using the techniques described above. Three tungsten masses were used: 28g, 38g, and 58g. The masses were mounted one at a time on the shaker, and measurements of pickup sensitivity were made over a range of frequencies. Sensitivity measurements were obtained at each of three positions, corresponding to the three mirrors. The sensitivities corresponding to the three mirror positions

were averaged to get the sensitivity for each mass. Figure 3 shows the results of this calibration for zero mass and for the three tungsten masses, normalized to the 5 kHz average.

DISCUSSION

Tests at NIST have demonstrated the feasibility of using a fringe-disappearance laser interferometer to calibrate a back-to-back accelerometer and to obtain sensitivities over a range of mass loads. The data in figure 3 show the effect of the mass load on the sensitivity. The effect of mass loading increases with frequency, and the sensitivity is lowered with an applied load. The data in figure 3 also show the experiment is starting to fail at 20 kHz, as can be seen from the inability to resolve the mass loading effect for the 28 and 38 gram cases. This most likely indicates nonuniform motion of the top surface of the accelerometer, in which case measurements at the three points do not accurately represent the motion of the accelerometer.

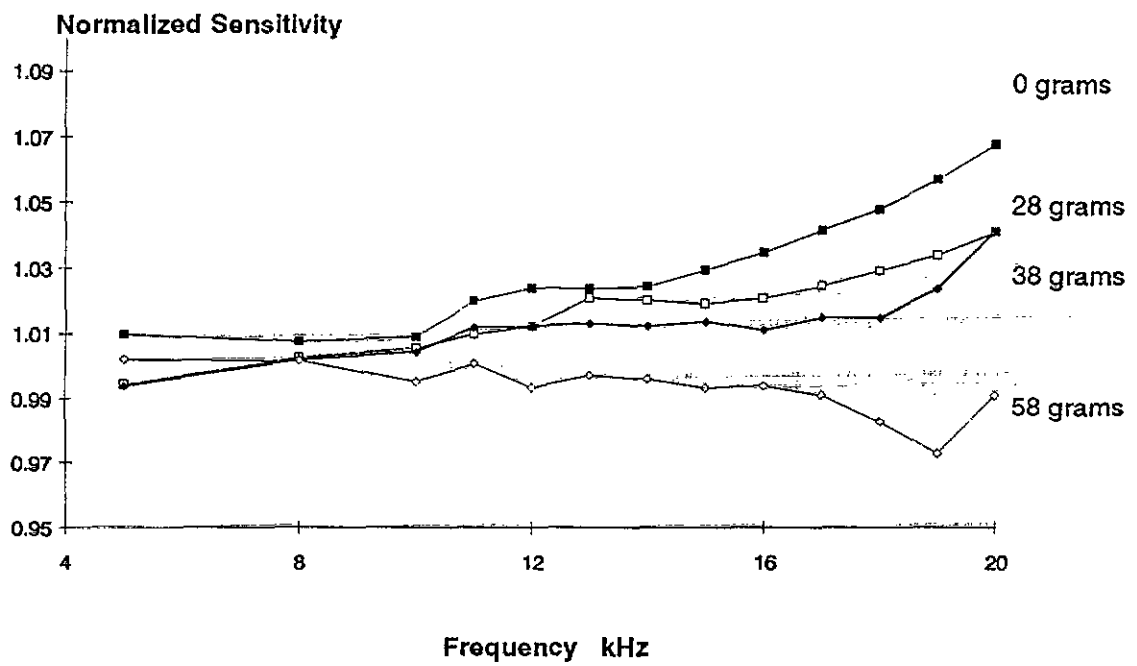

Figure 3. Results of BTB calibration for three masses and zero mass.

Figure 4 shows plots of least-square curves of degree two for the sensitivities corresponding to zero mass load and the three load masses of figure 3.

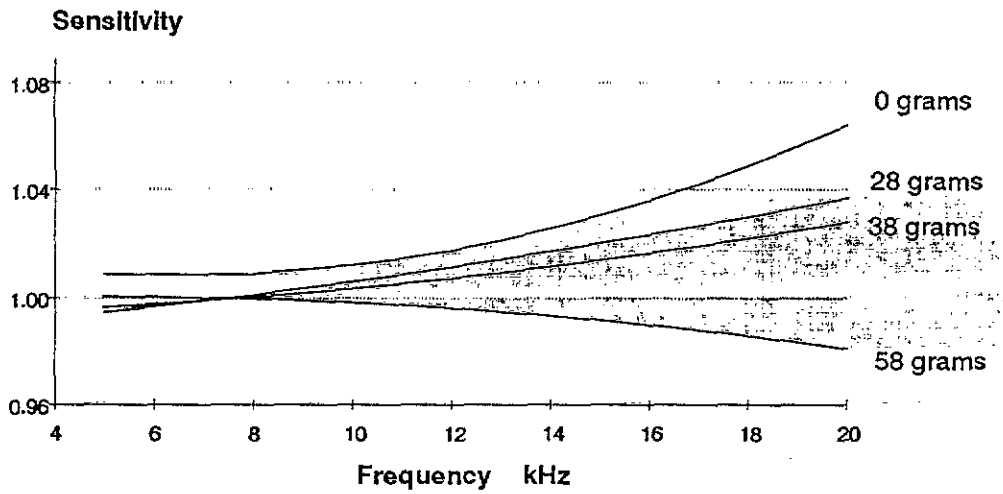

Figure 4. Least Square Curves for the Four Calibration Studies

It is possible to characterize BTB accelerometers for mass loading effects by the use of the interferometric calibration procedure outlined in this paper. One can calculate a mass loading coefficient defined as the percent sensitivity change per gram change of loading mass for an accelerometer, and include it as a specification along with the basic sensitivity, cross-axis sensitivity, etc. Figure 5 shows the mass loading coefficient as a function of frequency for the accelerometer tested and reported in this paper.

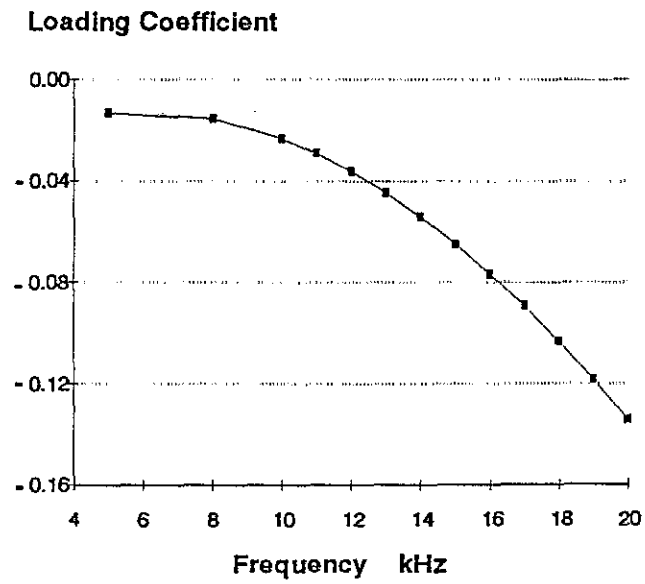

Figure 5. Mass Loading Coefficient vs Frequency

REFERENCES

1. Payne, B.F., "Absolute Calibration of Back-to-Back Accelerometers," Proc. ISA 27th Int. Instru.Symposium, Indianapolis, Ind. April 26-30, 1981, pp. 483-488.

2. Payne, B.F. , "The Application of Back-to-Back Accelerometers to Precision Vibration Measurements," Journal of Res., NBS, Vol88, no. 3 May-June 1983, pp. 171-174.

3. Robinson,D.C., Serbyn, M.R., Payne, B.F., "A Description of NBS Calibration Services in Mechanical Vibration and Shock," NBS Tech. Note 1232, Feb. 1987.

4. Payne, B.F., "Automation of Vibration Testing at the National Bureau of Standards," Proc. IES 30th Annual Tech. Meeting, Orlando, FL, May 1-3, 1984 (IES, Mt. Prospect, IL), pp.478-482.

ABSOLUTE CALIBRATION OF BACK-TO-BACK ACCELEROMETERS AT HIGH FREQUENCIES

SPEAKER: B. F. Payne, NIST

Q: Robert Sill (ENDEVCO). You say those numbers were averages of the readings taken on the three mirrors. Could you describe why those are not simultaneous readings?

A: No, they are not. With the present setup, we can only do one mirror at a time. We have the shaker mounted on an optical mount with micrometers which adjust the shaker, so that we just hit one mirror at a time.

Q: You are moving the shaker?

A: Yes, we are moving the shaker.

Q: Fred Alby (JPL). It would appear that the repeatability is at the 1/2 percent level. Could you comment on this, please?

A: Yes, the repeatability is very good; however, we really can't claim accuracy on it, just on the repeatability. If you have a structural effect, it can repeat very well.

Q: Thank you. It is still not absolute.

A: We claim up to 10 kHz, up to 2 percent; between 10 and 15 kHz, 3 percent; and above 15 kHz, 4 percent at present. The term absolute refers to the type of measurement. You should not imply that it is necessarily more accurate than another method just because it is measured in terms of a fundamental unit. Mistakes can be made in your test setup just as easily or more easily sometimes than other methods. I just wanted to clarify that one thing.

Q: Wayne Tustin (Tustin Tech Institute). I understand that you have a column resonance of aluminum cylinders with the rubber inserted. Was that aiming at around 20 kHz resonance?

A: Oh, no. The shakers were designed to go up to a region of 3 kHz to 80-100 kHz response. We cannot measure that high, because we are measuring 121 nanometers. At 20 kHz, we are in the hundreds of g's. We run out of steam at about 30 kHz. Although the stack of ceramic elements and dampers has a much higher usable range, it doesn't have the drive power.

Q: I was just curious as to what it does resonate at.

A: Each of these elements has a resonant frequency and is designed so that when one peaks out, the damper dampens that one, and you have a smoother response. Earl Jones wrote a paper in the Acoustical Society Journal back in the 1960s that gives a typical frequency response for that type of shaker. We have

copies if anyone needs one, or you can look it up in the journal.

Q: Thank you. That 121.1 nanometers; is that single or double amplitude?

A: I believe it is peak-to-peak.

Q: One more thing. Are your customers happy with 4 percent to 20 kHz?

A: Well, some of them would like a little better accuracy, but, right now, most people are satisfied to get anything. If we can get 4 percent right now that seems to satisfy most customers. There are always a few who would like better. Just like anything else, you want the best.

Q: Ed Peterson (MB Dynamics). Following up a little bit on Wayne's question about the 20 kHz situation, three companies, BTK, ENDEVCO, and MB, supplying systems right now are going to 10 kHz. I know that ENDEVCO sweeps out to approximately 50 kHz for resonant searches. I think I heard you say you are getting a lot of requests to go above 10 kHz to 20 kHz. If so, some of us on the suppliers side should be doing some work to make systems go higher.

A: It is not an everyday request; however, we are getting more requests than we used to.

Q: Is it 20 kHz? You are not saying 25 kHz or 30 kHz?

A: Some people ask for 25 kHz and some for 30 kHz, but mostly it is up to 20 kHz. We can go a little higher than 20 kHz if the accelerometer is a smaller unit. If we go to one of these miniature 5 or 10 gram types, then we can go a little higher than the 20 kHz. But, for this large type, 20 kHz is about the limit right now.

Q: Steve Kuehn (Sandia Labs). Are these three mirror mounts specially designed, and what effect is that having on your overall accuracy?

A: Are you talking about the mirrors that are mounted on the accelerometer?

Q: Yes.

A: The small mirrors are mounted on the surface of the accelerometer. These small mirrors are approximately 1/8-inch in diameter and were made in our optical shops. They are a normal type of optical mirror of about one fringe flatness across the surface that you could get from an optical company. We've tried different small mirrors, and they developed to be quite good. We would like to have the shaker have the reflective coating. We have tried that, and we have gotten pretty good results. For a

piggy-back accelerometer, you have to mount something or else you can polish the accelerometer until it is a mirror. In these two previous papers, we have did it that way. But, as soon as you use the pick-up again, you have to repolish it, and that is an expensive proposition. But the mirrors compare favorably with the results with the polishing.

Q: Could I ask you another question? I wasn't absolutely sure about the drawings, but are the three mirrors viewed through holes in the tungsten mask?

A: Yes.

VIBRATORY PRESSURE CALIBRATIONS

W. B. Leisher, Sandia National Laboratories

BACKGROUND

Researchers at the National Bureau of Standards during the early 1970's worked on various methods for calibrating pressure transducers with sinusoidal variations imposed on a static pressure level. The most promising method utilized the pressure variation at the bottom of a liquid column mounted on an electrodynamic shaker (1). The pressure amplitude during vibration, ideally, is equal to the product of the liquid density times the height of liquid times the g's of acceleration. Their techniques generated pressures up to 5 psig (peak) at a frequency range of 50 to 2000 Hz with the upper frequency limit restricted by resonant vibration in the liquid column. They evaluated several methods of damping the resonance to extend the usable range where pressure is proportional to acceleration. In this way, the calibration could be related to the fundamental measurements used to determine the acceleration. Their efforts formed the starting point of an on-going investigation at the Secondary Standards Organization of Sandia National Laboratories.

PRESENT WORK

A derivative method, using a reference pressure transducer instead of fundamental acceleration measurements, as suggested in the NBS report, is being investigated for calibrating pressure transfer standards for field use. Because pressure rather than acceleration is measured, liquid resonance effects are of little concern and tailored damping for the liquid column is not needed.

REFERENCE TRANSDUCER

Piezoelectric pressure transducers are considered to fit a second order spring-mass system model quite well and to have a flat response up to about 20 percent of their natural frequency. This can be partially verified by dynamically calibrating the transducer with pressure steps with rise times corresponding to the frequency range of interest. The quartz transducer selected as a reference has a resonant frequency of 60 kHz and a nominal sensitivity of 10 pC/psi. Static and step calibrations show the sensitivity to be essentially flat to at least 3 kHz.

TESTS AND RESULTS

Tests have been run at amplitudes of 0.5 and 1.0 psig (peak) over the frequency range of 30 to 2000 Hz using a flush diaphragm semiconductor type pressure transducer as the test gage. The transducers were mounted with their axis perpendicular to the direction of motion. Sensitivity using the vibrational method agrees with that measured during a static calibration within better than 1 percent up to 1 kHz. Large deviations encountered at higher frequencies were found to be caused by a nylon adapter used on the reference. New hardware is being designed to eliminate the problem and extend the usable range.

Results are sufficiently promising to warrant further work on this technique to explore both frequency and amplitude ranges.

(1) Vezzetti, C.F., Hilten, J.S., Mayo-Wells, J.F., and Lederer, P.S., A New Dynamic Pressure Source for the Calibration of Pressure Transducers, NBS Tech Note 714 (June 1976).

This work is supported by the US Department of Energy under contract DE-AC04-76DP00789.

VIBRATORY PRESSURE CALIBRATIONS

SPEAKER: William Leisher, Sandia National Laboratory

I suspect you may be going to ask if I looked at the transfer sensitivity of those transducers; and, yes, I did. You shake them in the air to be sure that there are no loud spikes. There is much that I did that I didn't cover.

Q: Pete Stein (Stein Engineering). Back in the 1970s, I asked Paul Letterer about the effect of the magnetic field on the transducer. Since you are on a shaker, this would be an ideal spot for a sample transducer mounted in a blind hole that didn't go through. You would be in the same magnetic field in the same acceleration area.

A: Yes. This is one of those jobs that got started and then the funding went away. I hope it will come back.

TECHNIQUES TO OPTIMIZE HIGH ACCURACY, COMPUTER CONTROLLED PRESSURE CALIBRATION

By
Martin Girard
DH Instruments, Inc.

ABSTRACT

The immediate and obvious benefit of computer controlled pressure transducer calibration is the automation of what is otherwise a labor intensive and highly operator dependent process. However, as is usually the case with automation, maximum benefit is not gained by merely reproducing traditional manual techniques automatically. This paper presents new techniques specifically designed to exploit the unique capabilities of computer control. These techniques, relative to traditional methods, improve test speed and quality while reducing hardware cost and complexity. Key words: pressure calibration, transducer calibration, automated calibration, pressure controller.

PRESSURE CALIBRATION

In the most general sense, pressure calibration is the determination of the relationship between pressure inputs and signal outputs for a pressure measuring device.

The basic technique used to perform a calibration is to simultaneously apply a static pressure to the device being calibrated and to a higher accuracy standard or reference. This is done at several increments over the operating range. At each increment the pressure set on the reference and the output of the device under test are recorded. The series of pressure vs. output relationships is then reduced in one way or another into an expression that can be used to translate output into pressure. The calibration data are also frequently used to predict the uncertainty associated with pressure measurements made with the device.

The quality of the calibration depends mainly on one thing: how well do you know the value of the pressure that is applied to the test device when its output is recorded.

Sources of error or uncertainty on the value of pressure actually applied to the test device include:

1) The accuracy of the reference device or standard.
2) Voluntarily integrated pressure control errors.
3) Pressure drops in the system due to leaks and flow.
4) Fluid heads between the reference device and the test device.
5) Random pressure instability in the system which a) can cause the pressure at the reference measurement point and the device under test measurement point to be different at the same moment in time and b) can cause pressure to have changed significantly in the time lapse between the reference measurement and the test measurement.

TRADITIONAL MANUAL CALIBRATION TECHNIQUE

Figure 1 gives the schematic of a traditional manual calibration system. The reference pressure measuring device and the device under test are connected together and to a pressure control system that includes an inlet and exhaust valve and a variable volume adjuster. The operator uses the pressure control system and the reference to set and stabilize the pressure at each increment and then records the test device output.

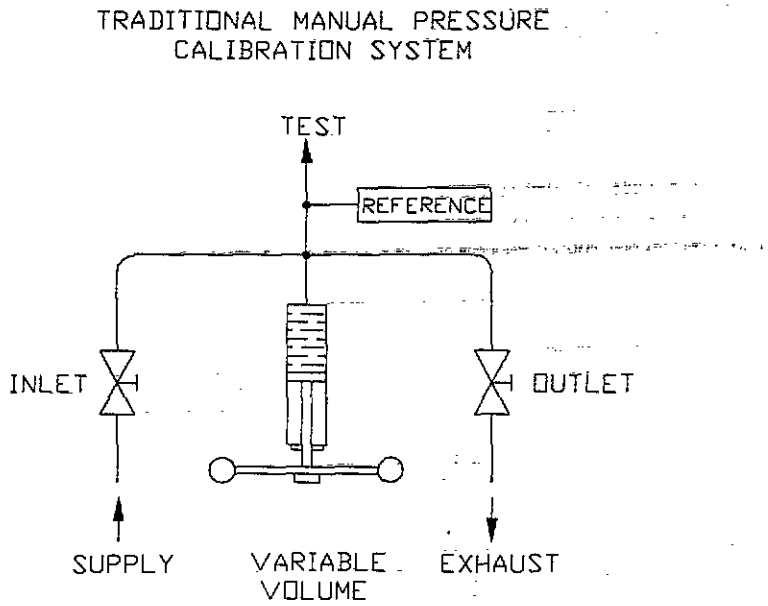

FIG. 1

Procedures dictate not only that the operator stabilize the pressure at each increment but that he set it at exactly the nominal increment value. This is necessary if the device he is calibrating is an analog gauge with fixed increments. It is also necessary even if he is calibrating a device with continuous output over the range such as a transducer because the data he is taking will go directly onto the calibration report. Neither he nor the user have the data reduction power available to be able to interpret the data without nominal, whole number calibration test points that are identical for ascending and descending increments.

The traditional manual calibration procedure is slow, labor intensive and highly operator dependent. Understandably, great efforts were made to automate it.

AUTOMATING THE TRADITIONAL MANUAL CALIBRATION TECHNIQUE

Early Automated Pressure Sources

In the 1970's the introduction of easily interfaceable computers that could control automated test systems made fully automatic transducer calibration a real possibility.

Pressure sources integrating automated pressure control with high accuracy pressure transducers were developed. These were designed to duplicate automatically, in response to remote computer commands or local front panel entry, the pressure setting and stabilizing function that was previously performed manually.

The new automated sources generally controlled pressure using the variable orifice technique. The basic principle of this technique is illustrated in Figure 2. Inlet and exhaust variable orifices are driven in a feedback loop with the pressure measuring device to adjust flow through the system. Adjusting flow adjusts pressure and allows the feedback signal to be nulled. In actual systems, the inlet and exhaust orifice functions are usually integrated into one servo-valve. Also, in lieu of a true variable orifice, later applications of the same principle use variations on the operating frequency of high speed solenoid valves to control flow. The principle and the result, however, are the same. Pressure control is achieved by continuous flow through the system and it is dynamic in that the servo-loop is always actively readjusting. The typical pressure controlling function at a set point of a high precision variable orifice controller is shown in Figure 3.

VARIABLE ORIFICE PRESSURE CONTROL
OPERATING PRINCIPAL

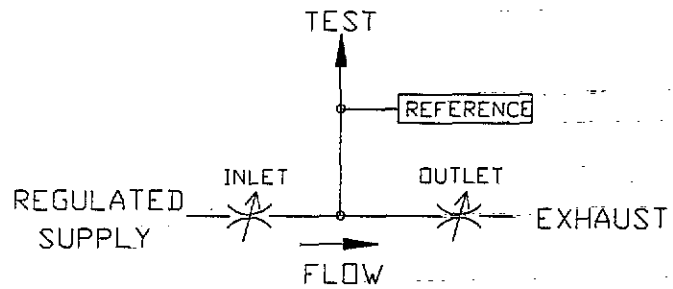

DA182

FIG. 2

TYPICAL VARIABLE ORIFICE
PRESSURE CONTROL

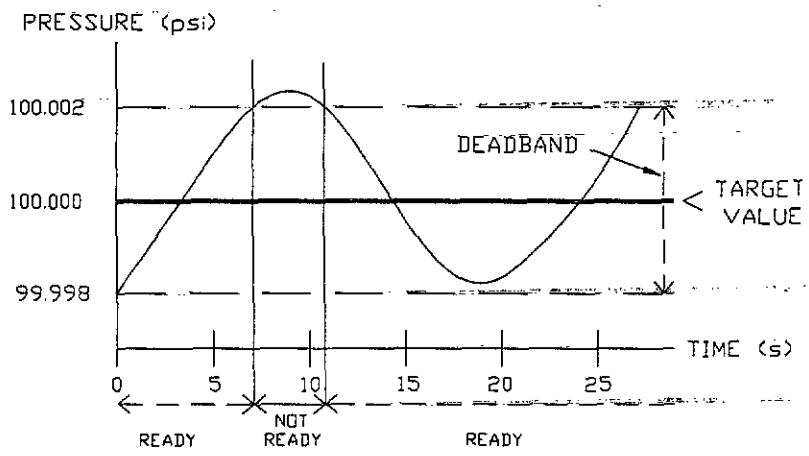

FIG. 3

DA183

Shortcomings of Early Automated Pressure Sources

Through the 1970's and 80's the accuracy of the devices to be calibrated improved continuously and volume multiplied as transducer use widened. Several shortcomings of traditional high accuracy controllers began to stand out. These include:

1) Speed - Existing high accuracy pressure controllers were designed for one mode of operation: setting pressure precisely at the commanded value without overshooting it and then actively maintaining it within a controlled deadband that is as narrow as possible. Keeping the deadband to a minimum is volume dependent and inherently requires highly dampened, very slow speed operation.

2) Accuracy limitations due to the integration of control errors - In normal use of a traditional controller deviations between the pressure actually set by the controller and the pressure requested or "target" pressure are integrated as errors. In Figure 3, the pressure that is requested is 100 psi. So long as the pressure is inside of the deadband, it will be considered to be equal to 100. Therefore, when the controller indicates that it has set 100.000 psi, it means that the pressure as measured by the reference is somewhere between 99.998 and 100.002 psi. The ± 0.002 psi control error may seem small but it represents an often unaccounted for additional uncertainty of ± 20% on a system claiming ± 0.01% F.S. uncertainty.

   Since the control error tends to be a function of the full scale of the controller, its relative significance increases as you go lower in the range. For example, at 10 psi it represents ± 0.02%. In other words, if you use the 100 psi controller to apply 10 psi twice, the difference between the first pressure and the second pressure could be as great as 0.04% not including the uncertainties on the reference measuring device itself.

   Despite the potential significance of integrated control errors, many manufacturers and users continue to compare pressure controllers based purely on the specification of their reference sensors with no consideration for control errors.

3) Dissimulation of leaks - The variable orifice controller does not discriminate between normal flow through its servo-valve and unintended flow in the test system due to leaks. It will feed leaks in the system causing pressure as read by both the reference and the test to stabilize. However, that the pressure is stable at both points is no guarantee that it is equal at both points. If there is a leak there will also be a pressure drop between the two points. The amount of the pressure drop is not readily predictable and can cause a significant difference between the pressure actually present at the test point and the pressure at the point where the reference is measuring.

   When using a controller that dissimulates leaks, separate leak tests must be performed over the pressure range at each test temperature and the possibility of unknowingly continuing a test with significant leaks present in the system still always exists.

4) Cost/complexity - Since control errors are integrated and they are a function of controller full scale, controller range, reference measuring device range and test device range must all be matched. Systems that are designed to calibrate multiple ranges of test devices therefore usually have to have multiple controllers as well as multiple references.

OPTIMIZING AUTOMATED CALIBRATION

Optimizing automated high accuracy calibration means increasing speed, improving accuracy and reducing the complexity of multi-range systems. This can be accomplished by developing new computer controlled calibration techniques that go beyond mere automated duplication of what was once done manually. One such technique consists of replacing the traditional variable orifice servo-controller with a positive shut-off pressure controller and measuring static pressure in the test system at each increment rather than insisting on precisely set actively controlled values. This will allow control errors to be completely eliminated while increasing calibration speed. Also, one controller can be used to cover a very wide range of pressure.

The Positive Shut-Off Pressure Controller

A positive shut-off pressure controller is one that sets the desired pressure value and shuts off from it rather than constantly adjusting flow through the system. This eliminates the dependence of pressure stability on the deadband limits of the controller so that truly static pressures can be set at any pressure.

Figures 4 and 5 show a positive shut-off pressure controller. Pressures are set using two fixed orifice inlet and exhaust valves. Flow controllers are used to keep differential pressure across the valves constant at all supply and system pressures and to maintain constant slew rates over a wide range of control volumes. There is flow through the flow controllers but the flow is independent of the test system. The control valves are slightly modified low speed industrial solenoid valves. Thanks to a proprietary algorithm and the high speed calculation and execution capabilities of an on-board microprocessor, the valves can be operated very predictably giving an extraordinary ability to control pressure.

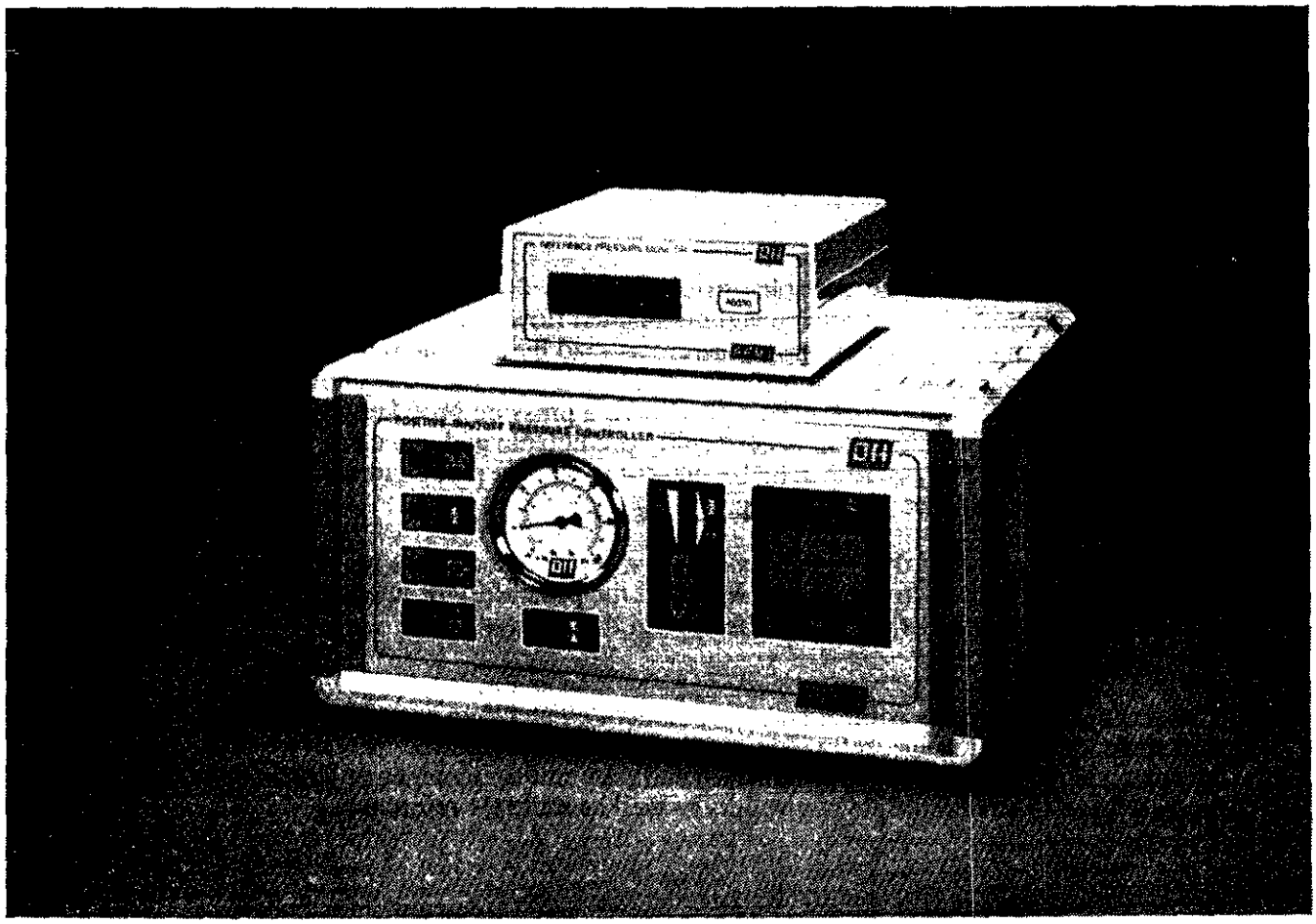

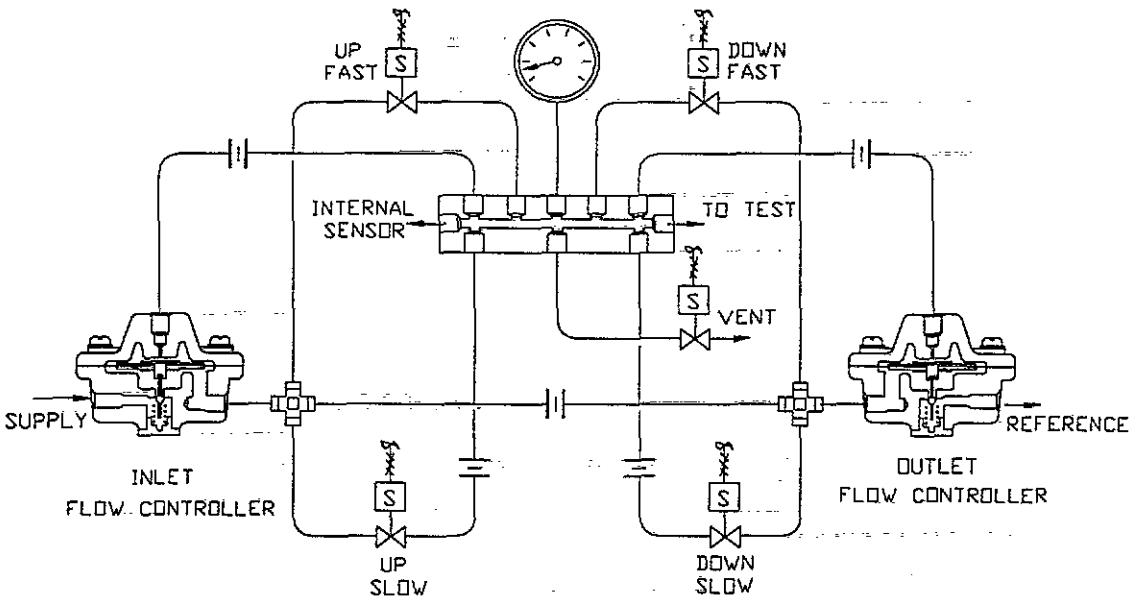

FIG. 5

The positive shut-off pressure controller does not have a built-in reference measuring device. It is made to be used in conjunction with an external reference device. This is so that the reference can be mounted to measure pressure close to the device being tested rather than in the controller enclosure. It also allows the user to choose the reference that he would like to use and to use multiple reference ranges with one controller. Finally, it means that the controller itself does not have to be removed from the test system for recalibration or range changes.

Positive shut-off pressure controller operation is characterized by three user adjustable operating parameters as illustrated in Figure 6.

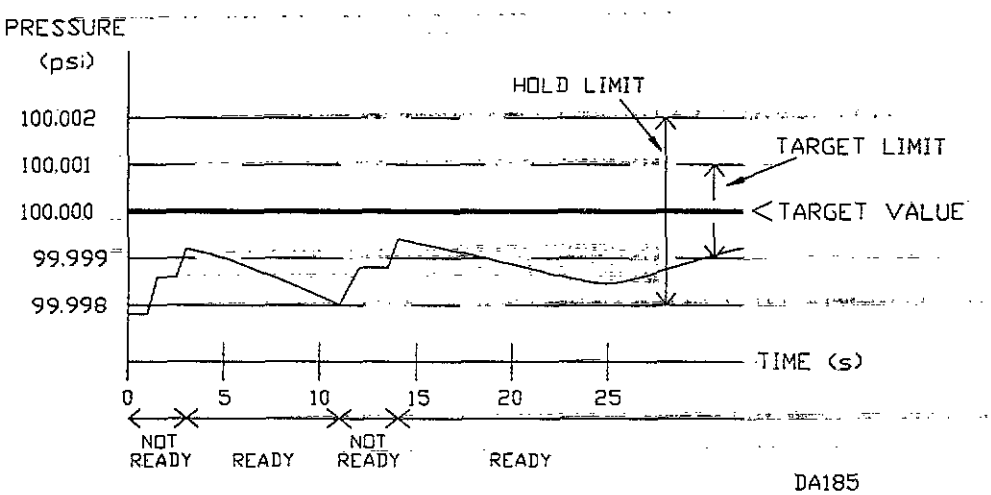

TYPICAL POSITIVE SHUT-OFF PRESSURE CONTROL

FIG. 6

1) Target limit - The target limit defines how close to the target value the pressure must be set before the pressure setting sequence is considered complete. In Figure 6 the target value is 100 psi and the target limit is ± 0.001 psi. When a pressure set command of 100 psi is given, pressure will be adjusted until it falls within 0.001 psi of 100. The controller then shuts off and does nothing further until another command is received (unless the "hold" function has been activated).

2) Hold limit - The hold function causes the controller to automatically readjust pressure to maintain it within certain limits of the target value. In Figure 6 the hold limit is ± 0.002 psi. When a pressure set and hold command of 100 psi is given, the pressure will be adjusted until it falls within 0.001 psi of 100. The controller then shuts off and monitors the pressure present in the system. If the pressure goes more than 0.002 psi above or below 100 psi, the pressure will automatically be readjusted to the target value within the target limit.

3) Stability test and ready indication - The controller constantly determines its status in terms of "ready" or "not ready". For the status to be ready, three criteria must be met: a) no valve can be operating; b) if hold is on the pressure must be inside the hold limit and c) the rate of change of pressure must meet the stability test. The stability test criterion is set by the user in terms of rate of change of pressure in pressure units/second.

   The "ready" or "not ready" condition is shown by a front panel indicator. It is also returned on the interface preceding the digital pressure information in response to a request for current pressure or in response to a status request.

   Figure 6 includes indication of when the system will be ready and not ready assuming a stability test of 0.001 psi/second.

Using a Positive Shut-Off Pressure Controller

The positive shut-off pressure controller can be used in exactly the same manner as a traditional controller. For this type of operation the user can select an alternate ready/not ready mode in which pressure resets short of the hold limit and ready is not dependent on lack of valve operation. Since is will be assumed that the pressure is equal to the target pressure there is no need to interrupt the ready condition so long as the pressure remains inside of the hold limits. Since the positive shut-off pressure controller can work with hold limits as tight or tighter than the minimum deadband of a traditional controller, in this mode its performance is at least equivalent in terms of both accuracy and speed.

The positive shut-off pressure controller, however, was designed to allow the application of a new technique. In this technique the actual static pressure in the shut off volume is read and used rather than assuming that the pressure equals the target pressure. From a practical standpoint, the only potential complication relative to the traditional technique is that the calibration points are not exact cardinal values. As explained below, in the vast majority of cases that is of no consequence and the benefits offered by the technique far outweigh this minor inconvenience. Those benefits include:

1) Elimination of control errors - Shutting-off and reading the reference to get back the exact current value of the static pressure present in the system eliminates any errors due to controller interference and inability to control perfectly. When the test device output is read, the only uncertainty on the pressure that is applied to it is the uncertainty on the reference device itself.

2) Increased speed - Since the hold limit is not going to be integrated as an error, it can be opened up to equal the maximum distance from the nominal point that the actual calibration point can be allowed to be. Working with wide hold limits and not requiring the controller to set and stabilize at a very specific point such as the 100.000 psi in our examples, greatly reduces the amount of time required to set and stabilize pressure.

   Independent testing has shown that replacing a traditional variable orifice controller with a positive shut-off pressure controller using the measured pressure technique can reduce the time required to complete a 21 step ascending/descending calibration sequence by a factor of two to three with equal or improved data quality.

3) Automatic full time leak detection - If there is a significant leak in the system the positive shut-off pressure controller using the measured pressure technique will make that obvious in two ways. First, the ready condition will very frequently be interrupted as the pressure reaches the hold limit. Second, if the leak is large enough, the ready condition will never exist since for a ready condition to occur, the pressure stability test must be passed.

   If the stability criterion has been set properly and the leak present is so large that a ready condition can never occur, the leak is too large to allow reliable data to be taken.

4) Use of one controller over a wide range of test instruments - Since the final stability of the pressure does not depend on the range of the pressure controller and no controller deadband errors are integrated, one controller can be used with several ranges of reference devices to cover multiple test instrument ranges. For example, a 1 000 psi controller can be coupled with 1 000 psi and 100 psi references. When calibrating a 100 psi device, the 100 psi reference is used and its full accuracy is obtained. There is no need for multiple controllers.

Questions Concerning Positive Shut-Off Pressure Control and the Measured Pressure Technique

Some of the most common questions and concerns relating to the possible application of positive shut-off pressure control and the measured pressure technique are:

1) The calibration points are going to end up being non-cardinal points and our calibration reports must show whole number values.

   Before computers were widely available, this was a real problem and it is probably the main reason that the tradition of taking data only at cardinal points is so strong. Today high powered computers are universally available. When given the choice it is more efficient, much faster and ultimately more accurate to use the computer to reduce data than it is to ask a mechanical pressure control system to set, stabilize and maintain exact cardinal points.

   Figure 7 shows the raw calibration data for a 100 psi transducer and the calibration report and output curve that were produced. In this case the hold limit used was ± 0.01 psi so the maximum distance between a nominal test point and the actual test point is 0.01 psi (0.01% of the transducer's full scale).

   In order to print a calibration report with cardinal points, the output at the cardinal point was extrapolated from the output at the actual test point using:

$$O_{car} = O_{cal}\left(\frac{P_{car}}{P_{cal}}\right)$$

   where:

   Ocar = output at the cardinal point
   Ocal = output at the calibrated point
   Pcar = pressure at the cardinal point
   Pcal = pressure at the calibrated point

In the worst case the difference between the calibrated point and the cardinal point is equal to the hold limit so the hold limit should not be set to a value greater than the distance over which it is safe to extrapolate output. In this case we have used 0.01% F.S. and for most instruments much greater values than that could be used with no detrimental effect to accurate characterization of the device. Another way to look at it is that if it is not safe to extrapolate over that distance, then your calibration points themselves should not be more than that distance apart.

The device output curve is drawn directly from the calibration points. Whether those points happen to fall at exact cardinal points or not is of absolutely no significance. It is equally insignificant in fitting the data.

2) How do you measure hysteresis when the ascending increment and the descending increment may not be exactly the same?

See 1) above, especially the first paragraph. Hysteresis can be quantified by comparing the ascending and descending value at the cardinal point or at any other point in the hysteresis curve. Also keep in mind that using a variable orifice controller and the traditional technique, the ascending and descending points were often significantly different due to the control errors; you just pretended they were the same.

3) If I am calibrating a group of same range test devices on a manifold, the actual calibration pressure at each increment may be different for each device.

See 1) above, especially the first paragraph. The computer is designed to handle large amounts of data and in most cases asking it to handle different pressure values for each transducer does not represent a significant additional work load.

4) It takes time to read my test device. What if the pressure changes between the time I read the reference and the time I read the device under test?

The ready condition is dependent upon the stability test being met. You set the stability test yourself and should set it as a function of the accuracy you are trying to achieve and the time it takes to read your test device. With the stability test thus set, when you make measurements in the ready condition, the rate of change of pressure is such that no significant pressure change can occur in the time it takes to read the test device. For best results, read the reference before and after you read the test. If both reference readings are "ready" average the two and use the average as the pressure applied to the test when the test was read.

5) I know that leaks can cause errors but my system will never be perfectly leak free. Can I still use positive shut-off pressure control?

When working with a leak, the hold function will activate more frequently and reestablish the pressure to the target. If the hold function cannot overcome the leak and/or if the stability test can never be met, the leak is so large that there is little or no chance of making meaningful measurements anyway regardless of the equipment and technique that you use. The advantage is that you will know that rather than continuing with the measurements only to end up with useless data.

6) What is the highest ratio of controller range to reference range that is acceptable?

That depends only on how close to the nominal calibration point your actual calibration point must be. A typical positive shut-off pressure controller has a minimum target limit of ± 10 ppm of full scale so you may end up being that far away from your nominal point. For example, a 1 000 psi controller has a minimum target limit of 0.01 psi. The final stability of the pressure is independent of controller range. If you can accept that the final pressure when you request 10 psi may be as low as 9.99 and as high as 10.01, you can use a 1 000 psi controller with a 10 psi reference to calibrate 10 psi test devices with the full accuracy of the 10 psi reference.

Raw Data

Pressure Up (psig)	Output Up (V)	Pressure Down (psig)	Output Down (V)
0	-0.00098	0	0.00097
19.9976	1.99984	20.0098	2.00290
39.9921	3.99737	40.0085	4.00269
59.9931	5.99647	60.0077	6.00161
79.9910	7.99734	80.0063	8.00071
99.9925	10.0004	-	-

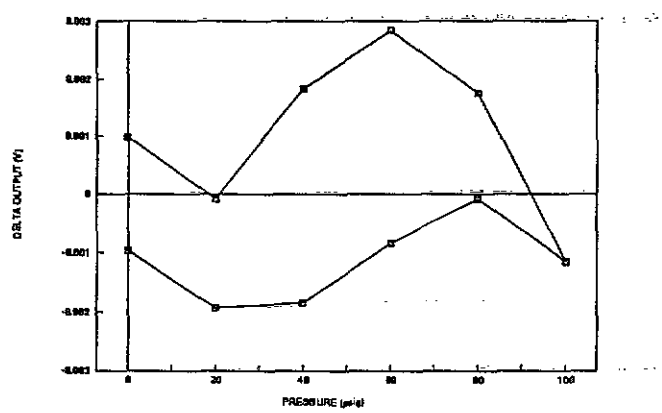

Calibration Certificate

Pressure (psig)	Output Up (V)	Output Down (V)
0	-0.00098	0.00097
20	2.00008	2.00192
40	3.99816	4.00184
60	5.99716	6.00084
80	7.99824	8.00008
100	10.0012	-

Raw Data, Calibration Certificate Data and Error Curve
From Measured Pressure Technique
Figure 7

TECHNIQUES TO OPTIMIZE HIGH ACCURACY, COMPUTER CONTROLLED PRESSURE CALIBRATION

SPEAKER: Martin Girard, DH Instruments, Inc.

Q: Scott Walton (Aberdeen Proving Grounds). In your internal references is that a managanin cell?

A: No, again the question really reflects the audience. The pressure controller is for up to 1000 psi. We are working out two new models: one for 3000 and one for 6000, so it is not the pressure range in which you would use the managanin pressure cells. The pressure reference was intentionally left out, because it could be almost anything. In the system design, the system is open so that the pressure controller and the reference are two separate things. We build some transducer-based and some piston cylinder-based references, but really it is up to the user.

Q: What reads 20 parts per million in a hundred psi?

A: Quartz pressure transducers. We have transducers with usable resolution of less than 10 parts per million. In that range, not at 100,000 psi, but at pressures up to 20,000 psi, those pressure transducers have absolute accuracy if I am allowed to use that term. Accuracy includes the uncertainty of the standards used to calibrate them on the order of 0.01 percent full scale.

Q: 0.01 percent. That's 100 parts per million?

A: Yes. Absolute accuracy of the transducer makes the measurements and has repeatability on the order of 10 parts per million and yields resolution of about 1.

SESSION 4

APPLICATIONS

MISSING PAGE

124

A NEW SOLID-STATE ROTARY VIBROMETER

P. W. WHALEY AND A. L. SHELDON
OKLAHOMA CHRISTIAN
UNIVERSITY OF SCIENCE AND ARTS
OKLAHOMA CITY, OKLAHOMA

ABSTRACT

A new class of rotary vibration sensors utilizing the amplitude modulated acceleration of a resonating tuning fork is described. Accelerometers mounted on the tines in two orthogonal directions are used to measure the acceleration which results from rotation of the assembly about an axis parallel to the tines. The Coriolis acceleration term is an amplitude modulation of the input angular velocity with the assembly resonant frequency as the carrier frequency. This capitalizes on the high-frequency effectiveness and dynamic range of accelerometers to provide a sensitive, broadband instrument potentially capable of functioning in hostile environments. A wide range of applications is possible including aircraft inertial navigation, guidance and control, tachometer requirements in severe industrial environments, trenchless technology in construction projects, directional drilling in the petroleum industry and automobile crash testing.

INTRODUCTION

This paper describes a new instrument which measures rotary oscillations. When a resonating tuning fork experiences an angular velocity about an axis parallel to the tuning fork tines, the Coriolis acceleration of a tine is the amplitude modulated angular velocity with the carrier frequency the same as the tuning fork resonant frequency[1]. Since the desired angular velocity signal is shifted upward in frequency by the amplitude modulation, accelerometers are ideal for this function. This new rotary vibrometer utilizes the high-frequency effectiveness and dynamic range of accelerometers to provide a sensitive, broadband instrument capable of functioning in severe environments.

The amplitude modulated angular velocity is proportional to the tuning fork resonant velocity. Therefore, maximum sensitivity is achieved when the resonant velocity is maximum. By driving the tuning fork with a piezoelectric actuator attached between the tines, the tuning fork is stiffened and its resonant frequency is increased. Since the piezoelectric actuator has very high impedance, its output displacement is not significantly influenced by the tuning fork. In this way the piezoelectric actuator stiffens the tuning fork and the tuning fork amplifies the system resonant deflection.

Since the fork/driver mechanical system is very lightly damped, small variations of excitation frequency result in large variations in the resonant velocity amplitude thus severely degrading sensitivity. Therefore the fork/driver system must be excited exactly at resonance to maximize the resonant velocity amplitude and minimize power consumption. Since the phase is a much more sensitive variable for precise control of resonance, a phase-locked loop is used to track the system resonant frequency and control the frequency and phase of the driver circuit at exactly the system resonant frequency.

An amplitude demodulator removes the base rotational information, which may be further processed to provide angular position, velocity or acceleration, as desired. A bandpass filter is used to eliminate unwanted frequency components and can also be designed to enhance the low frequency sensitivity.

For those applications requiring information at higher frequencies, the system resonant frequency can be increased. A wide range of applications is possible including aircraft inertial navigation, guidance and control, tachometer requirements in severe industrial environments, trenchless technology in construction projects, directional drilling in the petroleum industry and automobile crash testing. The design of an instrument for inertial navigation and control is described in this paper.

ACCELEROMETERS AND ANGULAR VELOCITY MEASUREMENTS

A tuning fork with piezoelectric driver attached between its tines is used to measure angular velocity, as illustrated in Figure 1. When the driver is excited by a sinusoidal voltage, the tuning fork vibrates in the y-direction according to:

$$r(t) = d + r_o \exp(j\omega_o t) \tag{1}$$

When there is a sinusoidal angular velocity, $\Omega(t)=\Omega_o e^{j\omega t}$, oscillating about the z-axis, the tuning fork tines will accelerate in two directions. The tine acceleration in the direction of the resonant motion is:

$$A_r = -\omega_o^2 r_o \exp(j\omega_o t) - \Omega_o^2 d \exp(j2\omega t) - \Omega_o^2 r_o \exp[j(\omega_o+2\omega)t] \tag{2}$$

The tine acceleration perpendicular to the resonant motion is:

$$A_\theta = j\omega\Omega_o d \exp(j\omega t) + j(\omega\Omega_o r_o + 2\omega_o\Omega_o r_o)\exp[j(\omega_o + \omega)t] \tag{3}$$

The second term in A_θ is the amplitude modulated signal of the input angular velocity, easily recognized by the shift in frequency. By attaching accelerometers A_1, A_2 and A_3 onto the tuning fork tines as illustrated in Figure 1, the angular velocity can be measured using accelerometer output signals.

Accelerometers A_2 and A_3 contain the desired angular velocity signal, but are contaminated by the motion in the r-direction. The output of either accelerometer is:

$$A = A_\theta + TS\, A_r\,, \tag{4}$$

where TS is the transverse sensitivity of A_2 or A_3. The desired term in the amplitude modulated signal is $2\omega_o\Omega_o r_o$, so equation (1) is normalized by this term:

$$A/j2\omega_o\Omega_o r_o = (\omega/\omega_o)(d/r_o)\exp[j\omega t] + (1+\omega/2\omega_o)\exp[j(\omega_o+\omega)t]$$
$$+jTS[(\omega_o/\Omega_o)\exp(j\omega_o t) + (\Omega_o/\omega_o)(d/r_o)\exp(j2\omega t) + (\Omega_o/\omega_o)\exp\{j(\omega_o+2\omega)\}]/2 \tag{5}$$

There are three dimensionless quantities in equation (2); (ω/ω_o), (Ω_o/ω_o) and (r_o/d). The ratio (ω/ω_o) quantifies the frequency of the input angular velocity as a fraction of the fork/driver system resonant frequency. The ratio (Ω_o/ω_o) quantifies the strength of the input angular velocity signal, also as a fraction of the fork/driver system resonant frequency. The ratio (r_o/d) quantifies the resonant amplitude of the tine as a fraction of the tine spacing. Figure 2 shows the normalized frequency spectrums of the first two terms in equation 2, illustrating the need for filtering the accelerometer signal from A_2, especially for small values of (r_o/d). Figure 3 shows the cross-axis sensitivity contamination terms as a function of the signal strength ratio. This illustrates the most serious contamination problem which must be solved. The contamination from cross-axis sensitivity becomes worse for low-level signals, which is the primary region for inertial navigation applications. Fortunately, a suitable configuration of A_3 can eliminate this contamination. Since the two tines of

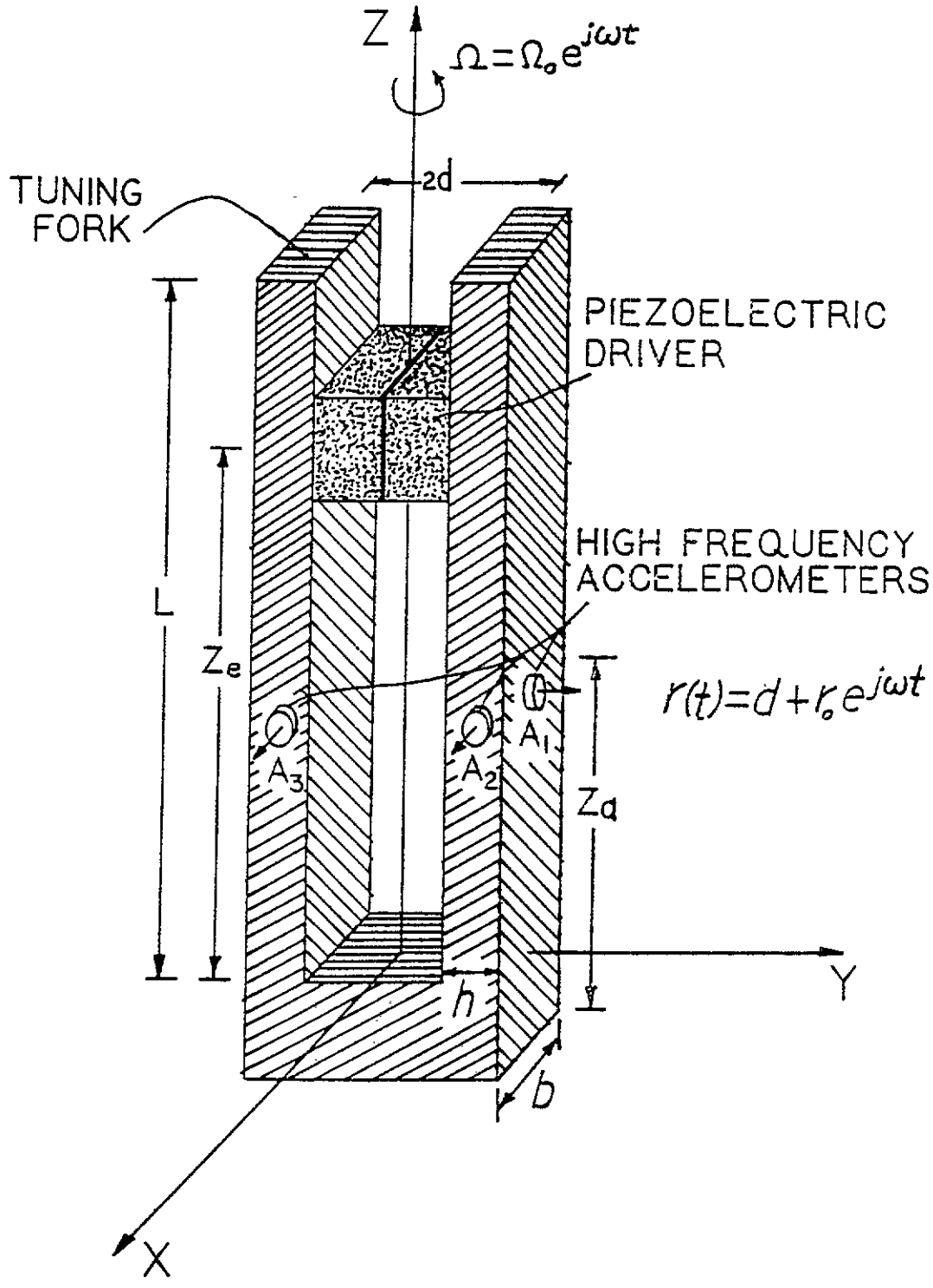

Figure 1. Schematic Diagram of a New Solid-State Rotary Vibrometer Based on Coriolis Acceleration of Resonating Tuning Fork Tines.

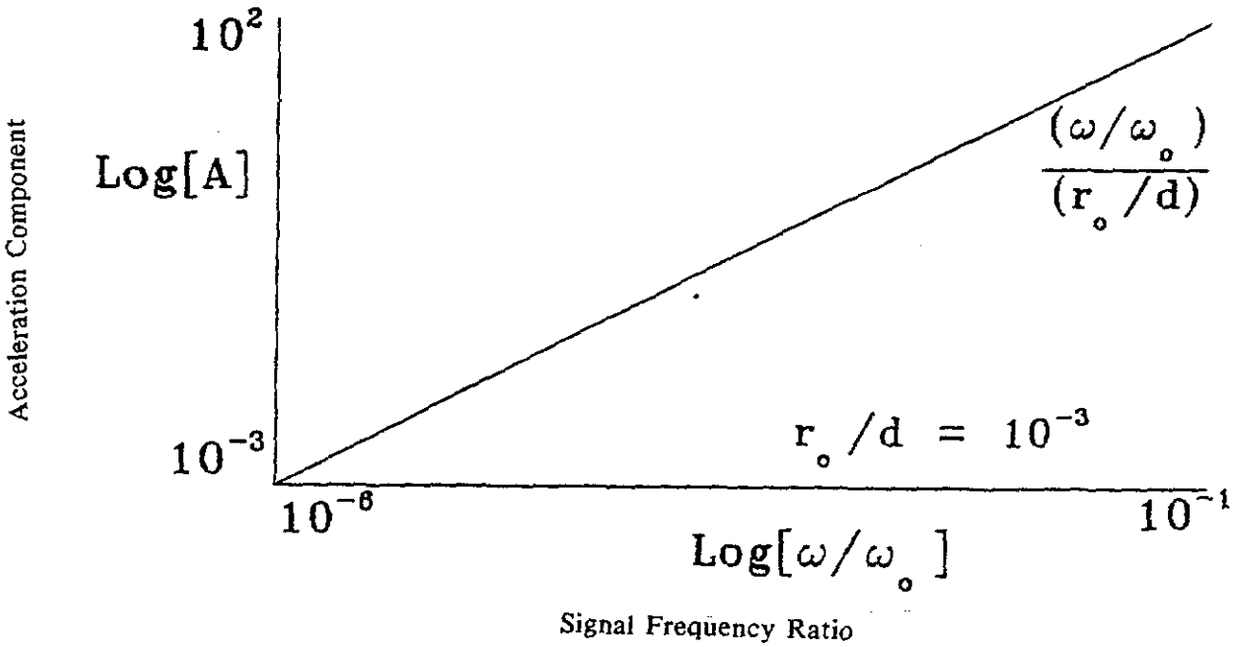

Figure 2a. Frequency Spectrum of the First Two Terms in the Transverse Accelerometer Equation: Component at ω.

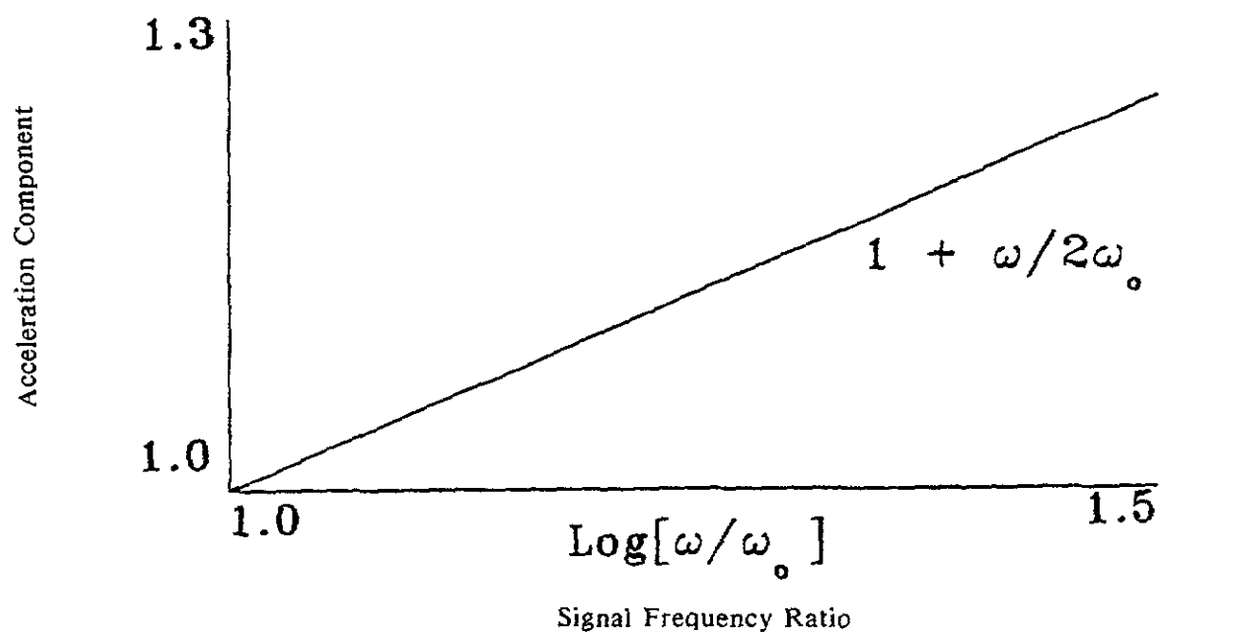

Figure 2b. Frequency Spectrum of the Amplitude Modulated Term in the Transverse Accelerometer Equation: Component at $\omega_o + \omega$.

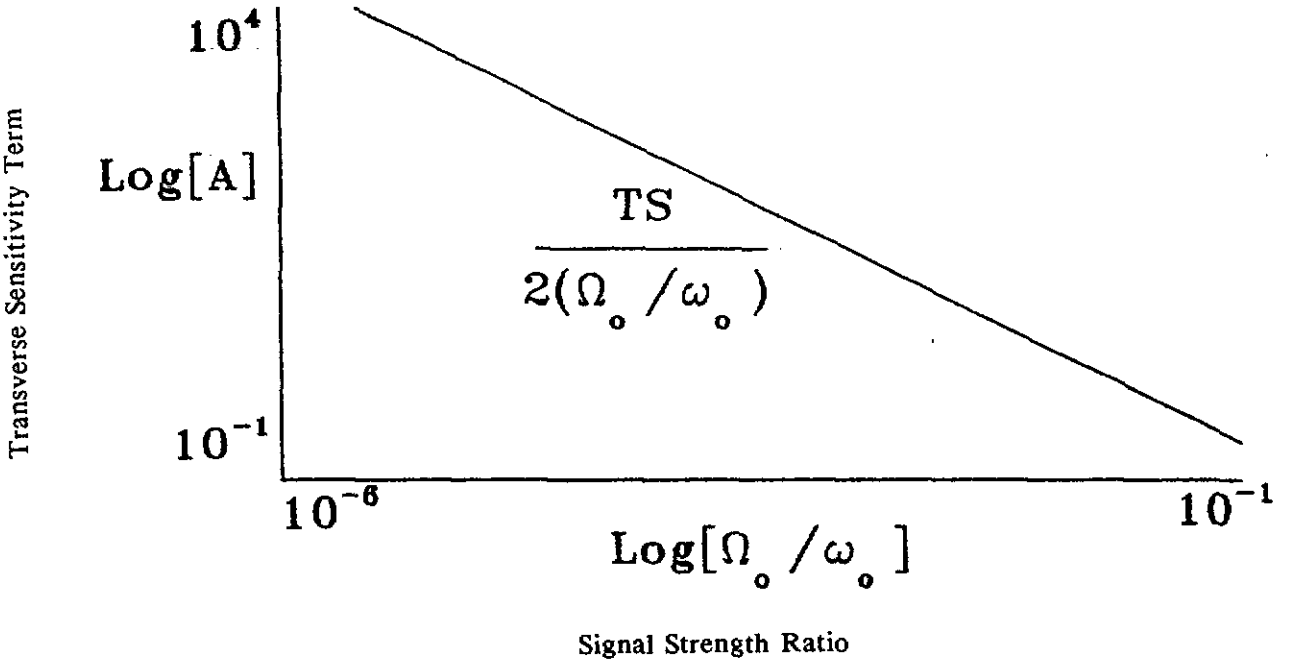

Figure 3a. Accelerometer Contamination from Transverse Sensitivity at the Carrier Frequency.

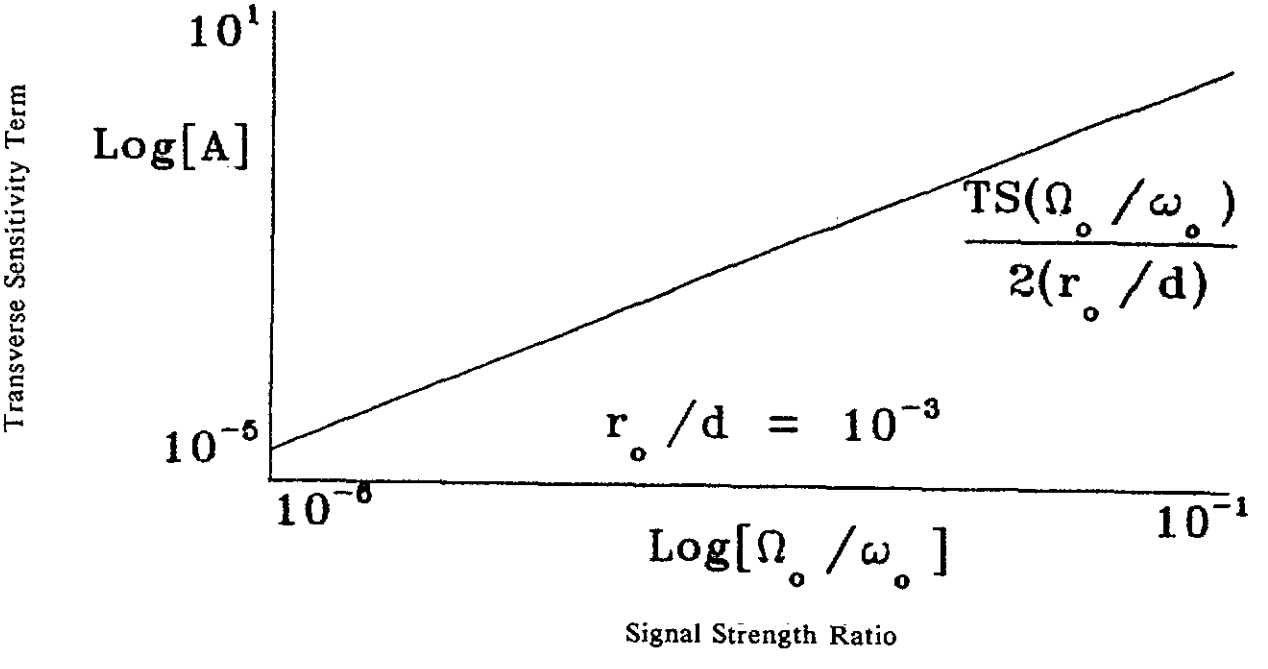

Figure 3b. Accelerometer Contamination from Transverse Sensitivity at 2ω and $\omega_o + 2\omega$.

the resonating tuning fork are vibrating exactly out of phase, the two cross-axis sensitivity component can then be removed by mounting A_3 on the opposite face of the opposite tine and then adding A_2 and A_3 together before signal processing. This will also double the desired amplitude modulation term.

After signal conditioning, the angular velocity signal is:

$$\Omega(t) = 4\Omega_o\omega_o r_o\, e^{j\omega t} \tag{6}$$

This equation illustrates that the angular velocity to be measured is proportional to the tuning fork/driver resonant velocity. The design of a prototype tuning fork/driver system is discussed in the next section.

DESIGN OF A TUNING FORK/DRIVER SYSTEM

The natural tendency for mechanical resonating systems is for the resonant displacement to decrease as the resonant frequency increases. The resonant frequency of the piezoelectric driver is very high, typically in the hundred kHz range. The displacement of the driver is very low, however, typically in the micron range. The resonant frequency of a tuning fork is very low, typically in the audible range. However, its resonant displacement amplitude is much higher than that of the piezoelectric driver. When the driver is attached between the tines of the tuning fork as illustrated in Figure 1, the combined system resonant velocity is much improved. The driver serves to stiffen the fork and the resonant frequency is increased. Alternately, the fork serves as a displacement amplifier for the driver and the resulting tuning fork/driver system will maximize the system resonant velocity amplitude.

It should be evident that the tuning fork/driver system resonant frequency must be high enough to enable the accelerometers to function properly. The amplitude modulated signal present in A_2 and A_3 permits accelerometers to operate at their best. Low frequency measurements are often difficult with accelerometers, but the zero frequency measurement of the amplitude modulation signal is at the system resonant frequency. By selecting ω_o sufficiently high, the accelerometer signal strength can be increased.

The most appropriate resonant velocity must be determined in order to estimate the application potential of this transducer and begin the design of the signal conditioning electronics. The configuration which maximizes the resonant velocity can be determined by evaluating the influence of the driver location. Because of the symmetry of the tuning fork, one of the tines can be analyzed independently. If the beam is thin compared to its length, the system resonant frequency can be determined using classical beam theory by assuming a piecewise mode shape[2]. The equation of motion of the Bernoulli-Euler beam is:

$$EI\,\frac{\partial^4 r}{\partial^4 z} + C\,\frac{\partial r}{\partial t} + \rho A\,\frac{\partial^2 r}{\partial t^2} = \phi(z-z_e)F_o\exp(j\omega_o t)\,, \tag{7}$$

where $\delta(z-z_e)$ is the delta function and F_o is the amplitude of the force supplied by the piezoelectric driver. The driver is modeled as a very stiff translational and rotational spring[3]. Equation (4) is solved using separation of variables, assuming $r(z,t) = \phi(z)q(t)$. The mode shape function, $\phi(z)$, will be discontinuous in the second and higher derivatives at $z = z_e$ due to the influence of the driver. The piecewise mode shapes can be written as follows:

for z between 0 and z_e

$$\phi_1(z) = C_1[\cos(kz)+\cosh(kz)] + C_2[\cos(kz)-\cosh(kz)] + C_3[\sin(kz)+\sinh(kz)] + C_4[\sin(kz)-\sinh(kz)]$$

for z greater than z_e

$$\phi_2(z) = B_1[\cos\{k(z-z_e)\}+\cosh\{k(z-z_e)\}] + B_2[\cos\{k(z-z_e)\}-\cosh\{k(z-z_e)\}]$$
$$+ B_3[\sin\{k(z-z_e)\}+\sinh\{k(z-z_e)\}] + B_4[\sin\{k(z-z_e)\}-\sinh\{k(z-z_e)\}]$$

The following boundary conditions are needed to evaluate the eight constants:

(1) Deflection is zero at z = 0
(2) Slope is zero at z = 0
(3) Deflection is continuous at $z = z_e$
(4) Slope is continuous at $z = z_e$
(5) The beam bending moment must balance the rotary stiffness at $z = z_e$[2]

$$\frac{d^2\phi_1}{dz^2} - \frac{d^2\phi_2}{dz^2} = \frac{k_\theta}{EI}\frac{d\phi_2}{dz}$$

(6) The beam shear must balance the translational stiffness at $z = z_e$

$$\frac{d^3\phi_1}{dz^3} - \frac{d^3\phi_2}{dz^3} = \frac{k_s}{EI}\phi_2$$

(7) Beam bending moment is zero at z = L
(8) Beam shear is zero at z = L

Boundary conditions (1) and (2) force C_1 and C_3 to be zero. The remaining boundary condition equations can be reduced to six equations in terms of the eigenvalue, λ=kL, and three dimensionless parameters $z^*=z_e/L$, $k_\theta^*=k_\theta/(EI/L)$ and $k_s^*=k_s/(EI/L^3)$:

$$[\cos(\lambda z^*)-\cosh(\lambda z^*)]C_2 + [\sin(\lambda z^*)-\sinh(\lambda z^*)]C_4 = 2B_1$$

$$[-\sin(\lambda z^*)-\sinh(\lambda z^*)]C_2 + [\cos(\lambda z^*)-\cosh(\lambda z^*)]C_4 = 2B_3$$

$$[-\cos(\lambda z^*)-\cosh(\lambda z^*)]C_2 + [-\sin(\lambda z^*)-\sinh(\lambda z^*)]C_4 + 2B_2 = -k_\theta^* B_3/\lambda$$

$$[\sin(\lambda z^*)-\sinh(\lambda z^*)]C_2 + [-\cos(\lambda z^*)-\cosh(\lambda z^*)]C_4 + 2B_4 = k_s^* B_1/\lambda^3$$

$$[-\cos(\lambda-\lambda z^*)+\cosh(\lambda-\lambda z^*)]B_1 + [-\cos(\lambda-\lambda z^*)-\cosh(\lambda-\lambda z^*)]B_2 +$$

$$[-\sin(\lambda-\lambda z^*)+\sinh(\lambda-\lambda z^*)]B_3 + [-\sin(\lambda-\lambda z^*)-\sinh(\lambda-\lambda z^*)]B_4 = 0$$

$$[\sin(\lambda-\lambda z^*)+\sinh(\lambda-\lambda z^*)]B_1 + [\sin(\lambda-\lambda z^*)-\sinh(\lambda-\lambda z^*)]B_2 +$$

$$[-\cos(\lambda-\lambda z^*)+\cosh(\lambda-\lambda z^*)]B_3 + [-\cos(\lambda-\lambda z^*)-\cosh(\lambda-\lambda z^*)]B_4 = 0$$

Figure 4a shows λ versus z_e/L for $k_s^*=10^4$ and $k_\theta^*=10^2$. When z_e/L is zero, λ = 1.875 corresponding to the cantilever beam. When z_e/L is one, λ = 4.730 corresponding to the clamped beam. The

maximum eigenvalue occurs at $z_e/L = 0.73$, where $\lambda = 6.3444$. Using the frequency equation $\omega_o=(\lambda/L)^2[EI/\rho A]^{0.5}$, the tuning fork resonant frequency has been increased by more than an order of magnitude due to the influence of the driver.

Since the piezoelectric driver is very stiff, its output displacement for a particular voltage is nearly constant over a wide frequency range, almost independent of the loading. The forced response can be calculated in terms of the force generated in the driver:

$$\frac{d^2q}{d^2t} + 2\zeta\omega_o \frac{dq}{dt} + \omega_o^2 q = \frac{\phi(z_e)F_o e^{j\omega t}}{\rho A \int \phi^2 dz} \qquad (8)$$

The mode shape function, $\phi(z)$, must be normalized such that $\int \phi^2 dz = L$. Then the amplitude of the resonant deflection is:

$$r_o(z) = \frac{\phi(z)\phi(z_e)(F_o/\zeta)}{2\lambda^4 (EI/L^3)} . \qquad (9)$$

This shows that the resonant deflection is proportional to (F_o/ζ) and allows evaluation of the corruption terms in Figures 2 and 5. The amplitude of the resonant velocity is:

$$\omega_o r_o(z) = \frac{\phi(z)\phi(z_e)(F_o/\zeta)}{2\lambda^2 (EI/L)} [EI/\rho A]^{0.5} . \qquad (9)$$

The energy dissipated per cycle is:

$$p = \frac{\phi(z_e)^2(F_o/\zeta)\pi}{2\lambda^4(EI/L^3)} \qquad (10)$$

Figure 4b shows the resonant velocity and power consumption plotted versus dimensionless driver location, z_e/L, with resonant velocity calculated at $z_e/2$. The distinct peak in the resonant velocity occurs at $z_e/L=0.73$, which coincides with the peak in the system eigenvalue. These results illustrate that the driver should be located at 0.73L. Figure 5 is a plot of $\phi(z)$ versus z/L and illustrates that the best location for the accelerometers is at $z=z_e/2$.

This simple analysis based on the Bernoulli-Euler beam is limited to beams that are very thin compared to the length. That limitation is likely to be violated for the final design, so a Timoshenko beam analysis may be necessary. Also, using the simple lumped spring model of the driver includes some inherent uncertainty in the parameter k_θ. Therefore, a finite element model of the tuning fork/driver system has been developed to investigate those effects.

DESIGN OF DRIVER AND SIGNAL CONDITIONING ELECTRONICS

A theoretical AM signal results from the Coriolis effect on an accelerometer mounted on the side of a vibrating beam. In Figure 1, the resonant displacement at the location of the accelerometers A_2 and A_3 is given by equation (1) which is repeated here:

$$r(t) = d + r_o \exp(j\omega_o t) \qquad (1)$$

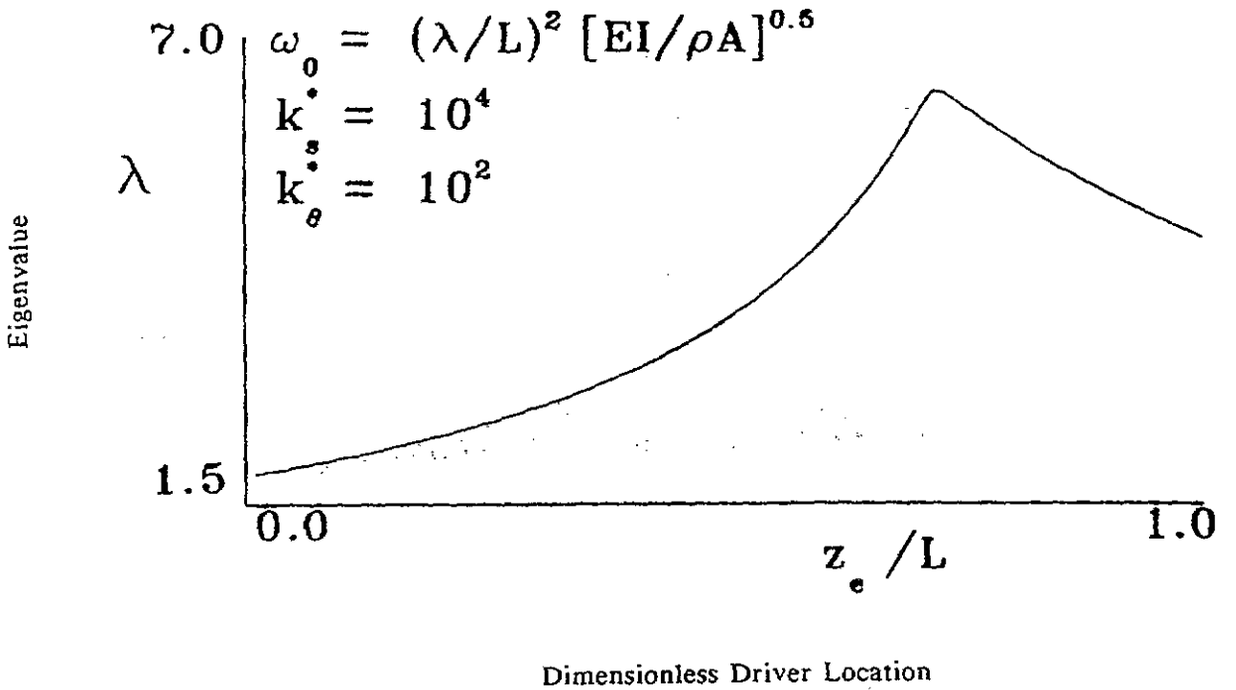

Figure 4a. Fork/Driver System Eigenvalue Plotter against Dimensionless Driver Location.

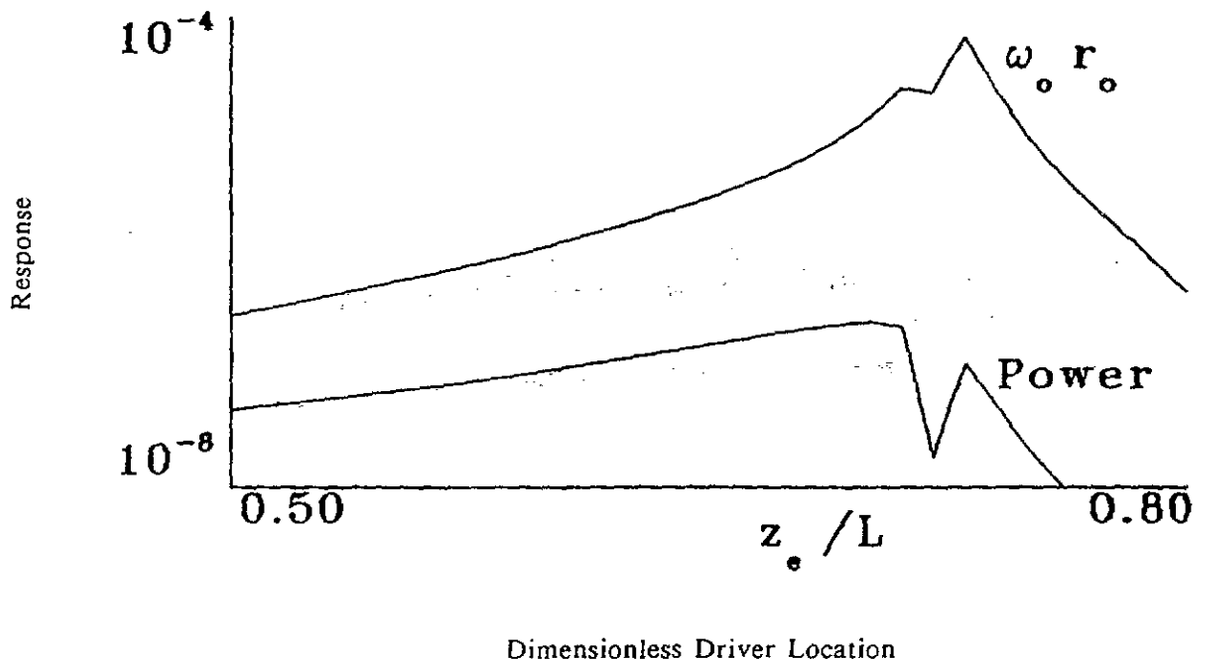

Figure 4b. Optimum Driver Location Based on Resonant Velocity and Power Consumption.

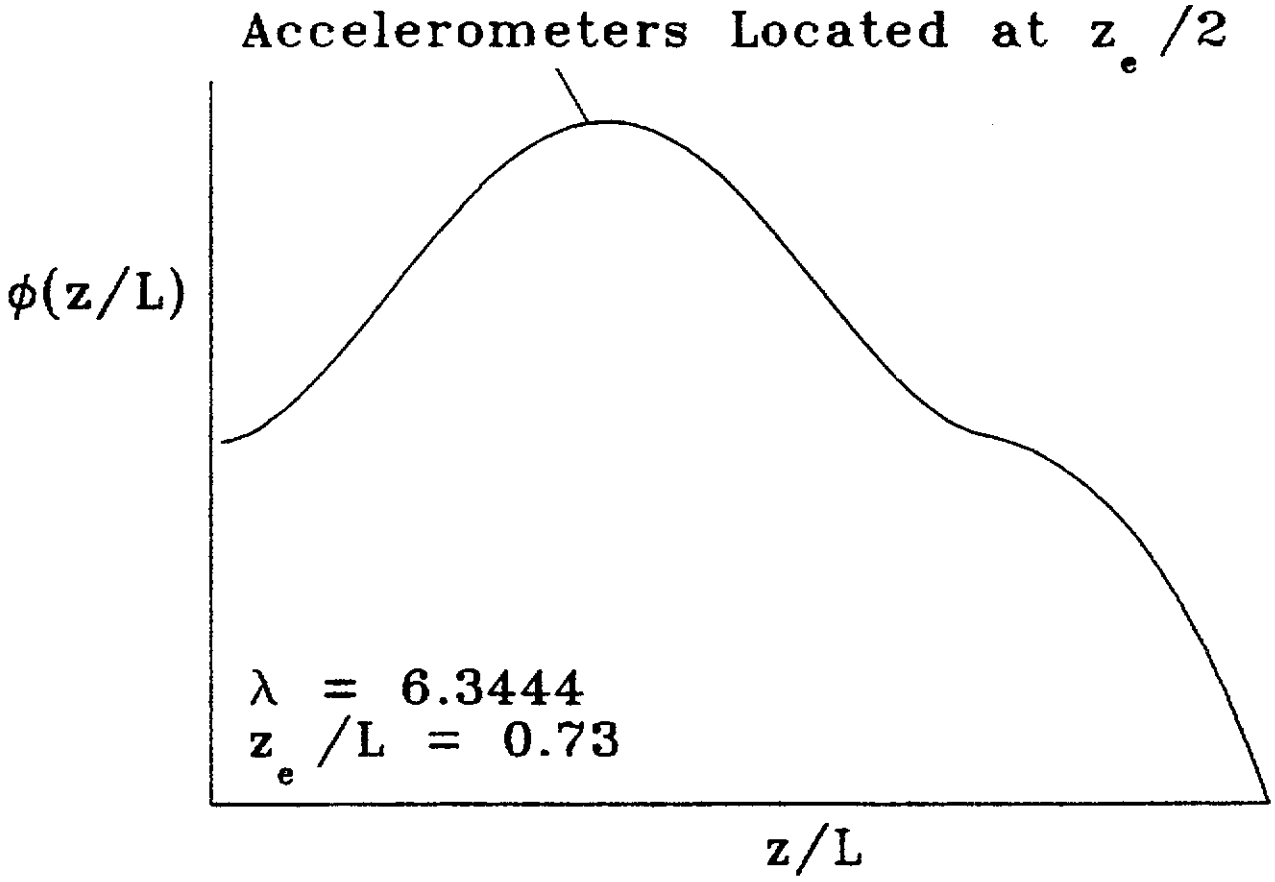

Figure 5. Mode Shape Function for Optimum Driver Location.

An angular input can be described as a velocity, $\Omega(t)$, which oscillates at a frequency (ω) about the Z-axis of the system at a velocity amplitude of Ω_o:

$$X(t) = \Omega_o e^{j\omega t} \tag{11}$$

Using the angular input, $\Omega(t)$, with the tuning fork's resonant amplitude, r(t), the following accelerations are experienced by accelerometers A_1 and A_2:

$$A_1(t) = r''(t) - \Omega(t)2r(t) \tag{12}$$

$$A_2(t) = \Omega'(t)r(t) + 2\Omega(t)r'(t) \tag{13}$$

where r'(t) and r''(t) are the first and second derivatives of r(t). Because of the location and orientation of A_3, its signal will be equal to the signal from A_2 except that the ω_o components will be 180° out of phase. Substituting equations (1) and (11), ignoring cross-axis sensitivity, gives:

$$A_1(t) = -\omega_o^2 r_o \exp(j\omega_o t) - \Omega_o^2 d \exp(j2\omega t) - \Omega_o^2 r_o \exp[j(\omega_o + 2\omega)t] \tag{14}$$

$$A_2(t) = j\omega\Omega_o d \exp(j\omega t) + j(\omega\Omega_o r_o + 2\omega_o\Omega_o r_o)\exp[j(\omega_o + \omega)t] \tag{15}$$

Examining equation 15, the first term of the signal $A_1(t)$ from accelerometer A_1 contains the resonant frequency of the system ω_o. $A_1(t)$ is then filtered to recover only the first term, which is the fundamental resonant frequency of the tuning fork.

$$A_1(t) = -\omega_o^2 r_o \exp(j\omega_o t) \tag{16}$$

Since the fork/driver mechanical system is very lightly damped, small variations of excitation frequency result in very large variations in the resonant velocity amplitude, thus severely degrading sensitivity. Therefore, the fork/driver system must be excited exactly at resonance to maximize the resonant velocity amplitude, maintain stability of resonant velocity amplitude, and minimize power consumption. Besides being driven exactly at the resonant frequency, it is equally important that the drive force be exactly in phase with the driven fork. Therefore, $A_1(t)$ is used as a reference signal for a phase-locked oscillator, that drives the piezoelectric actuator at the resonant frequency, in phase with the fork oscillations.

The piezoelectric driver selected is a highly capacitive device, and the displacement is proportional to the voltage developed across it. The voltage developed across a capacitor is equal to the integral of the current, divided by capacitance. The amplifier required to drive it must therefore have a very low output impedance but a high current capability, in order to develop sufficient voltage across a capacitive load. This may be achieved in several ways, but one way consists of a series resonant LC network, with the piezoelectric driver being the capacitive element. At resonance, this network reflects a very low impedance (ideally a zero impedance) to the amplifier, but the voltage developed across the piezoelectric driver can be made sufficiently high to excite the necessary displacement. This LC circuit also acts as a high Q filter developing voltage across the piezoelectric driver only at the fundamental resonant frequency, thereby reducing noise which would contaminate the desired signals from A_2 and A_3.

The signals from accelerometers A_2 and A_3 can also filtered to recover the amplitude modulated signals containing X(t). Equations 15 applies to both the signals from A_2 and A_3, except that the carrier ω_o is 180° out of phase from the signal from A_2. If the signal from A_2 is bandpass filtered to

remove the other unwanted frequency components (adjacent interferences), the signal remaining is of the form:

$$A_2(t) = 2\Omega_o\omega_o r_o \exp[j(\omega_o + \omega)t] \quad (17)$$

This equation has the original rotary input signal $\Omega(t)$, amplitude modulated onto a carrier frequency of the resonant frequency of the tuning fork. The signals $A_2(t)$ and $A_3(t)$ represent voltage signals:

$V_2(t) = (S_2)(A_2(t))$
$V_3(t) = (S_3)(A_3(t))$

where S is the accelerometer sensitivity in Volts/unit of acceleration. This can be expressed in an equation that represents an AM waveform according to the following general form for a given carrier amplitude A, modulating signal m(t), and carrier frequency ω_o:

$$AM = [A + m(t)] \cos(\omega_o t)$$

To put the accelerometer signal into this form of this equation,

$$m(t) = 2\Omega_o\omega_o r_o \exp(j\omega t)$$

$A = (TS^2)\omega_o^2 r_o$ (where TS = transverse sensitivity)

These signals from A_2 and A_3 can be summed together and filtered, to provide a suppressed-carrier amplitude modulated signal of twice the sideband amplitude. The polarity of the two transverse sensitivity terms will be opposite, due to the location and orientation, so after combining the signals from the accelerometers, the amplitude modulated signal will be:

$$AM = 4\Omega_o\omega_o r_o \exp[j(\omega_o + \omega)t]$$

which is the equation for a suppressed-carrier double-sideband amplitude modulated signal.

Summing the signals prior to filtering reduces the filtering requirements, resulting in simplified circuitry. That signal is then demodulated to provide the original rotational velocity signal, which can be further integrated or differentiated to provide angular position or acceleration. The critical elements of the signal conditioning circuit are illustrated in Figure 6.

Piezoresistive strain gage elements are solid state silicon resistors which change electrical resistance in proportion to applied mechanical stress. The accelerometer is etched from a single piece of silicon. This silicon chip includes the inertial mass and strain gages arranged in an active four-arm Wheatstone Bridge circuit complete with a novel on-chip zero balance network. The input and output resistances for the particular devices used are approximately 550 Ohms.

The output of the Wheatstone Bridge arrangement is applied to a high gain, low noise differential amplifier, providing a signal that includes the desired amplitude modulated or unmodulatated carrier. This arrangement is used for all three accelerometer signals, with the gain being adjusted as required for the particular channel application.

The low rotational amplitudes result in a low modulation index, producing a low signal-to-noise (S/N) ratio. Therefore the demodulator sensitivity is a primary design criteria, and the choice of a demodulator scheme is critical to recover the modulated signal from the carrier. Coherent demodulation was selected to provide the maximum sensitivity for signal recovery.

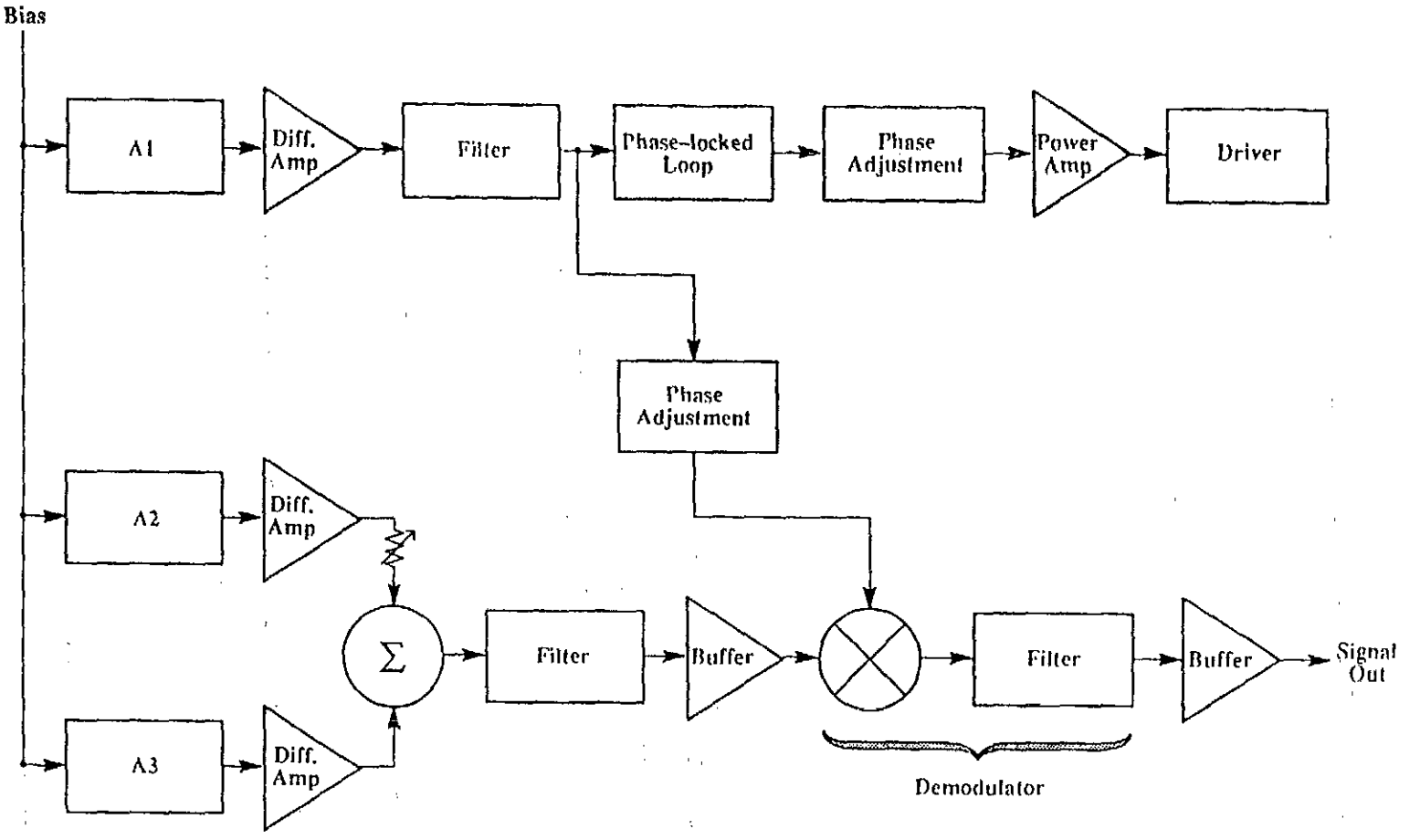

Figure 6. Basic Signal Conditioning Electronics Required with the Solid-State Rotary Vibrometer.

The signals from A_2 and A_3 are summed together to reduce signals introduced by accelerometer transverse sensitivity prior to filtering. The recovered signal is then filtered and down converted by mixing it with the reference signal ω_o from A_1. This mixing process provides three basic signals: The original signals applied to the mixer (the suppressed carrier AM signal and the reference signal ω_o); the sum of those signals; and the difference in those signals. The desired signal is now the difference signal out of the mixer, and the remaining signals are removed by filtering.

We have now recovered the original rotational signal. By differentiation for integration, we may provide that signal in any of several different forms.

CONCLUSIONS AND RECOMMENDATIONS

Accelerometers mounted orthogonally on the sides of the tines of a vibrating tuning fork, provide a suppressed-carrier double-sideband amplitude modulated signal, containing rotary motion information of the tuning fork about an axis parallel to the tines. By driving the tuning fork with a piezoelectric actuator attached between the tines, the tuning fork is stiffened and its resonant frequency is increased. The purpose of the tuning fork is to mechanically amplify and filter the displacement of the accelerometers at resonance, thereby increasing the sensitivity of the Rotary Vibrometer. Modulating the rotational information onto a carrier effectively widens the bandwidth of the accelerometer. Properly orienting the accelerometers orthogonally provides two carriers that, when summed together, suppress the carrier and cancel contaminating signals resulting from accelerometer cross-axis sensitivity. The carrier frequency is the resonant frequency of the tuning fork, and the modulating signal contains the rotary information. A phase-locked oscillator is utilized to drive the tuning fork exactly at resonance and in phase with the fork, to maximize purity of the carrier and minimize power consumption. This same signal may be used to demodulate the desired rotary information from the carrier. That rotational velocity information may further be processed by differentiation or integration to produce rotational acceleration or position.

Encapsulating the tuning fork and accelerometer assembly in an evacuated capsule would reduce the fluid damping on the fork and power consumption of the piezoelectric driver, while at the same time providing physical protection for the accelerometers. Coherent detection is the selected method of demodulation because of sensitivity, but for really low angular velocity measurement, digital circuitry would be required.

ACKNOWLEDGEMENTS

The University of Nebraska has supported the patent application process. Endevco has provided the piezoresistive accelerometers necessary to develop a prototype. Don Anderson, Ky Longley and Jim Yates have worked hard to develop the prototype described in this paper.

REFERENCES

1. Whaley, P. W., "A New Broadband Angular Velocimeter, U. S. Patent Number 4,958,519, September 25, 1990.

2. Whaley, P. W., and J. Pearson, "Computer Aided Design of Passive Vibration Isolators for Airborne Electro-optical Systems," Shock and Vibration Bulletin, No. 49, Part 2, pp. 81-86, September, 1979.

3. Kinsler, L. E., and A. R. Frey, Fundamentals of Acoustics, Chapter 12, "Ultrasonic and Sonar Transducers", pp. 333-374, John Wiley & Sons, New York, 1962.

LIST OF FIGURES

A ± 70 g FULL SCALE ACCELEROMETER DESIGNED TO SURVIVE 100,000 g OVERRANGE

Robert D. Sill, Sr. Project Engineer, ENDEVCO

Accelerometers using a silicon micromachined variable capacitance sensors survived 90,000 g overrange with small performance shifts. Design, packaging and performance testing for the ±70 g full scale device is described.

INTRODUCTION

The requirements of an inertial measurement unit (IMU) to survive 100,000 g call for the development of highly miniaturized and extremely rugged instruments. In one design, accelerometers are epoxied to the backs of ring laser gyros. In this configuration, accelerometer package design is driven by the need to reduce size and weight so that epoxy strength would be adequate to survive the launch. The result is a single-axis open-loop accelerometer weighing less than a gram and with dimensions of 10 x 10 x 3 mm.

This report will discuss the design of the accelerometer, and will describe some of the testing and results. Seven accelerometers were tested and survived shocks up to 90,000 g with small shifts in performance. The average magnitude of shifts of bias and sensitivity was <0.3% full scale (FS) and <0.7%, respectively. Analyses of performance gives direction for improvements to future versions of the accelerometer.

SUMMARY OF EXISTING DESIGN

Overall Design - At the heart of the accelerometer is a micromachined silicon variable capacitance acceleration sensor [1] and an ASIC (application specific integrated circuit), both of which were developed at Endevco. The packaging incorporated conventional chip-and-wire hybrid techniques on a thick film gold metallized alumina substrate. Internal connections were made with ultrasonic bonding of 1% Si aluminum wire. Discrete thin film resistors were actively laser trimmed to set bias levels after board assembly, before lid weldment. Conformal coating was used for component support during shock.

The accelerometer was electrically shielded and hermetically packaged in a titanium case with platinum feedthroughs, which provided considerable weight advantage compared to traditional iron-nickel alloy packaging. The ground pin was brazed to the titanium case, and two feedthrough pins were glass fired into the case wall.

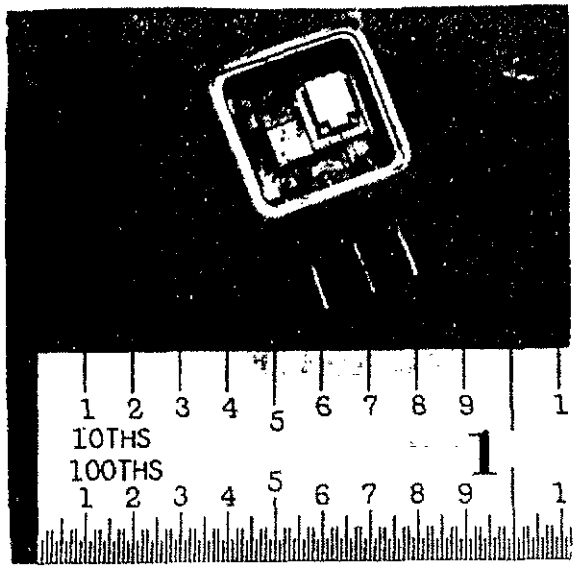

Figure 1. Photograph of the accelerometer. The lid is removed for clarity. The silicon sensor is seen at the upper right corner of the cavity, with a sensitive axis pointing up out of the lid. Its wirebonds are draped over a dam separating the sensor from the conformal coating used for structural reinforcement of components. The units on the measuring scale shown alongside are in tenths of inches. The 100,000 g shock is directed primarily transverse to the sensitive axis.

Design of the Sensor - The sensor consists of a sandwich of three micromachined silicon wafers: a moving flat plate in the center "core" wafer and two outer fixed plates (the "lid" and "base" wafers). The wafers are bonded to form a hermetically sealed assembly. It is a three terminal device in its present form, comprising a half bridge capacitive acceleration sensor. Positive acceleration (up into the base, normal to the mounting surface) causes capacitance between the core and the base to increase (because the plate-to-plate spacing decreases as the core moves downward relative to the base), while the capacitance between the core and the lid decreases.

To linearize the output, the ASIC output (a dc current) is proportional to the difference of the two capacitances. An earlier version of the sensor utilized only the gap between base and core, and was therefore a two terminal device which was used in matched pairs. That version of the sensor has been described previously [2], and incorporates the same air damping, stops, and glass inlays of the second generation device used in the accelerometer of this report. The newer sensor version is shown in Figure 2.

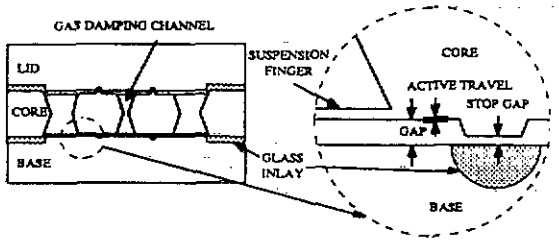

Figure 2. Cross-sectional depiction of the variable capacitance sensor used in the accelerometer. Dimensions are distorted in scale for clarity.

Compared to the first generation sensor described in [2],the sensor of this report differs primarily in the method of suspension of the inertial mass. The first version used a membrane around the mass at the centerplane, whereas the second uses suspension fingers of silicon on top and bottom surfaces of the core (similar to a trampoline or the spokes of a bicycle wheel) to connect the etch-freed mass mechanically and electrically to the edge rim. This is illustrated in Figure 3.

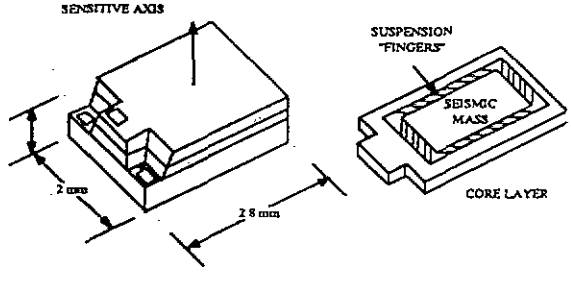

Figure 3. View of the sensor approximately to scale. Only the top layer of the suspension fingers is depicted. There is a matching array of fingers on the underside of the mass, with an opposite angle to the mass. Finite element analysis shows the asymmetry to cause insignificant warpage of the mass.

Several versions of the second generation sensor have been used. Differences exist primarily in the shape and thickness of the fingers (for which a patent is pending), to vary both the sensor sensitivity and the ratio of stiffnesses in the primary and transverse directions of motion. The shape is determined by patterning boron dopant into the silicon surface. Thickness is determined by the diffusion depth of the boron, high concentrations of which render the fingers resistant to the etchant used to free the mass from the rim in the core wafer. Two configurations are shown in Figure 4 which were involved in this project.

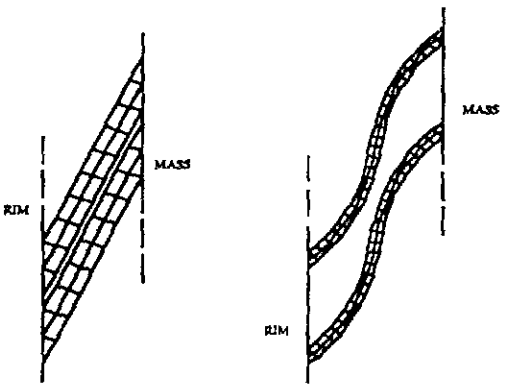

Figure 4. FEA models of two forms of suspension "fingers". The straight fingers on the left are those of the final configuration. Those on the right are used in more compliant (higher sensitivity) sensors also involved in testing in this program. A pair of each type is shown to depict the spacing used, and is shown approximately to scale. The rim-to-mass length of each finger is approximately 0.25 mm (10 mils). All fingers are planar with thicknesses of a few microns.

Finite element analyses (FEA) were performed on both types of suspension fingers shown in Figure 4. In Table I are comparisons of the results of FEA, using as-measured dimensions from the devices. The discrepancy between predicted and measured values of resonant frequency for the straight finger model was due to the initial failure to account for residual tension in the fingers left from processing. The geometry of the curved fingers reduces this effect.

Table I. FEA and measured results of two types of support fingers used in sensors of this program.

	Straight	Curved
Resonance in sensitive axis (FEA)	2.7 KHz	3.8 KHz
Actual res. freq. (as measured)	5.7 KHz	3.8 KHz
Full scale (measured)	70 g	35 g
Transverse resonance (FEA)	260 KHz	56 KHz
Stress per g transverse (FEA)	1.98 KPa	48.4 KPa
Stress per g sensitive (FEA)	393 KPa	365 KPa

Results concerning stresses support the conclusions from shock testing, that the stout design of the straight fingers generates considerably less stress for a given transverse shock. Samples from this design of sensors survived 125,000 g in the transverse direction on both the Hopkinson bar [3] and centrifuge testing. Because the overload stops limit motion of the mass to a few times full scale range, stresses in fingers due to shocks in the sensitive axis are small. The stops themselves see stresses of similar magnitude.

Samples of the curved design experienced partial failure between 30 000 g and 50 000 g at air gun and Hopkinson bar tests. Interestingly, for such levels there generally was not catastrophic failure. Performance change was on the order of a few percent. In shaker tests after the shocks, frequency response characteristics would change intermittently with acceleration amplitude, indicating particles (probably from broken fingers) were interfering with motion of the mass. It was concluded that the majority of the 188 fingers survived. From the FEA model, this indicates that many curved fingers survived stresses in excess of 2 Gpa (300 Kpsi).

As would be expected from the analysis, total failure occurred to samples with curved fingers on the Hopkinson bar at 100,000 g. All the fingers failed, and the mass occasionally burst out through the rim. The shocks on the bar were made more severe by the effect of overshoot of transverse deflection due to the relatively low transverse resonance. The natu-

ral period matched very closely the pulse duration of the shocks on the bar.

Sensor Mounting and Conformal Coating
In addition to shock survivability, good static performance is required of an accelerometer in an inertial measurement application. Dimensional stability is critical, particularly the flatness of the sensor base. (No discussion will be included on the electrical stability of circuit components.) Because the sensor is mounted on a surface of an active structural element (the base layer of the sandwich), thermal and mechanical strains from the mounting surface can be quite closely coupled to the sensor output. Using rigid epoxy to "hard"-mount the silicon sensor to a substrate whose thermal coefficient of expansion differed even slightly from that of silicon, such as aluminum nitride, resulted in significant changes in the sensor's thermal coefficient of capacitance. A compliant mounting scheme was necessary, which raised the problems of strength and of dealing with the displacements allowed by the interface during shocks.

A thin layer of silicone rubber (RTV) was used as mounting between the sensor and conventional 96% alumina substrate. Strength of the bond was adequate. At 100,000 g the weight of the 0.01 gram sensor stresses the bond at approximately 1.7 MPa (250 psi). Only in a comparatively long duration centrifuge test above 125,000 g (lasting minutes rather than the milliseconds experienced in shocks) has there been failure of the RTV interface. No failures of the bond have occurred in shocks in this program. However, wire movement and wirebond failure were the predominant accelerometer failure mechanisms in early tests, which may be related to the compliance of the RTV.

Thickness of the RTV determines the relative displacement between the sensor and the substrate during shock, and therefore the strain of the electrical wirebonds between. Methods of constraining wirebonds were found to be necessary since parasitic capacitances existed between the wires, and any displacement of the bonds represented changes of capacitance and therefore a bias shift. Alumina-filled structural epoxy was used to fix the lead wires in place, used as a thixotropic conformal coat. Because the sensor was strain sensitive, it was not permissible to allow the conformal coat to touch the sensor. Small dams were used to prevent flow of the coating onto the sensor. Draping the sensor lead wires over this dam permitted the shortening of the unsupported length of the wires from the sensor to the substrate. This was beneficial, minimizing displacements (and therefore output changes) due to shock. A compromise in length was necessary, however, since the unsupported wire length traversing the space between a rigidly held dam and the compliantly-held sensor needed to be long enough to provide strain relief for shocks.

TESTING

Transverse sensitivity - The dominate cause of transverse sensitivity, (that is, output due to accelerations transverse to the sensitive axis of the accelerometer), is simply misalignment of the sensor with the mounting surface. Present manufacturing procedures with RTV mounting allow misalignments on the order of 0.5°. Once corrections are made for this misalignment in the IMU, analysis shows no significant sources of transverse sensitivity, as described below.

Planar symmetry and the peripheral support structure of the seismic mass means the sensor has no "pendulous axis". Conditions of simultaneous primary and transverse accelerations can cause rotation of the mass, driving its edges toward the lid and base, but because of the peripheral support there is no tendency to drive the seismic center toward the neutral axis. The effect of the rotation that does occur is small because of spatial averaging of the capacitance (the capacitive contribution of the part of the gap narrowed by the mass rotation is compensated by the part widened). Analysis showed a 30 g static

acceleration in the sensitive axis and 300 g transverse acceleration resulted in rotation that would cause 3 milli-g of output. Testing this is difficult, and was not possible with available equipment. One possible configuration would have required an electrodynamic shaker carried on a centrifuge.

A test was performed to show that no nonlinear effects were created by transverse motion. The ring laser gyros of the IMU need "dithering" for operation, which is a sinusoidal angular motion imposed on the gyros to prevent "mode locking" at low angular rates. Since size constraints require the accelerometers mounted on the backs of the gyros, the operating environment of the accelerometer therefore includes several hundred sinusoidal g's transverse to the sensitive axis. This is several times larger than the full scale operating range.

To determine the effect of this motion, accelerometers were placed in the transverse direction on the end of a resonant rod, symmetrically mounted about the axis so no bending moments were imparted to the rod during vibration. The rod was driven axially by an electrodynamic shaker at the intended dither frequency (which at that time in the program, was near 1000 Hz). The high "Q" of the rod gave large amplitude high purity transverse motion to the accelerometers. Output by the accelerometers was about 1% of the value had the acceleration been on-axis, consistent with the transverse sensitivity due to mounting misalignment as determined by low g measurements. This was verified by further tests at high g, in which the accelerometers were then intentionally misaligned with shim stock, resulting in proportionate phase and magnitude changes.

By these tests the transverse acceleration performance was shown to be linear well beyond the full scale range, and that it would be correctable by IMU algorithms if misalignments are known. The effect of transverse input on bias was a simpler measurement, and also showed negligible non-linear effect. Bias shift during the 300 g 1060 Hz transverse test was less than 1.5 milli-g.

Bias rectification and nonlinearity - A potentially larger error due to non-linearity is that of bias shift due to vibration rectification. This can be visualized by considering one period of purely sinusoidal vibration. If monitored by an accelerometer with sensitivity which is greater with positive accelerations than negative, output would be larger going positive than negative, and the average would be non-zero, even though the the average of the input sinusoid was zero. A positive bias error would result from this hypothetical condition.

There are nonlinearities in the accelerometers, because capacitance is inherently a non-linear function of the gap. The differential nature of the sensor and the open-loop electronics eliminates most of the nonlinearity, but any non-linearity could cause rectification errors. The operating condition of the IMU could involve aerodynamic vibrations and nearly static accelerations, both of which are an appreciable fraction of full scale. This is a worst-case scenario for rectification, causing the accelerometer to operate with large vibrations in a region with significant (between 0.1% and 1%) non-linearities in its sensitivity.

It was impossible with existing facilities to do vibration testing of units in the presence of comparatively large static accelerations. Simulation was possible, however, by scaling sensitivity. Sensors were used with the curved fingers as described previously, but with thinner fingers, such that sensitivity was approximately 10 times that of the sensors in the final configuration. Amplitude linearity characteristics of these sensors were more like that of a ±7 g full scale transducer, as shown in Figure 5. (Accelerometers made from these ±7 g sensors in an IMU of a different program survived 15 000 g shocks, also in transverse directions, with performance shifts very similar to those in the program described in this paper.)

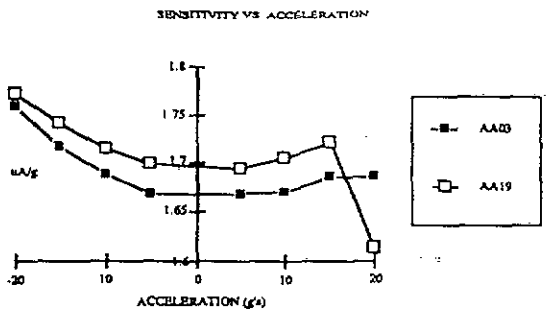

Figure 5. Amplitude linearity characteristics of ±7 g fullscale sensors. The curve of AA19 shows the effect of overrange stops at approximately 2 times full scale.

The scaling allowed simulation of 10 g static acceleration simply by orienting the shaker upward in earth's gravity. The results are listed in Table II.

damping has not yet been designed into the higher range sensors.

Too much damping can be a disadvantage. A separate test was performed on heavily overdamped sensors, with corner frequency of approximately 10 Hz, (compared to 200 Hz for the moderately overdamped units mentioned immediately above, and compared to 2000 Hz for the sensors in the the final configuration of the accelerometers in this program). The overdamped sensors exhibited highly nonlinear phase response along with higher-than-expected bias change due to vibration. Apparently the greater damping introduced other nonlinearities. This contrasts with nearly classic phase response for the moderately damped ±7 g units.

Table II. DC output in 1 g steady state at 0, 2.5, and 10 g rms vibration.

Ser. #	Sens (uA/g)	0 g rms (uA)	2.5 g rms (uA)	10 g rms (uA)
AA03	1.667	1.7456	1.7446 [-0.6]*	1.7306 [-0.9]
AA19	1.696	1.7727	1.7725 [-0.1]	1.7707 [-1.2]
AA03	transv.	0.0281	0.0281 [0]	0.0283 [0.12]

* [change relative to 0 g rms given in brackets, in milli-g's]

The third entry in the table is a transverse test, in which the unit was mounted with its sensitive axis oriented horizontally, so both steady state (gravity) and the vibration acceleration inputs were transverse to the sensitive axis. This placed the operating point of the accelerometer in the symmetric middle of the amplitude linearity curve, with the result of reduced rectification.

These more sensitive sensors had a moderately higher damping coefficient, which effectively reduced the bandwidth and amplitude of the vibrational input. Results were consistent with theoretical expectations and showed the possibility that the rectification could be acceptably small with an open-loop accelerometer. The 1 milli-g bias change at 10 g rms in the tests translates to a respectable 10 microg/g^2 over 2500 Hz. This level of

Closed-loop electronics is thought to offer the promise of performance improvement in bias rectification and amplitude nonlinearity. Holding the mass at the null point with feedback would prevent excursions into non-linear regions of operation.

Shock testing - The preliminary shock test was performed at Picatinny Arsenal's 2" air gun, and testing in the final round was the 2.5" diameter Hypervelocity Range/Track G Facility at Arnold Engineering Development Center (AEDC). In preparation, accelerometers were epoxied to the back of the ring laser gyros. Performance of the instruments was tested prior to and after each shock. Among accelerometer parameters tested was: scale factor and bias as a function of temperature, frequency response, transverse sensitivity, and amplitude linearity.

In the 2" gun at Picatinny the test piece is held in a projectile which is forced down a long closed tube when a metal diaphragm is ruptured by pressures up to 100 MPa or 15,000 psi. The projectile is caught softly as it compresses the gas in the end of the tube (which initially is kept at 2.7 MPa, or 400 psi). By measuring the mass of the projectile and the pressure of rupture, initial peak acceleration is calculated.

The diameter of the gun and the size of the gyros limited the Picatinny tests to one gyro/accelerometer stack, rather than the three-stack assembly of a full IMU able to be tested at AEDC. The projectile carries the stack on a fixture which orients them as they would be in the geometry of the IMU, with the mounting surface at a shallow angle to the direction of motion. This directs the majority of the shock along the direction of the support fingers in the sensor, primarily transverse to the accelerometer's sensitive axis. The sensor must survive without the benefit of engaging the mass onto the integral overload stops.

Accelerometers were shocked in two series of tests at Picatinny. The first group included tests of both the straight and curved finger sensors in larger test packages, the second group was the final configuration of sensors and packages.

Table III lists the change of performance parameters on the four accelerometers in the second test at Picatinny. Only one (AA11) came through unscathed, and even its performance did not meet the bias and sensitivity stability criteria. Other units showed some form of anomaly, in that AA12 showed a low stop level which worsened after the shock, and AA14 developed a drift that made the centrifuge testing of amplitude linearity difficult. Except for one unit which required a wire bond repair (AA13), there were no catastrophic failures. Results from AEDC are shown in Table IV.

Table III. Accelerometer performance shifts at Picatinny

Serial number	AA11	AA12	AA13	AA14
Shock level (g's)	87200	84000	85500	88400
Bias shift (g's)	0.09	0.56	-0.27	0.13
Sensitivity shift (%)	0.5	-1.1	0.6	-0.3
Non-linearity shift (%)	0.05	1.2	0.7	5
Transv. sens. shift (%)	0.07	0.07	-	-
Phase change @ 500Hz (°)	-0.1	-0.1	<0.1	-0.1

Table IV. Accelerometer performance shifts at AEDC

Serial number	AA25	AA15	AA24
Shock level (g's)	90000	90000	90000
Bias shift (g's)	-0.85	0.22	0.38
Sensitivity shift (%)	-0.9	0.01	-0.93

These were rigorous environmental tests. Although it is clear the design is not complete, the results are encouraging. Of these seven transducers, the average of the absolute values of shifts of bias and sensitivity was <0.3% full scale (FS) and <0.7%, respectively. Average values were smaller, 0.04% FS and -0.3%, respectively, averaging negative and positive-going shifts.

DISCUSSION OF POSSIBLE DESIGN CHANGES

Sensor and circuitry changes will be significant if closed-loop (servo feedback) electronics are to be incorporated. Structurally, two primary changes would be required in the sensor. Since the mass ideally would be held at a null position only by electrostatic forces, stiffness of the seismic mass support structure would need to be reduced severely. Transverse stop structures would be needed in the sensor, since no longer would the support fingers have the strength to support the mass during transverse shocks. Any damage to the stops which may occur during the shock would presumably not affect the performance. This would represent an improvement over the existing design, since any shock induced changes to the support fingers could directly affect performance.

Another possible structural change would involve the wire attachment. If strain isolation problems are attended to, (as well as other design and manufacturing problems), it would be desirable to change the electrical contact to the sensor from discrete wires to a solid contact, perhaps a "flip-chip" technique or the multichip interconnection techniques where conductors are grown in place. In this way the problem of bias shifts due to the varying parasitic capacitance associated with shock-displaced lead wires might be avoided, along with the complication of keeping conformal coating off of the sensor.

References:

1. Wilner, L. B., "Differential Capacitive Transducer and Method of Making",United States Patent 4,825,335

2. Wilner, L. B., "A High Performance, Variable Capacitance Accelerometer", IEEE Instrumentation and Measurement Technology Conference, 1988, pg 92-5.

3. Sill, R. D., "Shock Calibration of Accelerometers at Amplitudes to 100000 g Using Compression Waves", 29th International Instrumentation Symposium, Instrument Society of America, pg 503-16. Reprinted by Endevco as Tech Paper TP283.

Microprocessor Control of Transducer Signal Conditioning and Recording

Peter T. Frazer
Engineering Manager
Pacific Instruments, Inc.
215 Mason Circle
Concord, CA 94520

1. Introduction

The transducer amplifier field had its beginnings in manually controlled and calibrated electronic instruments. Filter and gain selections were made by turning knobs on front panels, and the screwdriver was the universal "calibrator", used to adjust parameters from gain accuracy and DC offset to excitation supply level and transducer bridge balance. In large research installations, many man-hours were consumed in the configuration and calibration of rack upon rack of amplifiers, and measurement accuracies were not always what the experimenters hoped for.

The 1980s brought the first introductions of programmable instrumentation amplifiers. Parameter setting by knobs and switches was replaced with parameter entry through the keyboard of a minicomputer or, later, a personal computer. Software simplified the control of large numbers of amplifiers. But calibration and "fine-tuning" of amplifier parameters still required that good old screwdriver, and there was no real "intelligence" in the channels themselves.

In the late 1980s relatively powerful single-chip microcontroller chips became available at low cost. This development created many new opportunities to simplify the use of instruments as well as improve performance of key parameters.

Pacific Instruments recently undertook a product development effort to investigate the use of a microcontroller to reduce the cost of and fully automate a programmable instrumentation amplifier, with the goal of creating a high-performance instrument that is versatile, easy to operate and maintain, and which saves the operator many man-hours of set-up and calibration time as compared with existing product offerings. This paper illustrates some of the accomplishments of this development effort.

2. Serial Data Links

One innovation inspired by the introduction of a microprocessor into an instrumentation amplifier is the use of "three-wire" serial data links between the processor, the circuitry it controls, and the hardware from which it retrieves information needed for control. A schematic representation of these links in the development unit appears in Fig. 2.1. The three wires are a "data" signal, a "clock" signal which marches the data through on-board serial shift registers, and a "latch enable" signal which enables the serial "string" stored in the registers to be applied to the circuitry being controlled. The individual signals pass from one instrument power supply to another via optoisolator ICs, used to maintain electrical isolation between the various supplies.

The use of serial links provides a number of advantages to the user as well as the hardware designer. For example, serial communication results in a reduction in the size, complexity, and cost of control circuitry. Consequently, more functions can be packed into the available printed circuit board space, and the cost savings can obviously be passed on to the customer in the form of a lower system price tag. Also, because fewer optoisolators are required for a serial communications scheme, (since only 3 signals must be passed from supply to supply), power consumption is reduced. Also, it has been our experience that failure rates are relatively high for optoisolators; reducing their numbers increases system reliability.

To understand a more subtle benefit of having fewer optoisolators, consider their inherent input-to-output capacitance. As suggested by the schematic in Fig. 2.2, any capacitance from input to output common will interact with the input signal source resistance to form an AC divider of the input signal. To the extent that these resistances and capacitances are not equal for both inputs, a differential signal will appear between the inputs and be amplified. The effect of this is to reduce the amplifier's common-mode rejection ratio (CMRR). Reducing the number of optoisolator connections between the floating front-end supply and the analog output supply decreases the amount of inter-supply capacitance, thereby improving the CMRR value for any given source resistance imbalance. CMRR values of more than 126 dB were easily obtained for the development unit at a gain of 1000.

3. Digital Gain Calibration

In a traditionally designed instrumentation amplifier, the gain must be calibrated, at the factory or at a calibration lab, to keep it within the required tolerance. This is typically done using precision potentiometers to vary the gain-setting resistances in the amplifier (see Fig. 3.1). To do this, a trained technician must take the amplifier from the instrumentation rack, open it up, and connect it to a special test fixture. He or she applies a known voltage to the amplifier's input, measures the corresponding output(s) with a calibrated voltmeter , and adjusts a potentiometer on the board. The procedure is repeated for each gain setting of the amplifier.

Using a microprocessor and digital-to-analog converters (DACs), a simpler, faster and more cost-effective method of gain calibration is possible. The secret of this approach is to use the DACs to create variable-gain amplifiers (VGAs). Schematically, the circuit behaves like the familiar inverting amplifier circuit shown in Fig. 3.2, which has a voltage gain G given by

$$G = - 2^N / D,$$

where N is the number of bits with which the DAC can be programmed, and D is an N-bit digital code. For a 12-bit DAC, for example, this equation reduces to:

$$G = - 2^{12} / D = - 4096 / D.$$

Fig. 3.3 shows how such gain elements can be used to digitally calibrate an amplifier. One of 7 feedback resistors is digitally connected to the "front-end" instrumentation amplifier circuit to set its gain. This stage, powered from a separate floating winding of the amplifier's isolation transformer, provides the common-mode rejection capability of the amplifier, accommodating input common-mode potentials of up to 300 volts. The output of this section feeds a series of two VGAs. Digital codes for the two DACs are programmed by the processor over one of the serial data links.

Gain calibration of this amplifier configuration is straightforward. (See Fig. 3.4.) With the instrument still installed in the rack, a signal from a calibrated GPIB-controllable voltage source is applied to the amplifier's input. The output signal for the channel drives a GPIB-compatible digital voltmeter. GPIB cables connect the test instruments and amplifier to an IBM-compatible personal computer equipped with a GPIB interface controller. An easy-to-use test and calibration program, written in MicroSoft QuickBASIC 4.5, is loaded by the operator. The program prompts the user for desired gain values; he or she either selects from "standard" values suggested by the program or enters values of his or her choice via the keyboard. A click of the mouse initiates an automatic gain calibration sequence.

The computer instructs the signal source to output a specific voltage level The computer adjusts the digital codes for the channel's two VGA DACs so that they produce an output voltage appropriate for the desired gain. The computer reads the value of this output voltage with the meter and checks the actual gain accuracy against the required value. This cycle is repeated automatically until the desired gain accuracy is achieved.

Why two VGAs in the channel? The answer has to do with their gain resolution. The gain of the DAC-based VGA is *inversely* proportional to the digital code written to it. One can show mathematically that the gain resolution of such an amplifier for a given input code is equal to the reciprocal of that code. For a 12-bit DAC and a code of 4095, the resolution is 0.025%, but for a code of 2048, this reduces to 0.05%. In order to calibrate overall channel gain to better than 0.1%, only the upper codes of the DACs can be used. The leading 8-bit

VGA acts as a "coarse" gain adjust which brings the overall gain to within a few percent of the desired value. The second, 12-bit VGA can then "fine-tune" the gain to better than +/-0.04% accuracy.

4. Variable Gain Capability

The mechanism described above opens up the possibility of configuring the overall channel as a variable gain amplifier. Suppose that a user wishes to have a 90% of full scale output for an input voltage of, say, 2.34-Volt produced by the transducer under a particular static-load condition. Using software routines, available as part of a standard package from the instrument manufacturer, he or she could set up the amplifier with the desired transducer input signal and, with a few simple keystrokes, instruct the software to adjust the hardware settings of the "front-end" and two VGAs to produce the desired percent-of-full-scale output. In addition, if the operator wished to use this custom gain setting in future applications, he or she could have the software store these hardware settings in the channel's on-board, nonvolatile memory, identifying the combination of gain settings with some mnemonic meaningful to the user. Thus, with the easy-to-use software and programmable hardware, gain can be customized by the user for a particular application--without the use of a screwdriver!

5. Autobalance

In the "good old days" of instrumentation, balancing an amplifier with a bridge-type transducer input was, at best, a tedious task. The operator had to go to each amplifier, meter and screwdriver in hand, and adjust a front-panel potentiometer to null out any DC offset resulting from bridge imbalance. In more recent times, progressive instrument manufacturers have offered "autobalance" capabilities in their amplifiers. In one such scheme, a small DC signal is introduced at the input of the amplifier by a programmable voltage source. This voltage is ramped over a range of values, while the resulting amplifier output voltage is monitored with a zero-crossing detector circuit. When the output crosses 0 Volts, ramping is terminated, and the amplifier is balanced. While requiring much less of the user's time than the old manual approach, this autobalance operation suffers from slowness (sometimes taking more than 10 seconds if the bridge is grossly imbalanced) and problems with accuracy and repeatability because of susceptibility of the zero-detecting circuit to electrical noise.

Use of an on-board microprocessor makes possible faster, more accurate and more repeatable automatic nulling of bridge imbalances. This is accomplished using "intelligent" algorithms administered by the processor in conjunction with an analog-to-digital converter (ADC) residing in each channel.

The arrangement is shown schematically in Fig. 5.1. A digitally controlled, bipolar current source is connected to one side of the

bridge through a solid-state switch, by means of which the autobalance signal can be enabled or disabled by the processor. The value (and direction) of the compensating current is determined by a digital code, generated by the processor, written to a DAC in the current source circuitry. The magnitude of the current is proportional to the excitation voltage applied to the bridge. With this ratiometric approach, once the offset of the bridge is nulled, the amplifier output will remain at zero even if the excitation voltage applied to the bridge is changed. When the user issues a command to balance the bridge, the ADC digitizes the DC amplifier output voltage and reads this value. Based on the its knowledge of the excitation voltage, the gain setting, and the value of "range resistors" located on the completion card (which determine the spread of bridge imbalances for which the circuit can compensate), the processor uses this digitized value to calculate the current source DAC digital code which will produce the current required to cancel the bridge's offset. After outputting this code to the autobalance circuit via the serial data link, the processor waits for the amplifier output to settle to its new value. If it finds that the amplifier output is still not at zero, it adjusts the DAC digital code to remove the residual error.

This approach allows nulling of bridge imbalances in less than one second, considerably faster than the less sophisticated autobalance approaches described earlier. Accuracy and repeatability are also enhanced because, unlike noise-sensitive zero-crossing detector circuits, the firmware-controlled ADC-based zero detector can desensitize itself to noise effects by using digital filtering techniques. These techniques include simple averaging as well as "glitch" detection and rejection algorithms.

6. Autozero

A similar approach can be used to remove DC offset errors in the amplifier electronics itself. In the traditional amplifier, zeroing is accomplished by sending out a technician to the amplifier itself and having him or her adjust "RTI" and "RTO" potentiometers used to cancel gain-dependent and gain-independent offset errors, respectively. Shorting the amplifier's input, monitoring the output with a voltmeter, and setting the amplifier gain to its highest value, the technician adjusts the RTI potentiometer until a 0-Volt output is achieved. With the amplifier at its lowest setting, the RTO potentiometer is similarly adjusted. Then, because of the inherent interaction of input- and output-related offset errors, the process is repeated one or more times until an acceptable "zero" is obtained for all gain settings.

Fig. 6.1 shows schematically how amplifier offset nulling is implemented when a microprocessor and an analog-to-digital converter are set to the task. When the command to zero the amplifier is given by the PC (or via the channel front-panel control interface, if available), the processor engages a high-performance relay at the amplifier's input to short both the positive and negative amplifier inputs to the amplifier's guard connection. The ADC then digitizes

the voltage level of the amplifier output. From the resultant digital code, the processor calculates a "first-pass" digital code to send to an "offset null" DAC; from this information it also selects the polarity of the reference voltage for the DAC. The voltage output of the DAC circuit is electrically summed with the amplifier output signal. This operaton results in a voltage that (assuming use of a 12-bit ADC with +/-10V full-scale input capability) is within about 4 mV of zero. The processor then routes the output signal to the ADC input through a preamplifier with a gain of 16. Reading this new, amplified value of output voltage, it adjusts the nulling DAC's digital code to get a output voltage that is much closer to zero. If a 12-bit DAC is used with a +/- 1-Volt input reference, zeroing to within 200 microvolts of zero can be achieved.

Because the processor can save DAC digital codes for each possible amplifier gain value, there is no longer a need to distinguish between RTI and RTO error sources--the controller treats all offset errors the same--and the need for front-panel offset adjust potentiometers is eliminated. Furthermore, with all channels under the control of a single PC, multiple amplifiers can be zeroed simultaneously. In fact, an operator could autozero as many as 160 amplifiers at once in about one second--even if the amplifiers are programmed to different gain settings--without ever having to go to where the amplifiers are located and without even having to locate that screwdriver.

7. Programmable Completion Card

Many instrumentation amplifier products feature plug-in modules, known as completion cards, containing circuitry which allows the user to alter the amplifier's configuration without having to remove the amplifier from its rack. Parameters such as local *vs.* remote sensing of excitation voltage, number and value of bridge completion resistors, and selection of voltage *vs.* current excitation monitoring can easily be customized for a given application by removing the card and modifying jumpers, switch settings and/or wirewrapped interconnections.

The advent of the on-board processor takes the convenience of customizable configuration one step further. In our development prototype we added to the standard completion card 16 miniature switches, again optically linked to the processor through a serial data path. (See Fig. 7.1.) Twelve of these switches were dedicated as user-definable configuration codes. Of these, four bits were used to select 1 of 16 possible combinations of amplifier parameters (gain, filter bandwidth, excitation voltage or current value). The remaining eight bits were left undefined, but could be used, for example, to identify the type and/or serial number of a transducer to be connected to that channel.

This "mechanical" programming capability provides an easy and inexpensive way for a user to set up a channel to a pre-defined configuration if he or she does not have ready access to a PC with GPIB capability or has not purchased an amplifier with a front-panel

instrument control option.

8. Excitation Interrupt

One technique used to calibrate a transducer involves isolating the transducer from the excitation power supply by physically breaking the connection between the positive terminal of the supply and the bridge network, upon which input offsets and noise can be readily measured. This interrupting is usually done with a relay or, in some cases, a semiconductor switch.

In the prototype instrument, the state of this excitation interrupt switch was easily controlled by the microprocessor in response to commands from a PC (or front-panel control interface, when so configured). Using the processor we were also able to implement some other features useful to the operator. For example, the processor automatically disables the excitation output to the transducer when the unit is turned on and the microcontroller is setting up a DAC in the excitation circuitry. As a result, the transducer is not exposed to potentially damaging voltage transients while the excitation supply is establishing its programmed value.

A second protective feature is invoked when the excitation supply is configured as a programmable current source. On power-up of the unit, no matter what the value of output current the supply was programmed to before the power was last removed, the processor initially sets the output current to its lowest possible value. Then, after the excitation output is connected to the transducer, the current is ramped up to its programmed value. This protects the transducer from damage which might occur when the excitation current source, whose output would normally rise to its compliance voltage level (typically 20 Volts or so) when not connected to a load impedance, is suddenly connected to the transducer load.

9. On-Channel Configuration Information

Once one has a microcontroller and a nonvolatile memory on the amplifier unit, the possibility arises for storing in the channel textual information describing the features of the unit and the current configuration of those features. Take as an example filter information. Text strings can be generated which detail the type of filter (*e.g.*, "4-POLE BESSEL") and the cutoff frequency for a particular filter selection ("10 kHz"); in addition, a numerical constant can be provided which tells the number of possible cutoff frequencies available for the unit in question.

This information can be read from an individual channel by a PC equipped with a GPIB interface. This allows the user of the applications software to retrieve information about the capabilities and current configuration of the amplifiers in his or her system without having to enter that information into the computer manually. This is true even if the channels have different features (*e.g.*,

different kinds of filters with different sets of cutoff frequencies).

Textual configuration information would be programmed into each amplifier at the factory when the unit is initially tested and calibrated. With the aid of a software package available from the manufacturer, the user could later modify these factory defaults as appropriate for his or her application.

10. Front Panel On-Line Display

A logical feature to offer in an instrumentation amplifier containing a microprocessor, an analog-to-digital converter, and a dot-matrix front-panel LED display element is what one might call an "on-line display". (See Fig. 10.1.) This can be thought of as a built-in digital voltmeter with which the user can display current values of such amplifier parameters as output voltage, excitation voltage, and excitation output current. Which parameter is displayed is selected either through a front panel control interface or by means of instructions from a remote computer. The display is updated about once a second.

This monitor provides the user with on-site diagnostic information about the amplifier. It allows him or her to check, for example, whether or not an autobalance operation completed successfully (confirmed by an output voltage reading of 0 Volts) or whether a transducer is actually connected to a given amplifier's input (indicated by a nonzero value on the excitation current monitor).

11. Conclusion

We at Pacific Instruments found that incorporation of an inexpensive microcontroller into a programmable instrumentation amplifier enhanced the unit's electronic performance, as evidenced in such areas as improved common-mode rejection, faster and more accurate autobalancing and output zeroing, and more versatile gain-setting capabilities. In addition, the user interface was greatly improved and simplified, with many of the mundane tasks (such as gain calibration and entry into the controlling PC of channel configuration information) automated by a combination of "intelligent" PC software and on-channel firmware. The result is an instrument that is flexible yet easy to use, both in large installations and in applications in which only a few channels are used, and promises to allow experimenters to spend more time to analyzing their data--and less time trying to find their screwdrivers.

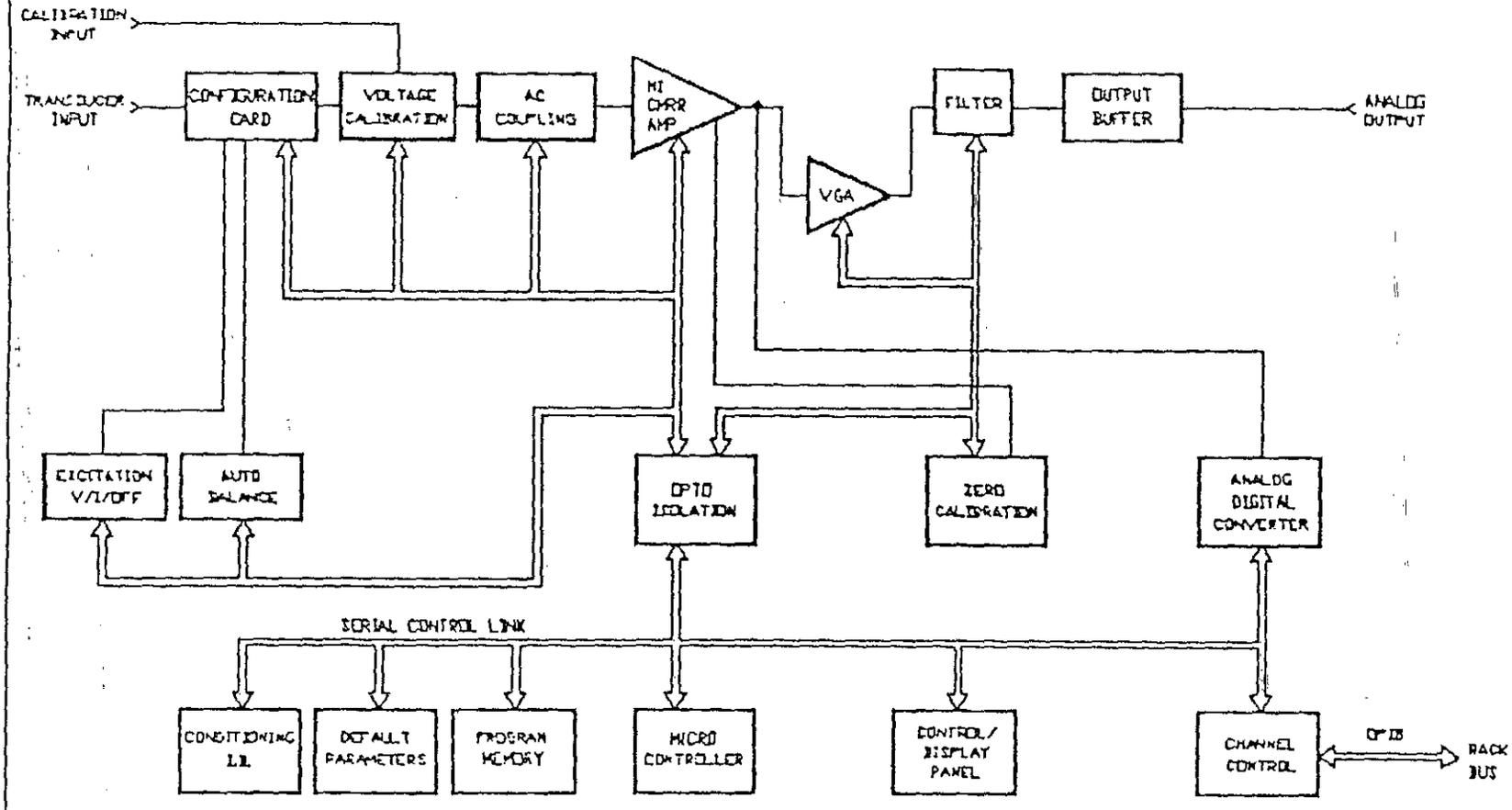

FIG. 1.1: MODEL 9355 PROGRAMMABLE INSTRUMENTATION AMPLIFIER

FILE NAME: MISC\SD71

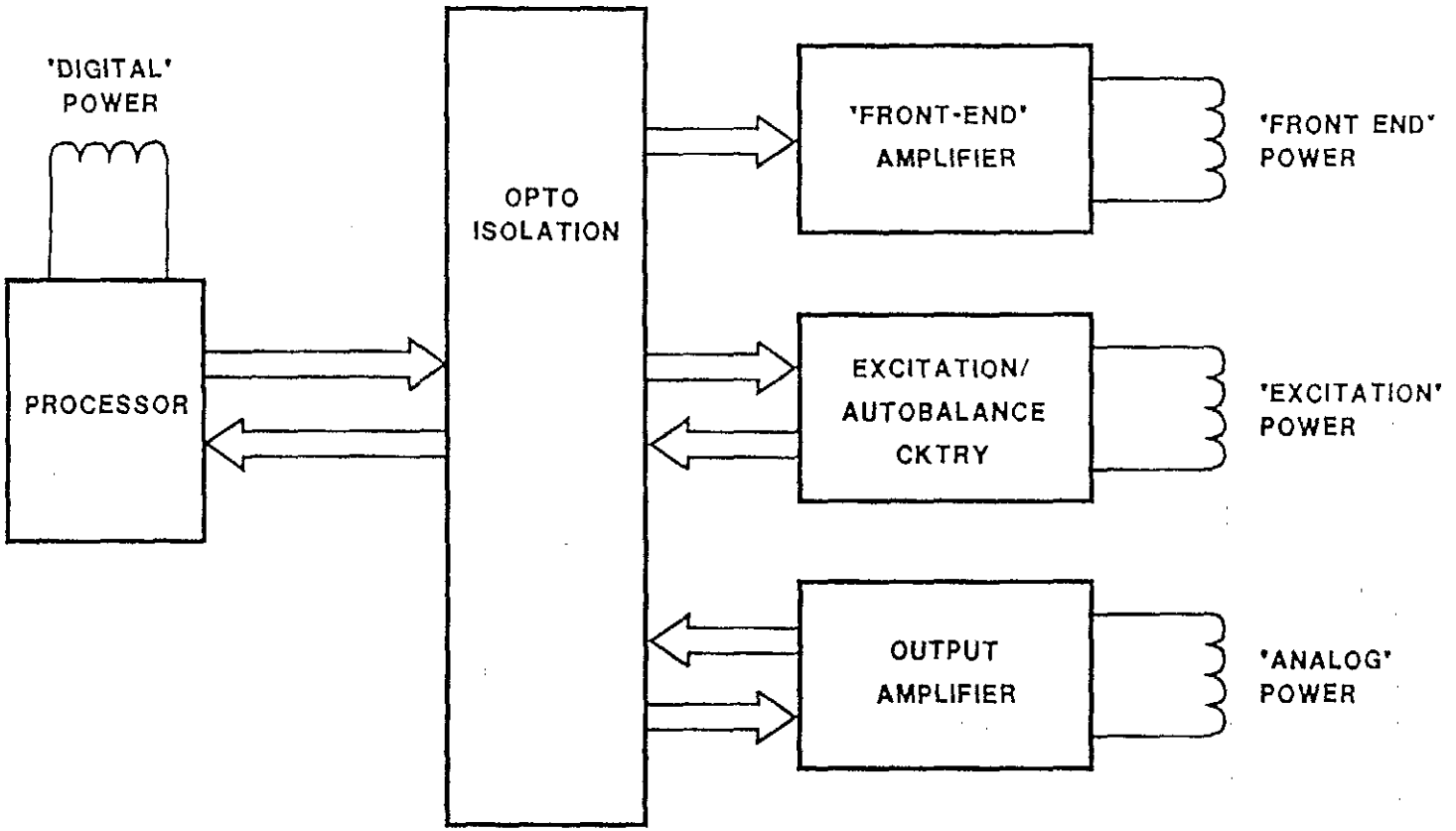

FIG. 2.1: SERIAL HARDWARE CONTROL LINK

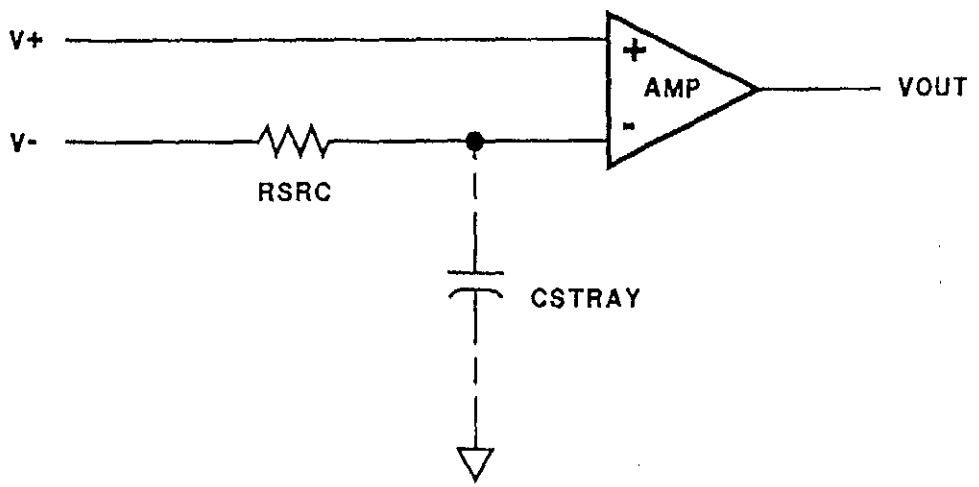

FIG. 2.2: COMMON-MODE ERROR SOURCE

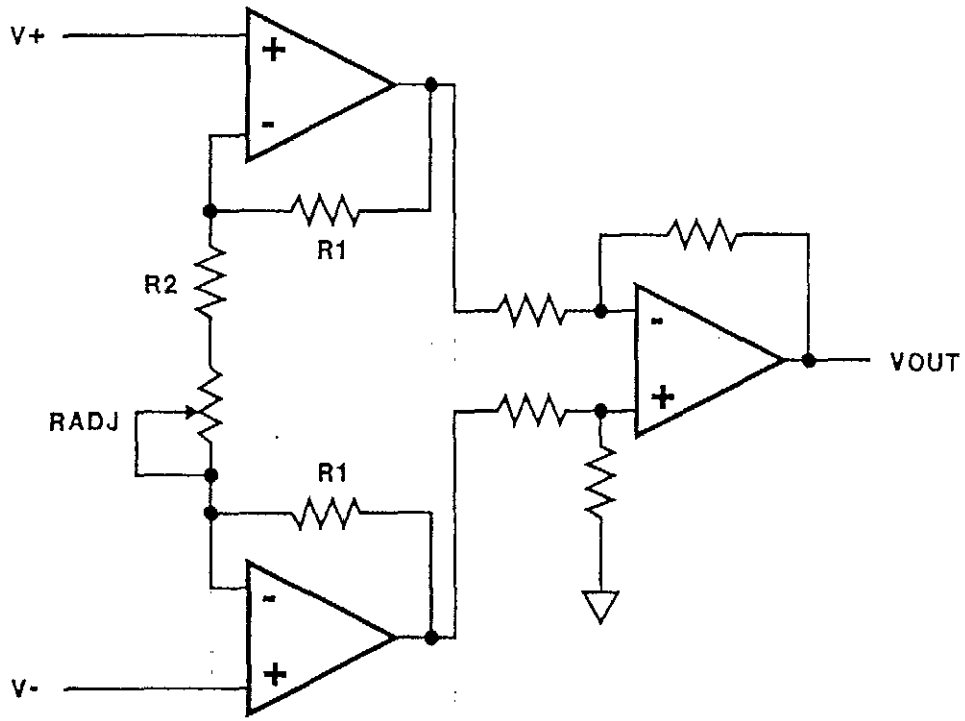

$$VOUT = 1 + \frac{2 * R1}{RGAINSET} (V+ - V-)$$

$$RGAINSET = R2 + RADJ$$

FIG. 3.1: POTENTIOMETER GAIN CALIBRATION

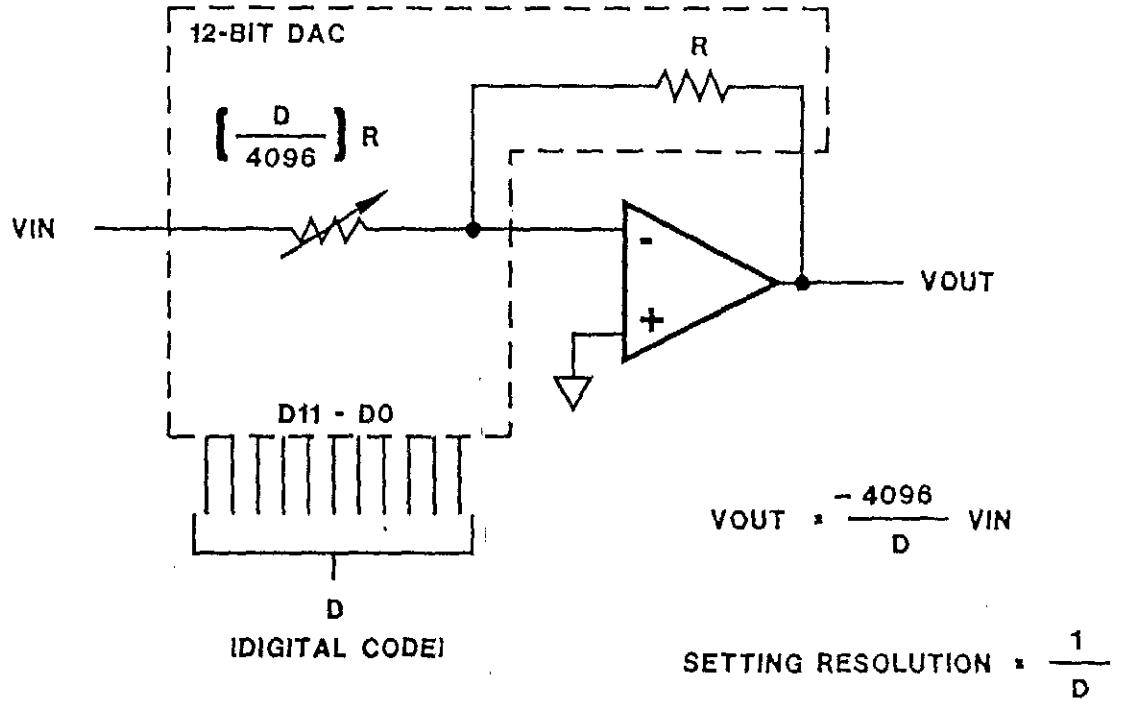

FIG. 3.2: DAC-BASED VARIABLE GAIN AMPLIFIER (VGA)

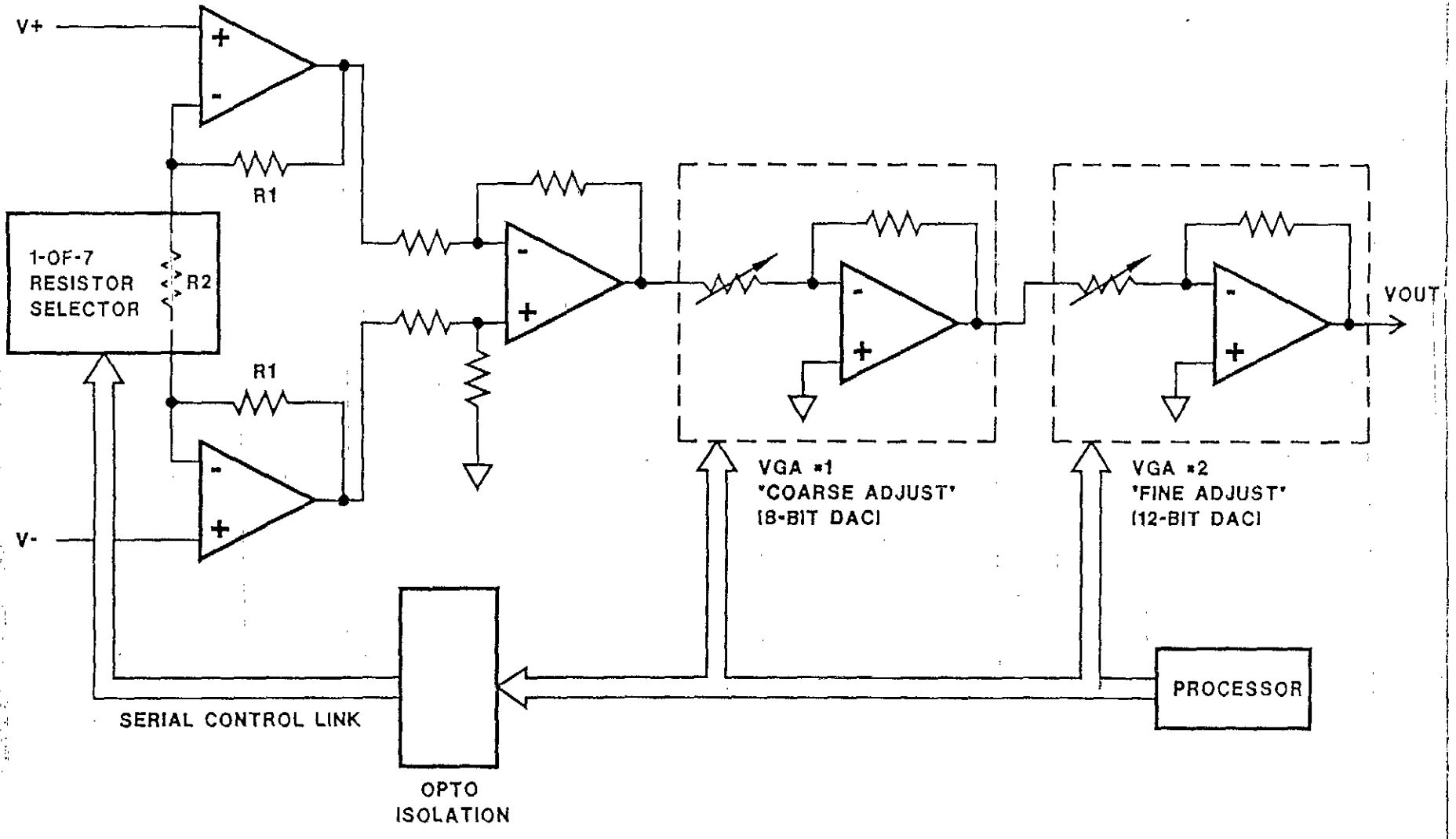

FIG. 3.3: PROCESSOR-BASED GAIN CALIBRATION

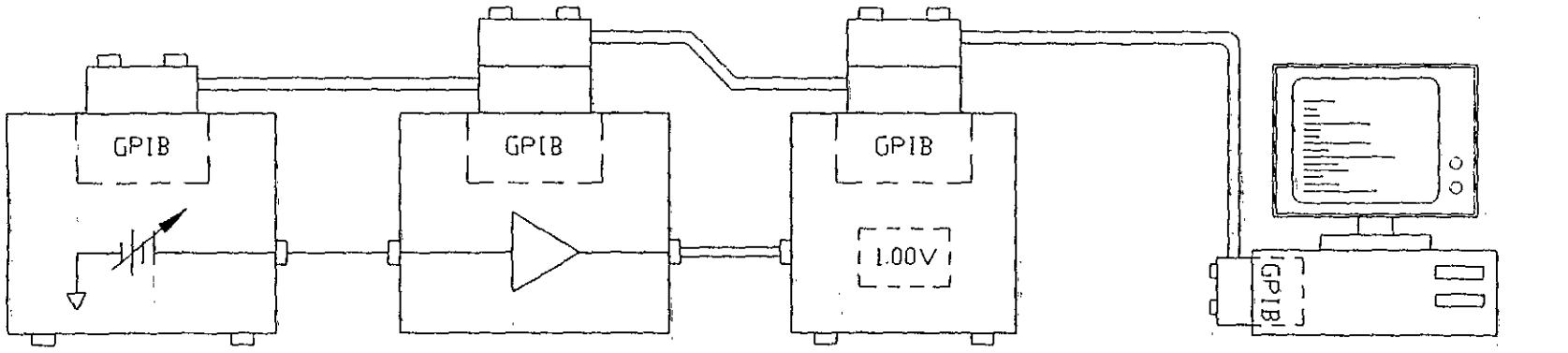

FIG. 3.4: PC-BASED AMPLIFIER GAIN CALIBRATION

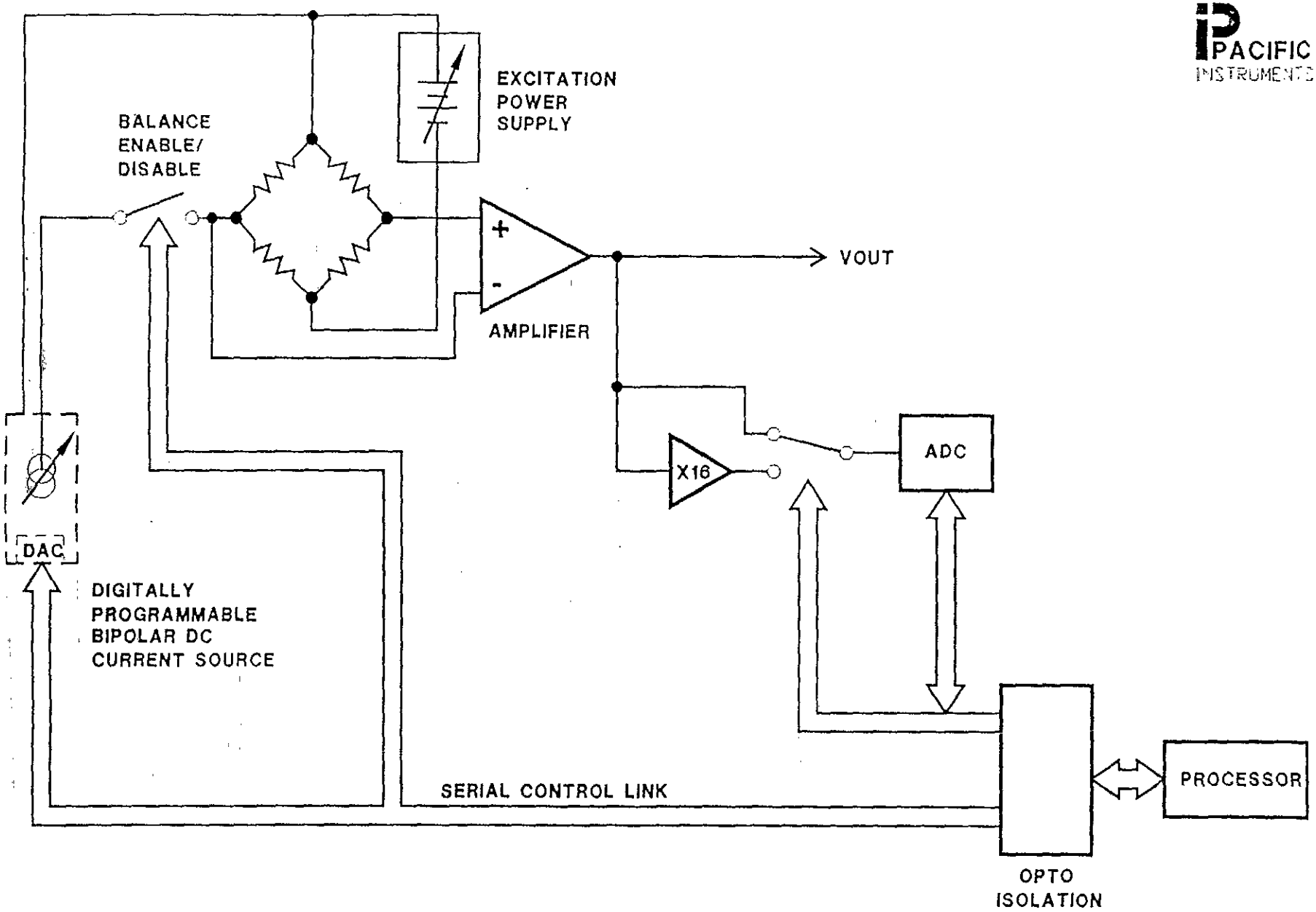

FIG. 5.1: AUTOBALANCE BLOCK DIAGRAM

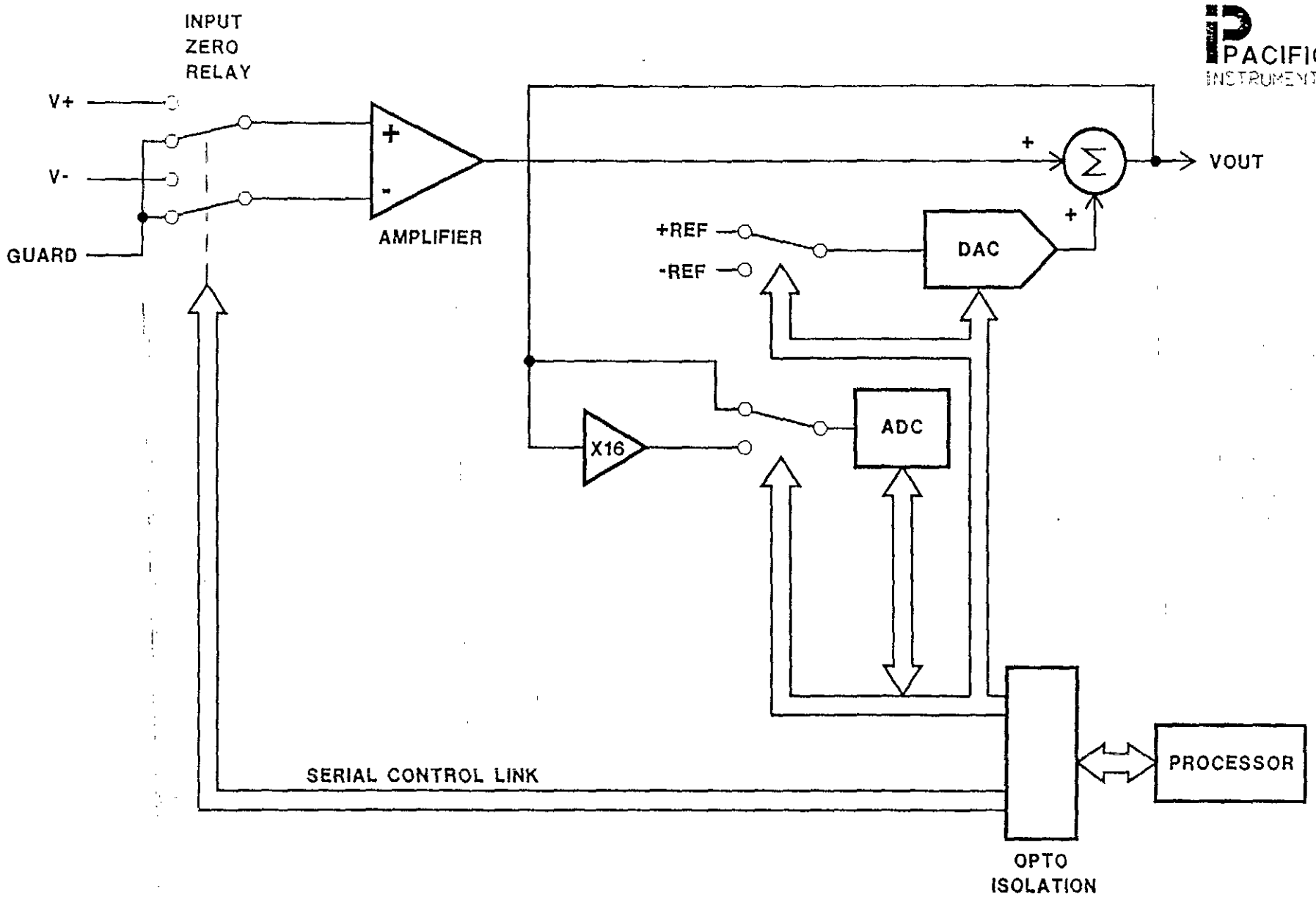

FIG 6.1: AUTOZERO BLOCK DIAGRAM

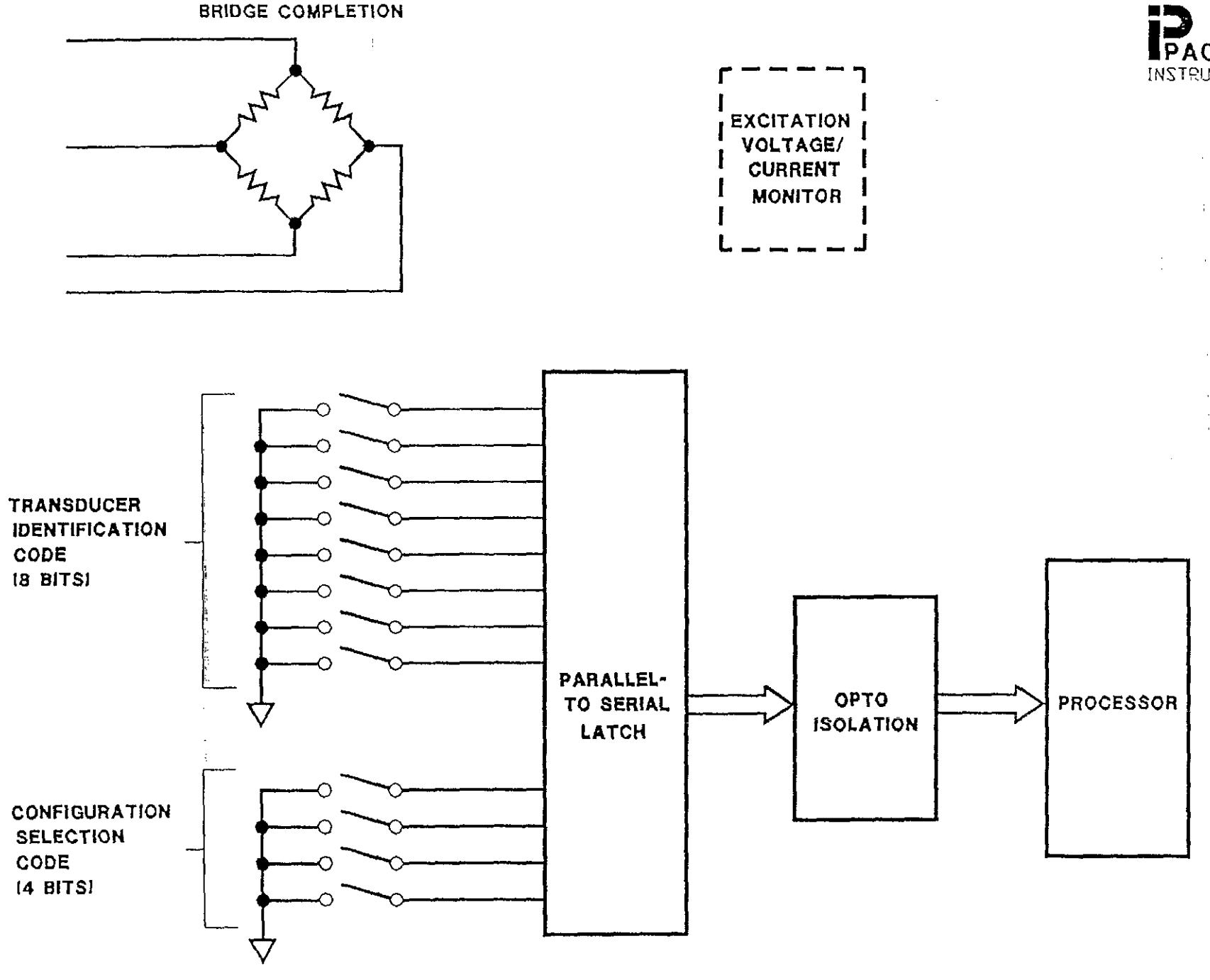

FIG. 7.1: PROGRAMMABLE COMPLETION CARD

FILE NAME: MISC\S073

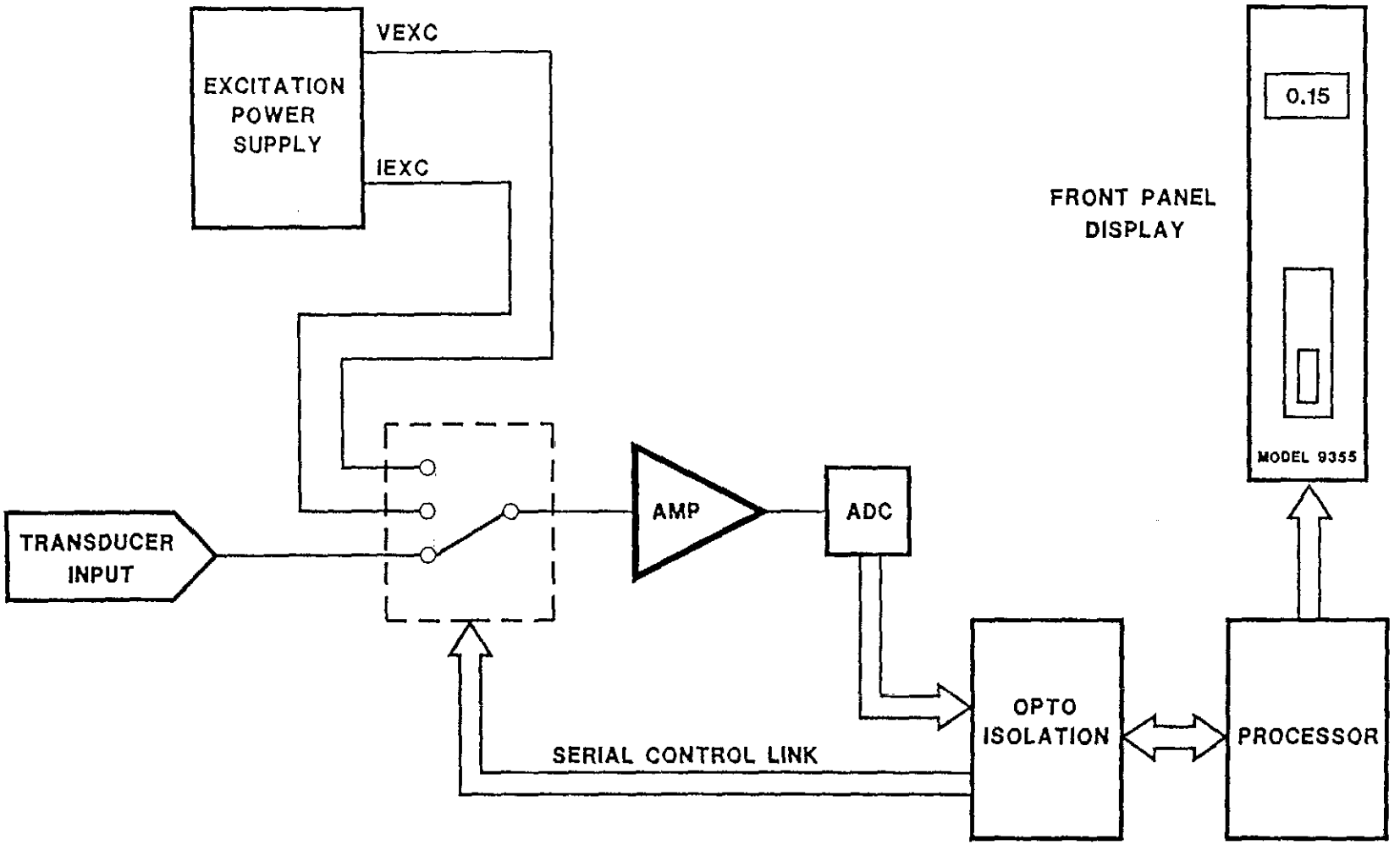

FIG. 10.1: FRONT PANEL ON-LINE DISPLAY

EVALUATION OF CHAMBER PRESSURE TRANSDUCERS FOR LARGE CALIBER WEAPONS

W. Scott Walton, US Army Combat Systems Test Activity

A study of several different chamber pressure transducers (100,000 psi range) is being conducted. The purpose of this test is to:

1. Find a transducer with performance that is superior to the widely accepted Kistler 6211 transducer.

2. Document the performance of the transducers, so that if a better transducer is found, field use of the transducer can begin without concern of causing an "instrumentation induced" shift in the nine years of data base accumulated using the 6211.

Four potential replacement transducers are being evaluated. A variety of different laboratory and field tests, using both static and dynamic pressure are being conducted.

A HIGH FREQUENCY, PIEZORESISTIVE TRANSDUCER FOR MEASUREMENT OF LOW LEVEL BLAST OVERPRESSURE

W. Scott Walton
U.S. Army Combat Systems Test Activity
Aberdeen Proving Ground, MD 21005-5059

ABSTRACT

Piezoresistive transducers have been developed to measure muzzle blast overpressure in the crew areas of Army weapons. Typical blast overpressures of interest range from 1 PSI to 10 PSI (7 KPa - 70 KPa or 170 dB - 190 dB). The most novel characteristic of these new transducers is the ability to drive long (150 m) cables at a high frequency (greater than 40 KHz). A variety of secondary benefits were also realized:

1. Improved calibration precision.
2. Reduced sensitivity to extraneous acceleration and thermal transients.
3. Improved aerodynamic response.

This paper describes a 3 1/2 year effort to develop a commercially produced transducer capable of meeting this specialized military need.

INTRODUCTION

The Army's effort to make weapons shoot farther and weigh less has created a situation that makes muzzle blast in the crew areas critical. An example of this problem is the M198 Howitzer. The muzzle brake on this weapon makes a light weight recoil system feasible, but forces such high pressures into the crew area that crewmen are restricted to no more than 12 rounds per day of the top charge during peacetime training.

Piezoelectric (PE) transducers used currently produce uncertainties on the order of $\pm$ 10% for field measurements where the direction of blast propagation is known [reference 1]. A typical field set-up of transducers is shown in Figure 1.

A transducer with a 100 PSI range is used to obtain a 500 KHz supressed resonance. The measurements of interest rarely exceed 10 PSI and are often as low as 1 PSI. The fact that the transducer is used at 1% to 10% of its full scale range makes it especially sensitive to thermal and vibration problems.

Errors due to off-axis shock waves in complex environments can be 50% to 150%. In a carefully controlled experiment using bare explosive charges, the extreme spread of a 5 round group was found to be 3% with a given transducer, yet the variation between two different transducers was as great as 20% [reference 2].

DESCRIPTION OF TRANSDUCERS

This effort was begun in 1987. The objective was to improve the overall acuracy of field measurements from $\pm$10% to $\pm$5% by using piezoresistive (PR) transducers. Previous experience in 1981 [reference 1] with PR transducers had shown them to be unacceptable because of:

(1) Sensitivity to light.

(2) Transducer resonance being excited by shock wave passage.

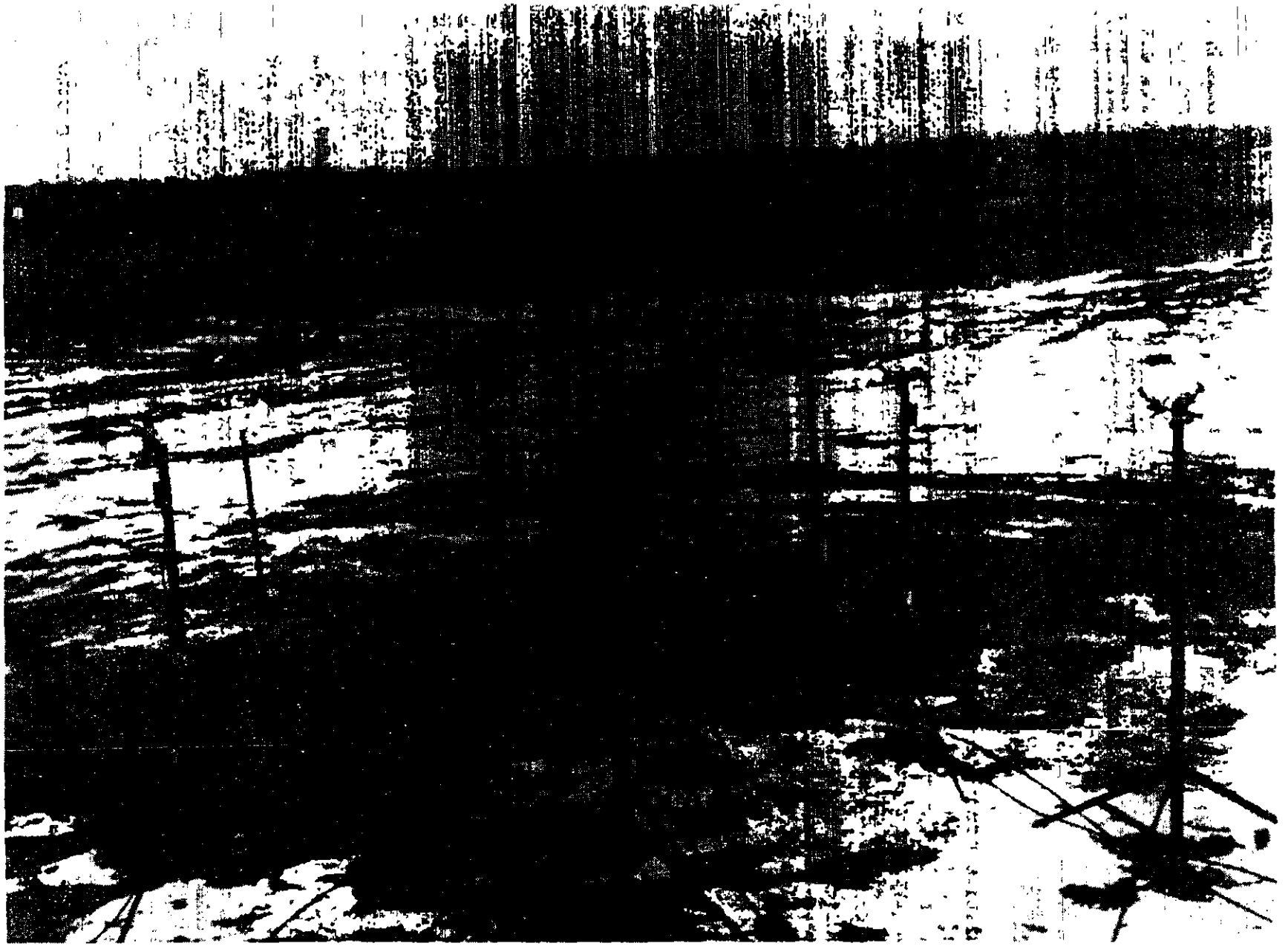

Figure 1. Example of transducer layout for blast overpressure measurement in the crew area of an 81 mm mortar.

Figure 2 Photograph of blast overpressure transducers

Figure 3. Photograph of Piezoresistive 1 transducer, showing line driver to drive long cables.

(3) Inability to drive long cables at frequencies above 10 KHz.

In the first round of development, prototype transducers from three different manufacturers were fabricated and tested in 1988. Due to continued problems of light sensitivity, and new thermal and vibration problems with the line drivers, none of the original prototypes were successful.

The "second generation" transducers and the piezoelectric transducer used presently are shown in Figures 2 and 3. The line driving amplifier is powered by transducer exitation voltage, such that normal Wheatstone bridge signal conditioning can be used.

THERMAL TRANSIENT TESTING

Thermal transients can cause significant measurement errors. Piezoelectric transducers are particularly sensitive to thermal transients, such as the hot exhaust gases from shoulder fired anti-tank rockets. One of the most severe thermal transient problems encountered in field measurements occurred during an evaluation of the effect of the accidental discharge of a Halon fire suppression gas bottle near the head of an armored vehicle crew member. The thermal cooling caused by a highly compressed gas expanding to atmospheric pressure caused such a dramatic thermal effect on the transducers that the blast overpressure levels could not be measured accurately.

Figure 4 shows an experimental set-up used to evaluate the sensitivity of blast overpressure transducers to thermal transients. Figure 5 shows the response of piezoelectric and the new piezoresistive transducers to the blast overpressure caused by rapid venting of a nitrogen gas bottle charged to 400 psi. Note that the erroneous thermal response of the unprotected piezoelectric transducer is larger than the actual blast overpressure. Also note that a thin layer of RTV delays and attenuates the thermal error, but does not eliminate it. Finally note that the thermal transient has essentially no effect on the piezoresistive transducers.

RESPONSE TO FLASH

Piezoresistive transducers are made of silicon, and can react as silicon photocells rather than pressure transducers if the silicon sensing area is not protected from light. This problem was severe on the first generation transducers obtained in 1988.

A layer of an opaque coating, such as RTV, Viton, or SES Black will reduce or eliminate the problem, but only if the coating has absolutely no pin-holes which allow light to pass. To check the response of the transducers, an electronic flash unit was functioned at 1" and 6" away from the transducer. It is interesting to note that the piezoelectric transducers also produced a significant signal during this test, but because of thermal effects rather than optical effects.

EFFECT OF AMBIENT TEMPERATURE

Blast overpressure transducers are typically calibrated in an indoor laboratory and then used outdoors. It is estimated that the temperature (of the transducer) can vary from 0^{o} F to 120^{o} F at Aberdeen Proving Ground. All transducers showed about a 3% change in sensitivity over this temperature range.

ELECTRICAL NOISE TESTING

A signal-to-noise ratio of at least 25:1 is required for blast overpressure measurement. Microphones are typically used for measurements below 1 PSI, and "blast transducers" are used for

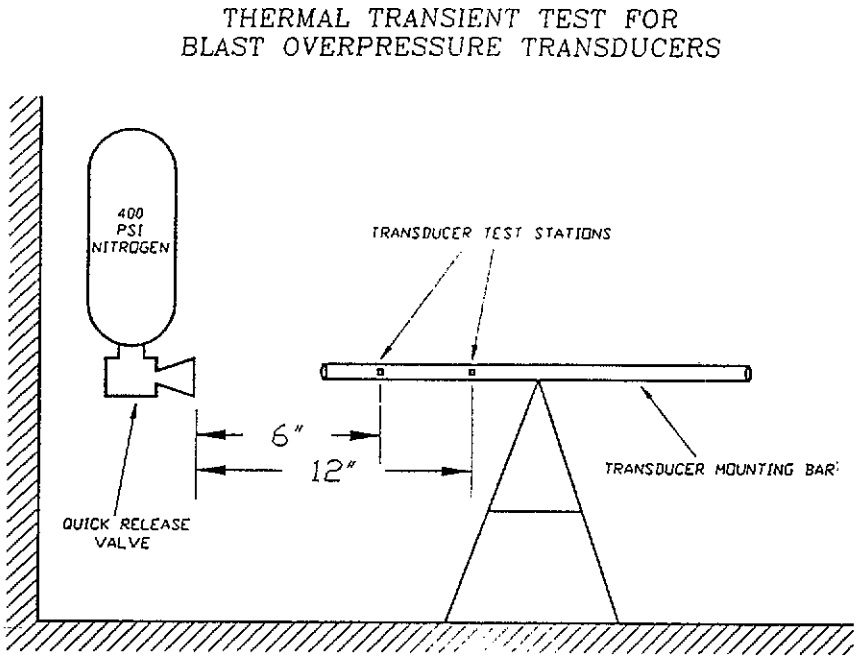

Figure 4. Experimental set-up to measure thermal transient response.

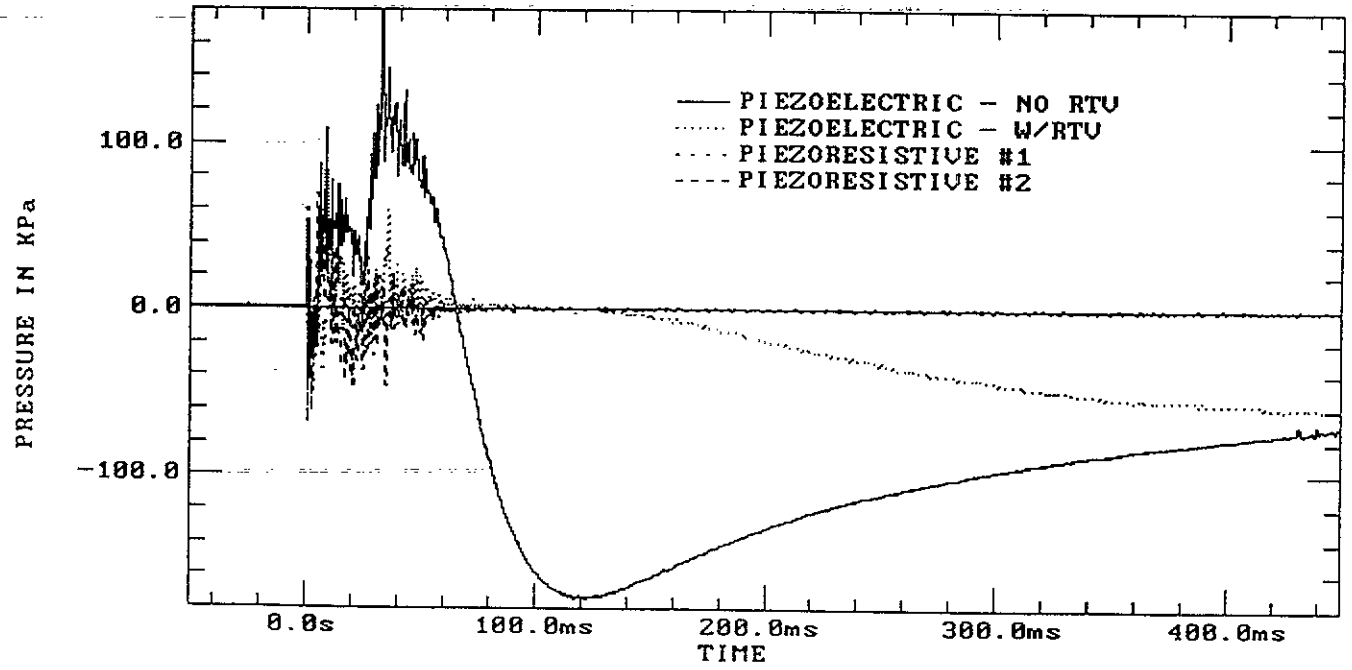

Figure 5. Response of Piezoelectric and Piezoresistive transducers to rapid venting of 400 PSI nitrogen bottle

measurements above 1 PSI. To avoid changing test set-up and transducer as pressure levels change during various test conditions, it is desirable to have the lowest possible electrical noise floor. It is unfortunate that the transducer which performed best in most situations ("Piezoresistive 1") had the highest electrical noise level.

ACCELERATION SENSITIVITY TESTING

The response of pressure transducers to acceleration must be minimized. The shock wave passing over the transducer creates an acceleration of the transducer. In field mounting situations, transducers must often be mounted rigidly, which transmits large acceleration levels to the transducer.

To evaluate acceleration sensitivity, the transducers were mounted on a steel plate. The plate was then hit by a hammer to produce levels of 100g's to 500g's. The resulting pressure transducer output was measured and divided by the acceleration level to obtain "KPa/g" levels. The piezoelectric transducer is typically about 10 times more sensitive to acceleration than the piezoresistive transducer.

Figures 6 and 7 illustrate the acceleration sensitivity problem. Pressure transducers were mounted in a long bar. When the shock tube fired, an acceleration is passed down the bar to the transducers (usually at a speed much faster than shock wave travels through the air). Hence the acceleration induced artifact on the pressure vs. times plot shown in figure 7 arrives before the blast overpressure arrives. Note that the acceleration induced artifact is not present on the piezoresistive transducers.

IMPROVED AERODYNAMIC RESPONSE

Compliance with the blast overpressure limits of MIL-STD-1474C (Noise Limits for Military Ground Materiel) (ref 3 and 4), requires measurement of side-on blast overpressure. Shock waves are directional. The "face-on" (0^0) value is more than twice the "side-on" (90^0) value. "Muzzle blast" produces shock waves from a variety of different sources (muzzle exit, ground reflections, secondary combustion of exhaust gases, etc.). Since a single transducer can only be oriented properly for a shock wave from a single direction, the complex nature of "muzzle blast" guarantees that several shock waves will strike the transducer "off-axis".

The difference between an "on-axis" measurement and an "off-axis" measurement could be as high as 150 percent. A transducer with "improved aerodynamic response" is desired, which will indicate as close to the "side-on" pressure value as possible, regardless of the transducer orientation. Figure 8 shows the transducers, mounted in cylindrical holders for blast overpressure measurement.

Testing of the new piezoresistive transducers indicated that the off axis discrepancy was reduced by a factor of two (i.e. from 100% "error" to 50% "error") when compared to current transducers. Figures 9 and 10 illustrate the difference between side-on and face-on response of the PE and PR1 transducers. Note that the PR1 transducer is an almost perfect stagnation probe when mounted in the "face-on" configuration.

DYNAMIC ACCURACY TESTING

It should be noted that all transducers provide very good accuracy when measuring simple pressure fluctuations, such as a 100 Hz sine wave. Measurement

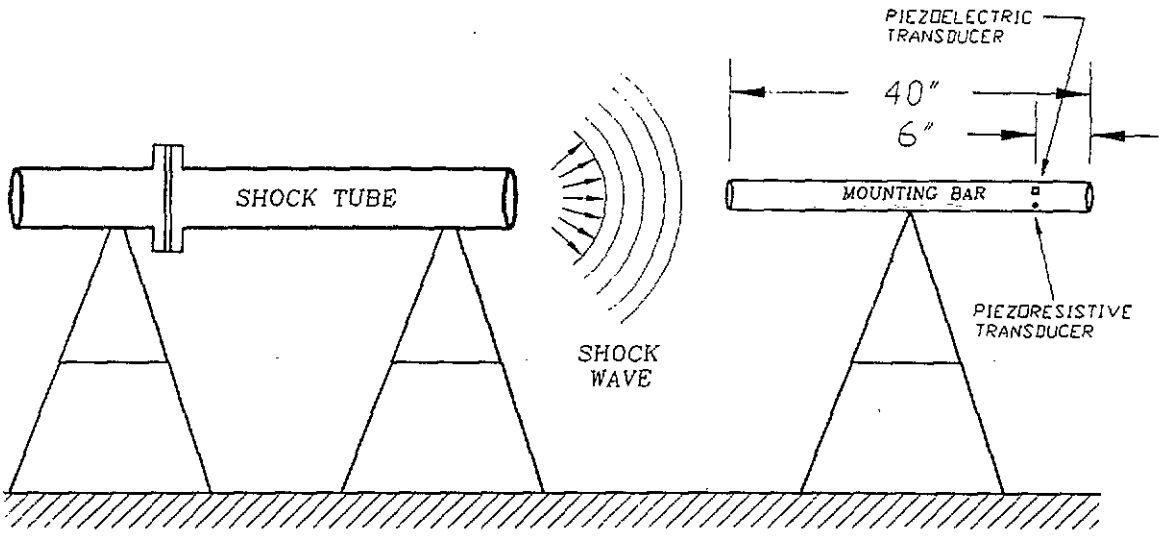

Figure 6. Experimental set-up for demonstrating acceleration sensitivity of blast overpressure transducers. Note that the blast wave hits the mounting bar first, and must then travel 34 inches before hitting the transducers.

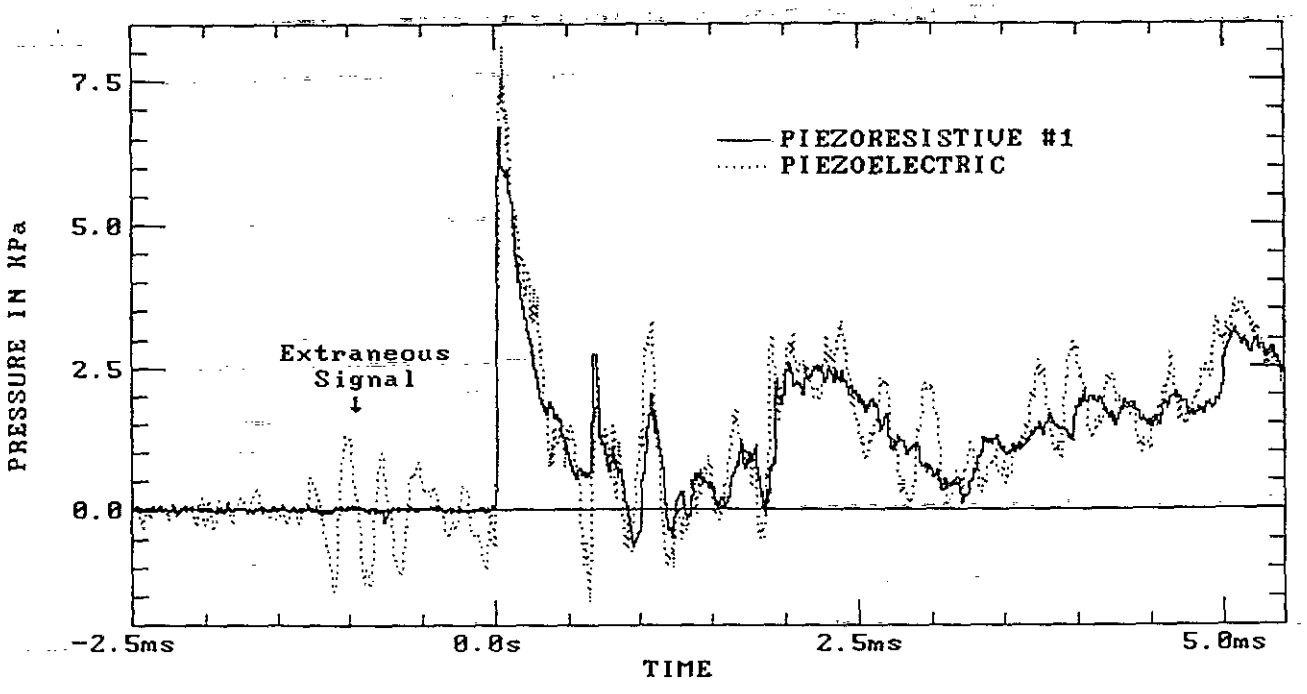

Figure 7. Response of piezoelectric and piezoresistive transducers to combined pressure and acceleration. Note the extraneous signals from the PE transducer.

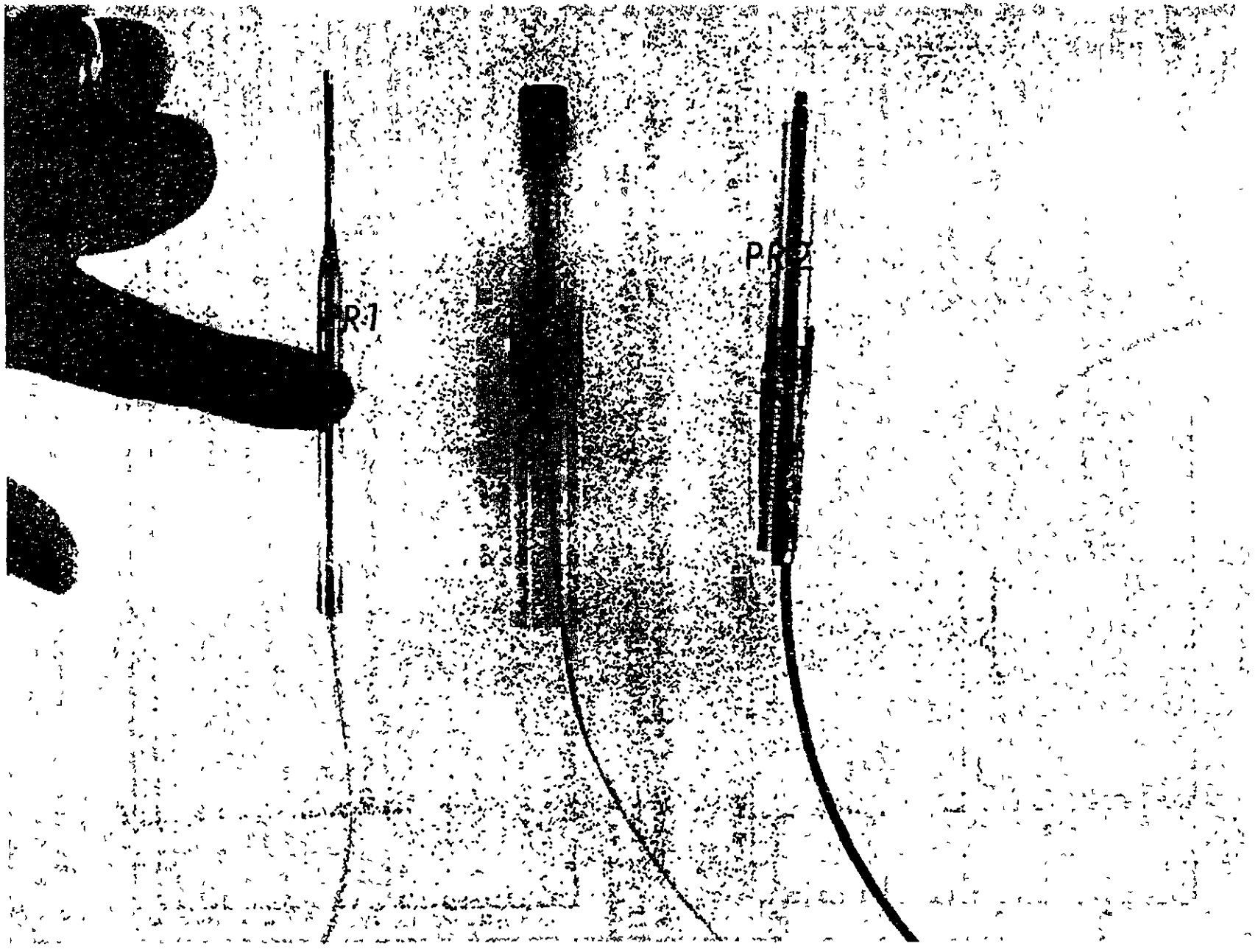

Figure 8. Blast overpressure transducers mounted in cylindrical holders to evaluate "aerodynamic response."

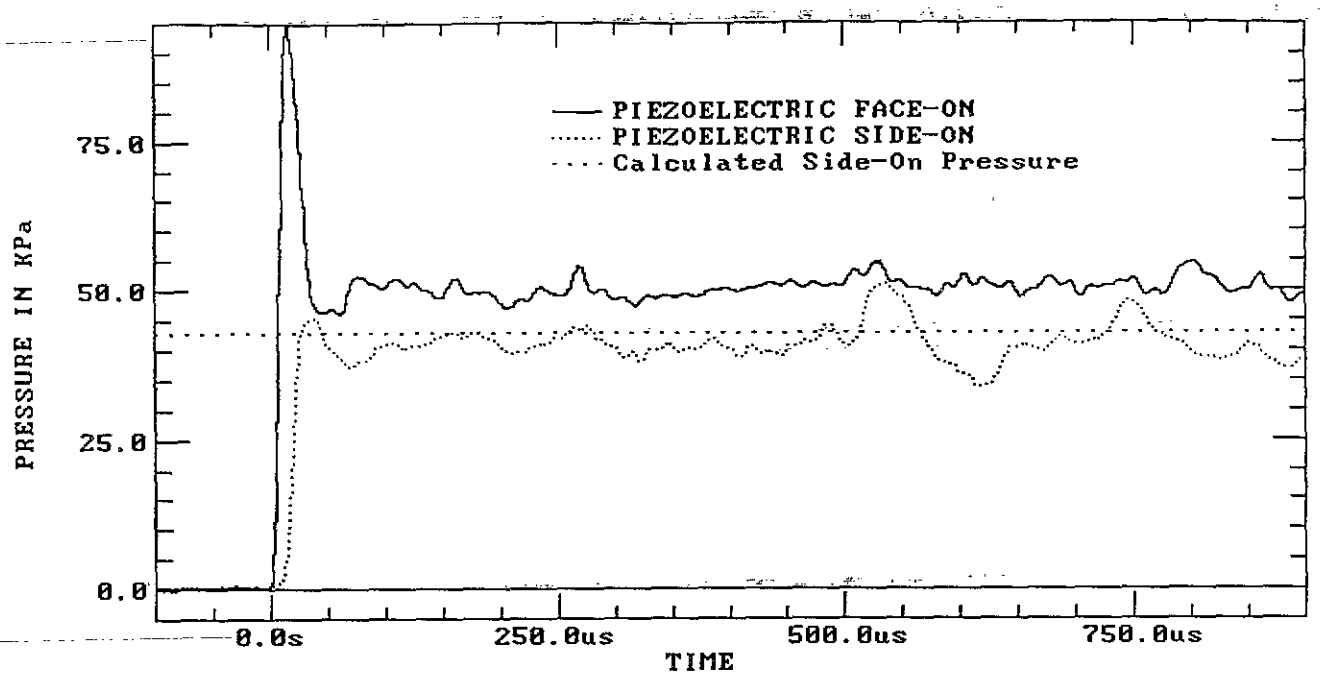

Figure 9. Response of piezoelectric transducer to side-on and face-on shock. Note that the face-on orientation produces a signal 124% higher than the side-on shock value.

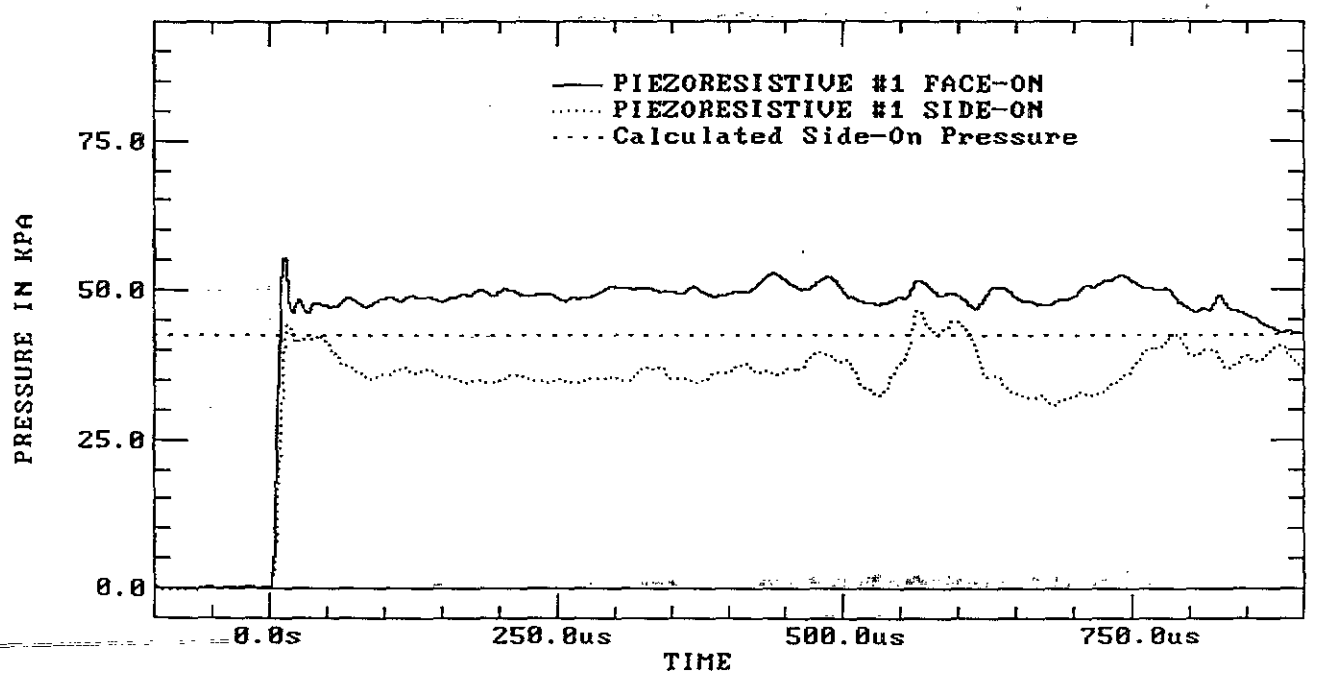

Figure 10. Response of piezoresistive transducer to side-on and face-on shock. Note that the face-on orientation produces a signal that is 34% above the calculated side-on shock value.

of shock waves is much more demanding. Peculiarities caused by minute variations on the sensing surface, the flow of the shock wave over the transducer, and the effect of transducer resonance (which is almost always excited by shock wave passage) can cause serious errors in the measurement of blast overpressure.

A facility to produce carefully controlled blast waves has been developed at USACSTA and is shown in Figure 11. In this Instrumentation Development Blast Chamber (IDBC), explosive charges from 28g (1 oz) to 227g (8 oz) are used. Several measurement aids are used to maintain the distance between the charge and the transducer at 3.000 meters ± 2mm. Two velocity probes, as shown in Figure 12, measure the shock propagation velocity. This velocity is used to independently calculate the shock wave pressure. Figures 13 and 14 show experimental transducers being installed in the IDBC.

Table 1 illustrates typical measurements from the IDBC. Table 2 summarizes the results of additional IDBC firing. Note that the most successful transducer (Piezoresistive 1) varied from 4.1% below to 1.1% above the readings of the velocity probes. Also note that the piezoelectric transducer currently being used varied from 0.1% to 16.5% above the readings of the velocity probes, hence asubstantial improvement in accuracy has been realized.

SUMMARY

Table 3 summarizes all the testing done and provides a quick comparison of the three types of transducers. In general, the objectives of the development effort have been achieved. The problems that remain to be solved are:

(1) The electrical noise floor of the Piezoresistive 1 transducer (0.5KPa) is too high. Measurements below 12 KPa can not be made with a 25:1 signal to noise ratio.

(2) The sensitivity of piezoresistive transducers to light remains a problem. A protective coating eliminates the problem, but any tear or abrasion of the coating will cause the problem to re-appear.

REFERENCES

1. W. Scott Walton, 1981: Improvement of Air Blast Measurement, ILIR Task 5, Report No. APG-MT-5481, U.S. Army Aberdeen Proving Ground, APG, MD.

2. W. Scott Walton, 1984: International Weapon Blast Overpressure Experiment, Report No. USACSTA-6109, U.S. Army Combat Systems Test Activity, APG, MD.

3. MIL-STD-1474C (MI), Military Standard, Noise Limits for Military Ground Materiel, 25 August 1988.

4. Test Operations Procedure 4-2-822, "Electronic Measurement of Airblast Overpressure", U.S. Army Test and Evaluation Command, 13 August 1987.

TABLE 1. Example of Instrumentation Development Blast Chamber (IDBC) Measurements. Peak overpressures in KPa for "Group 5", using 8 oz. Pentolite Spherical explosive charges, 30 July, 1990.

	ROUND NUMBER					
Transducer Type	1	2	3	4	5	6
Velocity Probe #1	38.15	38.01	38.43	38.75	37.23	37.51
Velocity Probe #2	38.53	37.85	37.61	38.76	38.64	38.08
Probe Mean	38.34	37.93	38.02	38.76	37.94	37.80
Piezoelectric	39.43	39.25	39.75	39.52	39.11	39.02
% from Probe Mean	+3.4%	+2.9%	+4.2%	+3.6%	2.5%	2.3%
Piezoresistive #1	37.76	38.53	38.25	38.85	38.64	36.60
% from Probe Mean	-1.0%	+1.0%	+ .3%	+1.8%	+1.3%	-4.1%
Piezoresistive #2	43.98	43.07	43.70	43.86	43.07	42.69
% from Probe Mean	+15.3%	+12.9%	+14.6%	+15.0%	12.9%	+11.9%

Grand Mean of Velocity Probes 38.13 KPa
Overall Mean of Piezoelectric Transducer 39.35 KPa (3.2% above probes)
Overall Mean of Piezoresistive #1 38.11 KPa (.05% below probes)
Overall Mean of Piezoresistive #2 43.40 KPa (13.8% above probes)

TABLE 2. Summary of Dynamic Accuracy test result from IDBC, groups 1 through 4, 27-30 July 1990. Mean peak overpressure values in KPa, and percent deviation from velocity probe measurement. NOTE: NS = No protective screen.

Group 1. 1 oz. Explosives, 6 rd.	Group 3: 1 oz. Explosives, 7 rd.
Velocity Probe Grand Mean= 14.03 KPa	Velocity Probe Grand Mean= 14.11 KPa
PE, S/N 1 14.69 KPa (+4.7%) PE, S/N 2 14.05 KPa (+0.1%) PE, S/N 3 14.37 KPa (+2.4%) PE, S/N 4 16.34 KPa (+16.5%) PE, S/N 5 14.36 KPa (+2.4%)	PE, S/N 1 14.56 KPa (+3.2%) PR 1, S/N 1 14.26 Kpa (+1.1%) PR 1, S/N 2 13.53 Kpa (-4.1%)
Group 2: 1 oz. Explosives, 6 rd.	Group 4: 4 oz. Explosives, 6 rd.
Velocity Probe Grand Mean= 13.91 KPa	Velocity Probe Grand Mean= 25.63 KPa
PE, S/N 1 14.58 KPa (+4.8%)	PE, S/N 1 26.51 KPa (+3.4%)
PR 2, S/N 1 15.53 KPa (+11.6%) (NS) PR 2, S/N 2 15.13 KPa (+8.8%) (NS) PR 2, S/N 3 16.17 KPa (+16.2%) PR 2, S/N 4 16.81 KPa (+20.8%)	PR 1, S/N 1 26.24 Kpa (+2.4%) PR 2, S/N 3 29.24 Kpa (+15.7%) PR 2, S/N 2 28.61 Kpa (+11.6%)

TABLE 3. Summary Comparison of Transducer Performance

	TYPE OF TRANSDUCER		
	PIEZOELECTRIC	PIEZORESISTIVE 1	PIEZORESISTIVE 2
Acceleration Sensitivity	.0096 to .037 KPa/g	.002 to .006 KPa/g	.003 to .005 KPa/g
Thermal Transient Sensitivity	Huge	Negligible	Negligible
Calibration shift w/ambient temp. change (0^{o} F-120^{o} F)	Approx. 3% (1981 study)	2.0% - 3.0%	2.4% to 2.7%
Response to Electronic Flash Unit			
at 6"	3.8 - 8.3 KPa	.31 - 1.7 KPa	.4 - 3.5 KPa
at 1"	41 - 83 KPa (thermal)	5.2 - 27 KPa (optical)	4.7 - 10 KPa (optical)
Electrical Noise Floor	.06 - .09 KPa	.4 - .5 KPa	.07 - .08 KPa
Off-Axis Error (Face-on vs. side-on)			
Free Field 38 KPa	114% Error	43% Error	60-76% Error
Shock Tube 46 KPa	124% Error	34% Error	68% Error
Dynamic Accuracy Error, Deviation from IDBC Velocity Probes			
1oz. sphere (14 KPa)	+0.1% to +16.5%	-4.1% to +1.1%	+8.8% to +20.8%
4oz. sphere (25 KPa)	+3.4%	+ 2.4%	+11.6% to 15.7%
8oz. sphere (32 KPa)	+3.2%	- 0.05%	+13.8%

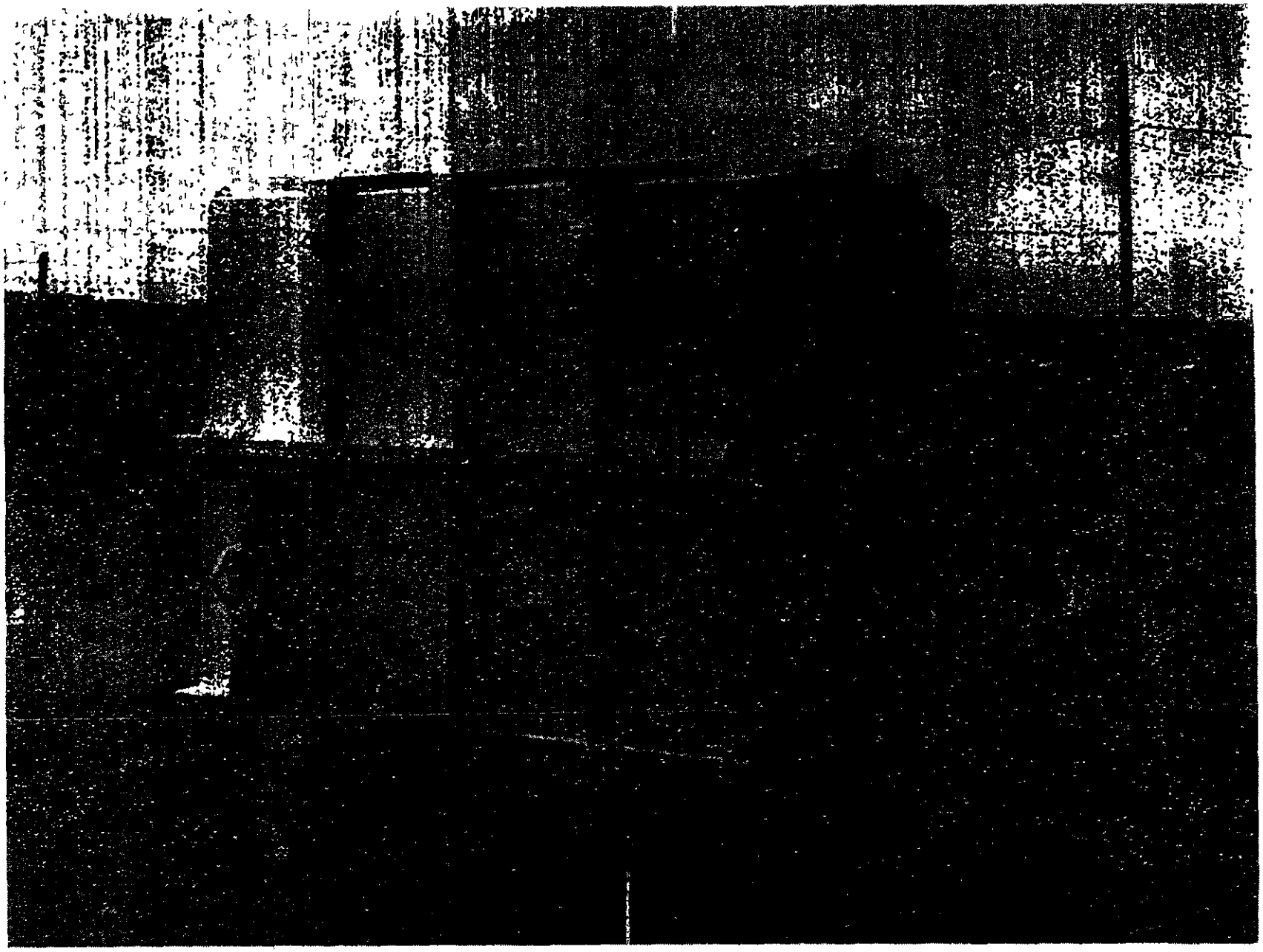

Figure 11. Photograph of the Instrumentation Development Blast Chamber (IDBC) used to test blast overpressure and ballistic shock transducers.

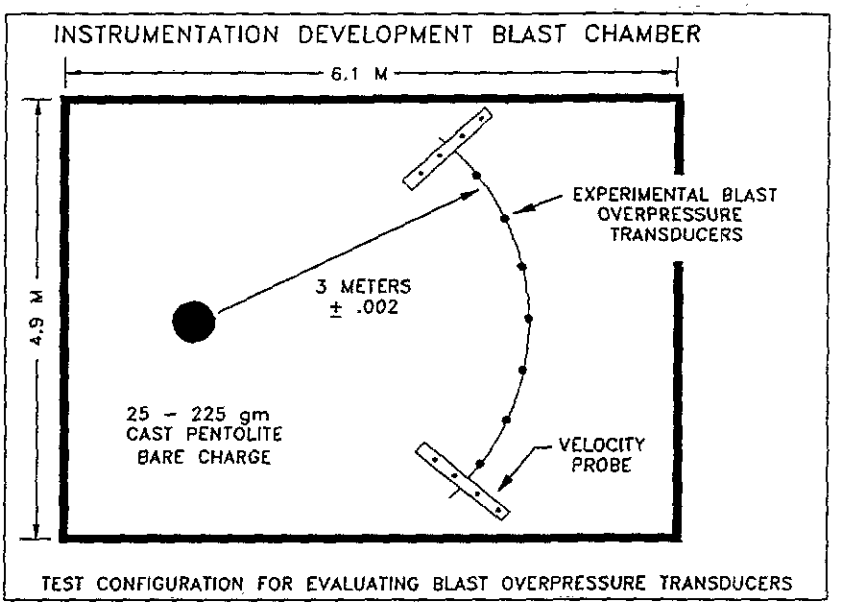

Figure 12. Sketch of IDBC configuration used to evaluate blast overpressure transducers.

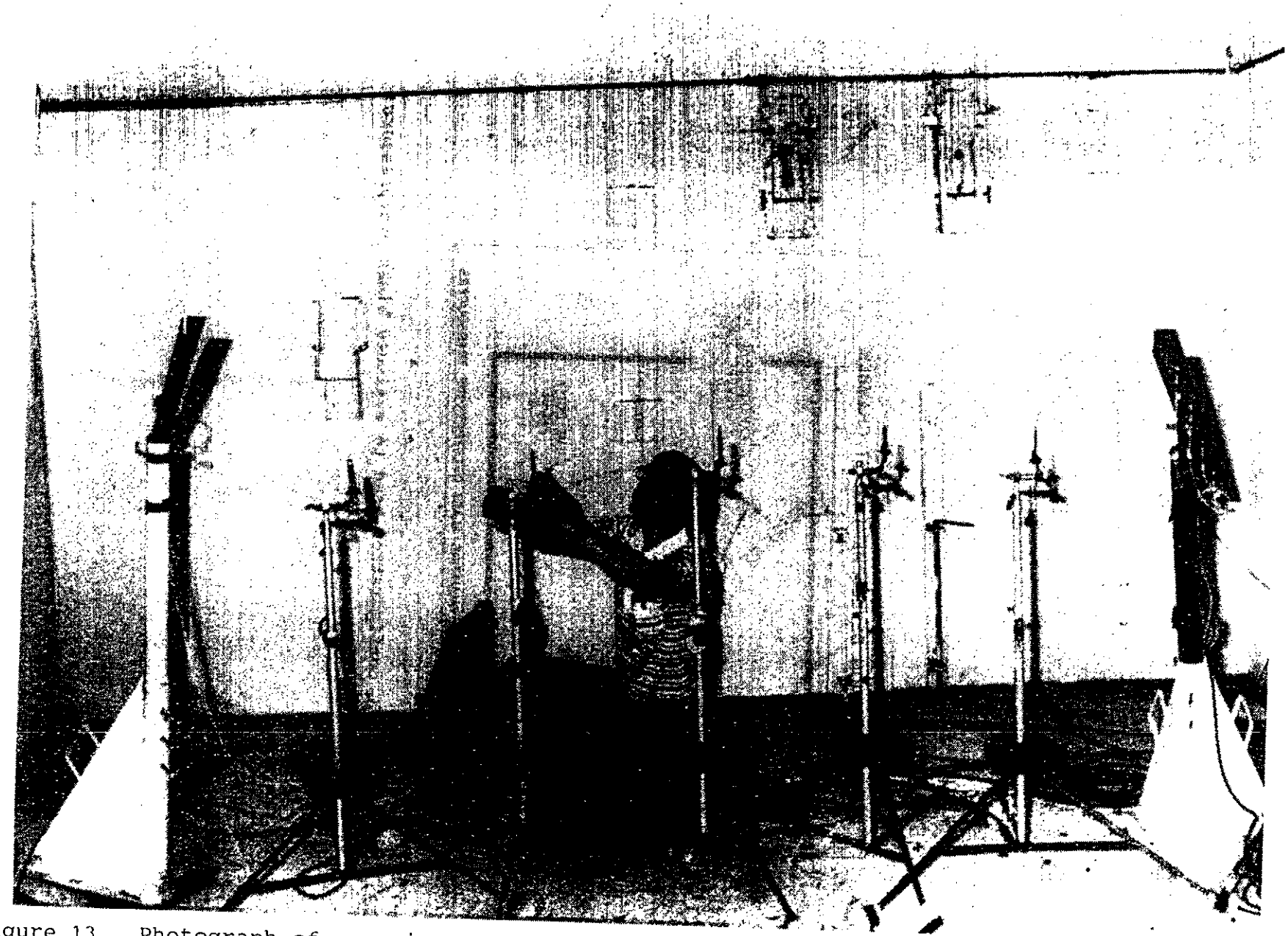

Figure 13. Photograph of experimental blast overpressure transducers being set up in Instrumental Development Blast Chamber.

Figure 14. Photograph of measurement technique used to insure that transducers are exactly 3.000 meters from center of explosive charge.

PVF_2 SHOCK STRESS SENSOR VALIDATION AND COMPARISON EXPERIMENTS

David B. Watts and David R. Wagnon
Wright Laboratory
Armament Directorate (WL/MN)
Eglin Air Force Base, Florida 32542-5434

ABSTRACT

A series of tests were conducted to validate the usefulness of Polyvinylidene Fluoride (PVF_2) as a shock stress sensor material in the five to twelve gigapascal region. Pentolite explosive charges introduced the shock wave into instrumented target materials. Varying thicknesses of polymethyl methacrylate (PMMA) and polytetra fluoroethylene (PTFE) accounted for the differences in shock velocity and pressure experienced by the gages. The experiments compared the response of PVF_2 stress sensors from two different vendors to that of the better known manganin stress sensors under similiar test conditions. The results of these experiments and empirically derived shock attenuation equations for PMMA and PTFE are contained in this paper.

INTRODUCTION

Conventional weapon technology development requires the accurate measurement of weapon performance and effectiveness. Current munition measurement techniques and sensors limit testing during weapon technology development programs. Poor frequency response and accuracy, high noise susceptibility, and limited data collection ability of present measurement technology provide only a small fraction of the desired data from munitions tests or lethality experiments. Investigation and application of innovative sensor materials such as PVF_2 are an attempt to solve some of these measurement problems.

A substantial data base containing the properties of PMMA under shock loading conditions from Pentolite provided the impetus for our experimental design. Pressure versus distance data was collected by the Naval Ordnance Laboratory in White Oak MD during calibration of the Large Scale Gap Test [1]. PMMA was used by NOL as an attenuator that was placed between two explosive charges. The thickness of PMMA was varied until the donor charge detonated the acceptor charge through the PMMA gap only fifty percent of the time. From this testing, NOL thoroughly characterized the shock attenuation properties of PMMA [2]. The availability of the NOL data base, access to a large quantity of Pentolite

(PETN/TNT 50/50), and the low cost of PMMA were determinants in the gage evaluation test design.

BACKGROUND

The objective of the experiment was to compare the response of PVF_2 stress sensors to that of manganin stress gages under similiar test conditions. Manganin gages were chosen as a standard for comparison because of their general acceptance as a stress sensor. PVF_2 is a thin piezoelectric polymer film that if poled, produces an electrical charge when subjected to stress. Manganin is a copper-manganese-nickel alloy with a low strain sensitivity, but a relatively high sensitivity to hydrodynamic pressure. Manganin gages are piezoresistive, which means they exhibit a change in resistance when subjected to stress.

Manganin gages require an external ciruit such as a wheatstone bridge and pulsed high voltage source to overcome signal to noise problems in explosive environments. Initially the bridge circuit is in balance. However, any change in resistance of the sensor due to stress will unbalance the bridge, producing a voltage across the output. The bridge output voltage is thus proportional to stress and is linear for small changes in gage resistance. This relationship is described as:

$$\Delta R_g/R_g = \frac{V_{out}(R_1+R_{gc})/R_g}{V_{in}(R_1/(R_1+R_{gc}))-V_{out}} \quad (1)$$

Where:
ΔR_g is the change in gage resistance due to stress (ohms)
R_g is gage resistance (ohms)
R_{gc} is gage plus cable resistance (ohms)
R_1 is a fixed bridge circuit resistance (ohms)
V_{in} is bridge excitation voltage (volts)
V_{out} is bridge output voltage (volts)

PVF_2 gages, on the other hand, do not require a power supply. They produce an electrical charge when stressed, which is often more than enough to overcome any noise. PVF_2 gages operating in the charge mode require a simple resistor and capacitor circuit. The charge generated by the stress gage is transfered to the capacitor in the external cicuit. The charge produced by the gage is proportional to the voltage across the capacitor which is, in turn, related to stress. This relationship is simply:

$$Q/A = C_c V_c(t)/A \quad (2)$$

Where:
Q is the charge released (uC)
C_c is the capacitance of the charge capacitor (uF)
V_c is the instantaneous voltage at the charge capacitor (v)
t is time (usec)
A is gage sensing element area (cm^2)

EXPERIMENT DESIGN

PVF_2 stress gages were purchased from two different vendors. Dynasen Inc. provided

stress gages made from uniaxially stretched, single cycle poled PVF_2 material manufactured by Pennwalt Corporation [3]. Ktech Corp. provided stress gages made from biaxially stretched PVF_2 manufactured by Rhone Poulenc Films in France and poled IAW the Institute Saint Louis (Bauer) method [4]. Metallized PVF_2 Kynar Piezo Film was also obtained in sheet form from Pennwalt Corp. In addition, manganin stress gages were purchased from Dynasen Inc. and Micro-Measurements Division of Measurement Group Inc. All PVF_2 film used was 26 microns thick.

A series of tests were conducted to validate the usefulness of PVF_2 as a shock stress sensor material in the 5 to 12 GPa range. The input shock wave was produced by 50.8 mm by 50.8 mm right cylinders of the explosive Pentolite (PETN/TNT 50/50) attenuated through various target materials. Targets consisted of two or three like discs 101.6 mm in diameter with thicknesses corresponding to the prescribed run distances. Two run distances of 6.35 mm and 12.7 mm were used in PMMA and PTFE to vary the expected stress levels. Most targets consisted of two discs epoxied together with either one or two gages mounted between them. In some cases, three discs were epoxied together with one gage mounted between each disc. The disc thicknesses in this configuration were each 12.7 mm thick. Therefore, one of the stress gages was a distance of 25.4 mm from the explosive/ target interface.

All gages were mounted between the discs near the centerline to minimize the wave "tilt" as it passed over the gage. In addition to the gage in the inerts, another gage was placed at the explosive/ target interface to act as a time-of-arrival (TOA) sensor to measure transit time. This transit time was used to calculate the expected stress levels in the materials from their known hugoniot constants. The gages mounted at the explosive/ target interface did not survive long enough or, in some cases, respond to the shock front in a way that the pressure level could be determined. Therefore, in many of the experiments, the top gage was replaced with a strip of Pennwalt metallized piezofilm to provide TOA data.

PVF_2 stress sensors were configured in the charge transfer mode. Manganin gages were configured in a wheatstone bridge using a pulsed power supply. Data was captured with a Textronix RTD710A digitizer operating at a sample rate of 10 nanoseconds per point. This digitizer has an analog bandwidth of 100 MHz. A wideband antenna centered around 400 MHz, was initially set up to monitor electromagnetic interference (EMI) from the bare charges. The antenna ended up providing accurate timing information of the shock wave through the target material. Large EMI spikes occurred at times corresponding to the shock front's arrival at the explosive/ target interface, the gage location, and the backside of the target. The largest EMI spikes occurred at

the locations where PVF_2 gages were mounted. Figures 1-3 are typical of the gage data and the corresponding antenna data indicating the shock wave TOA.

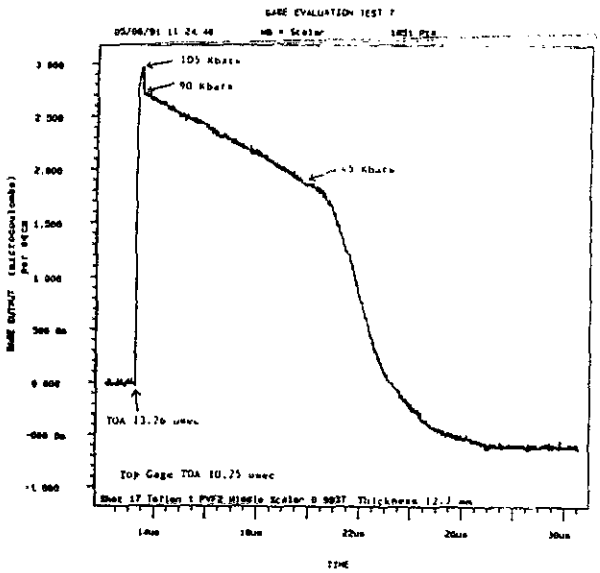

Figure 1. PVF2-11-.125-EK stress gage in 12.7 mm of PTFE.

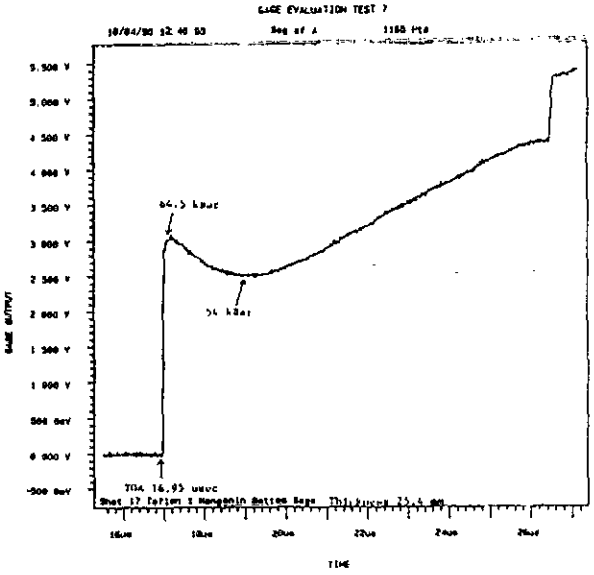

Figure 2. MN4-50-EK stress gage in 25.4 mm of PTFE.

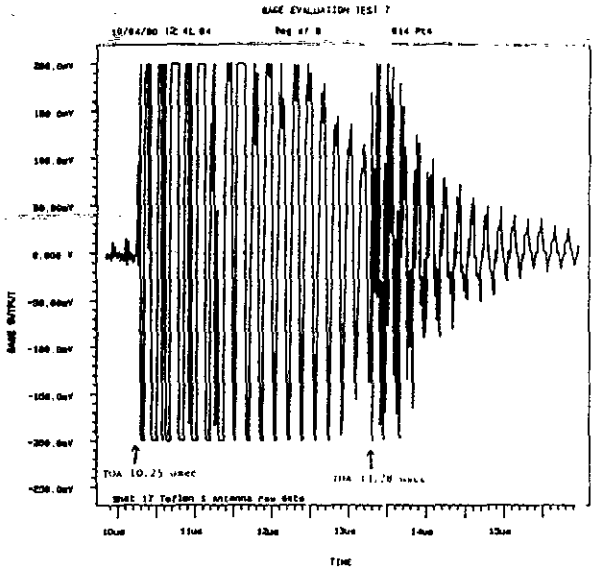

Figure 3. Antenna data indicating shock wave TOA.

SHOCK PHYSICS

The shock impinging on the gages is the result of a detonation wave adjacent to the inert material (target). The detonation drives a sharp shock whose properties are dependent upon certain material characteristics of the hot explosive gases and target. The initial, sharp rise in pressure will be followed by a much slower decay controlled by the detonation products as they expand. The calculation of the attenuating wave properties is impossible in closed form.

The strength of the shock waves of interest are greater than the yield strength of any of the targets. The shock wave is conveniently described as hydrodynamic since it behaves as a fluid. The conservation of mass and momentum lead to the key one dimensional

equation:

$$P = p_o u_s u_p \qquad (3)$$

Where:
P is pressure (GPa)
p_o is density (g/cc)
u_s is shock velocity (km/s)
u_p is particle velocity (km/s)

The particle velocity is the initial material flow rate induced by the shock. The equation assumes the material ahead of the shock is still prior to wave arrival. While the initial density of the material is certainly easy to obtain, there remain three unknowns and only one equation. This difficulty is circumvented since the shock velocity is approximately a linear function of the particle velocity:

$$u_s = c_o + s\, u_p \qquad (4)$$

Where:
c_o and s are constants

When substituted into the conservation of momentum:

$$P = p_o(c_o + s\, u_p)\, u_p \qquad (5)$$

The measurement of the particle velocity is sufficient to calculate the peak pressure.

Equation 5 produces a concave upward curve which is different for every material and is known as the hugoniot, figure 4. It represents the locus of states which a material can attain, not the series of states the material does attain during the shock process. Each state on the hugoniot can be connected to the origin (state u_p=0) by a line whose slope is $p_o u_s$ (reference eqn. 3). The shock velocity is much easier to measure, so this method is often used to calculate the pressure.

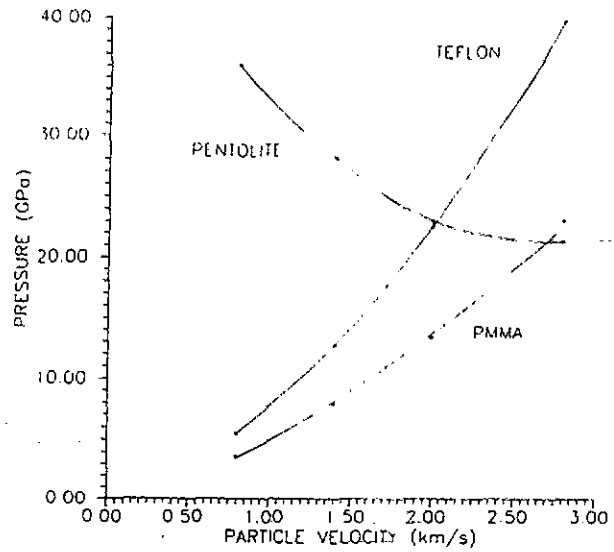

Figure 4. Pressure vs Particle Velocity.

The interaction of a detonation wave and target is difficult conceptually, since the explosive begins as a condensed material, but the interaction is between the detonation product gases and the target. The expansion of the product gases can be approximated by a products isentrope. While the isentrope is similar to the hugoniot previously described, its curvature is reversed since the products begin at a high pressure, a high temperature, and are in motion (u_p), figure 4. In other words, the interface interaction is the second shock for the gases. If the products are compressed and in motion, what happens if they encounter an obstacle which slows them down? They are further compressed and their pressure rises. If they reach

an interface which allows them to expand more easily, they become less dense and their pressure drops. This is exactly opposite the first circumstance addressed.

What happens at the interface? The calculation of the interface properties are possible because the two materials maintain contact. This means that the interface particle velocity is the same for both materials. The principle of continuity means the pressures are also the same. Another way of stating this obvious conclusion is that the products curve and target curve intersect at only one point, the unique state which both can attain (reference fig. 4).

WAVE CHARACTERISTICS

In this two dimensional test the shock wave is curved and continually affected by relief from the sides (edge rarefactions). Since the velocity of these rarefactions is the local sound speed in a moving medium, their range of effect can be calculated. This velocity will not exceed the shock velocity, so the singly shocked state can be bounded by a cone with a 45° included half angle. Since the charge radius is 25.4 mm, the edge effects will not reach the centerline until the target thickness exceeds 25.4 mm.

The wave curvature is equally simple. A Huygen's construction will adequately model the wave curvature in this geometry. Through the explosive, the curvature will be a simple radius from the detonator (assuming prompt initiation and ignoring the detonator radius). The detonator width will be invoked for gages that are at the limits of this test. The radius of curvature after 50 mm of run is 50 mm. Since Pentolite detonates at 7.5 km/s, the detonation wave arrives at the outer diameter of the end of the charge .78 microseconds after it reaches the center.

At the interface the velocity changes in an as yet unspecified manner. It could be higher or lower than the detonation velocity. The hugoniot of the target and products isentrope are used to obtain the initial pressure and shock velocity. The Huygen's construction is used at the interface to map out the shock wave in the target.

The gages should be struck simultaneously across their width to work correctly. The actual time for the wave to sweep the gage is a function of local wave curvature. The calculation is somewhat tedious but tenable. A right triangle is formed using the explosive centerline, the plane containing the gage, and the run distance from detonator to gage edge, figure 5.

The hypotenuse is found and the angle subtending the gage displacement is calculated. The distance from the centerline to the point where the hypotenuse crosses the explosive/ target interface is important. It determines the length run at the detonation velocity, and the length run at

the shock velocity in the target. The centerline explosive length and angle are used to determine these lengthes. These distances divided by their relative velocities sum to give the time-of-arrival at the gage edges. Because of the large runs involved and the small gages, the sweep time is relatively small (nanoseconds). Thus the non-planarity of the shock wave with respect to the gage surface was calculated and was determined to contribute a small error in comparison to other sources of error in the experiment.

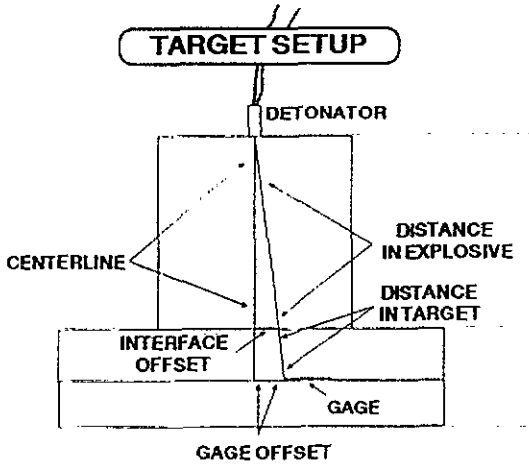

Figure 5. Diagram used for gage sweep time calculation.

RESULTS

Experimental results obtained by NOL for Pentolite on PMMA during calibration of card gap tests indicated the following pressures at the specified distances [2]:

Table 1. NOL Data

Distance	Pressure
0mm	21.33 GPa
6.35mm	10.37 GPa
12.7mm	8.07 GPa
25.4mm	5.71 GPa

Shock wave arrival times and the corresponding distances from the gages to the explosive/ target interface were used to derive equations representing the shock wave travel distance versus time for both PMMA and PTFE. The derivatives of these two equations provided equations for shock velocity versus time. Solving the shock velocity equation for time and substituting this into the corresponding distance equation and solving for shock velocity, yields an equation for shock velocity versus distance. For PMMA, the equation is:

$$u_s^2 = 30.45863177 - 0.4697088x \quad (6)$$

Where:
x is distance (mm)

Figure 6 is a graph of this equation for PMMA.

For PTFE, the equation is:

$$u_s^2 = 20.36252844 - 0.4280592x \quad (7)$$

Figure 7 is a graph of this equation for PTFE.

The calculated values for pressure in the two materials were determined by substituting the u_s obtained at the distance of interest into the hugoniot relation for that material, equation 4. The hugoniot constants for PMMA are [5]:

C_o= 2.555 and s= 1.556
also r_o= 1.186 g/cc

The constants for PTFE are [5]:

C_o= 1.845 and s= 1.693
also r_o= 2.152 g/cc

Solving equation 4 for u_p and substituting the appropriate values into equation 3, yields a pressure value for the distance of interest. Using this method the following pressures and distances were calculated for PMMA and PTFE:

Table 2. Calculated Pressure

PMMA	
Distance	Pressure
6.35 mm	10.73 GPa
12.7 mm	9.03 GPa

PTFE	
Distance	Pressure
6.35 mm	12.58 GPa
12.7 mm	9.91 GPa
25.4 mm	4.84 GPa

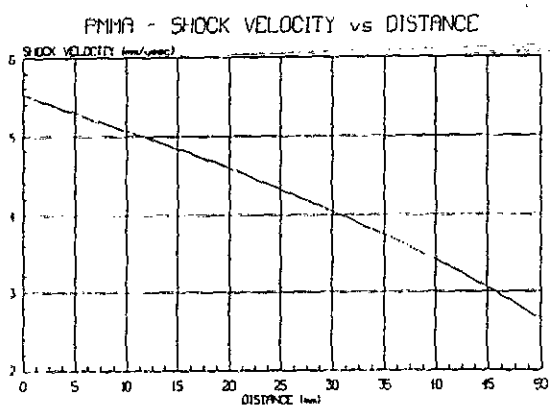

Figure 6. PMMA u_s vs x.

The calculated pressure in PMMA at 6.35 mm is similiar to that obtained by NOL. The calculated pressure in PMMA at 12.7 mm is 1.0 GPa higher than that obtained by NOL.

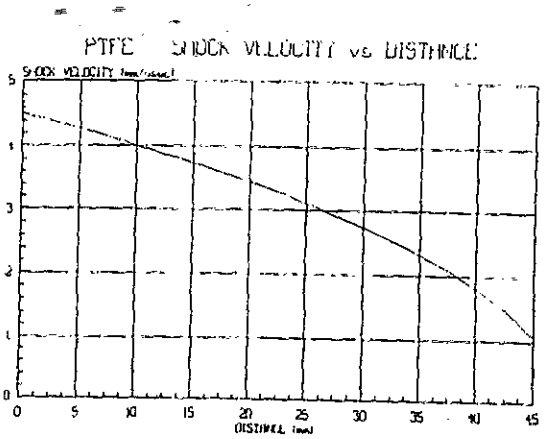

Figure 7. PTFE u_s vs x.

The equation representing the calibration curve for the Ktech PVF_2 gages for pressures above 1.0 GPa is [6]:

$$Q/A = 0.328244\ (P^{0.54633}) \quad (8)$$

The equation representing the calibration curve supplied with the Dynasen PVF_2 gages was determined for pressures above 1.0 GPa to be:

$$Q/A = -0.3148622 + 0.3194605\ (P^{0.5}) \quad (9)$$

Stress gages obtained from Ktech were PVF_2 model SNLA-26 with sensing element areas of 0.01 cm^2 and 0.09 cm^2 respectively. The Ktech gages were not encapsulated when purchased . The only SNLA-26 gages that were encapsulated later were the ones mounted at 25.4 mm from the explosive/ target interface in PTFE (Teflon). These gages were encapsulated in 1 mil (25 um)

thick Kapton polyimide film obtained from Dupont Company.

Stress gages purchased from Dynasen were also encapsulated in 1 mil of Kapton. The PVF_2 gages were model PVF2-11-.125-EK with a sensing element area of 0.1008 cm^2. The manganin gages were model MN4-50-EK and had a sensing element area of 0.1452 cm^2. Manganin gages delivered by Micro-Measurements were model LM-SS-210AW-048, option SP60 for encapsulation, with sensing element area of 0.3385 cm^2. Calibration curves supplied with the two types of manganin gages were used to find the stress.

The results of the pressure measurements for PMMA and PTFE are summarized in Table 3 and 4, for each gage model. Referring to figure 1, measurements were made at the peak which in most cases appeared as an overshoot. In some cases, the initial response to the shock wave appeared as an undershoot. Stress levels are also reported for the plateau near the peak which refers to the area where the peak settles down.

SUMMARY

The results of the gage evaluation experiments show a wide variation of responses of the PVF_2 stress gages to shock induced stress. Figure 1 is a typical trace from a PVF2-11-.125-EK stress gage in 12.7 mm of PTFE. Figure 2 represents the output of a MN4-50-EK stress gage in the same target as figure 1 but at 25.4 mm. The antenna data collected during the experiment with this target is shown in figure 3. The top gage was a strip of Pennwalt PVF_2 film. The first spikes in the antenna data correspond to the shock wave arrival time at the explosive/target interface represented by the top gage TOA of 10.25 usec. The second set of spikes occur at 13.28 usec which is the shock wave TOA at 12.7 mm corresponding to the PVF2-11-.125-EK position. No detectable spikes occurred at the time the shock wave impinged the MN4-50-EK gage, i.e. 16.95 usec. It appears that most of the EMI recorded during this shot was due to the shock wave impinging the PVF_2 material. The generation of EMI by the shocked PVF2 may be of some use as a technique to measure TOA or something to be shielded against if it would otherwise interfere with some other measurement system.

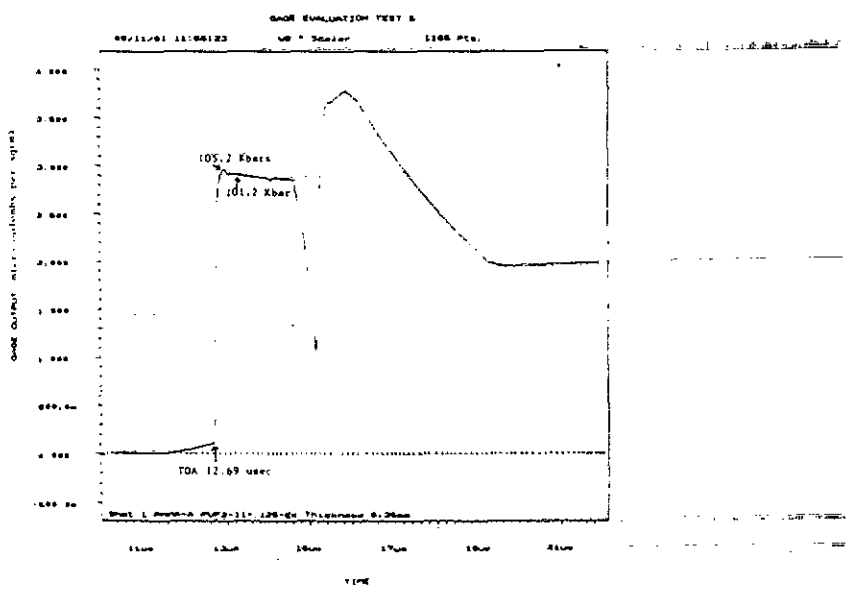

Figure 8. PVF2-11-.125-EK stress gage in 6.35 mm of PMMA.

Table 3. Pressure measured in PMMA.

Gage Model	Depth (mm)	Location	Output (uC/cm^2)	No. of Targets	Pressure (GPa)	Error Bars (GPa)
SNLA-26 0.01 cm^2	6.35	O	4.673 +/- 1.6975	4	12.92	5.65 - 22.78
		P	4.300 +/- 1.4329		11.09	5.28 - 18.77
	12.7	O	5.126 +/- 0.5163	4	15.30	12.60 - 18.24
		P	4.856 +/- 0.6298		13.86	10.75 - 17.32
PVF2-11 -.125-EK	6.35	O	3.007 +/- 0.2479	7	10.81	9.26 - 12.49
		P	2.986 +/- 0.1262		10.68	9.88 - 11.51
	12.7	O	2.821 +/- 0.2225	9	9.64	8.32 - 11.05
		P	2.805 +/- 0.1817		9.54	8.46 - 10.68
MN4-50-EK	12.7	O	17.5% +/- 1.1314%	2	7.60	7.40 - 8.00

Table 4. Pressure measured in PTFE.

Gage Model	Depth (mm)	Location	Output (uC/cm^2)	No. of Targets	Pressure (GPa)	Error Bars (GPa)
SNLA-26 0.01 cm^2	6.35	O	4.679 +/- 0.1084	3	12.95	12.40 - 13.50
		U	4.174 +/- 0.0276		10.51	10.38 - 10.63
		P	4.371 +/- 0.1022		11.43	10.95 - 11.92
	12.7	O	4.736 +/- 0.5821	3	13.24	10.41 - 16.37
		P	4.418 +/- 0.3373		11.66	10.08 - 13.34
SNLA-26 0.09 cm^2	6.35	O	3.634 +/- 0.3041	6	8.15	6.95 - 9.44
		U	3.167 +/- 0.4757		6.34	4.70 - 8.19
		P	2.900 +/- 0.4069		5.39	4.09 - 6.86

Table 4. Pressure measured in PTFE.

Gage Model	Depth (mm)	Location	Output (uC/cm^2)	No. of Targets	Pressure (GPa)	Error Bars (GPa)
SNLA-26 0.09 cm^2	12.7	O	3.183 +/- 0.4536	6	6.40	4.83 - 8.16
		U	3.188 +/- 0.0		6.41	none
		P	3.049 +/- 0.4446		5.91	4.43 - 7.59
	25.4	O	3.056 +/- 0.1454	3	5.94	5.43 - 6.46
		P	2.898 +/- 0.0425		5.39	5.24 - 5.53
PVF2-11 -.125-EK	6.35	O	3.285 +/- 0.0934	3	12.70	12.05 - 13.37
		P	3.103 +/- 0.1102		11.45	10.72 - 12.20
	12.7	O	2.756 +/- 0.2938	11	9.24	7.56 - 11.09
		P	2.484 +/- 0.2519		7.68	6.36 - 9.12
	25.4	O	2.255 +/- 0.1838	6	6.47	5.58 - 7.43
		P	2.068 +/- 0.1214		5.56	5.01 - 6.15
MN4-50-EK	6.35	O	26.53% +/- 1.1666	6	10.4	10.0 - 10.6
	12.7	O	20.29% +/- 0.9102	3	8.5	8.3 - 8.8
	25.4	O	14.60% +/- 0.2113	3	6.5	6.3 - 6.6
LM-SS -210AW-048	12.7	O	20.55% +/- 0.7142	2	8.0	NA

The response of PVF2-11-.125-EK stress gages mounted in 6.35 mm and 12.7 mm of PMMA are shown in figures 8 and 9, respectively. The gage measured stress levels are in the range of those reported by NOL, Table 1, as well as those calculated for PMMA, Table 2.

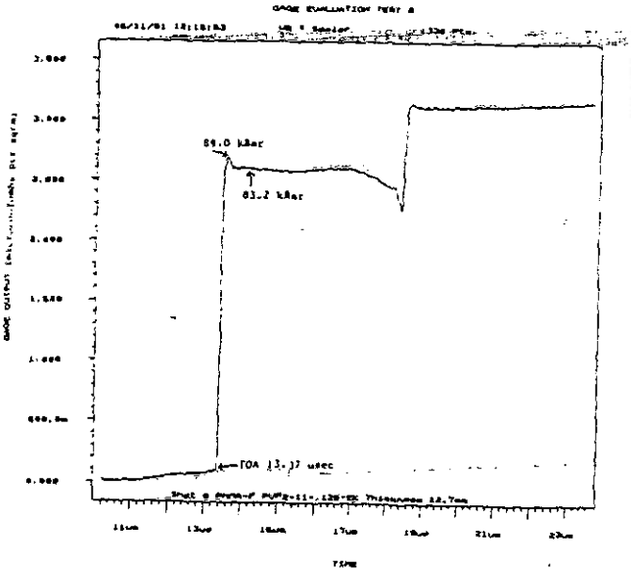

Figure 9. PVF2-11-.125-EK stress gage in 12.7 mm of PMMA.

The response of a PVF2-11-.125-EK gage in 25.4 mm of PTFE is shown in figure 10. The gage measured pressure is in near agreement with the calculated values in table 2. The graph in figure 11 is of a Kapton encapsulated SNLA-26 0.09 cm^2 stress gage. The SNLA-26 gages not ecapsulated appear to indicate a large variance in gage output. Once the gages were encapsulated the gage output was less erratic.

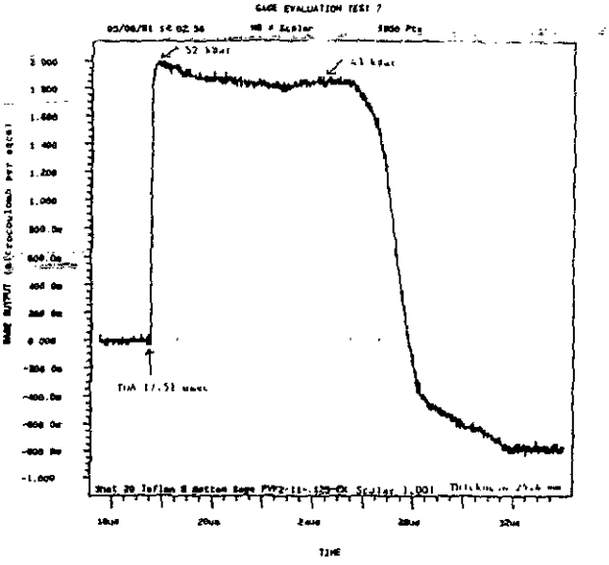

Figure 10. PVF2-11-.125-EK stress gage in 25.4 mm of PTFE.

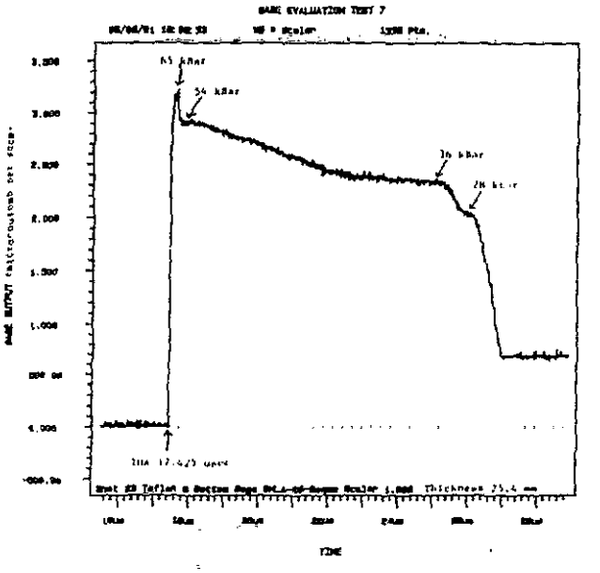

Figure 11. SNLA-26 0.09 cm^2 Kapton encapsulated stress gage in 25.4 mm of PTFE.

The switch from PMMA to PTFE as a target material was due to

the discovery of research investigating the shock induced polarization in plastics [7]. It was reported that PMMA exhibits strong electrical activity under shock loading conditions while the activity in PTFE is only feeble. The intent was to change to a target material that would not interfere with the performance of the unencapsulated gages.

Strong electrical activity is also reported for poly-pyromellitimide (PPMI), which is the composition of Kapton [7]. This same research reports that Kapton becomes highly conductive above a pressure of about 9 GPa. Therefore, a better encapsulation material for the present experimental setup may be PTFE instead of Kapton since some of the pressures encountered are above 12.5 GPa. The extent that the use of Kapton as an insulator in these experiments has affected the data is unknown. The fact that the Dynasen encapsulated gages seem to have faired somewhat better than the unecapsulated Ktech gages does lead one to consider encapsulation a benefit. The few Ktech gages that were encapsulated displayed very little variance in the data.

A series of experiments were also conducted with a new batch of Dynasen PVF2-11-0.125-EK stress gages. These gages were mounted on a 12.7 mm base of PMMA. The discs that were epoxied on top the gage, varied in thickness between 3.18 mm and 15.88 mm, in 1.59 mm increments. The pressure at these thicknesses was expected to vary between 7.4 and 13.2 GPa. Nearly all stress gages reported the same output. Consultation with Dynasen revealed the possibility that the new batch of PVF_2 material was overstretched by Pennwalt Corp. since the material was milky in appearance [8]. By being overstretched, this material may have dead spots or voids in it. The gages may be clipping due to saturation. Another possibility is that since this new batch of PVF_2 was poled to have a higher activity than the previous batch, the gage is short circuiting at high pressures. In any event, the distance and subsequent TOA obtained during this set of experiments was used to derive equation 6.

CONCLUSION

The usefulness of PVF_2 as a shock stress sensor material is promising. The high frequency response, high signal to noise ratio, and conformability of this material, make it useful in many unique measurement requirements. However, it is clear that careful attention must be paid in controlling the manufacturing process so that the material properties are consistent from batch to batch. It is also important to consider the gage packaging requirements for each unique application. Understanding the properties of the gage encapsulation material may help to reduce one more of the many variables present in munitions testing.

ACKNOWLEDGEMENT

The authors wish to acknowledge

the support received from Michael T. Van Tassel and Voncile Ashley. The dedication and professionalism of these two unique individuals was paramount to the success of this effort.

REFERENCES

(1) Price, D., A. R. Clairmont, Jr., and J. O. Erkman, "The Large Scale Gap Test. III. Compilation of Unclassified Data and Supplementary Information for Interpretation of Results", NOLTR 74-40, 8 March 1974.

(2) Erkman, J. O., D. J. Edwards, A. R. Clairmont, Jr., and D. Price, "Calibration of the NOL Large Scale Gap Test; Hugoniot Data for Polymethyl Methacrylate", NOLTR 73-15, 4 April 1973.

(3) Charest, J. A., and C. S. Lynch, "Comparitive Study of Commercial Piezofilm Stress Gauges", 39th ARA Meeting, Alburquerque, NM, October 1988.

(4) Lee, L. M., D. V. Keller, E. S. Gaffney, D. A. Hyndman, L. M. Moore, and F. Bauer, "Piezoelectric Polymer Shock Gauge Applications", Range Commanders Council 15th Transducer Workshop, Cocoa Beach, FL, June 1989.

(5) LASL Shock Hugoniot Data, Stanely P. Marsh ed., University of California Press, Berkeley, CA, 1980.

(6) Reed, R. P., and J. I. Greenwoll, "The PVF_2 Piezoelectric Polymer Shock Stress Sensor Signal Conditioning and Analysis for Field Test Applications", Fifth State-of-the-Art Blast Instrumentation Meeting, Alburquerque, NM, November 1988.

(7) Graham, R. A., "Shock Induced Electrical Activity in Polymeric Solids. A Mechanically Induced Bond Scission Model", The Journal of Physical Chemistry, Vol. 83, No. 23, 1979, pp. 3048-3056.

(8) Private communication with J. A. Charest of Dynasen Inc.

A COMMON TWO-WIRE

AUTOMATIC MONITORING SYSTEM

16TH TRANSDUCER WORKSHOP

18 JUNE 1991

BY
E. A. DAHL
LEROY BATES

Naval Ship Weapon Systems Engineering Station
Port Hueneme, California

19 JANUARY 1991

TWO-WIRE AUTOMATIC REMOTE SENSING AND EVALUATION SYSTEM (TWARSES)
SUPPLEMENTAL INFORMATION

1. The NSWSES Two-Wire Automatic Remote Sensing and Evaluation System provides, on a common two wire network, remote sensing and alarms from at least 160 locations with each location having 8 sensors which can be intermixed for many types of data - such as but not limited to - smoke (fire spreading), water level (progressive flooding), temperature, relative humidity, Ox Ho, NO. These automated 'smart' sensors will detect environmental conditions and will display on display boards - their status - and analog readout from these remote locations with both automatic alarms and printed data with time base.

2. This system was used for monitoring submarine battery cells on USS SUNFISH for three years. Now a system is installed in USS MEMPHIS, both for battery cell monitoring and environmental monitoring (PNO 38). The other systems have been used in USS ELLIOTT and USS LEYTE GULF for checking moisture and temperature content of vertical launch canisters.

3. This system is a portable, lay-in smokeless 1/8 diameter wire system and can be ship installed with all elements supplied in a "kit" or installed with ship assistance by NAVSESS.

4. The SCANNER DISPLAY for this system is 16" long, 12" wide, 4" deep, and is a dedicated display with only 117V 60V AC 50 watts supplied at one location. All sensors are powered from data line. This scanner control and alarm box can include data from the DCA status board. When any alarm appears, automatic readout of data from status board appears on LED readout. We can add readout of ship system if requested. A remote display unit 16x5x4 can be supplied and set anywhere in ship fed from either a two-wire copper or fiber optics line.

5. SENSOR BOX is 4 3/4" long, 3 1/8" wide, and 2 1/4" deep, held in position by double faced tape. This sensor box has variable addresses, will take 8 sensors selectable from the following list:

1 - Oxygen (in stock)
2 - Carbon Monoxide (in stock)
3 - Hydrogen Sulphide
4 - Sulphur Dioxide
5 - Hydrogen (in stock)
6 - Nitric Oxide (in stock)
7 - Nitrogen Dioxide
8 - Chlorine
9 - Hydrogen Chloride
10 - Hydrogen Cyanide
11 - Liquid Levels - Water, Oil, Fuel
12 - Smoke
13 - Pressure - Atmospheric
14 - Temperature - Atmospheric
15 - Relative Humidity
16 - Chilled Water - Pressure, Flow and Temperature
17 - 60 Cycle Power - Voltage, Frequency
18 - 400 Cycle Power - Voltage, Frequency
19 - Noise
20 - Vibration
21 - IR - Motion - Heat

We have in development, freon, carbon dioxide and toxic gas sensors. These could be ready for ship installation 40 days after funding. These sensors require local power.

6. Field calibaration would be done with a simple clip which would be placed over the front of the box with a nipple to connect a piece of gas tubing to a small calibration cylinder. This small cylinder will have a mixture of 500 ppm H2, 100 ppm NO, 250 ppm CO

NSWSES/TWARSES STANDARD DISPLAY

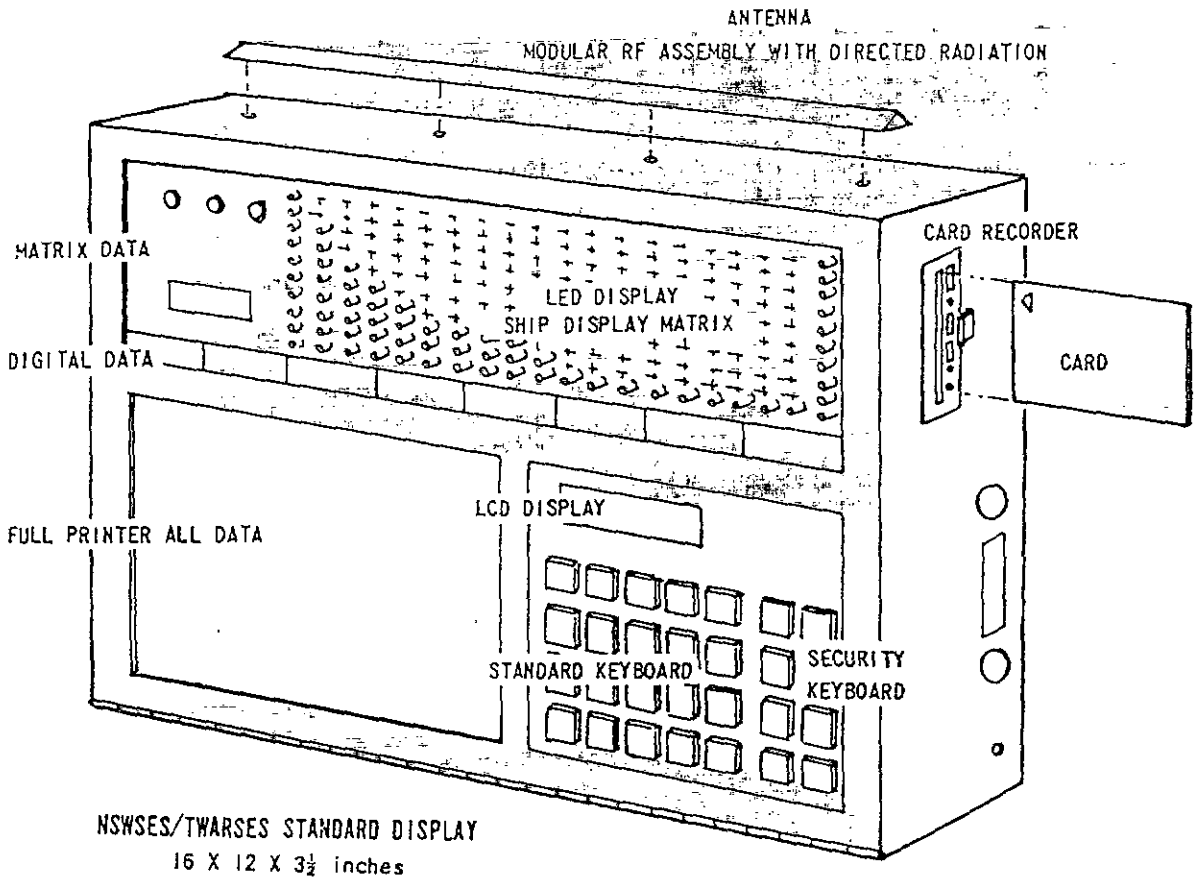

NSWSES/TWARSES STANDARD DISPLAY
16 X 12 X 3½ inches

1. WIRELESS DISTRIBUTION TWARSES SYSTEM
2. BLOCKED DATA
3. TWARSES FORMAT

HAND HELD EMERGENCY - LOCATION DISPLAY
3 X 5½ X 1½ inches (approx.)

LOOK NO WIRES !

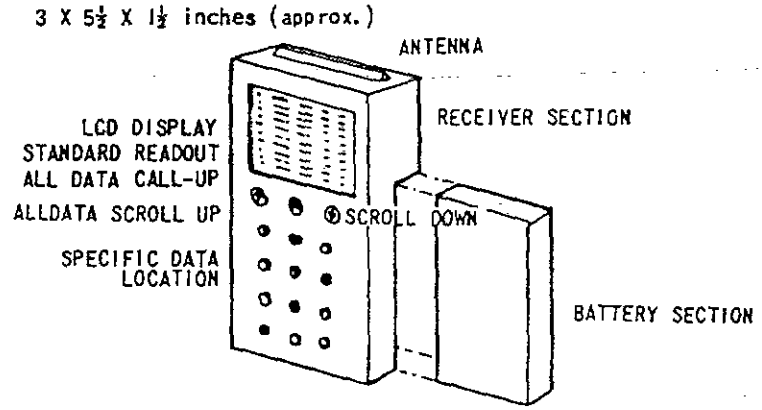

NOTE: CONTROLLED RADIATION - 360° OR DIRECTED

This Engineering and Artwork on RF-Pulse Coupler not done at Navy expense due to unavailable funding. E. DAHL

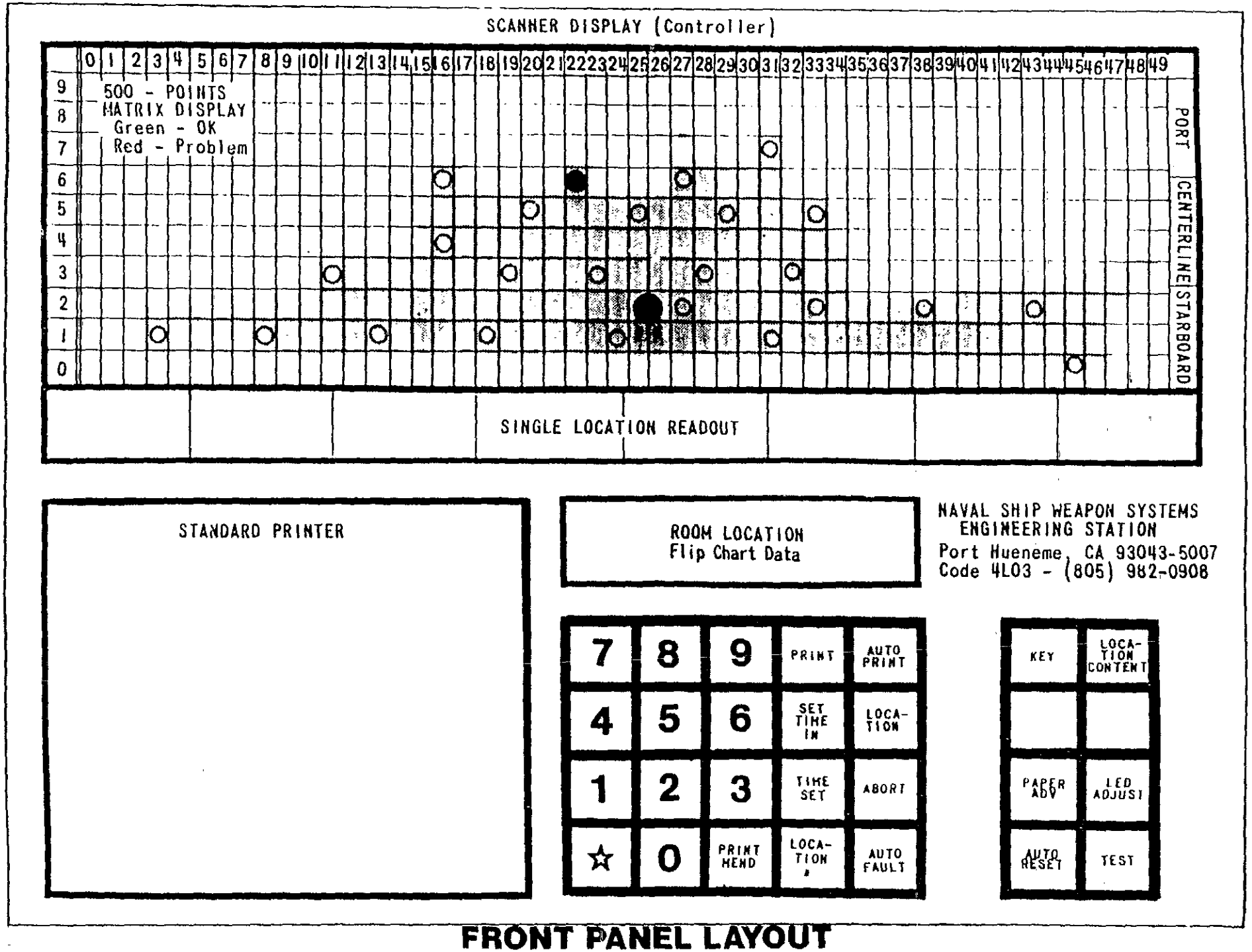

FRONT PANEL LAYOUT

NSWSES/TWARSES

TWO WIRE AUTOMATIC REMOTE SENSING AND EVALUATION SYSTEM

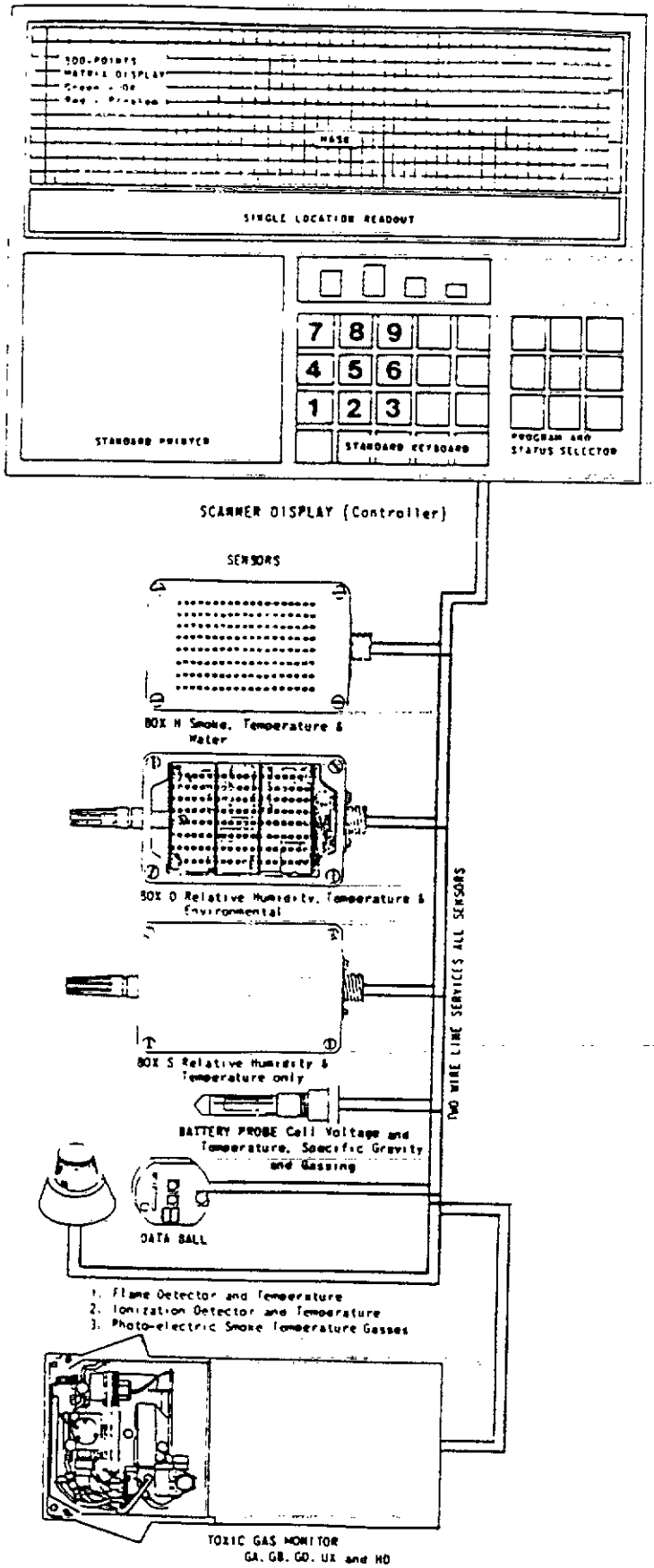

System Operation

The automatic monitoring system operates in a manner similar to an automatic, multi-scriber, party-line telephone system. The system is controlled by the Scanner/Display unit which interrogates each of the 150 sensors according to the program stored in a microprocessor. This patented system provides a *separate address for each sensor transponder*, permitting all of the transponders to be simply connected in parallel across a common, twisted-pair transmission line. The interrogating signal is also used to provide *power (6V-2MA) for the sensor* transponders and their associated sensors. This further simplifies the system by eliminating the need for a separate source of power at each sensor location.

Each sensor is interrogated with a 25-bit sequence which specifies: 1., the address of the sensor which is to reply, 2., the parameter to be reported (e.g., voltage, or temp-humidity etc.), and 3., the desired precision (which sets the length of the reply). The interrogation is transmitted as frequency-shift-keyed signal. Among the various types of interrogation signals which could be used (AM, FM, etc.,) frequency-shift-keying was selected because:

- FSK can be coded simply and inexpensively,
- FSK is basically a frequency-modulation technique, so the transmittal signal can be amplified and limited in the receiver without automatic gain control, and
- FSK is effected less by noise than amplitude-sensitive coding, because most noise or transient interference appears as amplitude format.

This FSK receiver in each transponder separates the two transmitted frequencies. Then demodulation is completed, when the separate tones are reconverted to the original data in serial binary format.

In order to minimize the cost of the sensor transponder, while at the same time achieving high quality telemetry, the analog signal from a selected sensor is not converted to digital form in the transponder. Instead, FM telemetry technique is used for the returned data. The analog sensor signal is used to modulate a voltage-to-frequency converter, and this tone signal is transmitted back to the Scanner/Display unit, which then converts is to digital form by counting it against a crystal reference.

Digital data from each parameter and each sensor is separately stored and averaged in the Scanner/Display unit. The averaged values are constantly compared against limit values. Whenever any one of the (1050) averaged value exceeds a limit, the Scanner/Display unit signals this fact by changing the color from Green to Red in an array of LED indicators, each one corresponding to an individual sensor.

In the automatic mode of operation, the unit also lights a flashing alarm lamp and sounds an aural alarm. If a printer is used as part of the system, the occurrence of an out-of-limit alarm also initiates a readout cycle on all sensor parameters with the out-of-limit parameters flagged for easy identification.

The operator may at any time obtain a digital readout of the parameter values and fault status for any selected sensor. This data is presented on a digital readout on the Scanner/Display unit front panel. When the system printer is used, the operator may, by keyboard command, select the automatic printout interval as well as initiating a complete printout cycle at any time.

Sensors

Almost any type of standard sensor, active or passive, can be adapted to the NSWSES Two Wire System.

The **SENSOR'S POWER**, if active, will also be supplied by the common two wire feed. The sensor output is connected to an A.C. signal in which the lowest or 0 reading of the sensor is 1V, the maximum reading of 100% of full scale of the sensor is 3V and of course, on half scale reading will be 2V. At the present time sensors are in use measuring battery sensors such as Cell Voltage, Specific Gravity, Temperature, Electrolite Level and Individual Cell Voltage.

ENVIRONMENTAL SENSORS which will permit monitoring of gasses throughout the hull of a ship. NSWSES has now in operation sensors measuring Oxygen, Carbon Monoxide, Hydrogen, Nitric Oxide, Humidity and Temperature with Freon and Toxic gasses in model stages.

With ***MACHINERY SENSORS*** we can monitor Mechanical parameters of machinery with this two wire system measuring Pressure, Liquid Level, Bearing Noise, Temperature, Air Pressure and Vibration.

Installation

Low cost installation - Uses existing wire ways, race ways or conduit runs. The smokeless, miniature, low voltage 2 wire cable may be added to existing structures at an economical cost.

Combined with adhesive mounted sensor boxes, the "off the shelf" system is truly cost effective.

Environmental

NSWSES D BOX

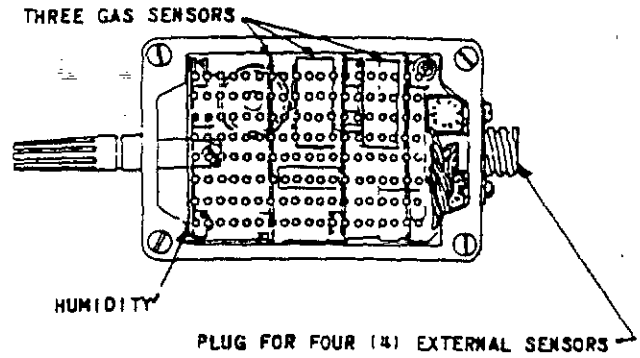

This wall mounted box is addressable for each location and provides data from seven sensors at the location.

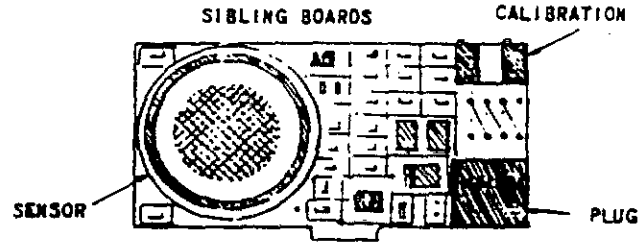

In stock are the following sensors:

- Carbon Monoxide, 7E0-7002-050
- Hydrogen, 7HY-000015-050
- Nitric Oxide, 7NT-045119-050
- Sulphur Dioxide, 3SF
- Oxygen, 077156080

In manufacture and available January, 1991 (IFP) are:

- Pressure
- Freon

These interchangeable sibling boards have an in-service life of two years with auto-alarm at a year and a half. The D Boxes permit through-case plug for three external sensors. Machinery, Sump alarms or Smoke, unit type B and local alarm available if requred.

NAVAL SHIP WEAPON SYSTEMS
ENGINEERING STATION
TEST AND ANALYSIS DEPARTMENT
Code 4L03 - (805) 982-0908

The NSWSES/NAVSES Smoke Alarm System is an adaption of the standard UL approved Cybernetic Smoke Detector Head # DT-6 using ionization principal as detection, or Head # R-902 using the Photo-electric principal.
The Standard Base # DB-4 is modified from a D.C. current shunt system to an A.C. two-wire NSMSES/TWARSES system in which one Control Board from the Control Base DB-4 is replaced with the Interchangeable NSWSES Board # 702-30. All mounting and screw holes are interchangeable. NOW this assembly, mounted the same, provides EXACT location, EXACT temperature at EXACT location - and displays with both, Illustrated Matrix Two-Color Status Display and Printed Readout with details of problem.

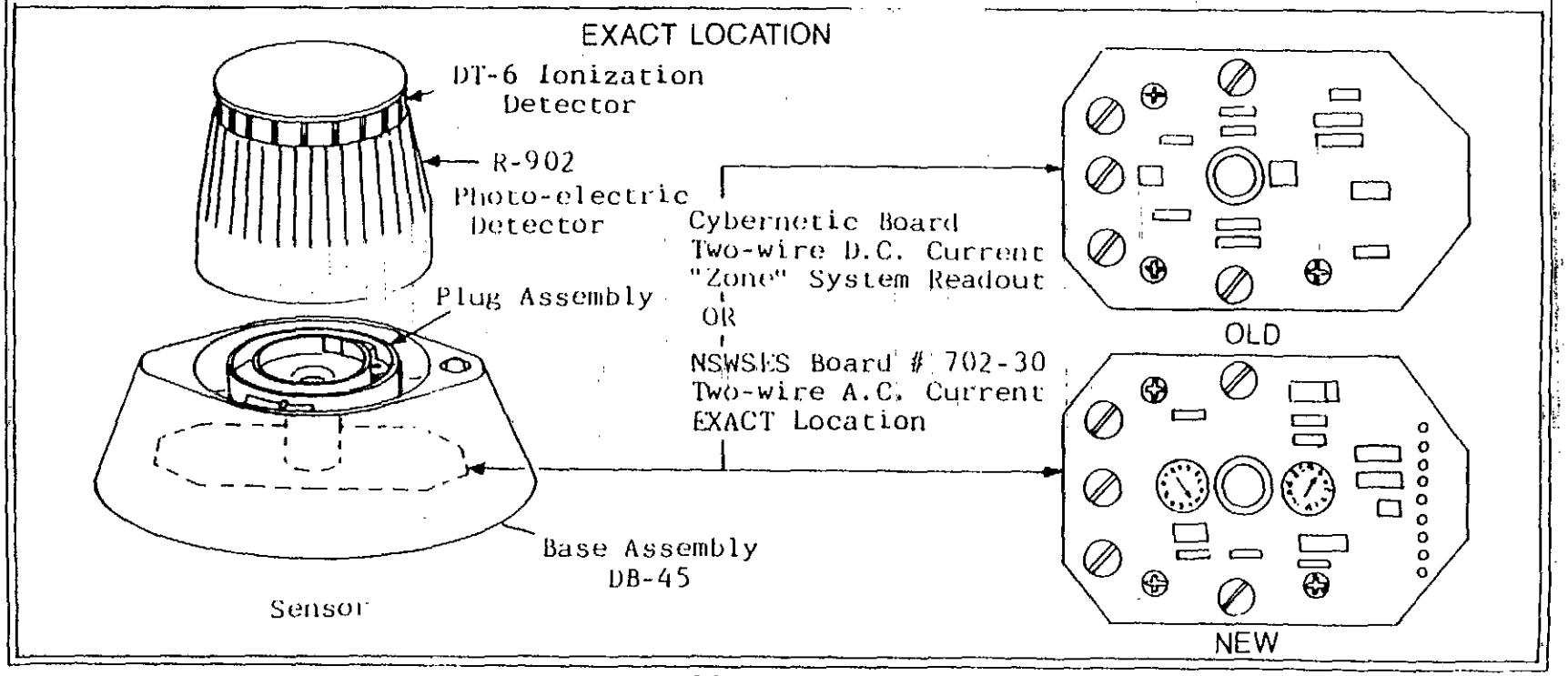

ASSEMBLY

SMOKE-TEMPERATURE-SUMP

SENSORS of 2 Dec 1990

SUBJECT	MEASUREMENT
1. CHILLED WATER	PRESSURE TEMPERATURE FLOW (?)
2. POWER 120 V 220 V 440 V	FREQUENCY 60 or 400
3. AIR FLOW For Dry Air Wave Guide	TEMPERATURE VELOCITY HUMIDITY
4. LIQUID LEVEL SENSOR	LIQUID YES or NO
5. GAS	AMOUNT

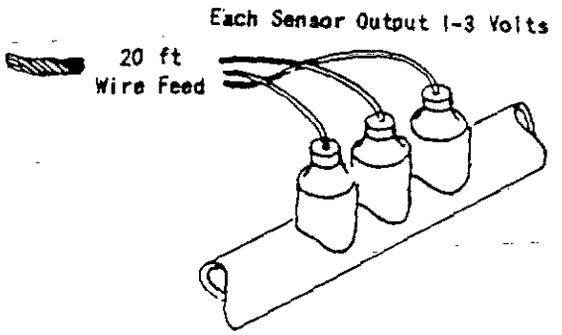

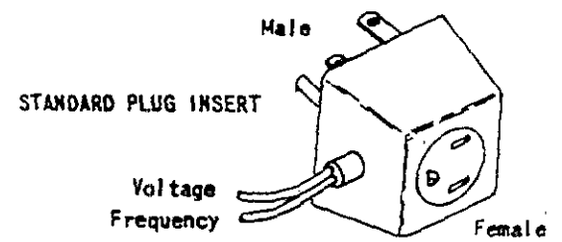

Each Output 1-3 Volts
Complete Isolation

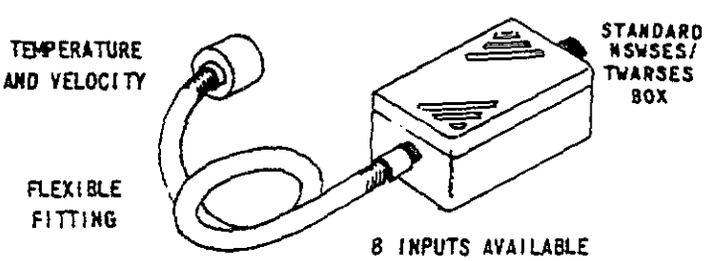

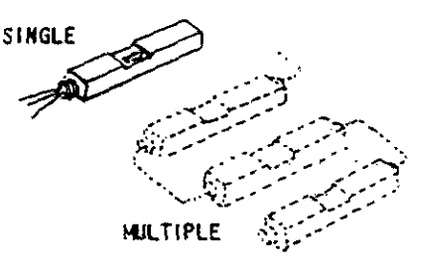

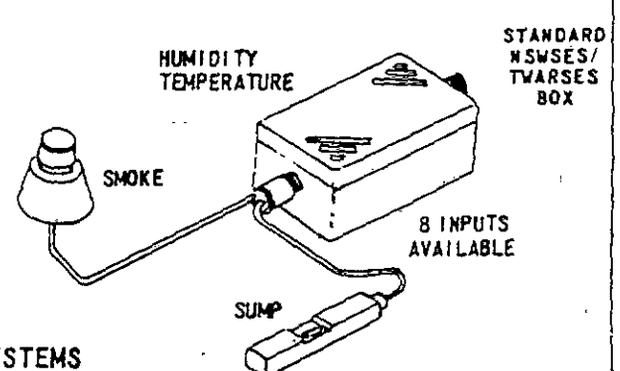

NAVAL SHIP WEAPON SYSTEMS
ENGINEERING STATION
TEST AND ANALYSIS DEPARTMENT
Code 4L03 - (805) 982-0908

JANUARY 1991 - USS MEMPHIS - Two Wire Automatic Remote Sensing and Evaluation System
PNO 38 TWARSES

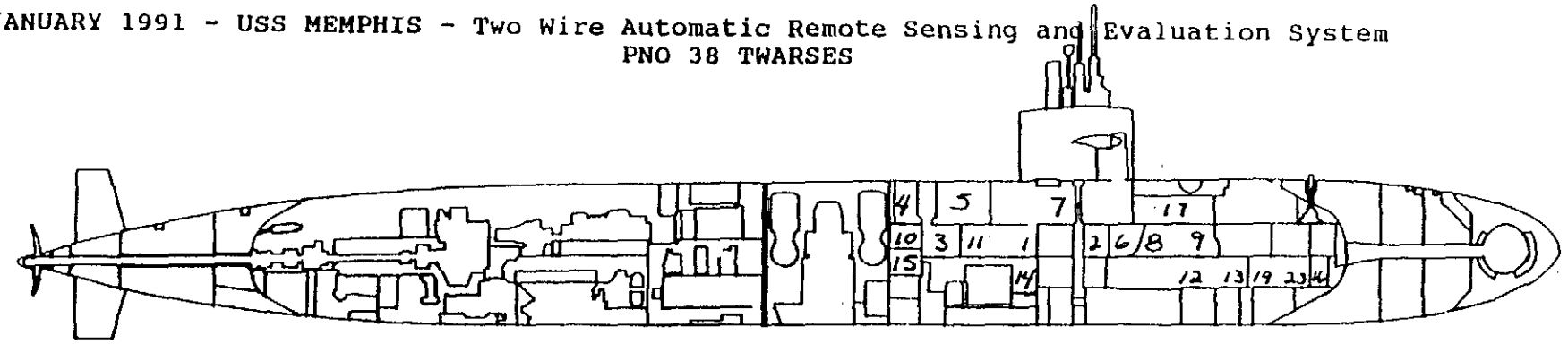

U - Upper Deck M - Middle Deck L - Lower Deck
Scanner Display Unit M Over Copy Machine

Sensors	Deck	Location
1	M	Offices' QTRS
2	M	Crews' Berthing
3	M	Chiefs' Berthing
4	U	Sonar Transmit Room
5	U	UYK Room
6	M	Crews' Berthing
7	U	Control Room
8	M	FWD Crews' Berthing
9	M	Passage way near Galley
10	M	Towed Array Space
11	M	FWD Crews' Berthing
12	L	Computer Room (Logging)
13	L	Crews' Berthing
14	L	Torpedo Room
15	L	Supply Room
16	L	Diesel Booth
17	U	Near Fan Room
19	L	Laundry Room
23	L	Machine Room

Ship's Printout

08:09 10 JAN 91 MEMPHIS (ver DEC 90)

Loc	Temp	RH	O2	CO	NO	H2	Alarm
1	70	37	--	--	--	--	--
2	60	51	--	--	--	--	--
3	69	37	--	--	--	--	--
4	62	52	--	--	--	--	--
5	65	46	--	--	--	--	--
6	67	40	--	--	--	--	--
7	56	27	--	--	--	--	--
8	71	32	--	--	--	--	--
9	68	38	--	--	--	--	--
10	71	37	21	--	--	--	--
11	58	57	20	--	--	--	--
12	72	36	21	--	--	--	--
13	70	34	20	--	--	--	--
14	71	32	--	--	--	--	--
15	69	36	21	--	--	--	--
16	59	57	21	--	--	--	--
17	63	50	22	--	--	--	--
19	57	57	--	--	--	--	--
23	61	52	--	--	--	--	--

AUTOMATIC DATA PRINTOUT

January 1991 - USS Memphis - Two Wire Automatic Battery and Evaluation System

PNO 38 TWARSES

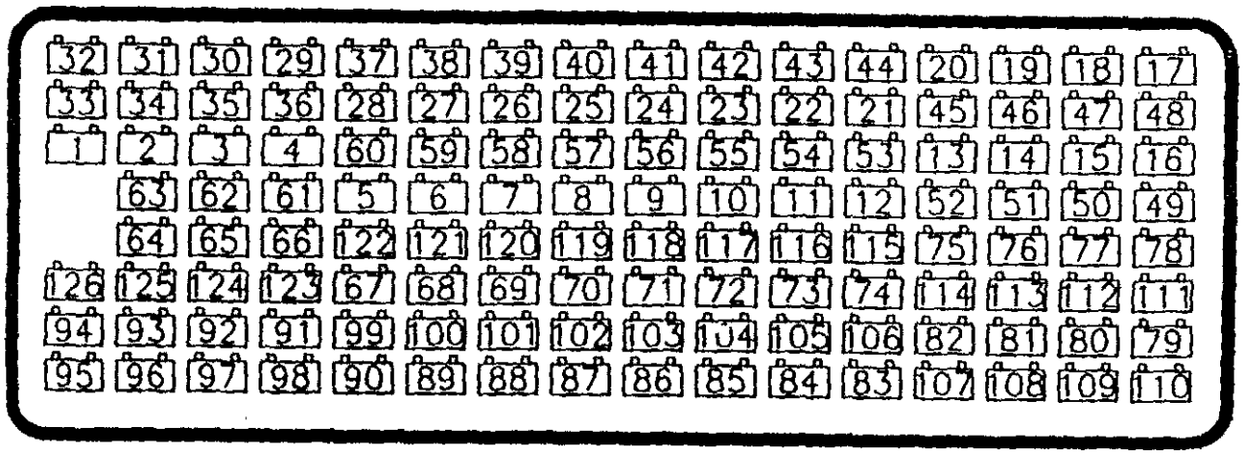

1*	2.107	< 1.275	62	2.451	LOW
2*	2.099	< 1.275	63	2.450	LOW
3*	2.088	< 1.275	66	2.441	LOW
5*	2.097	< 1.275	67	2.439	LOW
6*	2.099	< 1.275	66	2.439	LOW
7*	2.093	< 1.275	65	2.445	LOW
8*	2.089	< 1.275	67	2.439	LOW
9*	2.100	< 1.275	68	2.435	LOW
10*	2.102	< 1.275	67	2.436	LOW
11*	2.100	= 1.305	69	2.432	LOW
12*	2.099	< 1.275	70	2.430	LOW
13*	2.085	< 1.275	69	2.432	LOW
14*	2.099	< 1.275	68	2.435	LOW
15*	2.118	< 1.275	68	2.436	LOW
16*	2.099	= 1.305	65	2.445	LOW
17*	2.099	< 1.275	64	2.448	LOW
18*	2.093	< 1.275	65	2.443	LOW
19*	2.099	< 1.275	66	2.440	LOW
20*	2.095	= 1.285	65	2.442	LOW
21	2.122	< 1.275	69	2.431	OK
22*	2.091	< 1.275	67	2.439	LOW
23*	2.091	< 1.275	65	2.443	LOW
24*	2.088	< 1.275	65	2.444	LOW
25*	2.097	< 1.275	65	2.445	LOW
26*	2.099	< 1.275	65	2.445	LOW
27*	2.099	< 1.275	65	2.444	LOW
28*	2.087	< 1.275	65	2.444	LOW

29*	2.099	< 1.275	61	2.454	LOW
30*	2.097	< 1.275	62	2.454	LOW
31*	2.100	< 1.275	60	2.460	LOW
32*	2.097	< 1.275	60	2.459	LOW
33*	2.099	< 1.275	63	2.451	LOW
34*	2.100	< 1.275	62	2.451	LOW
35*	2.100	< 1.275	61	2.454	LOW
36*	2.088	< 1.275	65	2.442	LOW
37*	2.094	< 1.275	62	2.454	LOW
39*	2.100	= 1.285	62	2.451	LOW
40*	2.100	< 1.275	62	2.452	LOW
41*	2.093	< 1.275	64	2.447	LOW
42*	2.099	< 1.275	63	2.450	LOW
43	2.102	< 1.275	65	2.445	OK
44*	2.122	= 1.305	69	2.433	OK
45*	2.110	= 1.285	69	2.433	LOW
46*	2.094	< 1.275	65	2.442	LOW
47*	2.100	< 1.275	66	2.441	LOW
48*	2.021	< 1.275	64	2.448	LOW
49*	2.099	= 1.305	67	2.439	LOW
50	2.100	< 1.275	69	2.432	OK
51*	2.097	< 1.275	68	2.435	LOW
52*	2.100	< 1.275	70	2.430	LOW
53*	2.087	< 1.275	68	2.435	LOW
55*	2.099	< 1.275	67	2.436	LOW
56*	2.098	< 1.275	66	2.439	LOW
57*	2.111	< 1.275	65	2.443	LOW

58*	2.087	< 1.275	64	2.446	LOW
59*	2.099	= 1.305	67	2.439	LOW
60*	2.087	< 1.275	67	2.437	LOW
61*	2.093	< 1.275	68	2.433	LOW
62	2.099	< 1.275	66	2.441	OK
63	2.097	< 1.275	65	2.443	OK
67*	2.111	< 1.275	69	2.431	LOW
69*	2.088	< 1.275	67	2.437	LOW
70*	2.091	< 1.275	67	2.439	LOW
71*	2.099	< 1.275	68	2.436	LOW
72*	2.103	< 1.275	67	2.437	LOW
73*	2.099	< 1.275	68	2.433	LOW
74*	2.101	< 1.275	70	2.427	LOW
79*	2.099	< 1.275	63	2.450	LOW
81*	2.088	< 1.275	66	2.440	LOW
82*	2.103	< 1.275	68	2.436	LOW
83*	2.100	< 1.275	63	2.450	LOW
85*	2.082	< 1.275	63	2.451	LOW
86*	2.099	< 1.275	62	2.452	LOW
87	2.087	< 1.275	63	2.451	OK
88	SENSOR FAULT				
89	SENSOR FAULT				
90	SENSOR FAULT				
91	SENSOR FAULT				
92	SENSOR FAULT				
93	SENSOR FAULT				
94	SENSOR FAULT				
101	SENSOR FAULT				

1	2.1				
2	2.100	=			
3*	2.097	=	1.285	65	OW
4*	2.100	=	1.305	64	2.446 OK
5*	2.094	=	1.305	64	2.448 LOW
6*	2.111	=	1.285	64	2.446 LOW
7*	2.103	=	1.305	64	2.448 LOW
8	2.100	<	1.275	64	2.446 OK
9*	2.102	=	1.305	64	2.447 LOW
10	2.100	=	1.295	64	2.448 OK
11*	2.116	=	1.305	64	2.447 LOW
12*	2.111	=	1.305	64	2.448 OK
13*	2.114	=	1.305	63	2.451 LOW
14*	2.111	=	1.285	65	2.444 LOW
15*	2.099	=	1.305	64	2.448 LOW
16*	2.100	=	1.305	65	2.444 OK
17*	2.100	=	1.305	65	2.442 OK
18*	2.113	=	1.305	64	2.448 LOW
19*	2.100	=	1.295	63	2.448 LOW
20*	2.120	=	1.305	63	2.448 LOW
21*	2.100	=	1.305	62	2.452 OK
22*	2.090	=	1.285	62	2.452 LOW
23*	2.111	=	1.305	63	2.450 LOW
24*	2.113	=	1.305	65	2.445 OK
25*	2.088	=	1.305	66	2.441 LOW
26*	2.096	=	1.305	65	2.442 LOW
27*	2.099	=	1.285	65	2.442 LOW
28	2.107	>	1.315	67	2.439 OK
29*	2.100	=	1.305	66	2.441 LOW
30*	2.109	<	1.275	66	2.441 LOW
31*	2.100	>	1.315	66	2.446 LOW
32*	2.089	=	1.310	67	2.439 LOW
33*	2.100	=	1.305	66	2.441 OK
34*	2.111	=	1.285	66	2.441 LOW
35*	2.100	=	1.305	67	2.439 OK
36*	2.109	=	1.285	66	2.439 LOW
37*	2.099	=	1.305	66	2.440 LOW
38	2.111		CHANGE	65	2.444 OK
39*	2.098	=	1.305	66	2.440 LOW
40	2.099	>	1.315	66	2.440 OK
41*	2.091	=	1.305	66	2.441 LOW
42*	2.111	=	1.305	65	2.444 LOW
43*	2.122	=	1.305	64	2.447 LOW
44	2.112	=	1.295	65	2.444 OK
45*	2.097	=	1.305	67	2.437 LOW
46*	2.100	=	1.305	67	2.439 OK
47*	2.110	=	1.295	68	2.433 LOW
48*	2.100	=	1.305	67	2.439 LOW
49*	2.085	<	1.275	67	2.437 LOW
50*	2.099	=	1.305	66	2.441 LOW
51*	2.085	=	1.305	66	2.441 OK
52*	2.111	=	1.305	66	2.440 LOW
53*	2.116	=	1.305	67	2.437 OK
54*	2.099	<	1.275	67	2.439 LOW
55	2.074	=	1.285	66	2.439 OK
56*	2.100	=	1.310	66	2.441 LOW
57*	2.097	=	1.305	65	2.442 OK
58*	2.099	=	1.305	65	2.444 OK
59*	2.112	=	1.305	65	2.442 OK
60*	2.088	=	1.305	64	2.447 OK
61*					.OW
62*					.OW

5					
6					
66*	2.122				
67*	2.101	=	1.305	66	2.440 LOW
68*	2.111		CHANGE	67	2.439 LOW
69*	2.100	=	1.295	67	2.439 LOW
70*	2.104	=	1.285	68	2.436 LOW
71*	2.106	<	1.275	68	2.435 LOW
72*	2.100	<	1.275	68	2.435 LOW
73*	2.099	<	1.275	70	2.430 LOW
74	2.100	<	1.275	68	2.435 OK
75*	2.097	<	1.275	68	2.433 LOW
76*	2.096	<	1.275	68	2.433 LOW
77*	2.111	=	1.305	68	2.436 LOW
78*	2.110	=	1.305	67	2.436 OK
79	2.100	=	1.295	68	2.435 OK
80*	2.098	=	1.305	69	2.433 OK
81*	2.100	=	1.305	67	2.436 LOW
82*	2.111	=	1.305	66	2.439 LOW
83*	2.099	=	1.305	66	2.439 OK
84*	2.083	=	1.315	65	2.445 LOW
85*	2.099	=	1.305	64	2.446 LOW
86*	2.121	>	1.315	65	2.443 LOW
87*	2.100	=	1.305	66	2.441 OK
88*	2.100	=	1.305	66	2.439 OK
89*	2.111	=	1.305	66	2.441 LOW
90*	2.104	=	1.305	66	2.439 LOW
91*	2.122	=	1.295	66	2.440 LOW
92*	2.104	=	1.310	67	2.439 LOW
93*	2.099	=	1.305	67	2.439 LOW
94*	2.112		CHANGE	68	2.436 LOW
95	2.111		CHANGE	67	2.437 OK
96*	2.101	=	1.295	68	2.436 LOW
97	2.099	<	1.275	70	2.429 OK
98*	2.091	=	1.305	68	2.435 LOW
99	2.111		CHANGE	68	2.433 OK
100	2.100	=	1.285	68	2.435 OK
101*	2.111	=	1.305	67	2.436 OK
102*	2.116	=	1.305	68	2.433 OK
103*	2.077	=	1.305	68	2.435 LOW
104*	2.103	=	1.305	66	2.439 LOW
105*	2.099	=	1.305	65	2.443 LOW
106	2.097	<	1.275	65	2.442 OK
107*	2.099	=	1.305	66	2.439 LOW
108	2.108	=	1.295	66	2.440 OK
109	2.100	=	1.310	66	2.440 OK
110*	2.093	=	1.305	66	2.440 OK
111*	2.100	=	1.285	66	2.439 LOW
112*	2.104	>	1.315	66	2.440 LOW
113*	2.099	=	1.305	65	2.443 LOW
114*	2.117	=	1.310	66	2.440 LOW
115*	2.111	=	1.305	66	2.440 LOW
116	2.117	=	1.295	66	2.441 OK
117	2.100	<	1.275	65	2.442 OK
118*	2.113	=	1.305	65	2.442 LOW
119	2.122	=	1.285	65	2.444 OK
120*	2.100	=	1.305	66	2.441 OK
121*	2.088	=	1.305	65	2.442 LOW
122*	2.093	=	1.305	66	2.441 LOW
123*	2.111	<	1.275	65	2.443 LOW
124*		=	1.305	65	2.444 LOW
125					.OW
126					

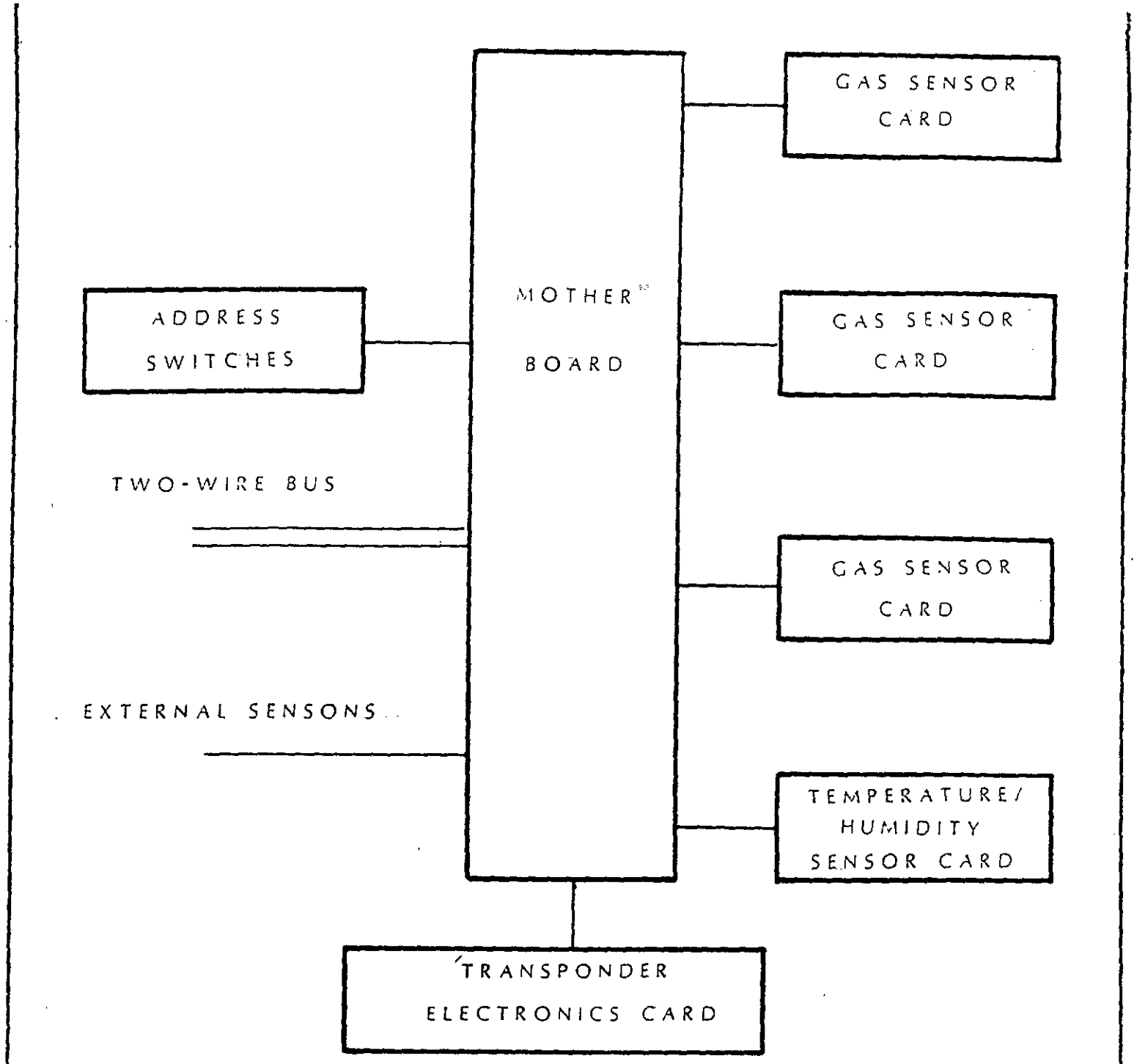

"D" TYPE MODULAR TRANSPONDER

8 - SENSOR INPUTS

SHIP AUTOMATIC SMOKE AND FIRE ALARM SYSTEM WITH DAMPER CONTROLS

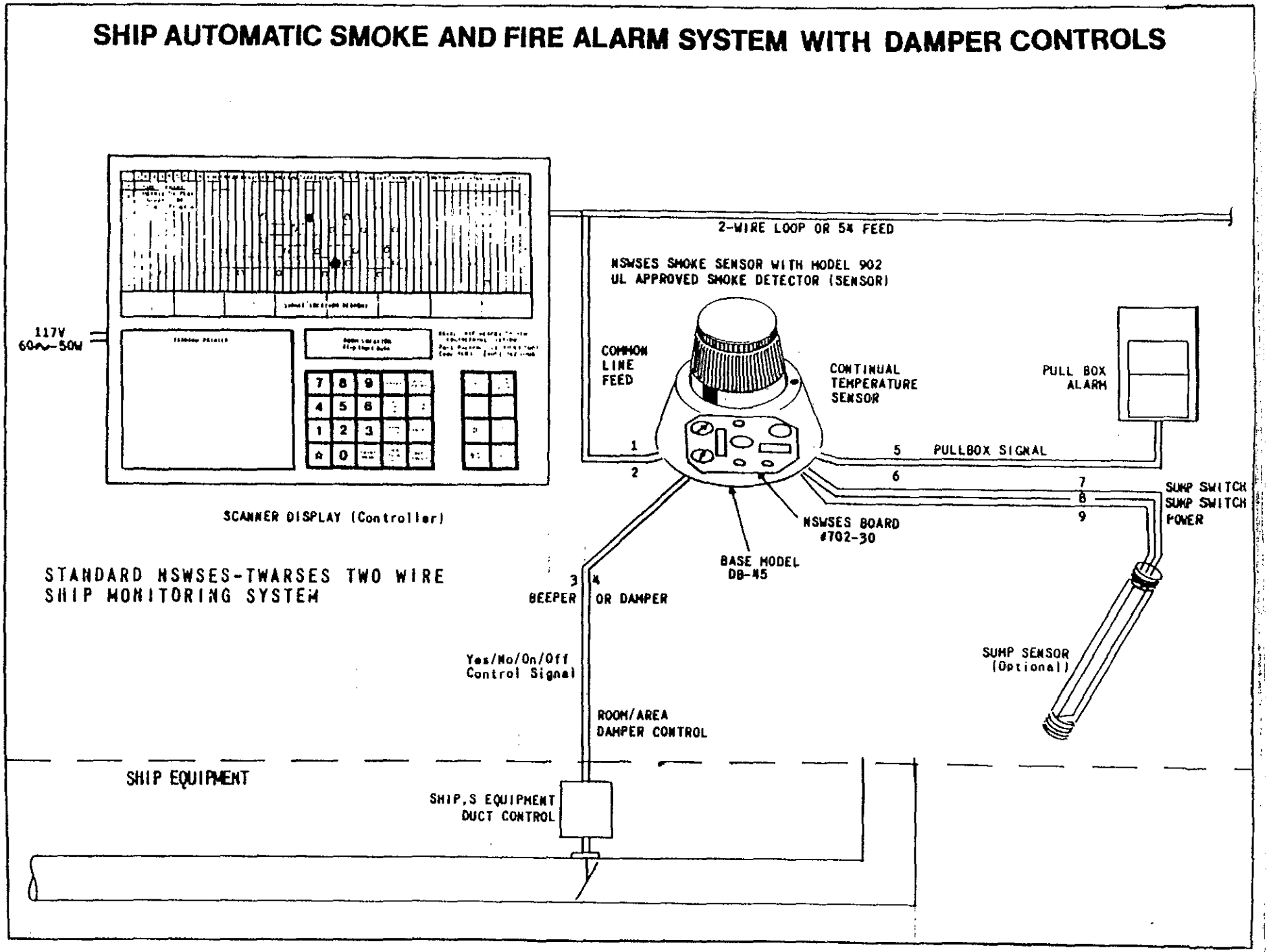

TWARSES SENSORS AS OF 1 JUNE 1991

0 - 1 - 3 VOLTS

The following sensors are available for connection to the TWARSES system for detection purposes.

1. OXYGEN ORDER CODE: MA240-074-00 MFG - CITY TECH

Sibling Board "A"

Low Oxygen levels are hazardous to health and in the extreme case can cause death through asphyxiation. Warning levels are often set in the region 17%-19% O2 by volume concentration. Low O2 levels may be due to leaks from cylinders/processes or the consumption of O2 by organisms in a confined space. Biologically it is the partial pressure of Oxygen in mBar's which is important rather than the concentration in volume %. Because of this we can, if required, also offer a sensor which will measure the partial pressure directly as oppose to the volume concentration. The sensor resolution is 0.05% O2.

POWER INTERNAL

2. CARBON MONOXIDE ORDER CODE: MB150-044-00 MFG - CITY TECH

Sibling Board "A"

Carbon Monoxide is a colorless odorless poisonous gas which is commonly produced in combustion processes. It is common to set alarm levels between 30 and 300 ppm. The sensor from City Technology includes an internal filter to increase the specificity to CO thus reducing the possibility of false alarms. The sensor resolution is 0.5ppm CO.

POWER INTERNAL

3. NITRIC OXIDE ORDER CODE: MF750-054-00 MFG - CITY

Sibling Board "A"

Nitric Oxide is produced from combustion sources especially diesel engines. It is spontaneously oxidized to NO2 by slow aerial oxidation. The NO2 is more hazardous and alarms are often set at 1-2 ppm. NO alarm levels are in the 50 ppm region normally. The

4. HYDROGEN ORDER CODE: ME550-064-00 MFG - CITY

Sibling Board "A"

Hydrogen is an explosive gas which can be produced during Lead acid battery charging. H2 is not explosive below 2% in air however alarm levels of 1000-2000ppm allow early warning of potential problems. The sensor resolution is 1ppm H2.

5. HYDROGEN SULPHIDE ORDER CODE: MC550-104-00 MFG - CITY

Sibling Board "A"

Hydrogen Sulphide is an extremely toxic gas with the characteristic smell of bad eggs. It is detectable by Humans at sub-ppm levels but unfortunately causes the nose to become accustomed to it's presence allowing high concentrations to build up undetected. Typical alarm levels are 10-20ppm. It is produced when some bacteria ferment anaerobically in water treatment areas and is often found associated with natural gas and oil deposits. The sensor resolution is 0.1 ppm H2S. The reaction that takes place in the sensor is the oxidation of H2S on a sensitive catalytic material which yields a tiny electrical current proportional to the number of molecules of H2S reaching the sensor's sensing electrode. The actual reaction is as follows:

$$H2S + 4H2O = H2SO4 + 8H+ + 8e$$

thus 8 electrons are produced from every 1 molecule of H2S.

The response time of the H2S sensor is measured as the time taken to reach 90% of it's final value on exposure to a step change in gas concentration. This varies slightly between different sensor types depending on the rate at which the reaction occurs on the catalyst. Foe the H2S sensor the 90% response time is less than 60 secs.

6. SULPHUR DIOXIDE ORDER CODE: MDA50-104-00

Sulphur dioxide is used in water treatment and produced in the combustion of sulphur containing fuels. It has a characteristic sweet taste and is hazardous at very low levels causing respiratory ailments. Alarm levels of 1-2 ppm are common. The sensor resolution is 0.1 ppm SO2.

7. NITROGEN DIOXIDE ORDER CODE: MG150-104-00 MFG - CITY

Nitrogen Dioxide is formed from NO and is also produced directly by combustion. It is an acidic gas with a dark brown color and acrid fumes. Alarm levels are usually in the 1-2 ppm area. The sensor resolution is 0.1 ppm NO2.

8. CHLORINE ORDER CODE: MH150-104-00 MFG - CITY

Chlorine is used in water purification and bleaching applications. It has a pungent smell and is highly toxic. Alarm levels of 0.5-1 ppm are common. The sensor resolution is 0.1 ppm Cl2.

9. HYDROGEN CYANIDE ORDER CODE: ML350-054-00 MFG - CITY

Hydrogen Cyanide is highly toxic and produced in acid reactions with cyanide containing salts. These are common in plating and refining works. It can also be produced by some explosives during their combustion and when certain plastics (e.g. polyurethanes) are burnt. Alarm levels of 10-50 ppm are common. THe sensor resolution is 0.5 ppm HCN.

10. HYDROGEN CHLORIDE ORDER CODE: ML350-104-00 MFG - CITY

Hydrogen Chloride is an acidic gas produced when PVC and other plastics are burnt. It is also used in the semiconductor industry as an etchant. The normal alarm levels are 5-20ppm. The sensor resolution is 1 ppm HCI.

11. CARBON DIOXIDE ORDER CODE: MP150-084-00 MFG - CITY

"D" CASE - STANDARD OUTPUT PLUG

Carbon Dioxide is present naturally at a background level of 340 ppm. It can be produced by combustion processes or by the action of acids on carbonates or through leaks from cylinders. A monitoring range of 0-1% is often used with an alarm at 5000 ppm. A prototype sensor is being produced as an engineering development sample. Power - 117V 60N - TWARSES - CODED

12. PRESSURE ORDER CODE: MZ1A0-094-00 MFG - CITY

An absolute pressure detector is available with the range 0-2Bar.

13. HUMIDITY & TEMPERATURE ORDER CODE: MFG - ROTRONICS

A. Sibling Board "B" is a probe assembly sitting the "D" box standardized to measure humidity 0-100%; temperature 40-140o.

B. Mother board Complete Assembly (CA) humidity and temperature. Order number is a standard box assembly designated as "E" with five external 0-3V inputs available at external plug configuration.

14. FREON ORDER CODE: MQ150-134-00 MFG - CITY

The detector is an infrared type and utilizes a 110V AC power supply with output indicating Freon data level. Power supply level and self check - four units available 26 July. Configuration to be used with mother board 702-30.

15. SMOKE DETECTOR ORDER CODE: MFG - PYROTRONICS

A. Photo-electric

B. Ionization

16. LIQUID LEVEL SENSOR ORDER CODE: MFG - LABAC MOLD CO

Use with mother board D-2 or 702-30

17. SPRING BEARING SENSOR ORDER CODE: MFG - LABAC MOLD CO

Oil level, temperature, conductor sensor. Use with mother board D-2 or 702-30.

THE FOLLOWING SENSORS ARE NOW BEING ASSEMBLED FOR NSWSES SYSTEM ANALYSIS USE:

18. CHILLED WATER - PROBE ASSEMBLY ORDER CODE: MFG -

19. DC CURRENT SENSOR ORDER CODE: MFG -

20. LINE VOLTAGE SENSOR

21. BATTERY CELL PROBE ASSEMBLY MFG -

UNIT BEING MODIFIED TO REDUCE SIZE AND COST. SAME CONFIGURATION.

22A. TANK LEVEL INDICATOR (POINT TYPE) MFG - LABAC

PART OF NAVSSES SMOKE DETECTOR SYSTEM.

22B. TANK LEVEL INDICATOR (CONTINUOUS READING) MFG - POLAROID

PART OF NSWSES SPRING BEARING SENSOR.

Secretariat

RANGE COMMANDERS COUNCIL

ATTN: STEWS-SA-R
WHITE SANDS MISSILE RANGE, NEW MEXICO 88002-5110

OFFICIAL BUSINESS